RNAi-mediated knockdown of the endogenous TCR improves safety of immunotherapy with TCR gene-modified T cells

D i s s e r t a t i o n

zur Erlangung des akademischen Grades

d o c t o r r e r u m n a t u r a l i u m

(Dr. rer. nat.)

im Fachbereich Biologie

eingereicht an der

Lebenswissenschaftlichen Fakultät

der Humboldt-Universität zu Berlin

von

D i p l o m - B i o c h e m i k e r M a r i o B u n s e

Präsident der Humboldt-Universität zu Berlin

Prof. Dr. Jan-Hendrik Olbertz

Dekan der Lebenswissenschaftlichen Fakultät

Prof. Dr. Richard Lucius

Gutachter/innen: 1. Prof. Dr. Wolfgang Uckert

2. Prof. Dr. Thomas Blankenstein

3. Prof. Dr. Christian Schmitz-Linneweber

Tag der mündlichen Prüfung: 12.12.2014

Zusammenfassung

Mithilfe von viralen Vektoren können T-Zellen *ex vivo* genetisch verändert werden. Der Transfer von Genen für die α- und β-Ketten des T-Zellrezeptors (TZR) programmiert T-Zellen spezifisch ein ausgewähltes Antigen zu erkennen und der Einsatz solcher genmodifizierten T-Zellen in klinischen Studien für die Immuntherapie von Krebs hat gezeigt, dass sie nach dem Transfer in den Patienten Tumore erkennen und abstoßen können. Genmodifizierten T-Zellen unterscheiden sich jedoch von normalen T-Zellen, weil sie zusätzlich zu den Genen des zelleigenen TZR auch die Gene des übertragenen TZR exprimieren. Diese Situation erlaubt die Bildung vier verschiedener αβ-TZR Heterodimere: der zelleigenen TZR, der übertragene TZR und zwei gemischte TZR, bestehend aus einer übertragenen und einer zelleigenen TZR Kette. Daraus ergeben sich zwei Probleme. Erstens entsteht eine Konkurrenzsituation. Die verschiedenen TZR Ketten konkurrieren miteinander um Heterodimere zu bilden und die Heterodimere konkurrieren um eine begrenzte Menge an CD3 Proteinen. Die Formation eines Proteinkomplexes aus TZR und CD3 Proteinen ist eine Vorrausetzung für die Oberflächenexpression und die Gesamtmenge des TZR an der Zelloberfläche ist beschränkt durch die verfügbare Menge an CD3 Proteinen. Zweitens stellt die Bildung von gemischten TZR ein Sicherheitsrisiko dar, weil die Spezifität dieser Rezeptoren durch den Zufall bestimmt ist und sie deshalb auch gesundes Körpergewebe erkennen könnten.

In dieser Doktorarbeit wurde ein neuartiger γ-retroviraler Vektor entwickelt um TZR Gene in T-Zellen zu übertragen und gleichzeitig die Expression des zelleigenen TZR durch RNA Interferenz (RNAi) zu unterdrücken. Dafür wurden zum einen die Gene des zu übertragenden TZR so verändert, dass sie von dem RNAi Effekt nicht beeinflusst werden, und zum anderen wurden Gene für Mikro-RNA (Abk. engl.: miRNA), die den RNAi Effekt auslösen, in den viralen Vektor MP71 eingefügt. Durch die Expression der miRNA reduzierte sich die Mengen des zelleigenen TZR auf der Oberfläche von genmodifizierten T-Zellen auf 6% und 12%, abhängig davon ob die miRNA die α- oder β-Kette des TZR unterdrückte. Anhand von Vektoren, die anstatt eines neuen TZR ein Markergen enthielten, wurde gezeigt, dass sich auch die Expression des Markergens in den genmodifizierten T-Zellen abhängig von der Position der miRNA in dem Vektor veränderte. Das Expressionsniveau betrug 32%, 2% und 15%, abhängig davon, ob die miRNA in das Intron am 5' Ende des Vektors oder direkt vor oder hinter das Markergen kloniert wurde. Die zwei miRNA für die Unterdrückung der beiden Ketten des zelleigenen TZR wurden deshalb in das Intron des retroviralen Vektors MP71 eingefügt und anschließend das Markergen gegen den P14 TZR, der das virale Antigen GP33 erkennt, ausgetauscht. Die Unterdrückung des zelleigenen TZR in genmodifizierten T-Zellen hatte zur Folge, dass beide Ketten des P14 TZR in etwa gleicher Menge auf der Zelloberfläche exprimiert wurden. Im Gegensatz dazu übertraf die Menge der β-Kette diejenige der α-Kette um das Zweifache, wenn ein unmodifizierter Vektor für die gentechnische Veränderung der T-Zellen verwendet wurde. Diese Beobachtung war ein klarer Beleg dafür, dass die Unterdrückung des zelleigenen TZR die Bildung von gemischten TZR bestehend aus einer β-Kette des P14 TZR und einer α-Kette des zelleigenen TZR verhinderte. Im Einklang mit dieser

Beobachtung konnte in einem Mausmodell gezeigt werden, dass die Unterdrückung des zelleigenen TZR in genmodifizierten T-Zellen auch die Entstehung von Autoimmunität verhinderte, die durch gemischte TZR verursacht wurde. Die Anwendung von gentechnisch optimierten P14 TZR Genen, um die Oberflächenexpression zu verbessern, führte im Gegensatz dazu weder zu einer Angleichung beider P14 TZR Ketten auf der Zelloberfläche, noch zu weniger Autoimmunität im Mausmodell. Unabhängig davon, ob die P14 TZR Gene kodonoptimiert wurden und eine zweite intramolekulare Disulfidbrücke enthielten oder nicht, entwickelten alle Tiere nach dem Transfer von genmodifizierten T-Zellen eine tödliche Autoimmunkrankheit. Dagegen überlebten 81% und 94% der Tiere, wenn die T-Zellen mit dem neu entwickelten Vektor genetisch verändert wurden, abhängig davon, ob der Vektor die unveränderten oder die optimierten P14 TZR Gene enthielt. In einem zweiten Tierexperiment konnte zudem gezeigt werden, dass die Expression der miRNA die Funktion der genmodifizierten T-Zellen nicht negativ beeinflusste. Die Doktorarbeit wurde mit der Entwicklung eines weiteren viralen Vektors abgeschlossen, der die Expression des zelleigenen TZR in menschlichen T-Zellen unterdrückt. Dafür wurden neue miRNA Gene konstruiert, die den zelleigenen TZR auf der Oberfläche von genmodifizierten menschlichen T-Zellen auf 10% und 22% reduzierten, in Abhängigkeit davon, ob die miRNA die α- oder β-Ketten des TZR unterdrückte. Im einem direkten Vergleich konnte gezeigt werden, dass der neu entwickelte Vektor die Mengen der Ketten eines TZR, der das "Cancer/Testis-Antigen" MAGE-A1 erkennt, auf der Oberfläche von genmodifizierten T-Zellen effizienter anglich, als die bereits etablierten Methoden für die Optimierung der TZR Gene.

Summary

T cells can be *ex vivo* genetically modified using viral vectors. The transfer of genes encoding the α and β chain of the T cell receptor (TCR) programs the T cells to specifically react towards an antigen of choice. Such TCR gene-modified T cells are currently employed in clinical studies of cancer immunotherapy where they are transferred back into the patient in order to launch an anti-tumor immune response. TCR gene-modified T cells differ from regular T cells. They express transferred TCR genes in addition to the genes of their endogenous TCR, which allows the assembly of four different TCR α/β heterodimers: the endogenous TCR, the transferred TCR, and two mixed TCR dimers, composed of endogenous and transferred TCR chains. This has two main consequences: First, the total amount of TCR on the cell surface is limited by the availability of CD3 proteins, which associate with the TCR dimers to form TCR/CD3 complexes. Hence, the TCR chains compete with each other for dimerization and CD3 proteins. Second, the formation of mixed TCR dimers represents a safety issue because their specificity is unpredictable and they may by chance recognize self-antigens.

In this thesis, a novel γ-retroviral RNAi-TCR replacement vector was developed that simultaneously expresses miRNA for the silencing of both endogenous TCR chains and a new pair of TCR chains, which were rendered RNAi-resistant by the introduction of silent mutations. First, miRNA directed at the mouse TCR chains were constructed and introduced into a GFP-encoding MP71 vector. In transduced mouse T cells, the surface level of the endogenous TCR was reduced to 6% and 12% by the expression of a TCRα or β chain-specific miRNA, respectively. However, the GFP expression was also affected by the modification of the vector. Depending on whether a miRNA was introduced into the 5' intron of the vector or at exonic positions 5' and 3' of the transgene, the GFP expression was reduced to 32%, 2% and 15%, respectively. Then, a miRNA cassette containing two miRNA for the simultaneous knockdown of both endogenous TCR chains was constructed and introduced into the 5' intron of a P14 TCR-encoding MP71 vector. The P14 TCR recognizes the viral antigen GP33. Silencing of the endogenous TCR in TCR gene-modified T cells resulted in equal surface levels of both P14 TCR chains, whereas more than twice as much P14 TCRβ chain compared to P14 TCRα chain was expressed at the surface of T cells transduced with an unmodified P14 TCR-encoding MP71 vector. This data strongly indicated that the formation of mixed TCR dimers composed of P14 TCRβ chain and endogenous TCRα chain is prevented by TCR silencing. Afterwards a mouse model of TCR gene therapy was used to demonstrate that the silencing of the endogenous TCR in TCR gene-modified T cells reduces mixed TCR dimer-dependent autoimmunity. Engineering of the P14 TCR by codon optimization in combination with the introduction of an additional inter-chain disulfide bond neither resulted in equal surface levels of the P14 TCR chains nor reduced the autoimmunity in the mouse model. All mice that received cells transduced with the native or optimized P14 TCR developed lethal autoimmunity, whereas 81% and 94% of the mice survived when the transferred T cells were transduced with the RNAi-TCR replacement vector encoding the native or optimized P14 TCR, respectively. A second mouse model was used to confirm that the expression of the miRNA did not negatively influence the

functionality of the TCR gene-modified T cells. The project was completed by the development of a second RNAi-TCR replacement vector for human T cells. New miRNA specific for the human TCR chains were constructed, which reduced the surface level of the endogenous TCRα and β chain in transduced T cells to 10% and 22%, respectively. Finally, a comparison of human TCR gene-modified T cells indicated that the surface levels of both chains of a TCR recognizing the cancer/testis antigen MAGE-A1 were more efficiently adjusted to each other by TCR silencing compared to established methods of TCR engineering.

1 Introduction

1.1 T cell progenitors in the thymus generate the TCR repertoire by somatic recombination

The adaptive immune system equips the host with a highly diverse repertoire of antigen-recognition receptors expressed by lymphocytes of the T- and B-cell linage. During lymphocyte development, the process of somatic recombination generates an individual and highly specific receptor for each cell. These receptors are currently investigated and already in clinical use for the immunotherapy of cancer, because they allow to direct the patient's immune system to a target of choice. Of particular interest is the T cell receptor (TCR) expressed by T cells, because they are capable of killing cells of the body showing aberrant protein expression. The TCR enables them to detect their target cells and T cells can reject tumors, if they express a tumor-specific TCR and if favorable conditions are induced.

The discovery of the TCR was enabled by experimentally produced antibodies raised against cell surface proteins and used to characterize lymphocytes [1,2,3,4,5,6]. This endeavor was facilitated by a method for the generation of clonal antibody-producing cell lines [7]. Using an monoclonal antibody (mAb) specific for an antigen only expressed by a particular T cell lymphoma, a surface protein was isolated that consisted of two different disulfide-linked polypeptide chains [8]. Importantly, a very similar heterodimeric protein was also found in normal T cells and other T cell lines, although those were not recognized by the mAb, suggesting a clonal nature of the heterodimer. Other mAbs able to block or activate antigen-specific T cell functions also precipitated the putative TCR, whose chains were made up of a clonal variable and non-clonal constant part as indicated by peptide digestion [9,10,11,12]. Two groups succeeded at the same time in isolating a TCR chain sequence by scanning cDNA libraries for genes that are differentially expressed in T and B cells [13,14,15]. The discovered mouse and human TCRβ chain sequences were homologous to the heavy chain of antibodies and consisted of variable (V), joining (J), diversity (D) and constant (C) segments, whereas the later identified TCRα chain sequence resembled the light chain of antibodies and consisted just of V, J and C segments [16,17,18]. The clonal expression in T cells and the composition of the TCR chains strongly suggested that TCR are generated by somatic recombination of distinct genetic segments, a process previously discovered in B cells to be responsible for the generation of antibodies [19].

The human TCR repertoire consists of around 1-4x10^6 different TCRβ chains and there is limited overlap between individuals [20,21]. The basis for this diversity are multiple TCR gene segments encoded in the TCR loci [22,23]. Precisely, the human genome contains 46 Vα, 50 Jα and one Cα segment, as well as 48 Vβ, 13 Jβ, two Dβ and two Cβ segments, that are involved in the generation of the TCR repertoire [24]. In the thymus, T cell progenitors start to express the recombination activating genes-1 and -2 (RAG1/2), which encode enzymes that recognize signal sequences flanking the TCR segments and mediate in combination with other factors the rearrangement of the DNA sequence [25,26,27]. RAG knockout mice showed a complete block in lymphocyte development [28,29]. A functional TCRα chain gene is generated by a productive Vα to Jα

recombination event, whereas in case of the TCRβ chain first a Dβ to Jβ, and then a Vβ to Dβ-Jβ recombination takes place. The TCR gene loci are rearranged successively starting with the TCRβ chain. Allelic exclusion prevents the recombination of the second TCRβ chain locus, if the recombination of the first locus was productive [30]. The recombined TCRβ chain then pairs with a germline-encoded α chain named pre-TCRα chain [31,32]. Pre-TCR surface expression signals to stop TCR recombination and induces a short phase of proliferation followed by the recombination of the TCRα chain loci, which, in consequence, generates T cell clones expressing the same TCRβ chain paired with different TCRα chains. Both TCRα loci are recombined simultaneously and several unproductive Vα to Jα recombinations may take place until a functional TCRα chain is generated. As a result, mature T cells can express two functional TCRα chains [33,34,35]. The frequency of such cells was determined to be approximately 30% among T cells from human peripheral blood lymphocytes (PBL) based on flow cytometry data [35]. Modern single-cell sequencing approaches however indicated a somewhat lower frequency, although this has not been studied in detail [36]. As an exception, mature T cells expressing two functional TCRβ chains were also reported to exist [37].

Besides the diversity generated by the recombination of gene segments and the formation of TCRαβ heterodimers, additional diversity is introduced at the joining sites. First, one strand of the DNA sequences is cut imprecisely and, second, nucleotides may be deleted by exonucleases or added by the enzyme terminal deoxynucleotidyl transferase [38,39]. Therefore, the highest degree of diversity is located at the V-J junction of the TCRα chain and the V-D-J junctions of the TCRβ chain. In analogy to antibodies, the hypervariable sequences at the junctions are called complementarity determining regions 3 (CDR 3). Intriguingly, the CDR3 encode for those amino acids that are mainly responsible for the specificity of the TCR. The CDR1 and CDR2 located in the V segments further contribute to ligand binding, but their variability is limited as their sequences are germline encoded.

1.2 The TCR associates with CD3 proteins for surface expression

The TCR dimer at the cell surface is non-covalently associated with different CD3 proteins and forms a large multimeric protein complex. Experiments with activating mAb directed either against CD3 proteins or the TCR demonstrated that the surface expression of both is modulated in a similar fashion [6,9]. In addition, TCR chains were co-precipitated with CD3 proteins [12]. Mutants of a human T cell line lacking either some of the CD3 proteins or one of the TCR chains demonstrated, that the presence of all components is required for the surface expression of the TCR/CD3 complex [40]. The first hint that the signal, which is induced upon antigen recognition, is transduced across the cell membrane by CD3 proteins was provided by the identification of signaling motifs in the intracellular domains of the CD3 proteins [41]. In contrast, the short intracellular tails of the TCR chains do not contain either the immunoreceptor tyrosine-based activation motifs (ITAM) encoded by the CD3 proteins or any other signaling domains. Although the structure of the TCR dimer was determined by x-ray crystallography and it was demonstrated how the TCR associates with CD3 proteins in the

endoplasmic reticulum (ER), there is still some uncertainty about the organization of the TCR/CD3 complexes on the cell surface.

Each TCR chain is composed of two extracellular domains that exhibit an immunoglobulin (Ig)-type fold structure, the N-terminal variable (V) domain and the C-terminal constant (C) domain [42,43,44,45]. This common folding motive consists of two anti-parallel β sheets forming a sandwich-like structure with a hydrophobic interior and an intra-molecular disulfide bond between the sheets. Heterodimerization is stabilized by the exclusion of hydrophobic residues from the solvent at the Vα-Vβ domain contact surface, by polar residues and by an inter-molecular membrane-proximal disulfide bond. Three loops that connect the β sheets extend from top of each V domain and mediate the contact to the antigen. They are encoded by the CDR 1 and 2 located in the V segments and by the CDR 3 located at the joining sites of the segments. The TCR heterodimer is stabilized by the association with the CD3 proteins, especially the Cα domain shows a distorted Ig-fold with some exposed hydrophobic residues. In addition, an extended loop of the Cβ domain with polar residues is likely involved in the formation of the TCR/CD3 complex. However, most important for the association of TCR and CD3 proteins are three basic residues in the transmembrane (Tm) domains of the TCR dimer. A single TCR dimer associates in the ER with three different CD3 dimers. First, a CD3δε dimer binds to the TCRα chain, then a CD3γε dimer binds to the TCRβ chain and eventually a CD3ζζ dimer is integrated into the TCR/CD3 complex. Since each CD3 chain encodes an acidic residue in their Tm domain, six acidic and three basic residues are present TCR/CD3 complex. In each assembly step, two polar residues of the CD3 dimers interact with a specific polar residue of the TCR chains. The sequence of the events, the involvement of the polar residues and the stoichiometry of the TCR/CD3 complex was determined by co-immunoprecipitation of *in vitro* translated TCR/CD3 components from ER-derived microsomes [46].

Several studies suggest that multiple units of the TCR/CD3 complex associate together at the surface of T cells and that the formation of multivalent TCR complexes is dynamically regulated. First, whether mono- or multivalent TCR/CD3 complexes could be isolated from T cell membranes was shown to depend on whether a detergent that destroys or preserves cholesterol-dependent protein complexes was used for solubization [47]. Second, multivalent TCR nanocluster were detected on the membranes of non-activated T cells using electron microscopy and photoactivated localization microscopy [47,48,49]. Third, TCR oligomerization was shown to be a key event in T cell activation and the different size of pre-formed TCR clusters on non-activated naive and memory T cells was suggested as an explanation for their different functional avidity [50,51,52].

1.3 Thymic selection imposes MHC restriction and self tolerance on the T cell repertoire

The ligands of TCR are peptides that are bound to major histocompatibility complex (MHC) molecules. "MHC restriction" describes the phenomenon that antigen-specific T cells cannot recognize antigen-positive cells expressing allogeneic MHC molecules. Virus-specific mouse T cells killed virus-

infected cells in *in vitro* assays only if the target cells shared MHC alleles with the T cell donor [53]. MHC restriction does not reflect a genetic determination, as T cells of bone marrow (BM) chimeras (F1 to parent) acquired a restriction to the MHC alleles of the graft recipient [54]. It was further demonstrated by transplantation of thymic tissues into thymectomized BM chimeras, that in particular the MHC alleles of the thymic grafts determined the restriction of the newly developing T cells [55]. The most significant data indicating that T cells are positively selected by thymic MHC molecules was provided by MHC knockout mice, in which T cell development is blocked in the thymus [56,57,58,59]. Likewise, the development of T cells in TCR-transgenic mice was largely dependent on the presence of the particular MHC molecule for which the transgenic TCR was restricted [60]. *In vitro* experiments using fetal thymus organ cultures from mice with deficiencies in peptide-MHC presentation demonstrated that the positive selecting ligands in the thymus consist of MHC molecules in combination with self-peptides [61,62]. Importantly, the signal that is generated by the interaction of the TCR with the peptide-MHC complexes during positive selection is much weaker than the signal that activates mature T cells in the periphery. In fetal thymus organ cultures, MHC-presented antagonist peptides were sufficient to positively select TCR-transgenic T cells [63]. In the absence of MHC molecules in the culture, positive selection of polyclonal T cells could be induced using a CD3-specific mAb under conditions that did not activate mature T cells [64]. Thus, positive selection generates a TCR repertoire with low-affinity for self-peptides presented by MHC molecules of the host. Another function of positive selection is that it segregates the MHC I-restricted CD8 T cell linage from the MHC II-restricted CD4 T cell linage.

After being positively selected, the T cell progenitors migrate from the thymic cortex to the medulla, where those TCR are deleted that recognize MHC-presented self-peptides with high affinity [65]. First evidence that highly activated T cell progenitors are deleted in the thymus was provided by mice expressing endogenously a viral superantigen. The presents of the superantigen in combination with a certain MHC molecule lead to the deletion of T cell progenitors expressing a particular Vβ TCR chain, which specifically reacted with the superantigen-MHC complex [66,67]. Antigen-specific clonal deletion was demonstrated in male TCR-transgenic mice, which expressed a TCR recognizing a male specific antigen [60]. Medullary thymic epithelial cells are the most prominent cell type involved in negative selection. They are capable to express otherwise tissue-restricted antigens through the action of the autoimmune regulator (AIRE) protein, which induces promiscuous gene expression [68,69]. Another cell type involved in the negative selection are dendritic cells, which might also be responsible for some degree of negative selection in the thymic cortex and during the transition to the medulla [70,71]. Through the process of negative selection, TCR with high affinity for self-derived peptides presented in the thymus are deleted from the repertoire.

1.4 T cells survey peptide samples of proteins produced by host and foreign cells

The peptides presented by MHC I and II molecules are protein degradation products derived from two distinct cellular pathways. MHC I molecules are loaded in the ER with peptides generated by the proteasomal degradation of cytosolic and nuclear proteins. Almost every cell expresses MHC I molecules, which allows cytotoxic CD8 T cells to survey samples of the proteome from individual cells throughout the body and to react towards those showing aberrant protein expression. In contrast, MHC II expression is mainly restricted to professional antigen presenting cells (APC) that are specialized in the uptake of foreign cells or debris by mechanisms such as phagocytosis. The engulfed material remains contained in a vesicle named phagosome, which matures and fuses with lysosomes to form phagolysosomes. MHC II molecules are loaded in this late vesicles with peptides generated by the degradation of exogenous material during the maturation process, so that CD4 T cells are assigned a major role in the adaptive immune response towards intruding pathogens and their products.

Studies on macrophages that were cultured with bacteria and used to stimulate CD4 T cells provided first hints for the requirement of antigen processing in the production of T cell epitopes. Macrophages could stimulate T cells only some time after they ingested bacteria, but the T cells were not able to recognize the macrophage immediately or the bacteria directly [72]. Furthermore, inhibition of lysosomal acidification in the macrophages reduced antigen-presentation in a dose-dependent manner [73]. Other experimental systems demonstrated presentation of MHC II-restricted antigens after incubation of APC with native or denatured antigenic protein, tryptic protein digests or synthesized peptides, further arguing for protein degradation as a critical step in antigen processing [74,75]. Short peptides were shown to directly bind to purified MHC II molecules *in vitro* [76,77]. Eventually lysosomal cysteine proteases, which are only active at low pH, were identified as the predominant enzymes involved in the production of peptides from proteins in phagolysosomes [78,79]. Incubation of target cells with exactly defined short peptides, whose sequence was derived from a viral protein, was also sufficient to elicit cell lysis by virus-specific MHC I-restricted CD8 T cells [80]. Before the cellular pathway producing MHC I-presented peptides was described, the first crystal structure of a human MHC I molecule (HLA-A2) indicated how such peptides were presented at the cell surface [81,82].

MHC I molecules consist of two polypeptide chains. The polymorphic α chain anchors the dimer in the membrane, folds into three distinct extracellular domains (α1-3) and is non-covalently associated with the smaller invariant β2-microglobulin polypeptide chain (β2M). A characteristic structure, the peptide binding cleft, is formed by the membrane distal α1 and α2 domains on top of the molecule: Two α helices are laying parallel on a plane β sheet and form the walls of a long groove, in which an extended peptide of about nine amino acids (aa) is deeply buried [81,82]. A similar peptide binding cleft was also found later on top of a human MHC II molecule (HLA-DR1), with the differences that the groove was open at its ends and composed of one domain from each of the two MHC II chains (α1 and β1) [83]. Whereas conserved residues at the end of the peptide binding cleft of the MHC I molecule

make contacts to both peptide termini, is peptide binding in case of the MHC II molecule mainly achieved through interactions of conserved residues along the cleft with the peptide backbone. Additional contacts between some side chains of the peptide and polymorphic residues of the MHC molecules confer additional allele-specific restrictions to the peptides.

Analysis of MHC-bound peptides, first isolated from cell lysates but then directly eluted from the cell surface, provided direct evidence that the natural produced determinants of known viral and minor histocompatibility antigens (mHAg) detected by T cells were indeed short peptides [84,85,86,87,88]. Moreover, the increasing number of characterized antigenic peptides presented by MHC alleles and the sequencing of eluted peptide pools, allowed the description of the peptide-binding specificity of MHC molecules [89,90,91,92]. Peptides of eight to nine and twelve to twenty five amino acids are preferentially bound by MHC I and II molecules, respectively. The affinity of a peptide for MHC I is usually dominated by two residues (anchor residues). The preference for a hydrophobic residue at the C-terminus is common, whereas the second anchor residue is more allele-specific. Peptide binding to MHC II molecules is more complex, because the position of the peptide and the length is not fixed, but common sequence patterns of two to three defined residues in a characteristic distance to each other could be identified.

The sequences of the MHC I-presented peptides identified them as derived from cellular proteins. During the constitutive protein turnover, the labeling of proteins with ubiquitin directs them to a large multicatalytic complex called proteasome, which is responsible for cellular protein disposal. Induction of decreased protein ubiquitination in a mutant cell line or pharmacological inhibition of the proteasome in lymphocytes was shown to coincidence with decreased antigen presentation by MHC I [93,94]. Though most peptides isolated directly from the cytoplasm or generated *in vitro* by purified proteasome complexes indeed possessed hydrophobic C-termini, the majority was longer than the peptides eluted from MHC I molecules [95,96]. ER aminopeptidase associated with antigen processing (ERAAP) was found to further trim the N-termini of the precursor peptides in the ER lumen until they acquire the optimal length. More long peptides were isolated from the ER and fewer peptide-MHC I complexes were expressed at the cell surface after knockdown of ERAAP by RNA interference (RNAi), whereas increased ERAAP expression resulted in the opposite effects [97,98,99]. Responsible for the shuttling of the peptides from the cytosol into the ER lumen are the transporters associated with antigen processing 1 and 2 (TAP1/2) proteins. Permeabilization of cells with a pore-forming bacterial toxin leaves the ER membranes intact. In such preparations, the transport of added model peptides into the ER depended on TAP1/2 and ATP [100,101].

1.5 Adoptive T cell therapy

1.5.1 Epitopes derived from tumor antigens are recognized by T cells

In the beginning of the last century it was suspected that the immune system constantly suppresses cancer development and that tumors can arise only if this suppression exceptionally fails [102]. This

hypothesis was inspired by experiments with transplantable tumor lines performed in mice and rats. In general, spontaneous tumors were more often rejected than accepted when transplanted from one animal to another. In addition, tumor graft rejection was augmented after immunization with tumor cells. It was further suspected, that lymphocytes, which frequently infiltrated the tumor grafts, mediated the rejection. However, almost all mice strains at this time were outbred, with the exception of the Japanese waltzing mouse. Although it was noticed, that tumor graft susceptibility varied between the mouse strains, Mendel's law could not easily explain the results of cross-breedings. This changed when the Japanese waltzing mouse was crossed to another mouse strain and the offspring were backcrossed to the parental generation [103]. In agreement with Mendel's law, tumor graft susceptibility seemed to depend on a small number of independent traits. The investigation of these genetic traits led to the discovery of the MHC in mice, which is named H-2 after its first characterized MHC-encoded gene [104]. Although strong allogeneic immune responses provoked by the transplantation of tumors across MHC barriers could be avoided, other individual genetic differences between donor and recipient that encoded mHAg continued to be a problem in transplantation experiments until pure inbreed mouse strains were established.

The central question whether tumors express antigens that would allow the adaptive immune system to recognize them, which is if they are immunogenic, was first answered using chemically induced tumors. Methylcholanthrene (MCA)-induced tumors that otherwise could be transplanted were indeed rejected by mice that were immunized before the tumor challenge with cells of same tumor line [105]. A comparison of several MCA-induced tumors with spontaneous mammary carcinomas in the same setting showed that the latter were not rejected, arguing against genetic variations within the mouse strain as an explanation, and for a characteristic immunogenicity of chemically induced tumors [106]. These findings were confirmed by a subsequent more detailed study [107]. Immunization protected mice against a tumor challenge in case of twelve out of fourteen MCA-induced sarcomas, but was unsuccessful in case of seven spontaneous sarcomas. In addition, the tumors also grew in mice that were immunized with normal tissue indicating the genetic homogeneity of the mouse strain. The protective immunity was in general specific for the immunizing tumor cell line, although few exceptions were observed. Eventually, it was formally proven that T cells recognized unique tumor-specific antigens in this model [108]. Immunization of the autochthonous hosts of MCA-induced sarcomas after the removal of the primary tumor induced a partially protective immunity and T cells isolated from the immunized mice recognized the respective tumor cells *in vitro*. No cross-reactivity between the independently derived sarcomas was observed.

1.5.1.1 Tumor antigens are grouped into categories based on their expression in normal tissue

The immunogenicity of chemically and viral-induced tumors and the description of T cell-mediated graft rejections stimulated the reformulation of the immune surveillance theory [109,110]. It was proposed that T cells would constantly prevent tumor development through the elimination of pre-

malignant transformed cells expressing tumor antigens. Others have later extended this theory and proposed that spontaneous tumors are in general of low immunogenicity [111]. It was stated that a constant immunological pressure would select very early for nascent tumor cells that do not present T cell epitopes. The proposed inability of the adaptive immune system to recognize spontaneous tumors is, however, questioned by the large number of tumor antigens that were described to be expressed for example in human melanomas. In general, the proteome of cancer cells differs from normal cells because of mutations in the genome and deregulated expression of non-mutated genes. Tumor antigens are grouped into categories based on their expression in normal tissue. MAGE-A1, the first described human melanoma antigen encoding a T cell epitope, was discovered by screening a tumor-derived DNA library with autologous tumor-reactive T cell clones [112,113]. MAGE-A1 is a typical tumor-associated antigen (TAA) generated by a non-mutated cellular gene. It belongs to the group of cancer/testis (CT) antigens, whose expression in normal tissue is mainly restricted to the germ cells of the testis. Tyrosinase and Melan-A/Mart-1 are further examples of TAA expressed in melanoma and were discovered by a similar approach using autologous tumor-reactive T cells [114,115,116]. Both belong to the group of differentiation antigens. Antigens of this group are characteristically expressed at a certain developmental stage in the cell linage from which the tumor originates. In contrast, tumor-specific antigens (TSA) are generated by somatic mutations and are therefore not expressed in normal tissue. A T cell epitope derived from a mutation in the cyclin-dependent kinase 4 (CDK4) gene of a melanoma was identified too using autologous tumor-reactive T cells [117].

The above examples are representative for a constantly growing list of immunogenic peptides from tumor antigens of which over 400 are listed in a current database [118]. It is therefore difficult to imagine how such immunogenic tumors can develop under the proposed constant pressure of the immune system. On the contrary, it was demonstrated in a mouse model that immunogenicity alone is not sufficient to elicit a destructive immune reaction in case of spontaneous tumors, which develop slowly in the host in the absence of acute inflammation from single cells [119]. Tumor growth induced by the stochastic activation of a viral oncogene resulted in systemic antigen-specific tolerance instead of tumor cell elimination. Immunotherapy of cancer therefore has to use means to break this tolerance, for example by the transfer of *ex vivo* activated T cells. The immunogenicity of tumors is a prerequisite for such a therapy.

1.5.2 Transfer of unmodified T cells

1.5.2.1 Donor-derived T cells can mediate the remission of relapsed myeloid leukemia in bone marrow recipients

The treatment of relapsed myeloid leukemia after BM transplantation with donor-derived T cells is one example from the clinic that shows both the benefit and risk of adoptive T cell therapy. In an MHC-matched setting, the donor-derived T cells recognize mHAg encoded by polymorphic genes expressed

by tumor cells and healthy tissue [120,121]. It was first demonstrated in mice, that transplantation of allogeneic but not syngeneic BM after irradiation mediates the elimination of residual leukemic cells [122,123]. However, in leukemia patients treated with allogeneic BM, the curative response, termed graft-versus-leukemia (GVL) effect, was associated with an autoimmune pathology, termed graft-versus-host disease (GVHD) that represents a life-threatening complication [124,125]. T cells co-transferred with the BM were identified to mediate both, the GVL effect and GVHD. Transplantation of T cell-depleted BM decreased the incidence of GVHD, but also increased the risk of leukemia relapse [126,127,128,129]. A breakthrough in the treatment of relapsed myeloid leukemia was the application of donor lymphocyte infusions (DLI) after allogeneic BM transplantation [130,131,132,133,134,135]. DLI induced complete remissions in the great majority of the patients and significantly decreased the risk of further relapse. However, GVHD remained to be a major complication and developed in 59% and 38% of the patients treated with DLI in one early and one recent study, respectively [136,137]. The difference in the incidence of GVHD is due to the application of incremental doses of DLI as compared to bulk regimes. One way to completely avoid GVHD while preserving the GVL effect would be the transfer of defined T cell populations specific for mHAg exclusively expressed on the hematopoietic cells of the recipient [138,139].

1.5.2.2 Virus-specific T cells confer immunological protection to immunosuppressed patients

De novo viral infections and reactivation of latent virus are common complications in immunosuppressed patients. Especially Epstein-Barr virus (EBV) and cytomegalovirus (CMV) related complications are difficult to avoid because of the high prevalence of latent infections in the population that are usually controlled in immunocompetent individuals. A mouse model that mimicked the clinical situation after BM transplantation demonstrated the critical role of CD8 T cells in fighting viral infections [140]. In a therapeutic setting, the transfer of small numbers of lymph node cells from immunized mice reduced viral replication and tissue damage, although the recipients were rendered immunosuppressed by irradiation before being infected with murine CMV. CMV-specific CD8 T cells were also detected in humans with latent CMV infections and it was suspected that were responsible to control the virus [141]. Furthermore, the recurrence of CMV-specific CD8 T cells in the blood of immunosuppressed patients correlated with protection against reactivation of CMV [142]. Based on these data, a first-of-its-kind study was performed in humans [143]. CMV-specific T cell clones of seropositive BM donors were expanded *in vitro* and infused into three patients after BM transplantation. A cytotoxic response towards CMV-infected autologous fibroblasts was detectable in blood samples from all patients up to four weeks after the infusion and none of the patients developed CMV viremia or pneumonia. In addition, no treatment-related toxicities were observed. This important study provided first clinical evidence, that the transfer of large numbers of allogeneic antigen-specific T cells did not cause GVHD, but conferred selective protective immunity to immunosuppressed patients. Consequently, donor-derived EBV-specific T cells were used with similar success to treat EBV

infections or EBV induced post-proliferative disease in BM recipients and third party-derived EBV-specific T cells were used to treat patients after solid organ transplantation [144,145,146].

1.5.2.3 Ex vivo expanded tumor-infiltrating T cells can mediate tumor regression in preconditioned patients

Late stage (IV) melanoma patients with disseminated metastasis have a poor prognosis with a low one-year survival rate of about 50% [147]. Such patients have already undergone conventional treatments or these options are not longer indicated because of the advanced status of disease. At present, however, the most effective treatments for these patients are provided by experimental studies of cancer immunotherapy, which report reproducible objective responses (>50% reduction in tumor volume) in a substantial fraction of patients and durable and complete remissions in some patients. Key for the success of cancer immunotherapy is the induction of an effective and long-lasting T cell response against the tumor and important progress has been made to achieve this goal. First clinical responses were induced by repeated cycles of high-dose interleukin-2 (IL-2), which nonspecifically activates T cell immunity. Adoptive T cell therapy (ATT) with *ex vivo* expanded autologous tumor-infiltrating lymphocytes (TIL) in combination with IL-2 was developed to further improve the treatment and recent data from small pilot studies indicate that this is possible if a conditioning regime is applied to the patient prior to the cell transfer (Fig. 1).

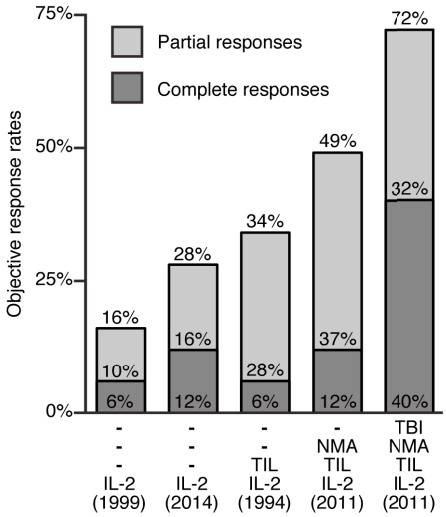

Figure 1: *Response rates of advanced melanoma patients treated with immunotherapy involving IL-2.*
Plot shows the objective response rates reported in clinical studies for patients with advanced melanoma that underwent immunotherapeutic treatments involving IL-2. The characteristic components of the treatments are indicated below the columns: Interleukin-2 (IL-2); Tumor-infiltrating lymphocytes (TIL); nonmyeloablative chemotherapy (NMA); 12 Gy total body irradiation (TBI). The years in which the reports were published are shown in parenthesis at the bottom of the picture. The number of patients for whom the results were reported from the left to the right: 270; 314; 86; 43; 25. All data from references 162, 164, 169 and 171. Figure modified from reference 159.

First discovered as a growth factor secreted by stimulated lymphocytes permitting on its own the continuous culture of T cells *ex vivo* [148], IL-2 was shown to enhanced T cell-mediated immunity in cancer mouse models when given systemically [149,150,151]. After the cloning of the IL-2 gene [152], recombinant IL-2 was produced in *E. coli* and eventually became available for clinical studies [153,154]. Low doses of IL-2 administered in the first trials were not sufficient to induce an antitumor effect, but induced a particular capillary leak syndrome as a main side effect next to minor

complications like fever and chills [155,156,157]. In contrast, the application of high escalating doses of recombinant IL-2 in short intervals (8 h) induced remissions of advanced metastatic cancer in a consecutive study [158]. Four of seven melanoma patients and three of three patients with renal cell carcinoma (RCC) exhibited objective remissions, providing first clinical evidence for the potency of IL-2 therapy. One melanoma patient of this study still alive and in complete remission since (>29y) [159]. Large clinical studies in the following years delivered proof that these responses were indeed induced by IL-2 and not by another treatment that was applied in parallel [160,161]. 16% of 270 patients with disseminated metastatic melanoma that were treated in eight clinical trials with high-dose IL-2 showed objective remissions, including 6% complete remissions (CR) and 10% partial remissions (PR) (Fig. 1) [162]. Similar results were reported for 255 patients with metastatic RCC, 14% showed objective remissions (5% CR, 9% PR) [163]. Since the establishment of the IL-2 therapy, the effectiveness of the treatment improved with the progress in clinical experience. Recently, objective response rates of 28% and 24% were reported for 314 melanoma patients (12% CR, 16% OR) and 186 RCC patients (7% CR, 17% PR), respectively (Fig. 1) [164].

These reproducible responses indicate that T cells specific for tumor-derived antigens are present in melanoma and RCC patients. However, the harsh conditions required to push those cells temporarily in an active state, the short duration of most responses and the fact that they occur only in a minor fraction of patients also argue against a natural tumor-specific T cell immunity. On the contrary, the potentially cancer-reactive T cells of the patients are inactive prior to immunotherapy, possibly due to the induction of tolerance by chronic inflammation, negative systemic effects on the immune system caused by tumor growth and unfavorable conditions within the tumor microenvironment. The rational of ATT is to overcome tolerance, immune suppression and homeostatic regulation by removing the tumor-reactive T cells from the host environment. This provides the opportunity to activate, expand and select the T cells *ex vivo*, before they are re-infused into the patient in large numbers and in conjunction with IL-2. A source of such tumor-reactive T cells are autologous tumor-infiltrating lymphocytes (TIL), which can be selectively expanded from resected tumor samples using IL-2 [165,166]. After being expanded *ex vivo*, TIL were capable to kill autologous tumors *in vitro* and to mediated tumor regression in mice [167]. In the first successful clinical trial using TIL plus IL-2, 20 patients with metastatic melanoma were treated and 11 of them exhibited objective cancer regression (55%) [168]. Treatment of 86 melanoma patients with similar protocols, resulted in an objective response rate of 34%, including 6% CR and 28% PR (Fig. 1) [169]. The *in vivo* functionality of the transferred cells was in part correlated with *in vitro* parameters of the TIL cultures such as short culture periods and fast doubling rates, as well as high cytolytic activity against autologous tumor. The induced partial responses, however, were only short-term (median 4 months), whereas complete responses lasted for 20 month or longer. Several lines of evidence indicated that poor engraftment and persistence of transferred cells were responsible for the limited therapeutic success in the initial studies, whose results are in the same range with those of present IL-2 therapy without ATT (Fig. 1).

The total size of the body's T cell pool is tightly regulated, mainly by a competition of the T cells for limited survival factors like IL-7 and IL-15. Adoptively transferred lymphocytes readily start to proliferate in lymphopenic mice even in the absence of antigen. Likewise, the transfer of TIL into patients, which were rendered lymphopenic by a nonmyeloablative (NMA) chemotherapy, resulted in an unprecedented expansion of the TIL and prolonged persistence at high levels [170]. Lymphodepleting regimes of different intensities were investigated in several clinical ATT trials and the report summarizing the results announced the highest response rates ever achieved in patients with advanced melanoma [171]. 43 patients were pre-treated with NMA chemotherapy only and 25 patients each were treated additionally either with 2 Gy or 12 Gy total body irradiation (TBI). For the three treatment modalities, objective response rates of 49% (12% CR, 37% CR), 52% (20% CR, 32% PR) and 72% (40% CR, 32% PR) were reported, respectively. TBI affects the gut integrity leading to the activation of the innate system by commensal bacteria and thus to signals of acute inflammation for T cells, which may explain the higher response rates. In addition, CD4 T cells and myeloid-derived suppressor cells, which both could have a negative influence on T cell-mediated immune reactions, may be more thoroughly reduced.

1.5.3 Transfer of TCR gene-modified T cells

1.5.3.1 TCR gene-modified T cells can mediate tumor regression and autoimmunity in patients

Transfection of TCR genes into a hybridoma T cell line provided definite proof that the specificity of a T cell is solely determined by the TCR [172]. At the same time, these experiments shed light on the possibility to redirect T cells by TCR gene transfer. In two seminal studies, a MART-1-specific and a virus-specific TCR were transferred by retroviral transduction into polyclonal human T cells to generate a cell population with a defined specificity for immunotherapy [173,174]. T cell clones expressing the transferred TCR were isolated and compared to the original T cell clone from which the TCR genes were obtained. Functional *in vitro* assays demonstrated, that some of the transduced clones were indeed comparable to the original clone. The application of TCR gene-modified T cells in the clinic offers several benefits (Fig. 2).

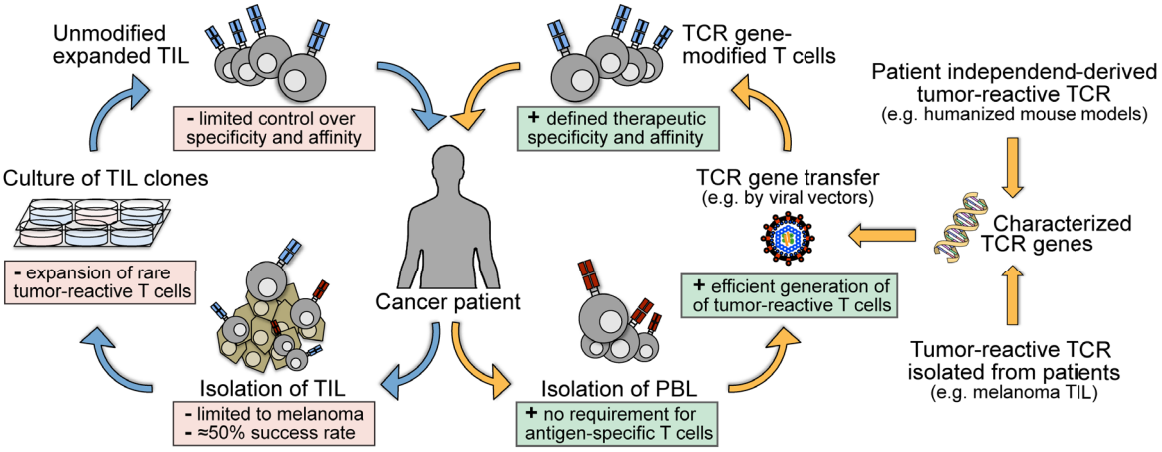

Figure 2: *TCR gene transfer broadens the applicability of adoptive T cell therapy.*
Adoptive T cell therapy using unmodified T cells for the treatment of cancer relies on the expansion rare tumor-reactive T cells from tumor-infiltrating lymphocytes (TIL), which is not possible for most cancer patients. In contrast, TCR gene transfer into nonspecific peripheral blood lymphocytes (PBL) generates large populations of tumor-reactive T cells independent of the patient's T cell repertoire. The therapeutic TCR can be obtained from other patients or patient-independent sources and selected for their specificity and affinity prior to their application.

Cancer immunotherapy using autologous TIL absolutely depends on the presence of tumor-reactive T cells in the patient and requires the isolation and expansion of these cells without compromising their *in vivo* functionality. In contrast, the generation of large pools of antigen-specific T cells by TCR gene transfer requires only limited *ex vivo* culture of the T cells and the transferred TCR can be selected for the right specificity and an optimal affinity in advance. Furthermore, not only other patients can be considered as possible sources for therapeutic TCR but also patient-independent sources such as *in vitro*-priming approaches or humanized mouse models [175,176,177]. In addition, the affinity of the TCR can be enhanced by directed *in vitro* evolution [178,179].

In the same manner as demonstrated for human T cells, mouse T cells could be redirected by viral transduction with TCR encoding-vectors [180]. Using a virus-specific TCR and a tumor cell line expressing the cognate antigen, it was shown that TCR-transduced T cells inhibited tumor growth after adoptive transfer [181]. In another model, which more closely resembled the situation of clinical TCR gene therapy trials, the transfer of TCR-transduced T cells recognizing a tissue-specific self-antigen was shown to overcome tolerance mechanisms that usually prevent autoimmune reactions [182].

Three TCR specific for shared TAA expressed in melanoma were applied in the first two clinical trials of TCR gene therapy: DMF4 and DMF5, which are two MART-1-specific TCR isolated from TIL, and one gp100-specific TCR isolated from an HLA-A2 transgenic mouse [183,184]. All patients received a NMA lymphodepleting regime prior to the transfer of TCR-transduced T cells and were treated afterwards with high dose IL-2. Partial response rates of 13% (4/31 patients) and 30% (6/20 patients) were reported for patients with advanced melanoma treated with DMF4 TCR- or DMF5 TCR-transduced T cells, respectively. The difference in the responses can be attributed to two factors: First,

an improved retroviral vector was used for the transduction of the DMF5 TCR and, second, the DMF5 TCR was of higher affinity. One complete and two partial responses were reported for 16 melanoma patients (6% CR, 12% PR) treated with transduced T cells recognizing gp100. The targeting of the melanoma differentiation antigens was connected with the destruction of epidermal melanocytes in case of the DMF5- and gp100-specific TCR only, indicating that the DMF4 TCR-transduced T cells were not able to recognize antigen on normal cells. 42% of the patients treated with the two high affinity TCR showed additional autoimmune symptoms in the eye and ear, which were clinically manageable and eventually resolved. In another clinical trial, three patients with metastatic colorectal cancer were treated with transduced T cells expressing a mouse TCR specific for human carcinoembryonic antigen (CEA), which was isolated from an HLA-A2 transgenic mouse and mutated *in vitro* to enhance the affinity [185]. The patients were lymphodepleted before the cell transfer and were treated afterwards with IL-2. One patient showed a partial response (33% PR, 1/3 patients). However, all patients developed severe inflammatory colitis and diarrhea leading to the halt of the trial. CEA is a tissue-restricted antigen that is overexpressed in colorectal cancers and expressed in normal intestinal epithelia. In case of the clinical studies above, mouse models correctly predicted the autoimmunity induced by transferred T cells recognizing either normal melanocytes or epithelial cells of the gastrointestinal tract [186,187].

On-target toxicity as described in the examples above is caused by the expression of the targeted antigen in normal tissue. Off-target toxicity caused by the cross-reactivity of the introduced TCR with other epitopes as the targeted one was observed in a clinical study, in which a TCR supposedly specific for the CT antigen MAGE-A3 was applied [188]. This TCR was isolated from a vaccinated melanoma patient and afterwards mutated i*n vitro* to enhance the affinity [189,190]. The first two patients, who received a mild lymphodepleting regime before the cell transfer, died within days after the infusion of TCR-transduced T cells due to severe cardiac toxicity [188]. It turned out that the introduced mutations changed the specificity of the TCR, which afterwards recognized a peptide encoded by the titin gene expressed in heart muscle cells in addition to the MAGE-A3-dervied peptide [190].

The definite reasons for the observed neurological toxicity, which developed in three out of nine patients and led to the death of two patients in a further clinical study, could not be resolved with sufficient certainty [191]. The TCR of this study was isolated from an immunized HLA-A2 transgenic mouse and recognized a peptide encoded by both CT antigens MAGE-A3 and -A9, but also a peptide with a single amino acid difference encoded by MAGE-A12 and to a lesser extend two peptides encoded by MAGE-A2 and -A6, which showed a difference to the MAGE-A3/9 peptide of two and one amino acid, respectively [192]. Furthermore, a single amino acid substitution was introduced into the TCRα chain to enhance the affinity. Highly sensitive methods, like direct mRNA quantification by the NanoString nCounter methodology [193], could detect MAGE-A9 and -A12 transcripts in normal human brain tissues at very low levels [191]. If these few transcripts resulted in on-target toxicity in the brain, than the question remains, why was it observed in three out of nine patients only? The

individually generated TCR gene-modified T cells could have introduced an unknown variable. For example, the authors of the study suggested differences in the total number and in the subtype composition of the TCR-transduced T cells as possible explanations [191]. However, this argumentation is difficult to follow as such correlations were not observed in the other trials.

The CT antigen NY-ESO-1 was targeted in the most successful clinical study of TCR gene therapy so far, in which no autoimmunity was reported [194]. Four of six patients with synovial cell sarcomas partially responded to the treatment (67% PR), and of eleven patients with advanced melanoma, three showed a partial and two a complete response (27% PR, 18% CR). The results of the melanoma patients in this trial and those of the TIL trials, in which the patients were treated also with a lymphodepleting regime before the cell transfer and with high-dose IL-2 afterwards, are in the same range. However, TIL can only be generated from 50% of the melanoma patients and for patients with synovial cell sarcomas this is not possible at all. Furthermore, this study demonstrated, that affinity-enhanced TCR not necessarily become unspecific. Two amino acid substitutions were introduced into the α chain of the NY-ESO-1-specific TCR, which was originally isolated from a melanoma patient [195,196].

1.5.3.2 TCR gene-modified T cells express different TCR dimers on their surface

TCR gene-modified T cells express at least two pairs of TCRαβ genes, which allow the assembly of four different TCRαβ dimers: the endogenous TCR, the transferred TCR, and two mixed TCR dimers, composed of endogenous and transferred TCR chains (Fig. 3). If the transduced T cell expresses two endogenous TCRα chains, than one additional combination of transferred and endogenous chains is possible. It has been suspected, that mixed TCR dimers are likely nonfunctional, because they are not positively selected in the thymus [174]. Technical factors might have contributed to establish this view. No method comparable to MHC multimer staining exists to quantify the amount of mixed TCR dimers on the cell surface and the specificity of mixed TCR dimers is extremely difficult to define after the transfer of a TCR into a polyclonal T cell repertoire. However, others have argued, that the formation of mixed TCR dimers poses a risk for TCR gene therapy [197]. As mixed TCR dimers are also not subject to negative selection in the thymus, they may by chance recognize self-antigens and induce autoimmunity. For almost a decade, such mixed TCR dimer-induced autoimmunity was not observed in mouse models of TCR gene therapy.

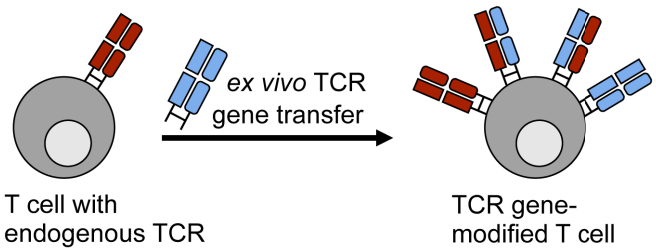

Figure 3: *The expression of two pairs of TCR genes in one T cell allows the formation of multiple TCR dimers.*
At least four different TCR dimers can be expressed on the surface of TCR gene-modified T cells: the endogenous TCR, the transferred TCR and two different mixed TCR dimers composed of endogenous and transferred TCR chains.

First evidence that mixed TCR dimers on TCR-transduced mouse and human T cells can recognize allo- and self-antigens, was provided by two recent studies [198,199]. Lethal mixed TCR dimer-dependent autoimmunity was observed in a mouse model of TCR gene therapy created to mimic the clinical situation closely [198]. In contrast to other models, the TCR-transduced T cells were transferred immediately after the transduction into irradiated mice, which were treated after a phase of lymphopenic expansion with high-dose IL-2. The autoimmunity, which was observed for five different TCR tested, strictly depended on the transfer of TCR gene-modified T cells and was not observed after the transfer of TCR transgenic T cells. Therefore, the mixed TCR dimer-depended autoimmunity was named TCR gene transfer-induced graft-versus-host disease (TI-GVHD). The incidence of TI-GVHD was characteristic for the individual TCR showing that some TCR are more prone to mixed TCR dimer formation than others. In the second study, seven TCR were transferred into five human virus-specific T cell lines. Each of the transduced T cell lines acquired specificities after the transfer of at least two of the TCR, which could neither be attributed to the endogenous nor to the transferred TCR [199]. Unexpectedly, the TCR-transduced T cell lines recognized allo- and self-antigens. The transfer of a single TCR chain was sufficient to endow the human T cell lines with alloreactivity and mouse T cells expressing a single transduced TCR chain induced TI-GVHD, which formally proved that mixed TCR dimer formation is the reason for both observations. The two studies showed that three factors influenced mixed TCR dimer formation: First, undefined characteristics of the transferred TCR, second the ability of the vector to ensure strong and stoichiometric expression of both transferred TCR chains and third, the usage of genetically engineered TCR genes.

1.5.3.3 TCR differ in their propensity for surface expression in TCR gene-modified T cells

In TCR gene-modified T cells, the TCR surface levels are the outcome of a competition between the endogenous and the transferred chains for heterodimerization and CD3 proteins. Overexpression of all four CD3 proteins (γ, δ, ε, ζ) was shown to be necessary to increase the total amount of surface TCR, which otherwise remains unchanged after the introduction of a second TCR [200]. By focusing the view on a single T cell expressing two TCR, three possible outcomes were defined in experiments with clonal T cell lines and T cell hybridoma depending on the competing TCR: either one of both TCR is predominantly expressed at the surface or both TCR are coexpressed [201]. Therefore, in the non-physiological situation of TCR competition, yet undefined properties of the individual TCR come into play and confer some TCR an advantage over others. A limitation of this view was pointed out through experiments in another study [202]. Since the transduction of single TCR chains was sufficient to reduce the surface levels of correctly paired endogenous TCR dimers, it was concluded that mixed TCR dimers also take part in the competition for surface expression. The authors further proposed, that those TCR dimers with the best-pairing properties might dominate the other possible combinations. Compared to these two-TCR/one-cell models, transduction of a TCR into polyclonal T cells is more complex. Both transferred TCR chains are confronted with a vast number of different TCR chains.

Whether well surface-expressed TCR tend to avoid the formation of mixed TCR dimers has not been shown. Considering that four TCR dimers compete in one cell for surface expression, it is very difficult to conclude from an increased level of one TCR dimer on the individual levels of the other three. Nevertheless, given the risks associated with mixed TCR dimer formation, it would be important to know, how to identify TCR that tend to pair with endogenous TCR chains when expressed in polyclonal T cells.

1.5.3.4 The quantity of TCR protein in TCR gene-modified T cells affects the composition of TCR on the cell surface

Transduction of T cells with more efficient TCR expression vectors results in an increase of both, the frequency of T cells expressing the transferred TCR chains and the surface expression levels of the transferred TCR chains, which demonstrates that the quantity of TCR protein has a strong influence on the outcome of TCR competition. In a direct comparison of retroviral vectors employing either the long terminal repeat (LTR) of Moloney murine leukemia virus (Mo-MLV) or myeloproliferative sarcoma virus (MPSV) to control GFP expression, the latter was shown to yield about ten-fold and 75-fold more GFP in transduced mouse and human T cells, respectively [203]. Two further factors contributed to the high expression levels achieved with the vector employing the MPSV LTR: First, the 5`untranslated region of the vector was optimized by the removal of all aberrant start codons and the reconstruction of the 5' intron by a minimal splice acceptor site and, second, the posttranscriptional regulatory element (PRE) of the woodchuck hepatitis virus was introduced into the 3' UTR. This optimized vector was designated MP71 [204]. Both vectors were used for TCR gene transfer into human T cells in a consecutive study, but only the MP71 vector-transduced T cells expressed the transferred TCR on their surface although the T cells were transduced with the same efficiency by both vectors and showed no difference in the number of integrated proviral copies [205]. Another mean to raise the yield of TCR protein is to optimize the sequence of the TCR cassette using synonymous codons. During such "codon optimization," rare codons and cryptic splice sites are removed and the GC content of the sequence is increased [206]. In contrast to the above mentioned vector features, the way in which the expression of both TCR chains is directed has a direct influence on the formation of mixed TCR dimers. Stoichiometric expression of both TCR chains is a prerequisite for correct pairing and this can be achieved by using a viral 2A peptide linker [206,207]. The coding sequence of the 2A element is placed between the two TCR chains, so that a continuous reading frame from the start codon of the first TCR chain to the stop codon of the last TCR chain is generated. The nascent polypeptide chain of the 2A element forms a secondary structure inside the ribosome that cause the ribosome to skip to the next start codon and to release the currently translated protein.

1.5.3.5 Improvement of TCR expression by protein engineering is not sufficient to prevent mixed TCR dimer formation

To give the transferred TCR an advantage in the competition with the endogenous TCR or to gain a direct influence on the pairing behavior, different strategies to engineer the TCR C regions were developed. It was noticed that mouse TCR are functional in human T cells and surprisingly well expressed on the cell surface [201,208]. The exchange of the Cα and Cβ regions of mouse TCR for the respective human TCR C regions decreased their surface expression in human T cells, whereas human TCR with mouse TCR C regions were better expressed than unmodified TCR [209,210]. In a particular experiment, human T cells were transfected by electroporation with equal amounts of mRNA encoding either the unmodified sequences of a human MART-1-specific TCR or the corresponding human-mouse hybrid TCR [209]. Engineering of the human TCR by "murinization" had two effects: First, the population of transfected T cells contained about double the amount of MHC multimer-positive cells (72.5% vs. 30.1%) and, second, the MFI of the MHC multimer staining was higher (88.5 AU vs. 44.8 AU). To avoid the usage of the complete mouse TCR C regions, which are potentially immunogenic in humans, nine critical amino acids in the mouse sequence were identified and were used to construct "minimal murinized" human TCR C regions that improved TCR surface expression almost as effectively as the mouse TCR C regions [211,212].

Another possibility of engineering the TCR C regions, which is applicable for mouse and human TCR, is to facilitate the formation of a second disulfide bond between both TCR chains by the mutation of two defined residues into cysteines [213,214]. The effect of the second disulfide bond on the surface expression of a human MART-1-specific TCR (termed F4) in T cells transfected with mRNA was comparable to the effect of murinization, the percentage of MHC multimer-positive cells was markedly increased (70% vs. 35%) and more MHC multimer was bound per cell as compared to T cells transfected with equal amounts of mRNA encoding the unmodified TCR (151 AU vs. 85 AU) [213].

Both strategies, the usage of mouse TCR C regions and the introduction of a second disulfide bond, were shown to induce preferential pairing of the transferred TCR chains. The surface levels of the correctly paired TCR dimers were less affected in transfected T cells by the expression of a second transfected competitor TCR as compared to the corresponding unmodified TCR [209,213]. However, the extent of these effects is depending on the particular TCR.

The usage of codon-optimized and 2A-linked TCR genes harboring a second disulfide bond completely prevented TI-GVHD in case of one TCR, but only reduced the incidence of TI-GVHD from 80% to 14.3% in case of another TCR [198]. Furthermore, TI-GVHD was observed in 59% of the mice in case of the latter TCR, when the optimized TCR genes with the second disulfide bond were used without the 2A element. Therefore, TCR engineering can induce preferential pairing, but it does not exclude the pairing of transferred and endogenous TCR chains. For example, if single TCR chains are transduced into T cells, than mixed TCR dimers are surface expressed despite of modified TCR C regions [215].

In contrast to the use of mouse TCR C regions and the introduction of a second disulfide bond, an attempt to rationally design the Cα-Cβ interface was less successful and possibly affected the overall stability of the TCR. The reciprocal exchange of a sterically and electrostatically complementary pair of interacting residues between the Cα and Cβ region disfavored the paring of the transferred and endogenous TCR chains, but the surface expression of the engineered TCR was considerably lower compared to the unmodified TCR [216]. Although the T cells were transduced with vectors encoding a selection marker and either the native or modified version of a gp100-specific TCR and were enriched by drug selection, the percentage of MHC multimer-positive cells was decreased from 81.3% to 56.4% by the introduced mutations.

In another study, the removal of *N*-glycosilation sites (N-X-S/T) in the TCR sequences by asparagine to glutamine mutations was demonstrated to increase the antigen-specific reactivity of TCR gene-modified T cells [217]. Transduced T cells that were sorted by flow cytometry for equal TCR surface expression showed improved cytokine production and lysis of target cells when expressing a TCR lacking a particular *N*-glycosilation site in the Cα region compared to cells expressing the unmodified TCR. However, this modification is unlikely to reduce mixed TCR dimer formation and it remains unclear if the TCR surface expression was influenced otherwise because only data of sorted T cells were presented. The authors speculated that the enhanced reactivity of the TCR gene-modified T cells was due to either facilitated oligomerization of the engineered TCR on the cell surface or a decreased energetic barrier for conformational changes in the TCR/CD3 complex.

Others have suggested another modification of the TCRα chain to improve TCR surface expression in TCR gene-modified T cells. Three mutations were introduced into the TCR Cα transmembrane region to change selected residues into hydrophobic residues [218]. Transduced human T cells expressing the modified α chain together with the unmodified β chain of the MART-1-specifc F4 TCR showed a higher percentage of MHC multimer-positive T cells compared to T cells transduced with a vector encoding the native sequences of both TCR chains (58.2% vs. 33.1%). It is reasonable to assume that not only the level of correctly paired transferred TCR chains is improved by this approach because the overexpression of just one of the transferred TCR chains favors the formation of mixed TCR dimers, which cannot be observed by staining the correctly paired TCR with MHC multimers.

1.5.3.6 Strategies that directly target the expression of the endogenous TCR

An alternative strategy to TCR engineering is to directly target the expression of the endogenous TCR. When this study was initiated, no strategies were reported how to decrease the amount of endogenous TCR protein in TCR gene-modified T cells. During this study, however, two different approaches were established. One the one hand, artificial zinc-finger nucleases (ZFN) were used to generate T cells with disrupted TCR genes, called TCRαβ-edited T cells [219]. Although this technique allows the generation of TCR gene-modified T cells completely devoid of functional endogenous TCR protein, the basic protocol requires approximately 40 days of *in vitro* culture including four

transduction steps and three sorting and expansion steps. The complex manufacturing process of TCRαβ-edited T cells also remained to be the main problem in a second study that employed more effective transcription activator-like effector nucleases (TALEN) instead of ZFN [220]. The reason why such extensive manipulations of the T cells are required will be pointed out later in the Discussion part of this thesis.

The downregulation of the TCR by RNA interference (RNAi) is an alternative approach to reduce the amount of endogenous TCR protein that can be easily integrated into established protocols for the generation of TCR gene-modified T cells. For this purpose retroviral vectors specific for human T cells were developed, which simultaneously express RNA molecules to trigger the RNAi mechanism and a codon-modified RNAi-resistant TCR [221,222]. Several distinct double-stranded RNA (dsRNA) molecules can be used to elicit the sequence-specific downregulation of target genes by RNAi (Figure 4).

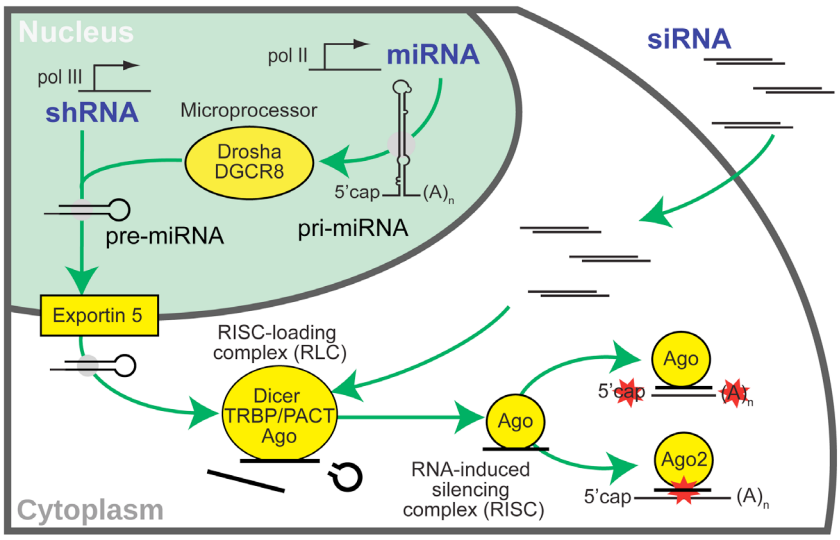

Figure 4: *Experimental post-transcriptional gene silencing is induced by double-stranded RNA molecules entering the RNA interference pathway.*
Transcription of micro RNA (miRNA) genes by polymerase II promoters (pol II) generates RNA molecules with characteristic secondary structures (pri-miRNA) that are recognized by the microprocessor complex composed of Drosha nuclease and RNA-binding protein DiGeorge critical region 8 (DGCR8). Polymerase III (pol III) promoters can be used to produce short hairpin RNA (shRNA) that resemble the pre-miRNA generated by the microprocessor complex. Exportin 5 mediates the nuclear export of double-stranded RNA molecules with 3' overhangs. Cytosolic Dicer in association with Argonaut proteins (Ago), trans-activation response RNA-binding protein (TRBP) or protein activator of PKR (PACT) mediates the cleavage of pre-miRNA and shRNA, but accepts also small interfering RNA molecules (siRNA) as substrates. The pathway culminates in the formation of RNA-induced silencing complexes (RISC) consisting of Ago proteins bound to 20-25-nt single-stranded RNA molecules that mediate the sequence-specific binding of the complex to complementary mRNA. Of the four mammalian Ago proteins, only Ago2 possess the catalytic activity to cleave the target mRNA, whereas the other Ago proteins attenuate mRNA translation and induce mRNA degradation.

They resemble endogenous intermediates of the RNAi pathway and enter the pathway at different points, but they all lead to the formation of RNA-induced silencing complexes (RISC) composed of an Argonaut (Ago) protein bound to a short single-stranded RNA molecule that directs the RISC to mRNA

with complementary sequence. Depending on which of the four mammalian Ago proteins is part of the RISC, the mRNA is either directly cleaved in case of Ago2 or the translation is attenuated and the mRNA stability is negatively affected in case of the other Ago proteins [223,224,225,226,227]. Transient protein knockdown can be achieved by transfection of small interfering RNA (siRNA) [228]. siRNA molecules are made of two complementary RNA strands of 21 nt forming a duplex RNA with 2-nt overhangs at the 3' ends that enter the RNAi pathway in the cytosol. Stable gene knockdown can be achieved by the continuous production of short hairpin RNA (shRNA) or micro RNA (miRNA), which enter the RNAi pathway in the nucleus and are then processed to siRNA-like molecules [229,230]. Transcription of miRNA genes by polymerase II (pol II) promoters produces capped and polyadenylated transcripts with distinctive secondary structures (pri-miRNA) that are recognized by the nuclear microprocessor consisting of Drosha nuclease and RNA-binding protein DiGeorge critical region 8 (DGCR8) [231,232]. The microprocessor then excises the miRNA hairpin from the transcript. Production of shRNA by polymerase III (pol III) promoters generates uncapped RNA hairpins without poly(A)-tails that resemble the intermediates (pre-miRNA) produced by the microprocessor complex. Hence, shRNA enter the RNAi pathway at this point. After the Exportin 5-mediated transport of the shRNA/pre-miRNA hairpins into the cytosol, the loops of the hairpins are removed by Dicer nuclease, which forms together with Ago proteins and RNA-binding proteins the RISC-loading complex (RLC) [233,234]. Exogenous siRNA resemble the dsRNA molecules generated by Dicer. Which strand of the dsRNA molecule is incorporated into the RISC and which one is removed, was shown to depend on the thermodynamic stability of both ends of the duplex [235,236].

The usage of miRNA as RNAi trigger for the knockdown of the TCR has the advantage that the same pol II promoter can be used to control the expression of the miRNA and the RNAi-resistant TCR. However, the construction of efficient RNAi-TCR replacement vectors has proven difficult. The first vector that was published suffered from a suboptimal vector design that likely results in the formation of enhanced levels of mixed TCR dimers [221]. In this vector, both TCR chains were expressed from different promoters and an exonic miRNA cassette was introduced at the 3' end of one of the TCR chains. The excision of the miRNA cassette from the mRNA by Drosha nuclease produces truncated mRNA, which reduces protein translation and results in mRNA degradation. Therefore, in T cells transduced with the first-generation RNAi-TCR replacement vector, the excess of one transferred TCR chain might induce mixed TCR dimer formation. In a subsequent study, a second generation RNAi-TCR replacement vector was presented, that employed an intronic miRNA cassette and a TCR cassette, in which both TCR chains were linked by a 2A element [222]. Although reduced endogenous TCR mRNA levels in human T cells were successfully correlated with higher surface levels of a second RNAi-resistant TCR, neither the amount of remaining endogenous TCR protein in the transduced T cells was determined nor if the transferred TCR chains reached endogenous surface expression levels. Therefore, it remained unresolved how effectively the endogenous TCR was indeed replaced by the

transferred TCR and whether the RNAi approach would reduce the formation of mixed TCR dimers and prevent the generation of self-directed specificities in the population of transduced T cells.

2 Aims of the thesis

The aim of this thesis was the establishment of an alternative strategy to reduce the level of mixed TCR dimers on TCR gene-modified T cells by directly targeting the expression of the endogenous TCR. The new technology should be more efficient compared to previously established methods that concentrated on improving the expression of the transferred TCR and should allow the generation of TCR gene-modified T cells in a clinically feasible protocol. This task should be solved by the construction of a γ-retroviral RNAi-TCR replacement vector expressing simultaneously miRNA targeting the endogenous TCR and a therapeutic RNAi-resistant TCR. The advantage of the RNAi approach over the use of genetically optimized TCR should be demonstrated in *in vivo* models of TCR gene therapy, which required to develop a vector specific for mouse T cells. A second vector specific for human T cells should be developed for further experimental investigations and a possible clinical application.

- The project was started by investigating whether the mouse TCR genes encode sequences that fulfill the criteria for efficient RNAi target sites. Answering this question involved the application of bioinformatic tools for the prediction of RNAi target sites and the empirical validation of the predicted target sites in an *in vitro* reporter assay that allowed using an established shRNA expression vector.

- How to trigger the RNAi mechanism and at the same time express a therapeutic TCR in T cells was addressed in the second part of the thesis. It was investigated whether an RNAi vector constructed by the introduction of miRNA directed at the predicted RNAi target sites into the γ-retroviral vector MP71 could meet this demands.

- TCR gene-modified mouse T cells were studied in the third part of the thesis involving *in vivo* models of TCR gene therapy and the detailed analysis of TCR surface expression. The following questions were in the focus of the experiments:
    - How is the TCR surface expression affected by TCR silencing in comparison to TCR gene optimization?
    - Does the expression of the miRNA negatively affect the *in vivo* functionality of TCR gene-modified T cells?
    - Does the silencing of the endogenous TCR in TCR gene-modified T cells prevent TI-GVHD caused by mixed TCR dimers?

- In the fourth part of the thesis it was asked whether it is possible to develop an RNAi-TCR replacement vector for human T cells and if so, whether TCR silencing has similar effects on the surface TCR composition of human TCR gene-modified T cells as observed for mouse TCR gene-modified T cells.

3 Results

3.1 Identification of target sites for the RNAi-mediated knockdown of mouse TCR

In the first part of the project, suitable target sites for the RNAi-mediated knockdown of the mouse TCR genes were identified. Such target site sequences have to fulfill certain requirements of the endogenous RNAi machinery and may not be present in any given gene sequence. Selected parts of the mouse TCR sequences were analyzed with bioinformatic tools and a list of potential target sites was generated. A limited number of target sites from the sequence analysis were then empirically confirmed in an *in vitro* reporter assay. To this end, it was demonstrate that the selected TCR sequences, which are shared by all TCR chains of a polyclonal repertoire, contained suitable target sites for the RNAi-mediated knockdown of the TCR.

3.1.1 Potential RNAi target sites have to be located in the open reading frame of the TCR constant regions

In order to knockdown every possible sequence of a polyclonal TCR repertoire, the target sequences should be located in the TCR C regions, which account for 60-70% of the TCR sequences (Fig. 5A). In addition, the targeting of untranslated regions (UTR) should be avoided, because they frequently contain binding sites for regulatory proteins or endogenous miRNA. RNAi directed at such sequences is likely inefficient and there is a higher risk of unspecific effects as similar sequences may be present in the UTR of other genes.

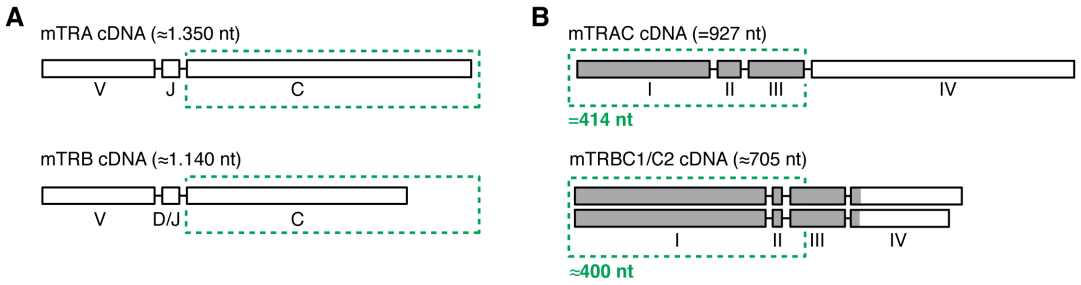

Figure 5: *RNAi target sites have to be located within the first 400 nt of the TCR constant regions.*
(**A**) The mouse TCRα (mTRA) and β (mTRB) chain cDNA sequences are drawn to scale. In order to knockdown all TCR of a polyclonal repertoire by RNAi, only the constant (C) regions (green box) and not the variable (V), joining (J) and diversity (D) regions can be targeted. (**B**) The exons I-IV of the mouse Cα (mTRAC) and Cβ regions (mTRBC1/C2) are drawn to scale. The open reading frame (ORF) is shown in grey. The green boxes mark the sequences that could serve as locations for RNAi target site. In case of the β chain, not the complete ORF but only the part that is homologous between mTRBC1 and mTRBC2 is suitable.

The mouse TCR Cα region (mTRAC) is composed of four exons of 261, 45, 108 and 513 nucleotides (nt). The first three exons are part of the open reading frame (ORF), whereas the last exon is not translated (Fig. 5B). Two different C regions are used in the TCRβ chains (mTRBC1/2). They resemble each other and are both composed of four exons. The first three exons have the same size of 375, 18 and 107 nt. The ORF extends to the first 18 nt of the fourth exon in both Cβ regions, but the length of

the following untranslated region (UTR) differs slightly and accounts for 217 and 192 nt in case of Cβ1 and Cβ2, respectively (Fig. 5B). The overall sequences similarity is very high for the first two exons and then deceases strongly towards the 3' end. There are only 4 nt difference in the first 400 nt, whereas the following sequences show a low overall similarity of 55%. Due to these characteristics of the TCR genes, the search for RNAi target sites was restricted to the first 400 nt of the Cα and Cβ sequences.

3.1.2 Potential target sites were selected using the overlap of the results from four RNAi target site prediction programs

Four different web-based programs for the prediction of RNAi target sites were used to analyze the first three exons of the mouse TCR Cα and Cβ regions. These programs use sequence-specific and thermodynamic parameters that reflect the requirements of the endogenous RNAi machinery to identify the most efficient RNAi target sites of a given sequence. On average 55% and 64% of the target sites predicted by any of the four programs were also predicted by at least one other program in case of the TCRα and β chain, respectively (Fig. 6, A and B). The overlap of the results was used to generate a list of potential RNAi target sites (Fig. 6C). The sequence of each target site was compare to mRNA in the reference sequence database (RefSeq) using the basic local alignment search tool (BLAST). Target sites with a continuous run of more than 15 matches or a run of 17 matches interrupted only by a

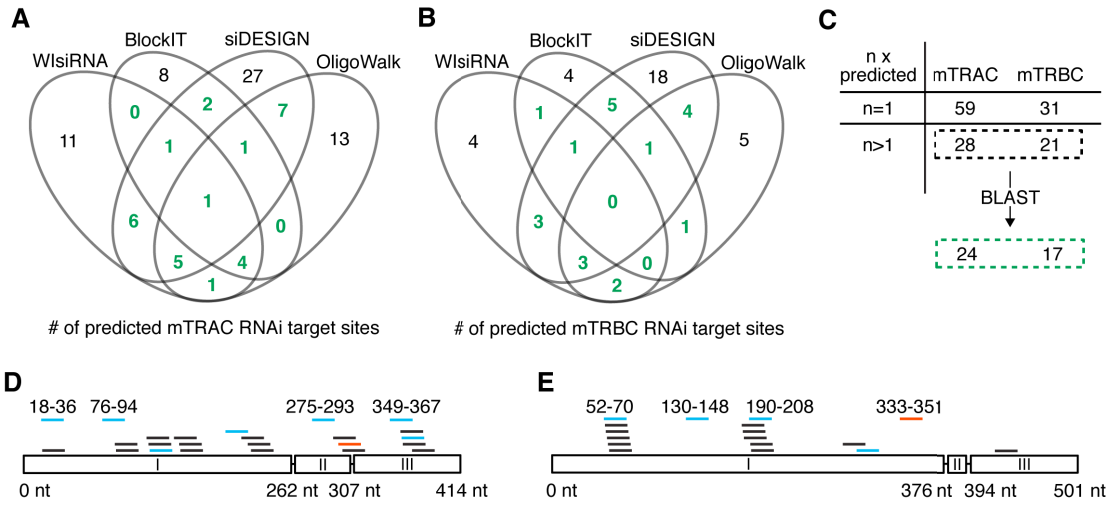

Figure 6: *A list of potential RNAi target sites was generated using the overlap of the results from four RNAi target site prediction programs.*
(**A-B**) The first three exons of mTRAC and mTRBC2 were analyzed using the RNAi target site prediction programs "WIsiRNA", "BlockIT", "siDESIGN" and "Oligowalk". Target sites that were not shared between mTRBC1 and mTRBC2 were removed. (**C**) The target sites that were predicted more than once were checked for their similarity with other genes using the basic local alignment search tool (BLAST). (**D-E**) Locations of the predicted RNAi target sites for mTRAC and mTRBC are shown in **D** and **E**, respectively. Blue or red color indicates that the target sites have been further investigated in this study. The positions of the target sites used in the *in vitro* reporter assays are indicated. The red target sites were used for the construction of the final miRNA cassette.

single mismatch were removed from the list. Furthermore, target sites with continuous runs of four or more identical nucleotides were discarded. Next, the positions of the remaining 24 and 17 target sites for the TCRα and β chain were analyzed (Fig. 6D and E). The TCRα chain target sites were more evenly distributed than the TCRβ chain targets sites, which were mainly clustered around two locations. Four target sites per TCR chain from different locations were selected to be further analyzed.

3.1.3 shRNA directed at the predicted target sites induced strong RNAi effects in an reporter assay employing plasmid vectors

An *in vitro* reporter assay was used to confirm empirically some of the RNAi target sites predicted by the sequence analysis. At this point in the project, a miRNA expression vector to analyze the knockdown of endogenous TCR in T cells had yet to be developed. Therefore, plasmid vectors that were already applied in previous studies in the literature were used in the assay. Cloning the native mouse TCR C regions into the plasmid vector siCHECK-2 generated three reporter plasmids. To investigate whether it is possible to shield the TCR sequences from the RNAi effect by silent mutations, two further reporter plasmids were constructed harboring the codon-optimized variants of the TCR C regions, which differed at the target sites from the native sequences by 3-4 nt. The resulting reporter vectors expressed a renilla luciferase whose mRNA encoded the cloned TCR sequences in the 3' UTR. Mouse NIH/3T3 cells were transfected with a mixture of an effector plasmid encoding an shRNA directed at a predicted target site and one of the reporter plasmids. After two days, the amount of renilla luciferase was determined in cell lysates based on the catalytic activity. A second luciferase (firefly), which was also expressed by the reporter plasmids, was measured in parallel and used to normalize the data. An shRNA directed at a site in the ORF of the renilla luciferase was used as a positive control and an shRNA not directed at any mouse gene was used as a negative control.

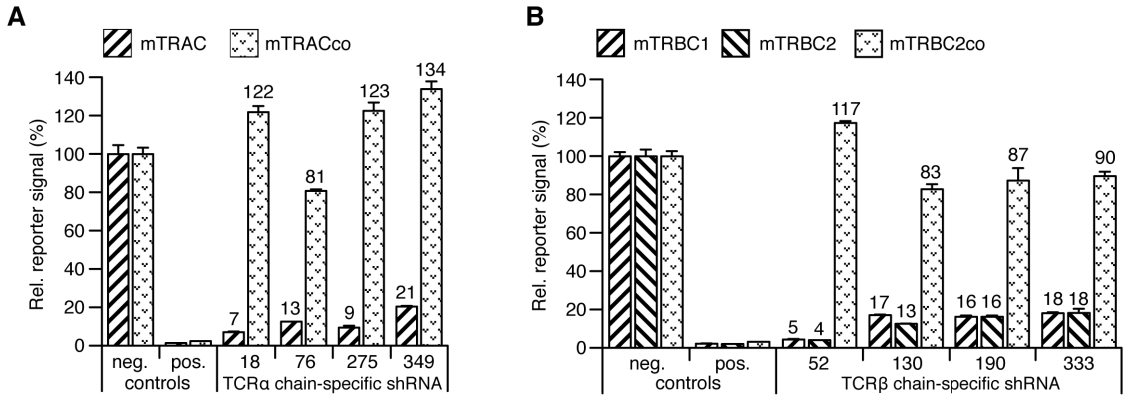

Figure 7: *Efficient knockdown of reporter genes encoding TCR sequences by shRNA directed at the predicted RNAi target sites.*
(**A-B**) Assessment of the silencing efficiency of shRNA targeting the TCR constant regions using a dual-luciferase reporter assay. Either native mouse TCR constant regions or codon-optimized (co) constant regions were fused as untranslated regions to a renilla luciferase gene (indicated above). An shRNA not targeting any mouse genes served as a negative (neg.) control and an shRNA targeting the coding region of the renilla luciferase gene served as a positive (pos.) control. The plots show the mean ±SD of triplicates.

All four shRNA directed at the predicted target sites in the mouse TCR Cα region (mTRAC) induced a strong RNAi effect and reduced the reporter signal by at least 80% (Fig. 7A). In contrast, either no or only a very small RNAi effect was observed, if the reporter plasmid expressed the codon-optimized TCR sequence (mTRACco). Similar results were obtained for four shRNA targeting TCRβ chain (Fig. 7B). The reporter signal was efficiently reduced whether Cβ1 (mTRBC1) or Cβ2 (mTRBC2) was targeted and only a small RNAi effect was observed when the codon-optimized variant (mTRBC2co) was targeted. The results of this assay indicated, that indeed suitable RNAi target sites were identified and that the sequence changes introduced through codon optimization were sufficient to avoid the RNAi effect.

3.2 Development of a γ-retroviral vector for RNAi-mediated TCR replacement

In the second part of the project a viral vector was developed accomplishing the following tasks in combination: first, efficient transduction of primary T cells, second, expression of RNA molecules that enter the RNAi pathway and knock down both endogenous TCR chains and, third, expression of transgenic proteins. The new RNAi vector was developed on the basis of the γ-retroviral MP71 vector, because this vector was previously shown to be superior to other vectors in regard to the ability to transduce primary T lymphocytes with efficiency and to confer stable transgene expression [203]. Although the MP71 vector was successfully employed in many studies for the generation of TCR gene-modified T cells, it was never used in an RNAi knockdown strategy before.

3.2.1 Harnessing the MP71 TCR vector for miRNA expression

A variety of different RNA molecules allow specific triggering of cellular RNAi. In this project, miRNA were chosen as RNAi trigger, because multiple miRNA can be combined to a cassette and expressed simultaneously. In addition, miRNA are expressed by polymerase II promoters, which allows to take advantage of the highly active LTR of the MP71 vector to express both the miRNA cassette and RNAi-resistant TCR. The first steps in the development of an MP71-based miRNA vector were to construct a functional miRNA directed at one of the TCR chains and to find a suitable position for the miRNA in the vector.

New miRNAs directed at the TCR genes were generated by exchanging the antisense sequence of endogenous and artificial miRNA. In principle, miRNAs are recognized and processed by the cellular RNAi machinery because of their secondary structure, which can be subdivided into the very characteristic highly base-paired miRNA hairpin encoding the antisense sequence and the more unstructured sequence that forms the backbone of the miRNA (Fig. 8A). Using the conserved structural features of miRNAs from different species, an artificial miRNA was constructed in a previous study [237]. The AmiR construct was synthesized according to the published sequence, with the exception that additional restriction sites were introduced into the central loop, which allowed sequential cloning of the miRNA base and hairpin (Fig. 8A). Following the examples presented in the

above study, a new AmiR hairpin was designed directed at the TCRα chain target site α275 (Fig. 8B). An antisense sequence of 19 nt was introduced by purpose, but together with the two adjacent 3' nucleotides of the hairpin, which were by change also complementary to the Cα sequence, the hairpin encoded an antisense sequence of 21 nt in total (Fig. 8C). The resulting miRNA "AmiRα275" was introduced at two different positions into a GFP-encoding MP71 vector (Fig. 8D). The mouse T cell hybridoma cell line B3Z was transduced with both vectors encoding the AmiRα275 either in an intronic position or exonic position 5' of GFP. The TCR surface and GFP expression levels of the transduced cells were analyzed by flow cytometry and compared to a control sample transduced with the unmodified MP71-GFP vector (Fig. 8E). The modification of the vector resulted in markedly decreased GFP levels in the transduced cells of 1% and 35% depending on whether the miRNA was introduced at the exonic or intronic position, respectively. In contrast, the RNAi effect was comparable for both vectors. The surface TCR levels were reduced to 70% and 75% by the expression of the exonic and intronic miRNA, respectively.

This data demonstrated efficient transduction of B3Z cells with modified MP71-GFP vectors expressing one miRNA and one transgene simultaneously. Although the advantage of the intronic miRNA was shown, the cells transduced with this vector still expressed only about one third of the GFP

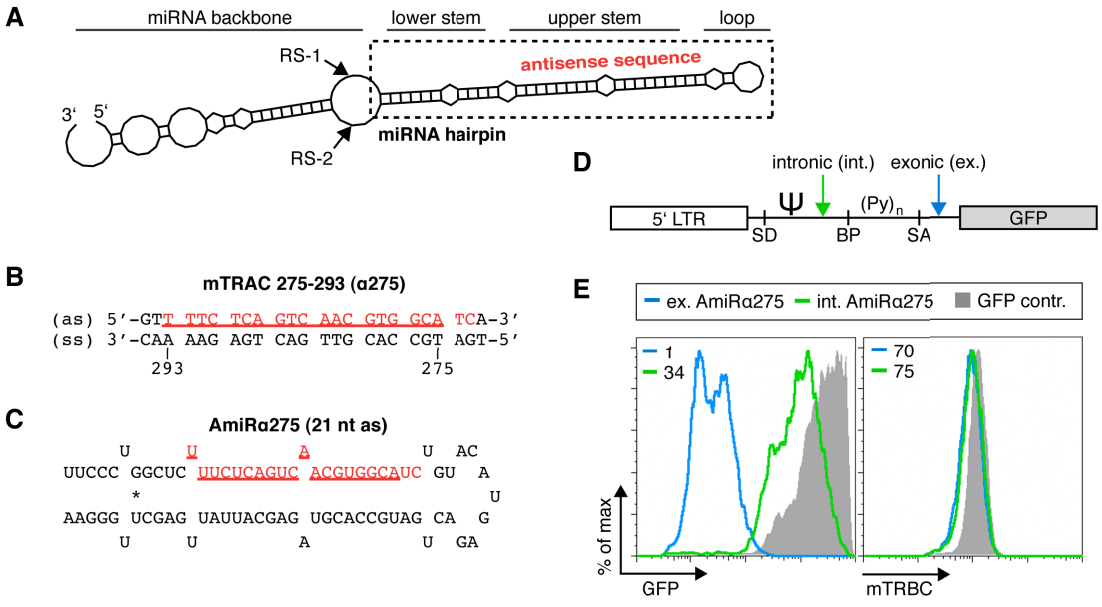

Figure 8: *The MP71 vector can be used for the simultaneous expression of miRNAs and transgenes.*
(**A**) Secondary structure of the artificial miRNA (AmiR). Restriction sites (RS) have been introduced at the indicated positions for cloning purpose. (**B**) 19-mer mTRAC target site sequence (underlined) and adjacent nucleotides. Red nucleotides are homologous to the AmiRα275 hairpin. Abbreviations: antisense sequence (as), sense sequence (ss). (**C**) The AmiRα275 hairpin was designed using the 19-mer antisense sequence of the target site α275 (underlined) but the complementarity to the TCRα cDNA (red) includes the two 3' adjacent nucleotides. (**D**) The AmiRα275 was introduced into an MP71-GFP vector at the indicated positions. Abbreviations: long terminal repeat (LTR), splice donor (SD), packaging signal (ψ), branch point (BP), pyrimidine bases (Py), splice acceptor (SA). (**E**) Surface TCR and GFP expression of transduced mouse B3Z hybridoma cells was analyzed by flow cytometry. Indicated are the relative MFI values (%) of the modified vectors compared to the unmodified parental vector (GFP contr.). Transduction efficiencies: ex. AmiRα275 (93%), int. AmiRα275 (89%), GFP contr. (72%).

compared to the control. In addition, the expression of the AmiRα275 had only a minor impact on the surface level of the endogenous TCR, which clearly would not compensate for this disadvantage. Consequently, the following experiments concentrated on the generation of highly efficient miRNA for the knockdown of the mouse TCR genes.

3.2.2 The length of the antisense sequence affects the knockdown efficiency of redirected miRNA

In addition to the AmiR, also endogenous miRNA were used in this study to design redirected miRNA for the TCR knockdown. For this purpose, the human miR-17-92 cluster was cloned into a plasmid, which served as a template to generate full-length redirected miRNA by overlap extension PCR. Two miRNA directed at the same target site were generated based on the miR-17, which is the first miRNA of the cluster. Expression of the native miR-17 sequence produces a mature miRNA strand of 23 nt according to miRBase (Fig. 9A) [238]. Using the TCRβ target site β052, which is a sequence of 19 nt, the miRNA miR17β52-A and -B, encoding an antisense sequence of either 19 nt or 23 nt, respectively, were generated (Fig. 9B-D). The secondary structure of the miR-17 hairpins was analyzed and if possible, a GU base pair was introduced in order to generate a structure comparable to the native miR-17. Both miRNA were cloned into the MP71-GFP vector and flow cytometric analysis of transduced B3Z cells showed comparable GFP levels for both samples (43% and 54%) (Fig. 9E). The surface TCR level was almost not changed (90%) by the miR17β052-A with the short antisense

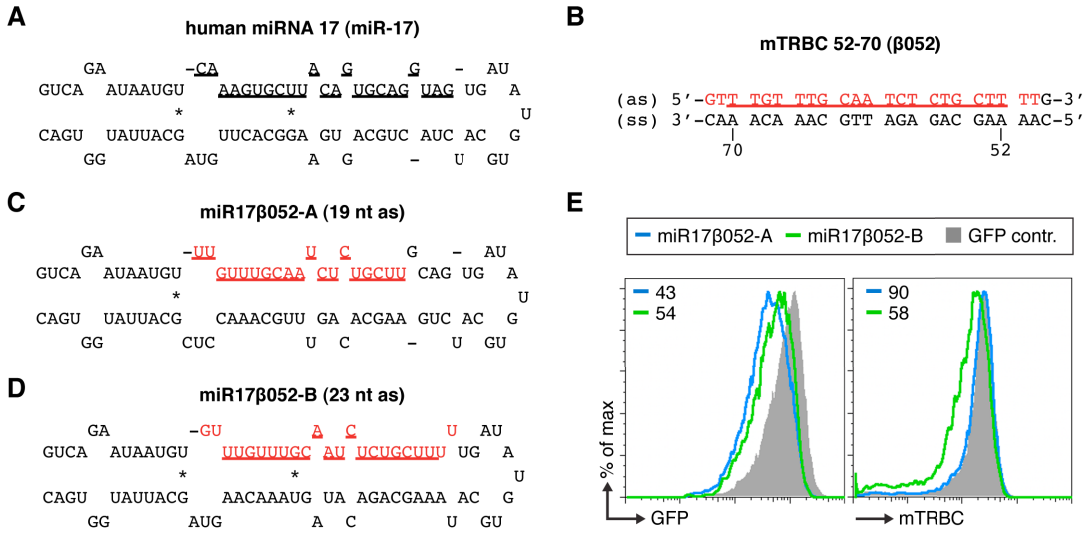

Figure 9: *Redirected miR-17 reduces the surface TCR on B3Z cells more efficiently when encoding a 23-mer antisense sequence compared to a 19-mer antisense sequence.*
(**A**) mTRBC cDNA sequence. The underlined nucleotides are complementary to the predicted 19-mer target site β052. Nucleotides in red were used for the design of the miRNA hairpins. Abbreviations: antisense sequence (as), sense sequence (ss). (**B**) Hairpin of the native human miR-17. The 23 nt of the mature miRNA are underlined. (**C-D**) miR-17-based hairpins targeting β052 and encoding antisense sequences of either 19 nt (C) or 23 nt (D). Nucleotides in red are complementary to the mTRBC cDNA and the underlined nucleotides are complementary to the target site β052 (**E**) Surface TCR and GFP expression of transduced mouse B3Z hybridoma cells. The MFI values relative to the parental control vector (GFP contr.) are indicated. Transduction efficiencies: miR17β052-A (90%), miR17β052-B (88%), GFP contr. (92%).

sequence, whereas the miR17β052-B encoding the long antisense sequence reduced the TCR surface level to 58%. This data suggested, that it could be beneficial to use an antisense sequence of more than 19 nt for the design of redirected miRNAs.

In the next step, it was investigated whether this finding also applies to other miRNA such as the AmiR. To facilitate the cloning of AmiR-expressing MP71-GFP vectors, the sequence of the AmiR base without the hairpin was introduced into an MP71-GFP vector at the intronic position. Then, two new AmiR directed at the β052 target site with an antisense sequences of 20 and 22 nt were generated and cloned into MP71-GFP vector encoding the AmiR base. The AmiRβ052-A hairpin was designed using the exact antisense sequence of the 19-mer target site and because the 3' adjacent nucleotide of the hairpin was by chance also complementary to the TCR sequence, the resulting antisense sequence was of 20 nt in total (Fig. 10A). The 22-mer antisense sequence of the AmiRβ52-B hairpin was generated by the addition of one nucleotide at the 5' end and two nucleotides at the 3' end of the predicted 19-mer sequence (Fig. 10B). In addition, a GU base pair was introduced at the 5' site of the antisense sequence to facilitate asymmetric strand loading. The analysis of transduced B3Z cells confirmed the previous results of the two miR-17 variants (Fig. 10C). There was only a small difference in the GFP levels of the two samples (33% and 23%), but a large difference in the RNAi effect. The expression of the AmiR with the short antisense sequence resulted in a TCR surface level of 123%, whereas the expression of the AmiR with the long antisense sequence reduced the surface TCR to 22%.

The data of the miR-17 and the AmiR variants directed at the same TCRβ target site demonstrated that an antisense sequence of more than 19 nt can improve the RNAi effect. Furthermore, the AmiR encoding an antisense sequence of 22 nt and a GU wobble at the 3' end showed the greatest knockdown efficiency of the four miRNAs. Therefore, further miRNA with the same design were investigated.

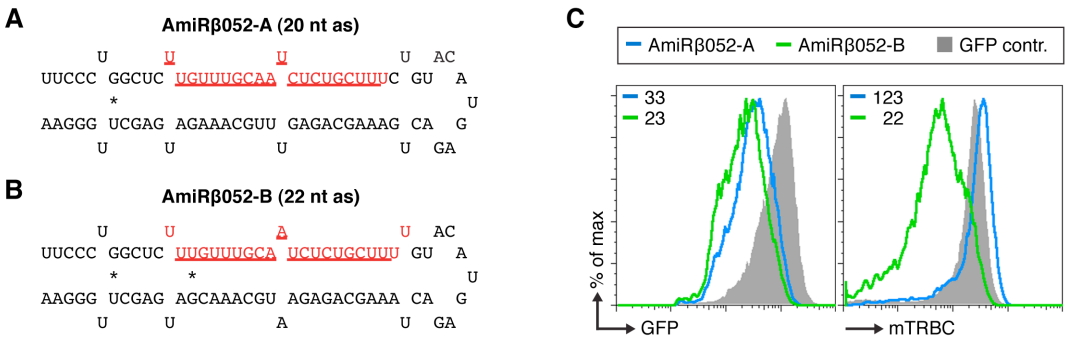

Figure 10: *An AmiR hairpin with a antisense sequence of 22 nt and a GU base pair at the 5' end shows improved TCR silencing efficiency.*
(**A-B**) Two AmiR hairpins directed at the TCRβ target site β052 with an antisense sequence of either 20 nt (A) or 22 nt (B) were compared. Nucleotides in red are complementary to the TCRβ chain. Nucleotides complementary to the predicted 19-mer target site are underlined. (**C**) The TCR surface level and GFP expression of transduced mouse B3Z cells was analyzed. The MFI values relative to the parental control vector (GFP contr.) are indicated. Transduction efficiencies: AmiRβ52-A (88%), AmiRβ52-B (73%), GFP contr. (92%).

3.2.3 Identification of an efficient miRNA for the knockdown of the mouse TCRβ chain

After a new design for the AmiR hairpin was established that resulted in an increased RNAi effect in case of the AmiRβ052-B, multiple hairpins with a long antisense sequence directed at different TCRβ target sites were analyzed. The AmiR hairpins were generated using synthesized oligonucleotides and then cloned into an MP71-GFP vector encoding the sequence of the AmiR base within the 5' intron.

Although the TCRβ target sites were tested before in the *in vitro* reporter assay using shRNA (Fig. 7B), only two of the four miRNA reduced surface TCR on transduced B3Z cells efficiently (Fig. 11). Multiple experiments with transduced B3Z cells expressing AmiRβ052-B and AmiRβ333-B were conducted and the AmiRβ333-B was identified as the best candidate for the TCR replacement vector. B3Z cells transduced with this miRNA showed throughout the experiments a stable reduction of the surface TCR level of 70-80% and stable GFP expression of about 20-30%.

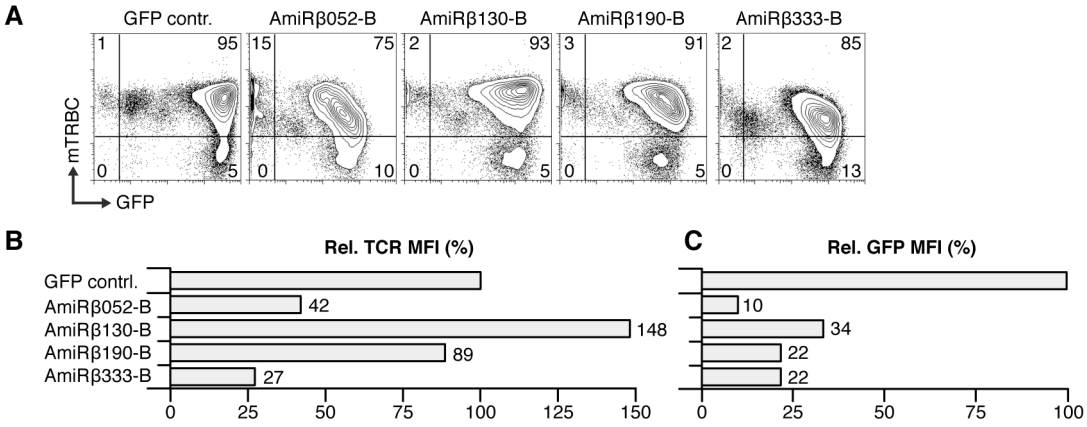

Figure 11: *The mTRBC target site β333 is most suitable for the design of an AmiR compared to three other target sites.*
(**A**) TCR surface levels and GFP expression of transduced B3Z cells were determined by flow cytometry. The percentage of gated cells is indicated. (**B-C**) The MFI were compared to the parental control vector (GFP contr.). Transduction efficiencies: GFP contr. (99%), AmiRβ52-B (85%), AmiRβ130-B (98%), AmiRβ190-B (96%), AmiRβ333-B (98%). Plots show the representative results of one out of multiple experiments.

Next, a new full-length miRNA encoding the AmiRβ333-B hairpin but without the restriction sites at the central loop was generated and designated as miRβ. Restriction sites were added at both ends of the miRNA enabling a successive cloning strategy to insert further miRNA into the vector after the integration of the first miRNA (Fig. 12, A and B). The analysis of transduced polyclonal splenocytes (C57BL/6) expressing either the AmiRβ333-B or the miRβ confirmed that the changes in the miRNA sequence did not influence the knockdown efficiency and hardly influenced the GFP expression (Fig. 12C-E). The surface TCR on the T cells transduced with MP71-GFP vectors encoding the AmiRβ333-B or the miRβ was decreased by 88%. The GFP levels ranged from 25% to 35% compared to cells transduced with the unmodified MP71-GFP vector.

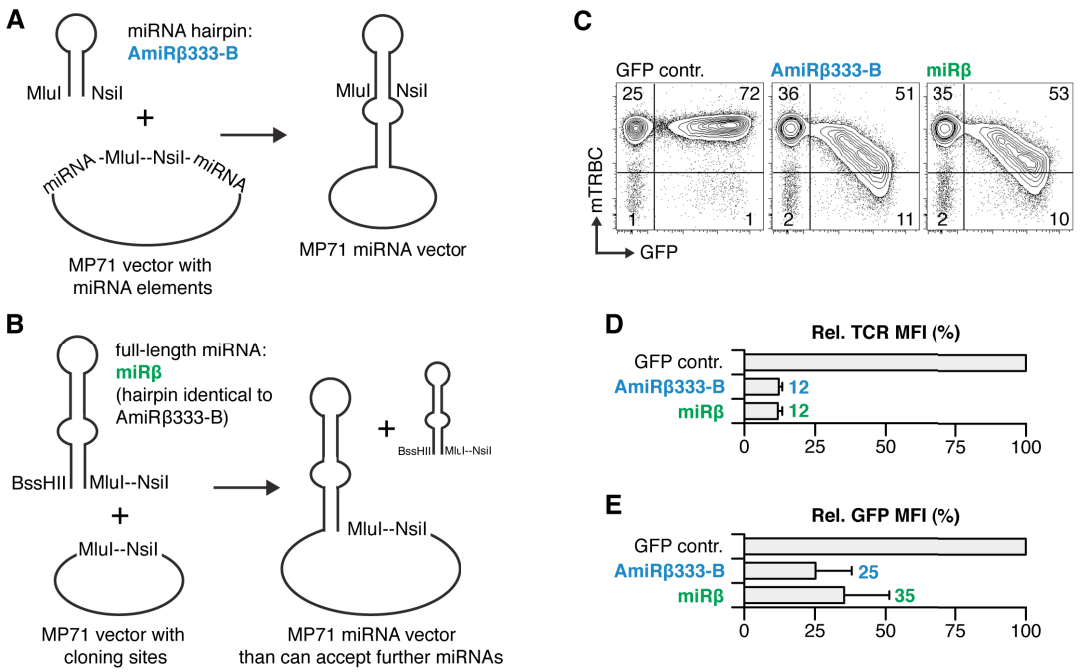

Figure 12: *The artificial miRNA targeting mTRBC-333 reduces the surface TCR of primary mouse T cells by more than 85%.*
(**A**) AmiR hairpins were cloned into a MP71-GFP vector that already encoded parts of the AmiR sequence. (**B**) Cloning strategy for the construction of vectors expressing multiple miRNAs. The redirected miRNAs were generated in full-length by overlap extension PCR with restriction sites at the 5' and 3' end. Introduction of the miRNA into the vector creates new restriction sites for the cloning of the next miRNA. (**C**) TCR surface levels and GFP expression of transduced polyclonal splenocytes (C57BL/6) were determined by flow cytometry. (**D-E**) MFI were compared to the parental control vector (GFP contr.). Transduction efficiencies: GFP contr. (84%, 73%), AmiRβ333-B (57%, 62%), miRβ (70%, 63%). Plots show the mean of two independent experiments ±SD (*n*=2).

3.2.4 Identification of an efficient miRNA for the knockdown of the mouse TCRα chain

To identify candidate miRNA for the knockdown of the mouse TCRα chain, AmiR hairpins with the same design as the miRβ, designated as format B, and a new hairpin design with a shifted antisense sequence, designated as format C, were investigated (Fig. 13, A and B). The antisense sequence of the new hairpin format was created by adding three nucleotides at the 3' end of the predicted target sequence, which resulted in a small shift of the 19-mer to the 5' end of the hairpin. The target sites for the miRNA were chosen according to the *in silico* prediction but irrespective of whether they were tested in the *in vitro* reporter assay using shRNA. The new AmiR were generated in full-length with restrictions sites at the 5' and 3' end and introduced into the intron of the MP71-GFP vector. Nine miRNA were analyzed in total: Six miRNA with both hairpin formats directed at three target sites (α018; α193; α395) and three miRNA with the new hairpin format C direct at three further target sites (α089; α121; α300). Two out of nine miRNA reduced the surface TCR on transduced B3Z cells to the

same level as the AmiRβ333-B, which was used as a positive control in this experiment (Fig. 13C). The RNAi effect was not as strong as in previous experiments, because of a lower overall transduction rate. The relative GFP expression levels ranged between 32% and 43% (Fig. 13D). The two most efficient miRNA encoded both a hairpin in the new format C and were directed at the target sites α018 and α300. Interestingly, in case of the α018 target site, both hairpin formats were tested in this experiment and the new format C resulted in a stronger RNAi effect (70% vs. 83%). To extend on this finding, a further miRNA was generated with a hairpin in the format B directed the α300 target site. Next, the two pairs of miRNA encoding hairpins in both formats directed at the target sites α018 and α300 were

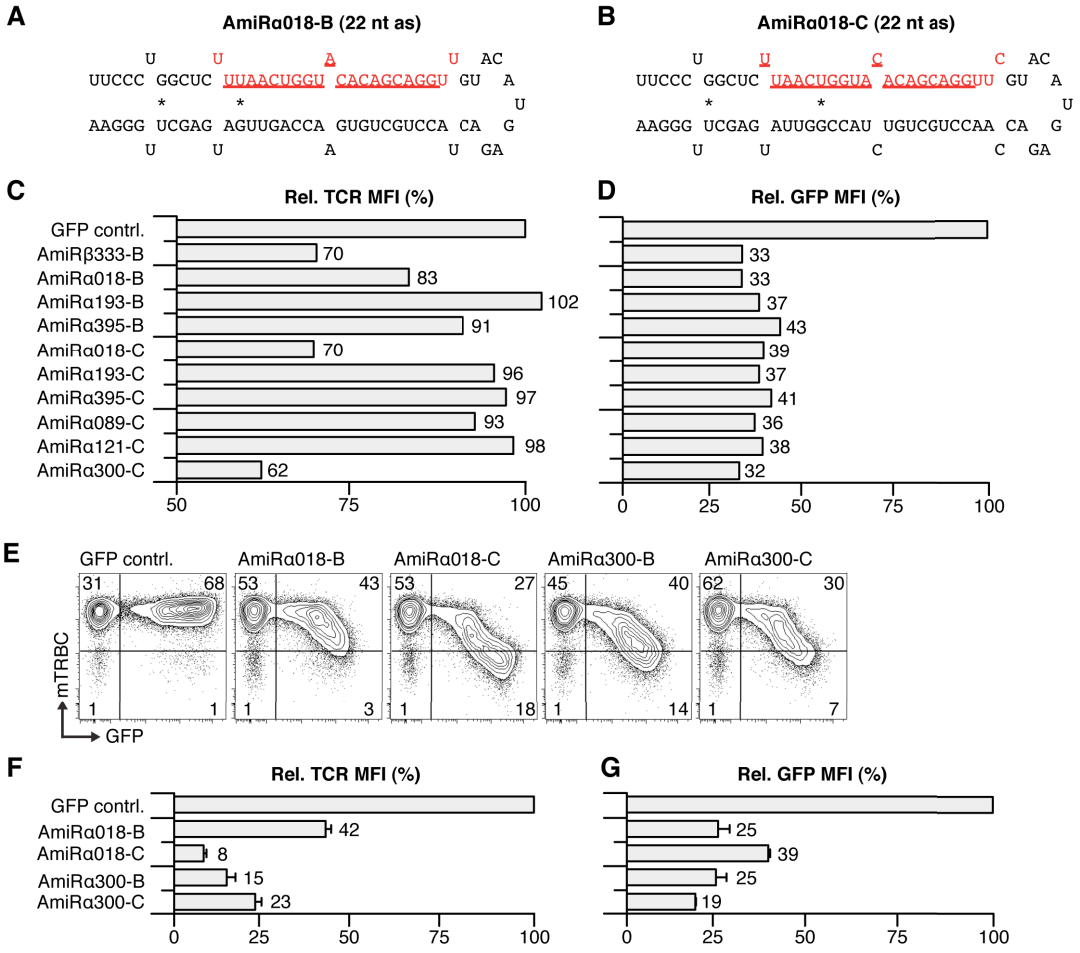

Figure 13: *Two candidate artificial miRNA were identified for the knockdown of the TCRα chain.*
(**A**) AmiR hairpin design B. The predicted 19-mer target sequence (underlined) is shifted by 1 nt towards the center of the antisense sequence (as, in red). (**B**) AmiR hairpin design C. The predicted 19-mer target sequence (underlined) starts exactly with the first nucleotide of the antisense sequence (red). (**C-D**) B3Z cells were transduced with nine vectors that expressed miRNA directed at six different TCRα target sites. TCR surface levels and GFP expression were compared to cells transduced with the GFP control (contr.) vector. The AmiRβ333-B vector served as a positive control. Transduction (Td) efficiencies were evenly low (mean: 20%). (**E**) TCR surface levels and GFP expression of transduced polyclonal splenocytes (C57BL/6) were determined by flow cytometry. (**F-G**) MFI were compared to the parental control vector (GFP contr.). Td efficiencies: GFP contr. (49%, 70%), AmiRα018-B (40%, 47%), AmiRα018-C (37%, 46%), AmiRα300-B (33%, 55%), AmiRα300-C (27%, 38%). Plots show the mean of two independent experiments ±SD (*n*=2).

expressed in transduced polyclonal splenocytes (C57BL/6) (Fig. 13E). In case of the miRNA pair directed at the α018 target site, the hairpin format C resulted in a stronger RNAi effect (8% vs. 42%) (Fig. 13F). However, the opposite was found in case of the second miRNA pair, although the difference between both miRNA was smaller. Expression of the AmiRα300-B and -C reduced the TCR surface level to 15% and 23%, respectively. The GFP expression in the transduced T cells ranged between 19% and 39% (Fig. 13G).

Up to this point, two highly efficient miRNA for the knockdown of the TCRα chain were identified, which reduced the TCR surface level of transduced T cells by 80-90%. Both miRNA were constructed using the AmiR sequence, which was also used before to construct the miRNA targeting the TCRβ chain. In order two combine two miRNA in a cassette for the simultaneous knockdown of both TCR chains, new miRNA based on different sequences had to be generated, because direct sequence repeats are not stable in retroviral vectors. Therefore, in the next step, the backbone sequence of the endogenous mouse miRNA-155 (miR155) was used to construct miRNA to replace AmiRα018-C and AmiRα300-B.

Four miRNA based on the mouse miR155 sequence were constructed analogous to the AmiRα018-C and AmiRα300-B but with some modifications oriented on the secondary structure of the native miR155 (Fig. 14A-D). The hairpins were designed with a central mismatch of two base pairs and without a GU base pair at the 5' end of the antisense sequence. Two miRNA for each target site were generated either with an antisense sequence of 21 nt, similar to prevoius publications, or with an extendent antisense sequence of 22-23 nt. Full-length miR155-based miRNA were generated with restriction sites at both ends to allow the combination of multiple miRNA to one cassette by a successive cloning strategy. The extended antisense sequence resulted only in a small improvement of the RNAi effect in transduced splenocytes (C57BL/6) in case of the miRNA directed at the α018 target site and both miRNA directed at α018 were much less efficient as the corresponding AmiR (Fig. 14E-H). However, the construct with the shorter antisense sequence showed the same knockdown efficiency as the corresponding AmiR in case of the two miR155-based miRNA directed at the α300 target site. This miRNA (miR155α300-B) was chosen for the construction of the miRNA cassette and was therefore designated miRα. Expression of miRα reduced the TCR surface level of transduced splenocytes more than 90%.

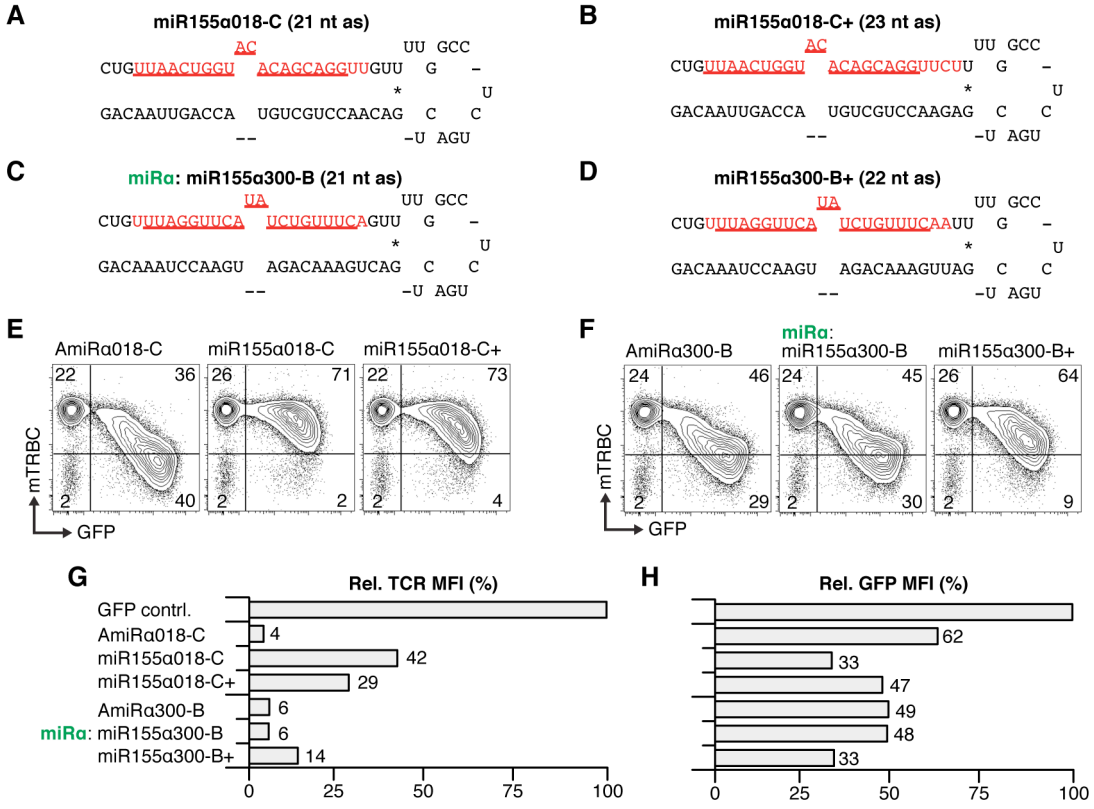

Figure 14: *The miRα demonstrated the best knockdown efficiency out of four miR155 constructs directed at two different TCRα target sites.*
(**A-D**) Secondary structure of miR155 hairpins designed analogous to AmiRα018-C and AmiRα300-B with a variation in the length of the antisense sequence (as, in red). The predicted 19-mer target sequence is underlined. (**E-F**) TCR surface levels and GFP expression of transduced polyclonal splenocytes (C57BL/6) were determined by flow cytometry. (**G-H**) MFI were compared to the parental control vector (GFP contr.). Transduction efficiencies: GFP contr. (74%), AmiRα018-C (77%), miR55α018-C (73%), miR55α018-C+ (77%), AmiRα300-B (75%), miR55α300-B (75%), miR55α300-B+ (73%). Representative results out of multiple experiments are shown.

3.2.5 Intronic miRNA results in superior transgene expression compared to 3' exonic miRNA

Previous experiments in this thesis (Fig. 8) indicated, that intronic miRNA is superior to exonic miRNA in terms of transgene expression. However, a miRNA with a low silencing efficiency was used in the experiment, which was probably not well recognized and processed by the cellular RNAi machinery. In addition, only an exonic position 5' of the GFP and not another possible exonic position located 3' of the GFP was investigated. To confirm the previous findings with a highly efficient miRNA and to include the 3' exonic position, three MP71-GFP vectors were compared encoding the miRβ either at one of the two exonic positions 5' and 3' of GFP or at the intronic position within the 5' untranslated region (Fig. 15A).

All three positions allowed the generation of functional miRNA as the surface TCR on GFP-positive T cells (C57BL/6) was decreased compared to T cells transduced with the unmodified vector and nontransduced GFP-negative T cells (Fig. 15B). Furthermore, a linear relationship of GFP expression and TCR silencing was observed when the miRβ was located at either the 5' intronic or the 3' exonic position, whereas the location of the miRβ at the 5' exonic position resulted in a heterogeneous cell population composed of GFP-negative cells with decreased surface TCR and weak GFP-positive cells with almost no surface TCR. On average, the miRβ reduced the surface TCR by more than 90% independent of its position (Fig. 15C). However, at the same time the expression of the GFP transgene was also diminished by the introduction of the miRNA compared to the parental vector. Depending on the miRNA position, expression levels ranged from 32% for the 5' intronic position to 2% and 15% for the 5' and 3' exonic positions, respectively (Fig. 15D). These data confirmed previous findings of this study and further demonstrated that intronic miRNA results in superior transgene expression compared to 3' exonic miRNA.

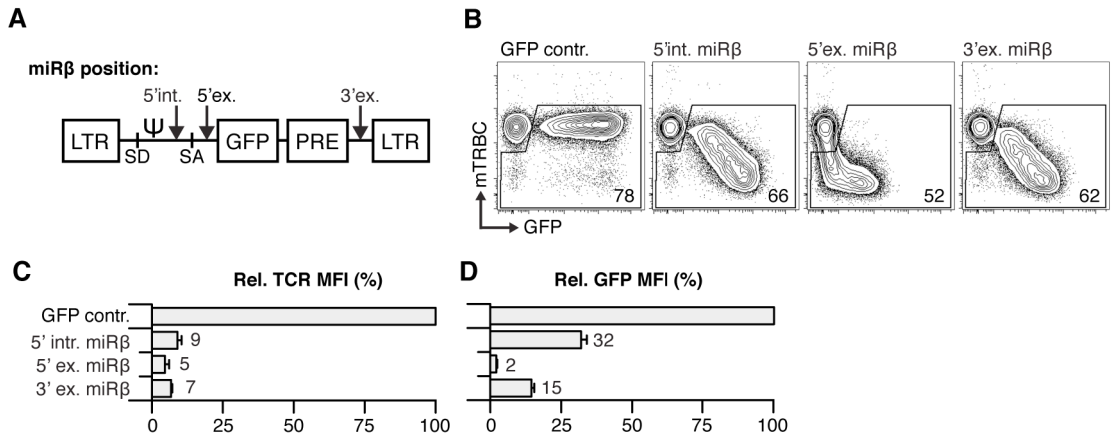

Figure 15: *Intronic miRNA results in superior transgene expression compared with exonic miRNA.*
(**A**) The miRβ targeting at the TCRβ chain was introduced in GFP-encoding MP71 vectors at following positions: 5' intronic (5' int.), 5' exonic (5' ex.) and 3' exonic (3' ex.). Abbreviations: long terminal repeat (LTR), splice donor (SD), packaging signal (Ψ), splice acceptor (SA), post-transcriptional regulatory element (PRE). (**B**) TCR surface levels and GFP expression of transduced polyclonal splenocytes (C57BL/6) were determined by flow cytometry. The percentage of gated cells is indicated. (**C-D**) The MFI were compared to the parental control vector (GFP contr.). Transduction efficiencies: contr. GFP (83%, 78%), 5' int. miRβ-GFP (66%, 68%), 5' ex. miRβ-GFP (52%, 45%), 3' ex. miRβ-GFP (62%, 63%). Plots show the mean of two independent experiments ± SD (*n*=2).

3.3 Analysis of RNAi-TCR gene-modified mouse T cells

Vectors expressing a single miRNA and GFP were used to identify two highly efficient miRNA for the knockdown of the mouse TCR and to quantify the RNAi effect on the protein level with single-cell resolution by flow cytometry. In the third part of the project, the GFP transgene was exchanged for an RNAi-resistant TCR cassette with silent mutations at the RNAi target sites and a cassette with both miRNA was introduced into the vector. It was then investigated whether the RNAi effect of the miRNA

compensates for the lower transgene expression levels of the miRNA-encoding vectors and whether the TCR gene-modified T cells with silenced endogenous TCR bear an advantage over TCR gene-modified T cells generated with conventional vectors. How the expression of the miRNA affect the surface expression of the transferred TCR chains was analyzed in *in vitro* experiments by flow cytometry. The functionality of the RNAi-TCR gene-modified T cells was analyzed in two mouse models. In the first model, the ability of adoptively transferred RNAi-TCR gene-modified T cells to engraft, to expand upon antigen-specific stimulation and to exert antigen-specific effector functions was analyzed in tumor bearing mice. Afterwards, a second mouse model was used to investigate the formation of self-reactive mixed TCR dimers on TCR gene-modified T cells generated either with the RNAi-TCR replacement vector or with conventional vectors. The experiments using the TI-GVHD mouse model were conducted in cooperation with G. Bendle and C. Linnemann (group of Prof. T. N. Schumacher, The Netherlands Cancer Institute, Amsterdam) and the analysis of the histological specimens were performed in cooperation with S. Schulz (Institute of Pathology, Charité Campus Mitte, Berlin).

3.3.1 Silencing of the endogenous TCR supports the expression of an RNAi-resistant second TCR

To analyze how the reduced transgene expression strength of the miRNA vectors influences their ability to express a second TCR in T cells and how the RNAi-mediated silencing of the endogenous TCR in turn supports the surface expression of a transferred TCR, the GFP of the miRNA vector was exchanged for a P14 TCR cassette with silent mutations at the RNAi target sites. This TCR recognizes the MHC class I-restricted GP33-41 epitope of lymphocytic choriomeningitis virus (LCMV) glycoprotein. Three vectors were compared encoding in addition to the RNAi-resistant P14 TCR cassette either the miRα and miRβ separately or combined (miR) (Fig. 16A). In T cells transduced with the miR cassette-encoding vector (miR-P14), only the net result of the negative and positive influences can be measured. However, in T cells transduced with vectors encoding a single miRNA, one of both P14 TCR chains is not supported by the RNAi effect. The surface expression of this TCR chain can be compared to the surface expression of the same chain on T cells transduced with vectors encoding the appropriate miRNA to determine the supportive RNAi effect. 62% of the T cells expressed both P14 TCR chains (Vα2, Vβ8) at high levels after transduction with the miR-P14 vector, whereas T cells generated with similar transduction efficiencies using vectors encoding single miRNA expressed only one of the P14 TCR chains at a high level (Fig. 16B). Only the P14 TCR chain was preferentially expressed whose endogenous counterpart was silenced by miRNA. Specifically, miRα-P14 vector-transduced cells showed relative Vα2 and Vβ8 chain levels of 76% and 41%, whereas miRβ-P14 vector-transduced cells showed relative Vα2 and Vβ8 chain levels of 16% and 117% (Fig. 16C). These data demonstrated two points: First, the expression of the miR cassette resulted in simultaneous silencing of both endogenous TCR chains and second, the low transgene expression level of the miRNA vector could be compensated by the reduction of TCR competition in TCR gene-modified T cells.

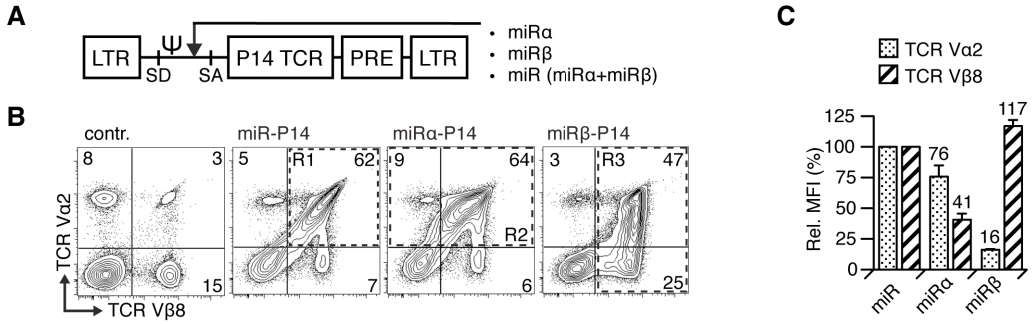

Figure 16: *Silencing of the endogenous TCR supports the expression of a transferred RNAi-resistant TCR.* (**A**) P14 TCR-encoding MP71 vectors expressing either each miRNA for the silencing of the TCRα (miRα) and β chain (miRβ) separately or both miRNA together (miR). (**B**) The P14 TCRα (Vα2) and β chain (Vβ8) surface levels of transduced polyclonal T cells (C57BL/6) were analyzed by flow cytometry. CD8 T cells are shown. Numbers indicate the percentage of cells in each of the quadrant gates. Nontransduced T cells served as control (contr.). MFI of the transduced cells were calculated using the gates R1 (miR-P14), R2 (miRα-P14) and R3 (miRβ-P14). (**c**) MFI of cells expressing only one miRNA were compared to cells expressing both miRNAs. Transduction efficiencies: miR-P14 (62%, 62%); miRα-P14 (73%, 65%); miRβ-P14 (72%, 70%). Plot shows the mean of two independent experiments ± SD (*n*=2).

3.3.2 MHC multimer staining of transduced TCR-transgenic T cells demonstrates the knockdown of the endogenous TCR

P14 TCR gene-modified T cells with and without silenced endogenous TCR were further characterized in an experimental setting that allowed the staining of the endogenous and transferred TCR using MHC multimers. In this setting, TCR I-transgenic T cells instead of polyclonal T cells were transduced either with the P14 or miR-P14 vector. TCR I specifically recognizes the simian virus 40 large tumor antigen epitope I ($SV40_I$) presented by MHC I. Furthermore, differences in the transduction efficiency between the two samples were avoided by the use of viral supernatants equilibrated in titer. The surface levels of the P14 TCR chains on the transduced cells differed between both samples despite similar transduction rates (Fig. 17, A and B). Silencing of the endogenous TCR increased the surface level of the P14 TCRα chain (Vα2) by more than two fold and resulted in a small increase of the P14 TCRβ chain (Vβ8). A more striking difference between both samples was observed, when the T cells were stained with MHC multimers specific for the transferred P14 TCR (Db-GP33) and the transgenic TCR-I (Db-$SV40_I$). The whole population of Db-GP33-positive T cells generated with the conventional P14 vector did still bind the Db-$SV40_I$ multimer clearly indicating that both TCR are expressed at the cell surface (Fig. 17C). The MFI of the Db-$SV40_I$ multimer was only reduced to 72% by the expression of the P14 TCR compared to nontransduced TCR I-transgenic T cells (Fig. 17D). In contrast, two third of the Db-GP33-positive T cells that were generated with miR-P14 vector did not bind the Db-$SV40_I$ multimer anymore due to the downregulation of the transgenic TCR. The MFI of the Db-$SV40_I$ multimer was reduced to 4% compared to nontransduced T cells and the MFI of the Db-GP33 multimer was almost doubled compared to the T cells transduced with the P14 vector. These data

confirmed directly that the expression of the miR cassette reduces the surface levels of the endogenous TCR in RNAi-TCR gene-modified T cells and thereby facilitates the expression of the transferred TCR.

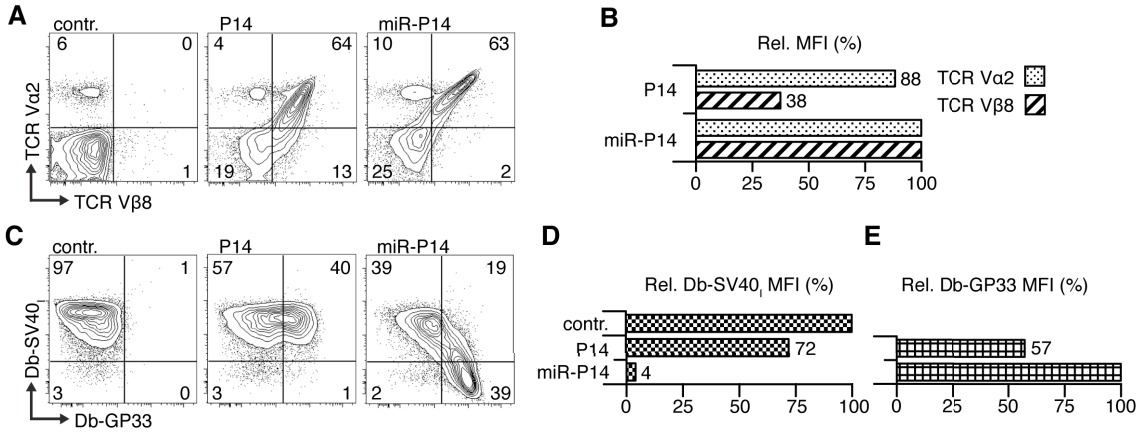

Figure 17: *MHC multimer staining demonstrates RNAi-assisted TCR replacement in transduced TCR I-transgenic T cells.*
(**A**) The P14 TCRα chain (TCR Vα2) and P14 TCRβ chain (TCR Vβ8) surface levels of transduced SV40I-specific TCR I-transgenic T cells were determined by flow cytometry. Nontransduced T cells served as a control (contr.). The percentage of gated cells is indicated. (**B**) The MFI of the transduced cells expressing the P14 TCR without the miRNAs were compared to the MFI of the cells transduced with the miRNA vector. (**C**) The transduced cells were also stained with a TCR I-specific (Db-SV40$_I$) and with a P14 TCR-specific (Db-GP33) MHC multimer. (**D-E**) The MHC multimer staining of the endogenous SV40$_I$-specific TCR was analyzed by comparing the transduced samples to the nontransduced control. The MHC multimer staining of the transferred P14 TCR was analyzed by comparing the miR-P14 vector-transduced T cells with the P14 vector-transduced T cells. Representative results of one out of two experiments are shown.

3.3.3 RNAi-mediated TCR replacement in contrast to TCR gene optimization results in equal surface levels of the transferred TCR chains

After it was established that both miRNA of the RNAi-TCR replacement vector are functional and that both transferred TCR chains are efficiently expressed at the surface of transduced T cells, experiments were conducted to analyze in detail, how the silencing of the endogenous TCR affects the surface expression of the transferred TCR in comparison to other optimization strategies. For this purpose, an optimized P14 TCR cassette was constructed by the introduction of a second disulfide bond into the TCR C regions and codon optimization. Then, the native P14 TCR cassette of the P14 and miR-P14 vector was exchanged for the optimized P14 TCR cassette generating the vectors P14opt and miR-P14opt. Furthermore, the transduced T cells were compared to population of nontransduced T cells expressing endogenously the Vα2 and Vβ8 chain at a 1:1 stoichiometry. Through this comparison, it was possible to assess the degree of TCR replacement and the molar ratio of the transferred TCR chains. Although the TCR gene-modified T cells were generated with comparable transduction efficiencies using supernatants equilibrated in viral titer (Fig. 18A), the surface levels of the P14 TCRα and β chain differed markedly between the samples (Fig. 18, B and C). Compared to the Vα2- and Vβ8-

positive nontransduced T cells, the P14 vector-transduced cells showed reduced and disparate TCRα and β chain levels of 24% and 64%, respectively (Fig. 18C). Notably, silencing of endogenous TCRs strongly reduced the difference between both TCR chain levels. For example, the TCRα chain level was improved from 24% to 36%, whereas the TCRβ chain level was reduced from 64% to 42% if the miRNA cassette was expressed in addition to the native P14 TCR. Importantly, this adjustment of the MFI values was a unique effect of RNAi-mediated TCR silencing, because TCR gene optimization as employed in the P14opt vector did not change the difference between the MFI values similarly, but instead raised them individually to 46% and 78% for the TCRα and β chain, respectively. Overall, the expression of the transferred TCR chains on miR-P14opt vector-transduced cells, which combined high TCR surface levels with a 1:1 stoichiometry (TCRα chain 81%, TCRβ chain 86%), resembled most the surface TCR on the nontransduced T cells expressing endogenously the Vα2 and Vβ8 chain. Likewise, the miR-P14opt vector-transduced T cells showed the highest percentage of Db-GP33-positive cells with the highest MFI, followed by the cells transduced with the P14opt, miR-P14 and P14 vector, respectively (Fig. 18, D and E). However, TCR gene optimization (codon optimization in combination with an additional disulfide bond) improved MHC multimer binding more effectively than the silencing of the endogenous TCR. In particular, the ratio of P14 TCR expressing cells to Db-GP33-positive cells was improved from 0.41 to 0.50 if the miR cassette was expressed in addition to the native P14 TCR, but optimization of the P14 TCR improved this ratio to 0.65 (Fig. 18D). Furthermore, compared to P14 vector-transduced cells the Db-GP33 MFI was 1.14 fold improved by TCR silencing and 1.65 fold by TCR gene optimization (Fig. 18E). Notably, the combination of the miR cassette with the optimized P14 TCR resulted in a greater improvement of the Db-GP33 MFI than the combination of the miR cassette and the native P14 TCR. Collectively, these data revealed that silencing of the endogenous TCR and TCR gene optimization affected the P14 TCRα and β chain levels in different ways. The amount of transferred P14 TCR on the cell surface was increased to a greater extent by TCR gene optimization but, in contrast to TCR silencing, this technique did not result in equal P14 TCRα and β chain surface levels, which implied that the amount of mixed TCR dimers was not concomitantly reduced.

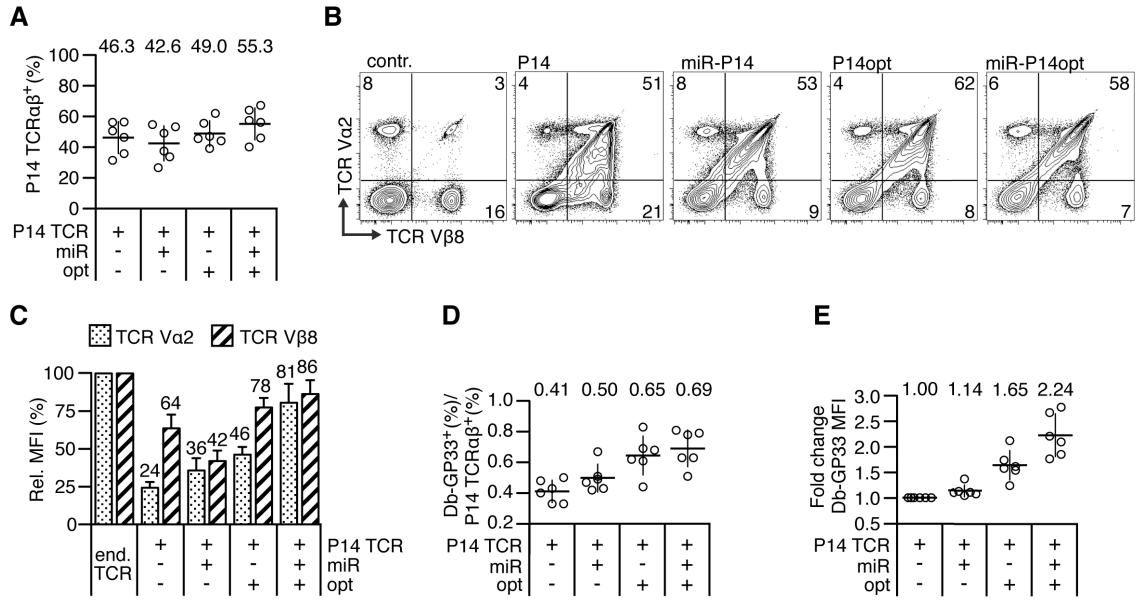

Figure 18: *RNAi-mediated TCR replacement results in equal surface levels of the transferred TCR chains.*
(**A**) Polyclonal T cells (C57BL/6) were transduced with four P14 TCR vectors differing from each other by the presence of the intronic miR cassette (miR) and the usage of the optimized P14 TCR cassette (opt). Comparable transduction efficiencies were achieved using viral supernatants equilibrated in titer. (**B**) T cells were stained for CD8 and for both P14 TCR chains (TCR Vα2, TCR Vβ8). CD8 T cells are shown and the percentages of the gated cells are indicated. Nontransduced T cells served as control (contr.). (**C**) MFI of transduced CD8 T cells were compared to nontransduced Vα2/Vβ8 double-positive CD8 T cells (end. TCR). (**D**) Plot shows the proportion of CD8 T cells expressing both P14 TCR chains that bind the Db-GP33 multimer. (**E**) Plot shows the fold change of the Db-GP33 multimer MFI relative to the P14 vector-transduced sample. Horizontal bar (group mean, indicated on top). Vertical bar (SD). Data of six independent experiments are shown in **A**, **C**, **D**, **E** (n=6). Representative data of these experiments are shown in **B**.

3.3.4 RNAi-TCR gene-modified T cells show anti-tumor reactivity and increased antigen-specific proliferation

After the specific RNAi effects of the miR cassette were studied in the previous experiments, the functional reconstitution of the T cells with silenced endogenous TCR by the expression of RNAi-resistant P14 TCR was analyzed. Hypothetically, the expression of the miRNA cassette could induce off-target effects, either in a sequence specific manner or by saturation of the endogenous miRNA pathway, resulting in impaired cell survival, proliferation or effector function. No differences were found in the proliferative capacity and stability of TCR expression between P14 and miR-P14 vector-transduced T cells after three weeks of *in vitro* culture (Fig. 19, A and B). Furthermore, TCR gene-modified T cells generated with all four P14 TCR vectors showed no differences in INF-γ production or peptide-sensitivity after stimulation with titrated amounts of GP33 peptide (Fig. 19C).

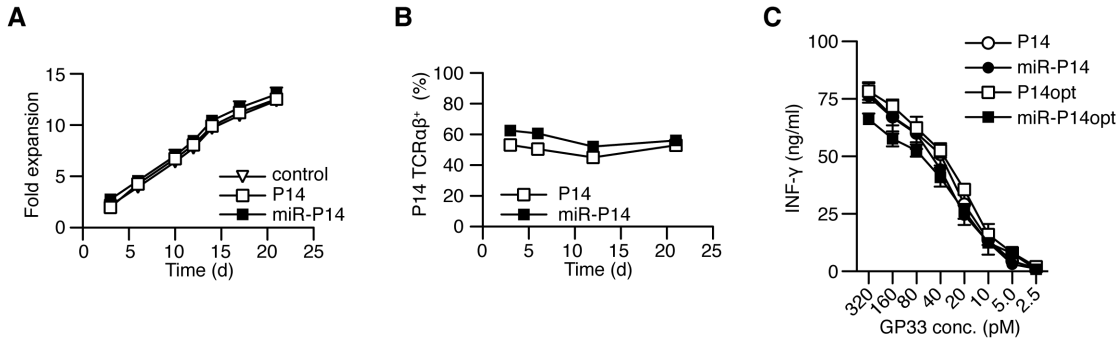

Figure 19: *No miRNA off-target effects were detected in* in vitro *assays testing proliferative capacity and antigen-stimulated cytokine production.*
(**A**) The fold expansion of polyclonal T cells (C57BL/6) transduced either with the P14 vector or with the miR-P14 vector was determined over three weeks of *in vitro* culture. Nontransduced T cells served as a control. Plot shows means of replicates (2-3) ± SD. (**B**) The percentage of CD8/P14 TCRαβ T cells was determined by flow cytometry. (**C**) INF-γ secretion of P14 TCR-transduced polyclonal T cells stimulated with titrated amounts of peptide. Plot shows means of duplicates ±SD. Representative results of one out of two independent experiments are shown. Transduction efficiencies: P14 (51%), miR-P14 (53%), P14opt (62%), miR-P14opt (58%).

Furthermore, the *in vivo* functionality of RNAi-TCR gene-modified T cells was analyzed in a tumor suppression model. Mice that were injected with GP33-expressing B16.F10 melanoma cells were treated with transduced T cells and the engraftment and expansion of the transferred cells, as well as suppression of tumor growth was analyzed. Enhanced on-target effects due to differences in the P14 TCR surface levels, however, might not be observable as it was demonstrated that even P14 TCR-transgenic T cells were hardly more effective than P14 vector-transduced T cells in this model [239]. Indeed, comparable suppression of tumor growth was achieved irrespective of the particular vector used for transduction as no significant differences in the number of experimental pulmonary metastasis among the treatment groups were observed (Fig. 20A-C). The average number of experimental metastases was 27 for the P14 group and 25 for the P14opt group, showing that the increase of the P14 TCR level by TCR gene optimization did not significantly alter the outcome. No negative effects of the miR cassette were detected either, as on average 30 and 22 experimental metastasis were found in the groups that received T cells expressing the miR cassette and either the native or optimized P14 TCR. Successful engraftment, proliferation and stable TCR expression was confirmed by analyzing peripheral blood samples at day seven and 14 after transfer (Fig. 20D-G). Regardless of whether the miR cassette was expressed together with the native or optimized P14 TCR, the percentage and MFI of Db-GP33-positive cells were significantly increased. After one week, on average 36% and 55% of the transferred CD8-positive T cells were stained by the Db-GP33 multimer in the P14 and P14opt group, respectively, whereas 59% and 83% Db-GP33-positive cells were detected in the miR-P14 and miR-P14opt group, respectively (Fig. 20D). The Db-GP33 MFI was increased from $1.8x10^3$ AU to $2.3x10^3$ AU if the miRNA were expressed in addition to the native P14

TCR and from 2.8x10³ AU to 3.8x10³ AU if they were expressed in addition to the optimized P14 TCR (Fig. 20E). Similar results were obtained from a second measurement at day 14 (Fig. 20, F and G). These data provided no evidence for RNAi-related off-target effects. On the contrary, the data indicated that the increased amount of P14 TCR resulted in enhanced antigen-driven proliferation of transferred T cells expressing either the miR cassette or the optimized P14 TCR, with the greatest levels of proliferation being seen with the combination of both.

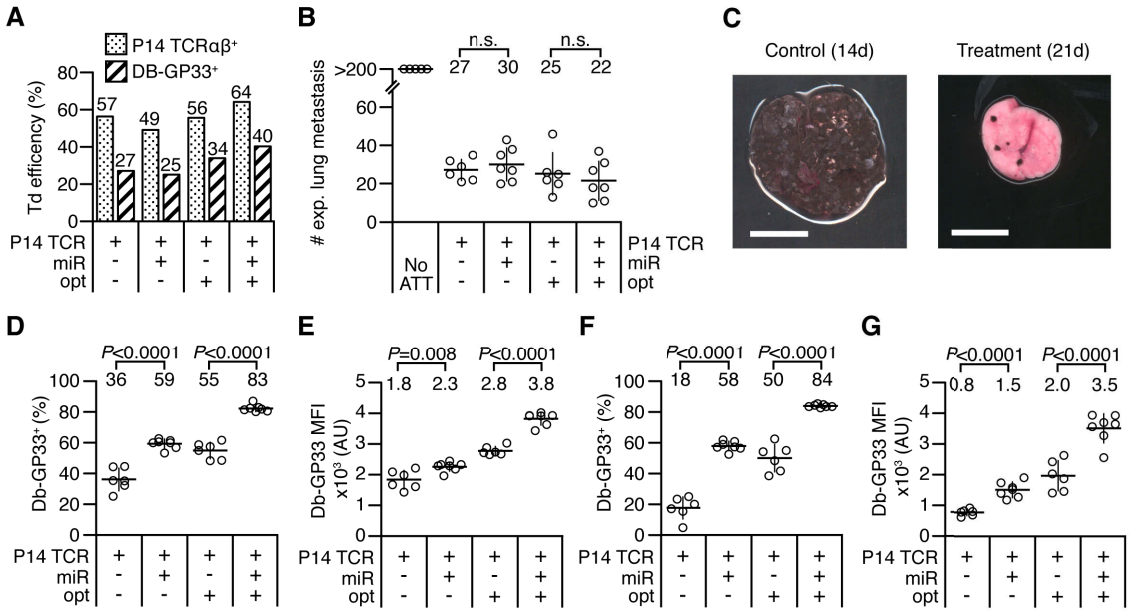

Figure 20: *miR-TCR gene-modified T cells show anti-tumor reactivity and increased antigen-specific proliferation.*
(**A**) Transduced polyclonal T cells (B6.SJL) were analyzed either for the expression of both P14 TCR chains (P14 TCRαβ) or binding of the P14 TCR-specific MHC multimer (Db-GP33) at the day of adoptive T cell transfer (ATT). 2x10⁶ congenic CD8/P14 TCRαβ T cells were transferred into recipients (C57BL/6) that received 3 days before 1x10⁶ GP33-expressing tumor cells (B16-GP33) intravenously. (**B**) Plot shows the number of macroscopically visible experimental (exp.) lung metastasis 21 days after ATT. The mice of the control group without ATT were sacrificed after 14 days. (**C**) Representative lungs of the control and treatment group at the indicated days after ATT. Scale bar: 1 cm (**D-G**) Transferred T cells (CD8/CD45.1) in peripheral blood were analyzed either at day 7 (**D** and **E**) or at day 14 (**F** and **G**) after ATT. Symbols represent individual mice. Horizontal bar (group mean, indicated on top). Vertical bar (SD). Group sizes: P14 (*n*=6), miR-P14 (*n*=7), P14opt (*n*=6), miR-P14opt (*n*=7), control (*n*=5).

3.3.5 P14 TCR gene transfer induces the formation of self-reactive mixed TCR dimers

The formation of self-reactive mixed TCR dimers on P14 TCR-transduced T cells was analyzed in a mouse model, in which mixed TCR dimers induce TI-GVHD. This model closely mimics the clinical protocol of TCR gene therapy. First, the TCR gene-modified T cells were transferred into hosts that were rendered lymphopenic by nonmyeloablative total body irradiation and, second, the hosts were treated after the cell transfer for three days with high-dose IL-2. The autoimmunity in this model is

characterized by a rapid decrease in body weight in combination with a general destruction of the hematopoietic compartment leading to anemia and the depletion of lymphocytes in the secondary lymphoid organs. The previous data in this thesis indicated that the P14 TCR would very likely cause a high incidence of TI-GVHD because the P14 TCR chains were highly unequal expressed on the surface of transduced T cells even when using a vector encoding a TCR cassette with a 2A element (Fig. 18C). Indeed, all mice (C57BL/6) that received transduced T cells expressing the native P14 TCR developed lethal TI-GVHD within 30 days, whereas no autoimmunity was induced after transfer of P14 TCR-

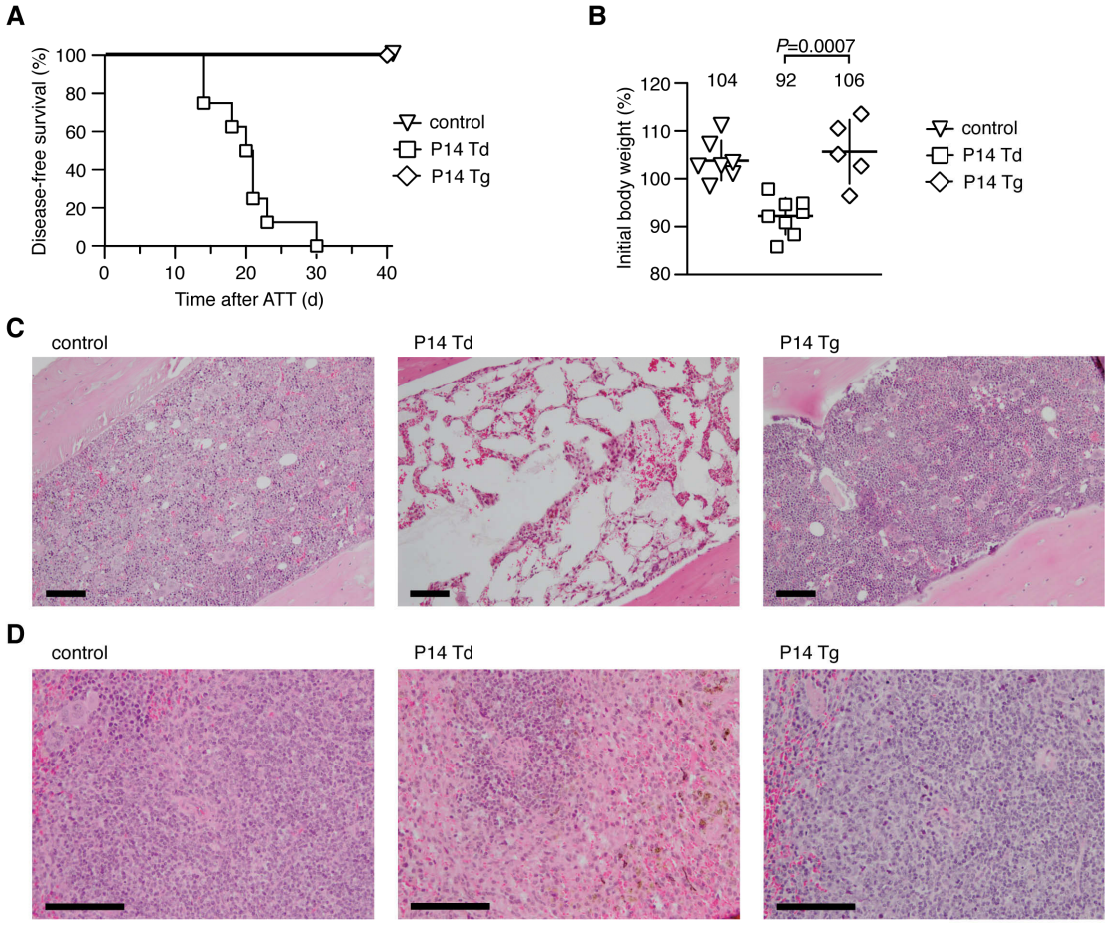

Figure 21: *TI-GVHD is induced by P14 TCR-transduced but not by P14 TCR-transgenic T cells.*
(**A, B**) Cell populations containing 1x10^6 P14 TCR-expressing CD8 cells were transferred into irradiated mice (C57BL/6). 10 days after adoptive T cell transfer (ATT) the mice were treated for 3 days with IL-2 twice a day and monitored for autoimmune symptoms. The control group was treated identical but received nontransduced T cells. A Kaplan–Meier plot of disease-free survival and the change of body weight at day 14 after ATT are shown in **A** and **B**, respectively. Horizontal bar (group mean, indicated on top). Vertical bar (SD). Group sizes, Td efficiency: control (n=7), P14 Td (n=8, 20%), P14 Tg (n=5). (**C, D**) Femur and spleen were collected either at the time point when the mice had to be sacrificed because of TI-GVHD (P14 Td) or 40 days after ATT (P14 Tg, control). Sections of formalin-fixed and paraffin-embedded tissue were stained with H&E. Bone marrow sections in **C** demonstrate the disappearance of hematopoietic cells in recipients of P14 TCR-transduced T cells (P14 Td). Spleen sections in **D** demonstrate that also the periarteriolar lymphatic sheaths (PALS) are significantly reduced in mice of this group (P14 Td). Samples of four mice from each group were analyzed. The scale bars in **C** and **D** represent 100 µM.

transgenic T cells or nontransduced T cells (control) (Fig. 21A). The observed symptoms and kinetics were similar to those described for other TCR in this model, including the rapid weight loss (Fig. 21B). The disappearance of hematopoietic cells in the bone marrow and the massive reduction of the periarteriolar lymphatic sheaths (PALS) in the spleen, two characteristic manifestations of TI-GVHD, were confirmed in recipients of P14 TCR-transduced T cells (Fig. 21, C and D). The same organs from recipients of P14 TCR-transgenic or nontransduced T cells did not show pathologic changes. The data indicated, that the autoimmunity observed in this mouse model was mediated by self-reactive mixed TCR dimers expressed on the surface of P14 TCR-transduced T cells.

3.3.6 RNAi-mediated TCR replacement severely reduces the incidence of TI-GVHD

The previous experiment established, that the P14 TCR is particularly prone to induce autoimmunity in the TI-GVHD mouse model. This experimental setting therefore represented a very stringent *in vivo* assay for strategies to reduce the formation of self-reactive mixed TCR dimers after TCR gene transfer. How the development of TI-GVHD is affected by TCR silencing or by the usage of codon-optimized TCR genes that harbor a second disulfide bond was investigated using the four P14 TCR vectors, which differed from each other by the presence of the intronic miR cassette (miR) and the usage of the optimized P14 TCR cassette (opt).

All mice (C57BL/6) that received transduced T cells expressing the native or the optimized P14 TCR developed lethal TI-GVHD (Fig. 22A). In contrast, despite the high incidence of TI-GVHD observed following gene transfer with the native P14 TCR, only three out of 16 mice that received P14 TCR-transduced T cells with silenced endogenous TCR developed TI-GVHD. Moreover, when RNAi-mediated knockdown of the endogenous TCR was combined with the expression of the optimized P14 TCR genes, only one mouse out of 16 developed TI-GVHD. The body weights of the two groups that were treated with T cells just expressing the native or optimized P14 TCR differed significantly from those two groups that were treated with T cells expressing the same TCR but in addition also the miR cassette (Fig. 22B). Analysis of peripheral blood confirmed engraftment and expansion of transduced T cells. These data demonstrated that in case of the P14 TCR only the silencing of the endogenous TCR and not the use of optimized TCR genes efficiently reduced the amount of mixed TCR dimers on TCR-transduced T cells and the incidence of lethal TI-GVHD in mice receiving these cells.

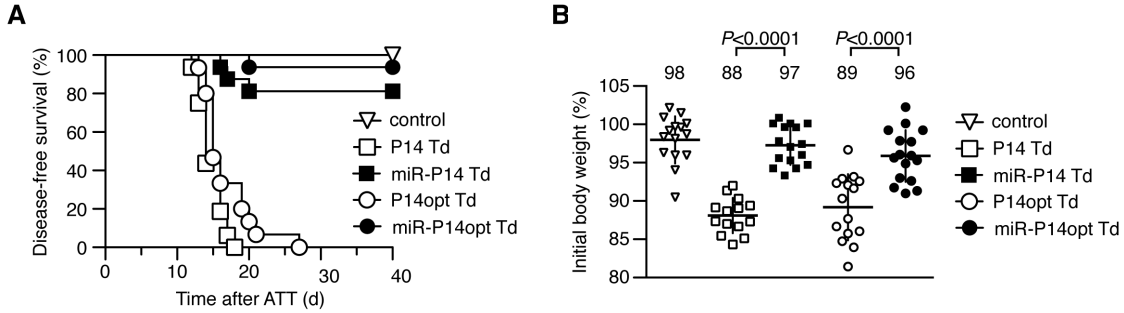

Figure 22: *RNAi-assisted TCR protein replacement severely reduces the incidence of TI- GVHD caused by mixed TCR dimers.*
(**A**) 1x10^6 polyclonal P14 TCR-transduced T cells (C57BL/6) were transferred into lymphopenic hosts (C57BL/6) that were treated 10 days after the adoptive T cell transfer (ATT) for 3 days with high dose IL-2 twice a day and closely monitored for autoimmune symptoms. The control group (contr.) was treated identical but received nontransduced T cells. (**B**) Change of body weight at day 12 after ATT. Symbols represent individual mice. Two mice of the P14 group had to be sacrificed because of TI-GVHD at day 11 and were therefore not included. Horizontal bar (group mean, indicated on top). Vertical bar (SD). Cumulative results of two independent experiments are shown. Group sizes and transduction efficiencies: control (*n*=15), P14 (*n*=16, 55%, 56%), miR-P14 (*n*=16, 35%, 62%), P14opt (*n*=15, 44%, 21%), miR-P14opt (*n*=16, 65%, 57%).

3.4 Generation and analysis of human TCR gene-modified T cells with silenced endogenous TCR

The RNAi strategy, which was developed in the previous parts of the project for mouse T cells, was translated to human T cells in the last part of the project. New highly efficient miRNA specific for the human TCRα and β chain were identified and an RNAi-TCR replacement vector for the generation of human RNAi-TCR gene-modified T cells was constructed. The effect of TCR silencing on the surface expression of a human TCR specific for the CT antigen MAGE-A1 was compared to established strategies of TCR gene optimization, which included the introduction of a second disulfide bond and minimal murinization. The analysis of the human TCR gene-modified T cells was hampered by the fact, that the TCRα chain of the transferred TCR could not be stained directly by using mAb. Therefore, an indirect staining strategy was established: The endogenous TCR chains expressed on TCR gene-modified T cells instead of the transferred TCR chains were stained. This staining strategy allowed to analyze whether the two transferred TCR chains were unequally expressed at the cell surface and how the surface expression was affected by TCR silencing and TCR gene optimization.

3.4.1 Identification of efficient miRNA for the knockdown of human TCR

The analysis of the human TCR sequences and the prediction of RNAi target sites was performed as previously described in this study for the mouse TCR. Ten miRNA directed at the human TCR Cα sequence and 13 miRNA directed at the homologous parts of the human TCR Cβ1 and Cβ2 sequences were constructed. The new AmiR hairpins were designed as described for the mouse TCRα chain-specific AmiRα018-C (format C), which showed the highest silencing efficiency of all mouse TCR-

specific miRNA (Fig. 13 and 14), and cloned into the MP71-GFP vector encoding the AmiR backbone sequence as described (Fig. 12A).

About half of the TCRα chain-specific miRNA reduced the surface level of the TCR/CD3 complex on transduced Jurkat cells by more than 40% (Fig. 23A). Cells expressing the two most efficient constructs AmiRα109 and AmiRα319 showed CD3 levels of 20% and 15%, respectively. The relative GFP expression levels of the samples ranged between 40% and 63% (Fig. 23B). In contrast, only two of the 13 miRNA directed at the human TCRβ chain reduced the CD3 levels to 50% or lower (Fig. 23C). Expression of the AmiRβ034 and AmiRβ433 resulted in CD3 levels of 50% and 45%, respectively. One of the vectors (AmiRβ204) resulted in an exceptional high GFP level of 90%, but the mean value of the other samples was 47% (Fig. 23D). Overall, the GFP levels of the transduced Jurkat cells were somewhat higher compared to similar experiments in the mouse B3Z cell line. The two most efficient miRNA for each TCR chain were selected to be further analyzed in primary human T cells.

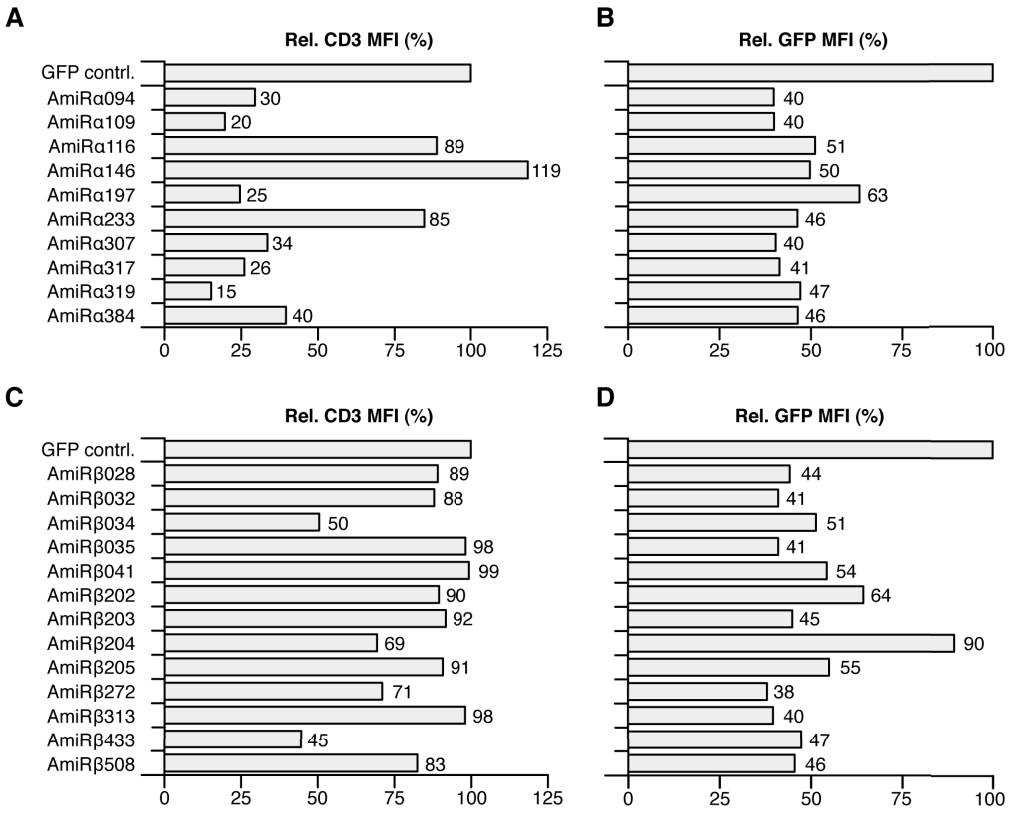

Figure 23: *Decreased surface levels of the TCR/CD3 complex on Jurkat cells transduced with vectors expressing miRNA directed at the human TCR.*
(**A-B**) The human Jurkat T cell line was transduced with GFP-encoding vectors expressing artificial miRNA (AmiR) directed at the human TCRα chain. The cells were stained using a CD3-specific mAb. TCR/CD3 surface levels and GFP expression was determined by flow cytometry. Mean Td rate: 25%. Plots show mean values of two independent experiments (*n*=2), except for AmiRα109, AmiRα197 and AmiRα319 (all *n*=1). (**C-D**) TCR surface levels and GFP expression of transduced Jurkat cells expressing AmiR targeting the human TCRβ chain. Mean Td rate: 28%. Plots show mean values of two independent experiments (*n*=2), except for AmiRβ041, AmiR β205, AmiRβ313, AmiRβ508 (all *n*=1) and AmiRβ032 (*n*=3).

3.4.2 Construction of a miRNA cassette for the knockdown of both human TCR chains

The four miRNA selected in the previous experiment, two for each TCR chain, were all based on the AmiR backbone and cannot be combined in a cassette, because direct sequence repeats are not stable in retroviral vectors. Therefore, a second variant for each of the four miRNA was generated based on the mouse miR155 sequence and with the same hairpin design like the mouse TCRα chain-specific miRα (Fig. 14C). In addition, new full-length versions of the four miRNA based on the AmiR sequence were generated. The new miRNA encoded restrictions sites at both ends that allowed the construction of a miRNA cassette as previously described for the mouse TCR-specific miRNA (Fig. 12B).

The two miRNA directed at the target site α319 were more efficient in human T cells as compared to the Jurkat cell line and they outperformed the other two TCRα chain-specific miRNA. In particular, transduction of human T cells with a vector encoding miR155α319 generated a homogenous cell population of which 87% appeared to be surface TCR/CD3-negative in the flow cytometric analysis (Fig. 24A). The MFI of the TCR/CD3 complex was reduced to 10% compared to control cells transduced with the unmodified GFP vector (Fig. 24B). Based on this data the miR155α319 was chosen as miRα for the human RNAi-TCR replacement vector. The relative GFP expression level of the T cells expressing this miRNA was 23%, whereas the GFP levels of the other samples were 31%, 32% and 48% (Fig. 24C). The AmiRβ034 was the most efficient of both TCRβ chain-specific AmiR, although the difference was small (Fig. 24D). Expression of the AmiRβ034 and AmiRβ433 in transduced human T cells reduced the TCR surface level to 22% and 24%, respectively. In addition, the AmiRβ034 sample showed a relative GFP expression level of 50%, which was the highest value of all four samples (Fig. 24E). Therefore, the AmiRβ034 was designated miRβ and combined with miRα to a miR cassette.

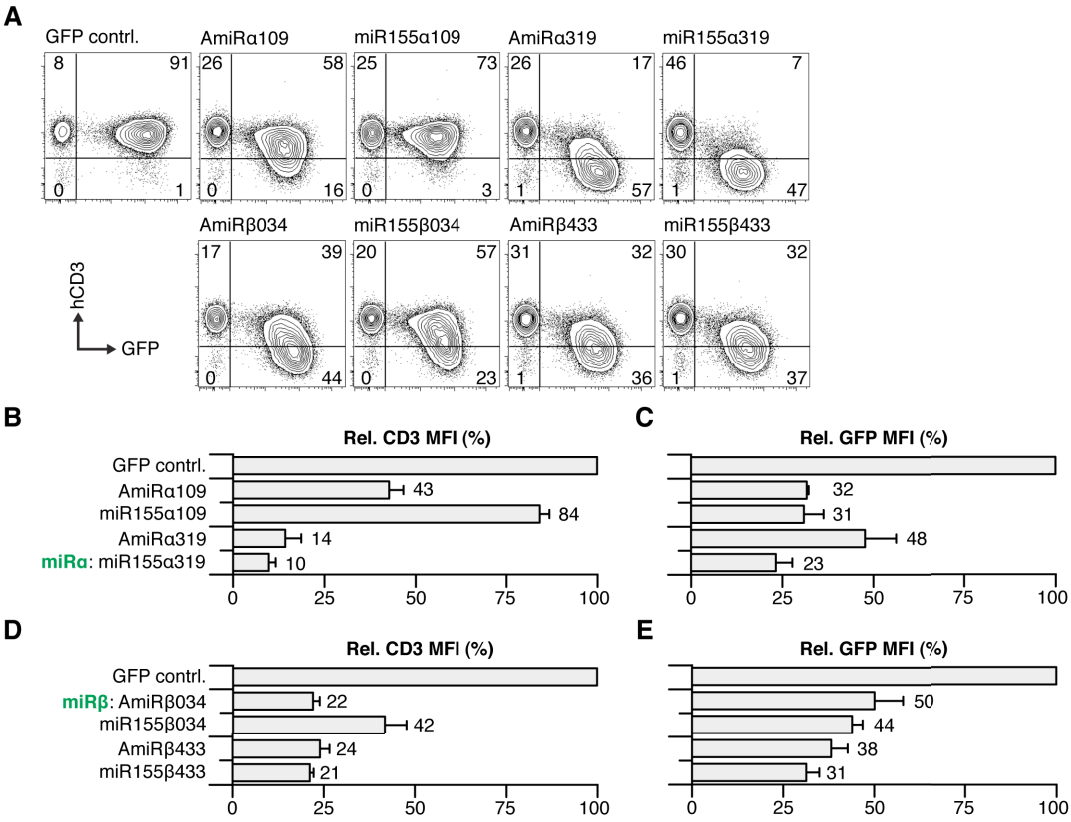

Figure 24: *Knockdown of the endogenous TCR in human transduced T cells.*
(**A**) Human T cells were transduced with four vectors expressing GFP and a miRNA targeting either the TCRα or β chain. The TCR surface levels were measured using a CD3-specific mAb. The percentages of gated cells are indicated. (**B-E**) Plots show TCR surface levels and GFP levels of transduced T cells expressing a miRNA directed at the TCR. Plots in **B** and **C** show mean values (±SD) of two independent experiments (*n*=2), except for AmiRα319 and miR155α319 (*n*=3). Mean Td rate=63%. Plots in **D** and **E** show mean values (±SD) of two independent experiments (*n*=2), except for AmiRβ034 and miR155β034 (*n*=3). Mean Td rate=67%.

3.4.3 RNAi-mediated TCR replacement in human T cells

The 1367 TCR, which recognizes a peptide derived from the CT antigen MAGE-A1 presented on HLA-A2, was used as a model TCR for the analysis of RNAi-mediated TCR replacement in human T cells. This TCR was isolated by M. Obenaus and C. Leitao (group of Prof. T Blankenstein) from transgenic mice expressing a human TCR repertoire and HLA-A2.

To compare the effect of TCR silencing with current strategies to improve TCR pairing by engineering of the TCR C regions, three vectors were constructed each harboring a codon-optimized 1367 TCR cassette. The 1367 vector represents a standard TCR expression vector without further modifications besides codon optimization. Engineering of the TCR C regions by the exchange of nine amino acids of the human sequence for the respective amino acids of the mouse sequence (minimal murinization) and by the introduction of an additional disulfide bond generated the 1367opt vector.

Introduction of the codon-optimized TCR cassette into the RNAi-TCR replacement vector generated the miR-1367 vector. The usage of the three different vectors resulted in slightly different amounts of MHC multimer-positive T cells after transduction. 54%, 42% and 49% of the CD8 T cells transduced with the 1367, 1367opt and miR-1367 vector, respectively, bound the specific MHC multimer (Fig. 24A). Although there was not much difference between the samples in the percentages of cells expressing the transferred TCRβ chain (Vβ3, Fig. 25, B and C), the analysis of the MFI values strongly indicated, that the expression level of the transferred TCRα chain differed between the samples (Fig. 25, D and E): The T cells transduced with the 1367opt and miR-1367 vector bound almost twice as much MHC multimer per cell as compared to 1367 vector-transduced T cells, although no great change in the amount of Vβ3 per cell was detected. Changes in the expression of the transferred TCRα chain, for which no mAb was available, could explain the improved MFI of the MHC multimer staining. To determine whether the transferred TCRα and β chains were expressed at unequal levels on the cell surface and how the engineered TCR C regions or the TCR silencing influenced the surface levels, the transduced T cells were stained with a mix of mAb specific for endogenous TCR chains (Fig. 25, B and C). The mix for the detection of the endogenous TCRα and β chains contained three Vα-specific mAb (Vα2, Vα7.2, Vα12) and six Vβ-specific mAb (Vβ1, Vβ2, Vβ5.1, Vβ13.6, Vβ14, Vβ22), respectively. The mAb mixes, as shown by the nontransduced control sample, stained 15% and 30% of the endogenous TCRα and β chains, respectively. These values and the percentages of double-positive cells from the transduced samples were used to calculate how much Vβ3-positive T cells coexpress endogenous TCR chains if all endogenous TCR V regions would have been stained (Fig. 25F). 64% of the Vβ3-positive T cells express endogenous TCRα chains on their surface, whereas only 33% express endogenous TCRβ chains. In other words, the TCRβ chain of the 1367 TCR is a better competitor compared to the TCRα chain and completely replaced the endogenous TCRβ chains in 67% of all transduced T cells, whereas the endogenous TCRα chains are only replaced in 36% of the transduced T cells. The most prominent effect of the engineered TCR C regions and the silencing of the endogenous TCR was the reduction of the percentage of Vβ3-positive T cells positive for endogenous TCRα chains (Fig. 25F). Only 32% and 21% of the T cells transduced with the 1367opt and miR-1367 vector, respectively, expressed endogenous TCRα chains. The smallest difference between the numbers of T cells coexpressing endogenous TCRα or β chains was detected in the sample transduced with the miR-1367 vector (endo. Vα 21%, endo. Vβ 17%). In addition, these values were also the lowest of the three samples. The functionality of the transduced T cells was confirmed in an INF-γ release assay, which showed no difference between the samples (Fig. 25G).

In conclusion, the TCRα and β chain of the human 1367 TCR showed a similar surface expression pattern as the mouse P14 TCR chains. Staining of the endogenous TCR on the surface of transduced T cells indicated, that the TCRβ chain of the 1367 TCR more efficiently replaced the endogenous TCR chains than the TCRα chain. Furthermore, the data indicated that the RNAi technology established in the mouse model could be successfully translated to human T cells to reduce the formation of mixed

TCR dimers and to improve the safety of TCR gene therapy. Silencing of the endogenous TCR in human T cells prevented that the different abilities of the transferred TCR chains to replace the endogenous TCR chains came into full effect and resulted in equal replacement of the endogenous TCRα and β chain by the transferred TCR chains.

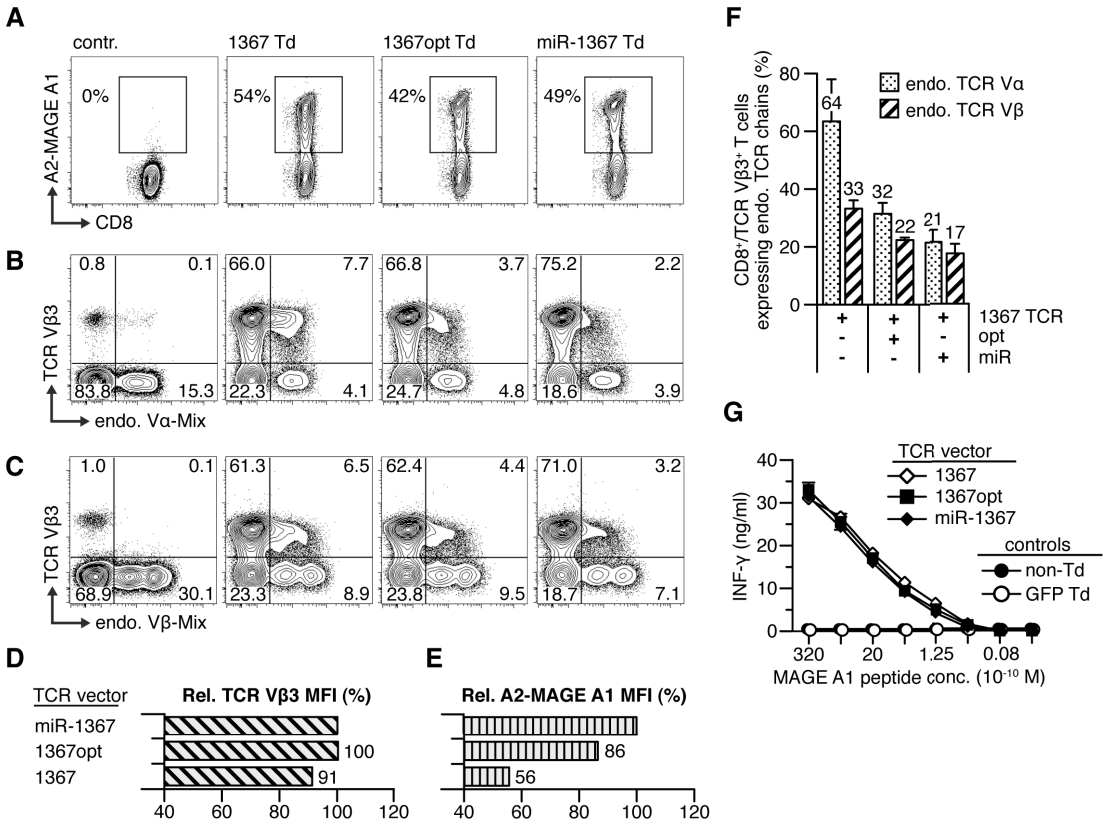

Figure 25: *TCR silencing and engineering of the TCR C regions reduce the expression of endogenous TCR in human TCR-transduced T cells.*
(**A**) The surface TCR on human T cells transduced with either of three vectors encoding codon-optimized genes of the MAGE-A1-specific TCR 1367 was analyzed by flow cytometry. The TCR C regions in the 1367opt vector were modified by minimal murinization and the introduction of a second disulfide bond. In contrast, the miR-1367 vector expresses miRNA for the silencing of the endogenous TCR in addition to the 1367 TCR. Nontransduced T cell served as control (contr.). Plots show MHC multimer (A2-MAGE A1)-stained CD8 T cells. Percentages of positive cells are indicated. (**B-C**) Analysis of the endogenous TCR on transduced CD8 T cells expressing the transferred TCRβ chain (Vβ3). Three Vα-specific mAb (Vα2, Vα7.2, Vα12) were used to detect endogenous TCRα chains (endo. Vα-Mix) and six Vβ-specific mAb (Vβ1, Vβ2, Vβ5.1, Vβ13.6, Vβ14, Vβ22) were used to detect endogenous TCRβ chains (endo. Vβ-Mix). Numbers indicate the percentage of cells in each of the quadrant gates. (**D-E**) The relative MFI of CD8/Vβ3-positive cells and CD8/MHC multimer-positive cells are shown. (**F**) The total amount of transduced CD8 T cells expressing endogenous TCRα (endo. TCR Vα) or β chains (endo. TCR Vβ) on their surface was extrapolated from the data shown in **B** and **C.** Data are represented as the means (±SD) from at least two independent experiments (*n*=2). Data of the TCR 1367 vector are from three experiments (*n*=3). (**G**) INF-γ secretion of the transduced T cells stimulated with titrated amounts of peptide. Plot shows means of duplicates ±SD.

4 Discussion

The treatment of patients with autologous T cells that have been redirected to a target of choice by TCR gene transfer is the most promising approach of immunotherapy to date. The unique capability of T cells to destroy metastasis at virtually any side of the body has already been demonstrated with great success in a significant number of late stage melanoma patients treated with IL-2 alone or in combination with TIL. TCR gene therapy will make this highly effective treatment available for a much broader range of patients whose endogenous T cell repertoire lacks the required therapeutic specificities and who suffer from other forms of cancer.

The high cytotoxic potential of adoptively transferred T cells is accompanied with the risk of autoimmunity if antigens are recognized on healthy tissue. Unfortunately, such side effects were seen in almost every clinical trial of TCR gene therapy so far. On-target toxicity caused by the choice of the wrong antigen as target and off-target toxicity due to the application of unspecific TCR can be avoided in the future, but also preventive measures should be taken into account, so that the number of observed side effects does not unnecessarily expand further.

Contrary to the belief that mixed TCR dimers formed by the combination of endogenous and transferred TCR chains after TCR gene transfer are either not functional or only expressed at insufficient levels to induce side effects, two studies demonstrated that under certain experimental conditions mouse and human TCR gene-modified T cells can be activated by mixed TCR dimers recognizing self-derived antigens. The mixed TCR dimer-induced autoimmunity in the TI-GVHD mouse model depended on the particular TCR that was transferred, how the TCR gene-modified T cells were generated and how the recipients were treated. Each of these parameters is going to be varied in upcoming clinical studies. It is therefore difficult to argue against preventive measures to avoid mixed TCR dimer formation solely because TI-GVHD was not observed in the past clinical studies.

It has been demonstrated in this thesis, that the RNAi-mediated knockdown of the endogenous TCR in TCR gene-modified T cells is superior compared to currently employed modifications of the TCR C regions in preventing the formation of mixed TCR dimers. The translation of this technology to other vectors systems, which are available for the genetic modification of human T cells, will allow the construction of more efficient RNAi-TCR replacement vectors in the future. Alternative technologies that allow the sequence-specific introduction of mutations in the genome to completely shut down the TCR expression are still technically highly demanding and further development is needed before they can be introduced into clinical protocols. Future directions of TCR gene therapy will include the production of T cell grafts with improved *in vivo* functionality and the targeting of tumor-specific antigens. These goals might be only achievable with vector systems that are fast to produce and enable protocols that do not require extensive *ex vivo* manipulation of the T cells.

4.1 Analysis and prevention of mixed TCR dimer formation

This thesis provides first evidence that RNAi-mediated silencing of the endogenous TCR minimizes the expression of mixed TCR dimers on TCR gene-modified T cells and severely reduces the risk of autoimmunity in an *in vivo* model of TCR gene therapy. Previously it has been shown, that an additional disulfide bond in the TCR C regions and the linkage of both TCR chains by a 2A element avoided TI-GVHD in case of one TCR and greatly diminished TI-GVHD in case of another TCR [198]. The data presented here demonstrates, that these measures are not sufficient for TCR such as the P14 TCR for which mixed TCR dimer formation is pronounced (Fig. 22). The unequal surface levels of the P14 TCRα and β chain on transduced T cells indicate that they possess different abilities to compete with the endogenous TCR chains for surface expression (Fig. 18). This difference between the two P14 TCR chains remained dominant even after the TCR genes were codon-optimized and an additional disulfide bond was introduced. The reduction of mixed TCR dimers by these strategies therefore depends on the particular TCR that is transferred. Silencing of the endogenous TCR on the contrary mitigated the TCR competition and resulted in equal surface expression levels of both P14 TCR chains. Since this strategy acts on the endogenous TCR, the mode of action is in principle independent of the particular TCR that is transferred. Furthermore, the unequal TCR chain surface levels after the transfer of both TCR genes could be directly linked to the development of mixed TCR dimer-dependent autoimmunity in an *in vivo* model. All mice in those two groups that received TCR gene-modified T cells with unequal TCRα and β chain surface levels developed fatal TI-GVHD, whereas 86% of the animals survived in both groups that received TCR gene-modified T cells expressing the transferred TCR chains but at equal levels (Fig. 22).

In case of the P14 TCR, the determination of the surface levels of both TCR chains has proven to be a more useful indicator for the amount of mixed TCR dimers compared to either MHC multimer staining or the calculation of the ratio of T cells binding the MHC multimer to T cells expressing the P14 TCR chains (Fig. 18). The reason for this is that the amount of correctly paired P14 TCR per cell might reflect either that a higher percentage of the surface expressed TCR chains is correctly paired or the expression of more correctly paired TCR chains without a change of the ratio of correctly paired TCR chains to mixed TCR dimers. Per definition, MHC multimer binding provides only information about one of the four possible TCR dimers expressed on the surface of TCR gene-modified T cells. It was an unexpected finding of this study that TCR gene optimization improved the MHC multimer binding to greater extends than TCR silencing, although TCR silencing more efficiently reduced the amount of mixed TCR dimers. These results warrant caution in interpreting MHC multimer binding with regard to the amount of mixed TCR dimers. Instead, the determination of the TCR chain surface levels might serve to identify TCR that are prone to induce autoimmunity in the future. Even though the notion that unequal surface levels indicate the formation of mixed TCR dimers has already been made in one of the first studies on human TCR gene-modified T cells [174], the prevalence of this

phenomenon among the TCR that were either suggested for or have already been used in clinical trials of TCR gene therapy is currently unknown. Equal surface levels of the transferred TCR chains on the other hand are a prerequisite for correct TCR chain pairing, but give no information about the pairing itself. For example, both chains of the ovalbumin-specific mouse OT-I TCR are expressed at about equal levels on transduced T cells, although a high incidence of TI-GVHD was observed after the transfer of OT-I TCR-transduced T cells [198]. Hence, equal surface levels of the transferred TCR chains alone do not indicate the absence of mixed TCR dimers, whereas unequal surface levels positively confirm the presence of mixed TCR dimers.

For the majority of mouse and human TCR, the direct staining of both TCR chains is not possible because of a lack of the required TCR V region-specific mAb. For example, commercial suppliers offer three human TCR Vα-specific mAb only. For the human 1367 TCR investigated in this study, only a TCRβ chain-specific mAb was available. For that reason, an alternative staining strategy was employed (Fig. 25). Rather than measuring the surface levels of both transferred TCR chains directly, the percentage of cells expressing endogenous TCR chains in addition to the transferred TCRβ chain was determined. The results indicated that the human 1367 TCR, very similar to the mouse P14 TCR, is also prone to induce mixed TCR dimers, because the transferred TCRβ chain more efficiently replaced the endogenous TCR chains compared to the transferred TCRα chain. Twice as much TCR-transduced T cells expressed endogenous TCRα chains on their surface compared to TCR-transduced T cells expressing endogenous TCRβ chains (Fig. 25).

So far, there is no data connecting mixed TCR dimers on transduced polyclonal T cells with autoreactivity. TI-GVHD has not been observed in past clinical studies using TCR gene-modified T cells [240]. However, mixed TCR dimer-dependent allo- and autoreactivity has been observed *in vitro* after the transfer of TCR in oligoclonal virus-specific human T cells [199]. It is reasonable to assume, that such specificities are present at very low frequencies in TCR-transduced polyclonal T cells, but are not detectable in assays that are typically used to analyze the specificity of the transferred TCR. Furthermore, only nonmodified TIL and not TCR-transduced T cells have been transferred into irradiated patients, but irradiation is a precondition to observe TI-GVHD in the mouse model. Compared to other TIL trials using the same preconditioning of the patient as in the TCR gene therapy studies, an enhanced *in vivo* activity of the transferred T cells was observed after the transfer into irradiated patients [171]. At this point, it can only be speculated whether particular differences between mice and men exist that exclude TI-GVHD in future TCR gene therapy trials employing new TCR and improved protocols. Preventive measures to avoid mixed TCR dimer formation seem advisable.

The initial data from the flow cytometric analysis indicated, that the engineering of the TCR C regions in case of the human 1367 TCR was more effective compared to the mouse P14 TCR. Eleven mutations were introduced into the human TCR C regions, nine mutations that exchanged the amino acids of the human sequence for the respective amino acids of the mouse sequence (minimal

murinization) and two mutations that changed two amino acids into cysteines allowing the formation of a second disulfide bond [211,212,213,214]. For the mouse P14 TCR, naturally only the introduction of a second disulfide bond was applicable. The usage of the engineered human TCR C regions improved the surface expression of the transferred TCRα chain and resulted in higher surface levels of correctly paired TCR as indicated by an increased MFI of the MHC multimer staining. However, whereas the percentage of TCR-transduced T cells coexpressing endogenous TCRα chains was reduced to one-half by the engineered TCR C regions, TCR silencing reduced the percentage to one-third (Fig. 25). In addition, the difference in the replacement of the endogenous TCR chains between the transferred TCR chains was lower for the T cells with silenced endogenous TCR compared to the T cells expressing the genetically engineered TCR chains. Considering that every single of the eleven mutations is potentially immunogenic and that immune reactions towards full mouse TCR have already been observed in patients [241], it is an clear advantage of the RNAi technology to prevent the surface expression of the endogenous TCR more efficiently without the need for any mutations in the TCR protein sequence.

Although this study provided a first view on unequal expression levels of transferred TCR chains on transduced human T cells, additional data is obviously needed to confirm the formation of mixed TCR dimers and, more importantly, to demonstrate that they indeed endow transduced T cells with self-directed specificities. A straightforward approach would be to use the transgenic mouse developed by Li et al. that harbors the full human TCRα and TCRβ chain loci and HLA-A2 to analyze the induction of TI-GVHD by T cells transduced with human TCR [177]. Since the presence of just one MHC molecule represents an unnatural situation that likely limits TI-GVHD, the expression of further MHC I molecules and additional MHC II molecules may be required. To analyze the surface expression levels of both TCR chains, one might considerer alternative molecular probes to mAb for flow cytometry. Aptamers are short nucleic acid oligomers that were demonstrated to bind specifically and with high-affinity to a target of choice [242,243]. The generation of aptamers does not rely on immunization, as they are generated *in vitro* by selecting high-affinity binders in repeated cycles from random libraries of folded single-stranded nucleic acid oligomers. After each selection step, the binding molecules are eluted from the target, amplified by PCR and again selected under more stringed conditions, a method called systematic evolution of ligands by exponential enrichment (SELEX). It has been demonstrated, that whole cells can be used in this procedure for the selection and counter-selection of aptamers binding to cell surface structures (cell-SELEX) [244,245,246]. The usage of syngeneic clonal T cell lines differing in just one TCR chain for cell-SELEX should allow the identification of aptamers specific for TCR V regions for which no mAb are available.

With the required TCR V region-specific probes at hand, it might be possible to answer the question of the prevalence of TCR that are prone to mixed TCR dimer formation, because they are composed of chains that differ in their ability to replace endogenous TCR chains upon expression in polyclonal T cells. In case of the mouse P14 TCR, the human 1367 TCR and at least one other human TCR mentioned in the literature [247], the TCRβ chain was expressed at higher surface levels than the TCRα chain.

Based on the assumption that this phenomenon could be explained by a promiscuous pairing behavior of the TCRβ chain as opposed to a more selective pairing behavior of the TCRα chain, one might further speculate that such TCRβ chains could be overrepresented in the naive TCR repertoire. The TCRβ chain loci are rearranged first during T cell development in the thymus and the TCRα chain loci are only rearranged after a phase of proliferation. In consequence, every TCRβ chain has the chance to pair with a variety of different TCRα chains. The number of positively selected clones expressing the same TCRβ chain but different TCRα chains might be greater for TCRβ chains showing a promiscuous pairing behavior.

4.2 Knockdown of the TCR genes by RNAi

One of the most critical tasks in the development of the RNAi-TCR replacement vectors in this study was the construction of highly efficient miRNA. In a rational approach first suitable RNAi target sites of 19 nt length were identified within selected regions of the TCR sequences using bioinformatic tools, then the guide strands of miRNA hairpins were replaced by the predicted antisense sequences. Mismatches and a central bulge were introduced in the hairpin *via* the passenger strand to generate a secondary structure comparable to endogenous miRNA. Similar strategies have been used successfully in previous studies in the literature for the generation of redirected miRNA [230,248,249]. The knockdown efficiency was quantify in this study on the protein level by flow cytometry in T cells and T cell lines transduced with vectors expressing GFP and the hairpins embedded in miRNA backbones.

Eventually two highly efficient pairs of miRNA for the knockdown of the mouse and human TCR chains were identified. Expression of these miRNA in transduced T cells reduced the surface levels of the mouse TCRα and β chain to 6% and 12%, respectively, and those of the human TCRα and β chain to 10% and 22%, respectively. In the flow cytometric analysis, 40% and 16% of the transduced mouse T cells expressing the miRα or β, respectively, appeared to be completely devoid of surface TCR (Fig. 12 and 14). The silencing efficiency was strictly proportional to the GFP expression and varied within the population of transduced T cells. Differences in the vector copy number and vector integration sites within the cell population could explain this observation. TCR silencing appeared to be more homogenous in the transduced human T cells. A high proportion of 87% and 53% of the transduced T cells expressing miRα or β, respectively, were negative for surface CD3 (Fig. 24). However, the mouse T cells showed a higher staining intensity compared to the human T cells, which could have contributed to the high amount of transduced human T cells in the CD3-negative gate. During this study, Okamoto et al. published another RNAi-TCR replacement vector for human T cells [221,222]. A comparison of the silencing efficiencies is complicated by the fact, that Okamoto et al. quantified the RNAi effect on the mRNA level only. They reported relative endogenous TCRα and β chain mRNA levels of about 35% in MHC multimer-sorted transduced human T cells.

The data presented here provides first indications that a complete knockdown of the endogenous TCR can be achieved in a subpopulation of the transduced T cells using the described miRNA. These

data need to be confirmed by further studies establishing the relationship between the proviral copy number, mRNA expression levels and the amount of TCR protein expressed at the cell surface. Possibly, residual endogenous TCR protein in some of cells might be responsible for the few cases of TI-GVHD observed after the transfer of T cells transduced with the RNAi-TCR replacement vectors (Fig. 22). It was reported, that even low-level expression of a second TCR induces mixed TCR dimer formation [250]. An analysis of the self-reactive T cells would be necessary to verify this hypothesis and to exclude the possibly that the silencing efficiency was reduced due to other reasons.

One way to further improve the silencing efficiency is to introduce additional miRNA into the vector directed at the same or new target sites. For this purpose, one might consider the AmiRα018-C targeting the mouse TCRα chain or miR155β433 targeting the human TCRβ chain (Fig. 13 and 24). The latter targets the same sequence as the miRNA used by Okamoto et al. For viral vectors, however, new miRNA have to be constructed using distinct backbone sequences to avoid recombination events during the production of viral particles. This complicated step can be avoided using non-viral vectors for the generation of RNAi-TCR gene-modified T cells.

4.3 The risk of RNAi-induced off-target effects

The most critical aspect of the RNAi technology is the risk of inducing off-target effects. It has been reported, that sustained high-level expression of certain shRNA in the liver of adult mice resulted in liver dysfunction (36/49 shRNA) and fatal toxicity (23/49 shRNA) [251]. The shRNA differed among each other in their sequence and length. It was suspected that they were produced or processed with different kinetics, so that some of them might have accumulated leading to the saturation of components of the cellular RNAi pathway like Exportin 5, which is responsible for the transport of shRNA and processed endogenous miRNA into the cytosol. Cytotoxic effects were also observed in transduced T cells and depended on the strength of the promoter controlling the shRNA expression [252,253]. The use of polymerase II promoters instead of the more active polymerase III promoters for the expression of miRNA or shRNA avoided the cytotoxic effects in T cells and other cell types [253,254,255,256]. Moreover, in a direct comparison, exogenous miRNA in contrast to siRNA and shRNA did not saturate the RNAi-induced silencing complexes (RISC) in the cytosol [257]. siRNA and shRNA resemble intermediates of the miRNA pathway and might therefore circumvent early rate limiting steps, whereas exogenous and endogenous miRNA share the same entry point into the pathway and underlie the same endogenous control mechanism.

Sequence-specific off-target effects are caused by the binding of the loaded RISC to mRNA with imperfect complementarity to the guide strand. Endogenous miRNA exhibit only a limited sequence complementarity of about 6-8 nt to their natural targets. These so called seed region is located at the 5' end of the guide strand starting with the second nucleotide and mediates the binding of RISC to target sites located in the 3' UTR of mRNA transcripts [258]. Since the RNAi pathway ends in the formation of RISC irrespective which kind of RNA molecule was the initial trigger, similar rules that govern

endogenous miRNA target recognition also apply for experimentally induced RNAi. Gene expression profiling revealed, that many unintentionally regulated transcripts indeed encoded sequence motifs that were complementary to the seed region of the respective siRNA and that these motifs were often located in the 3' UTR [259,260,261]. However, the presents of a seed region match in the 3' UTR alone is not sufficient for the prediction of miRNA targets. Features like the position of the binding motif within the 3' UTR, the AU-content of the surrounding sequence and the presence of other miRNA target sites represent additional constrains [262]. In case of experimentally induced RNAi, it can be assumed that RISC binding to full complementary mRNA is preferred. In addition, the likelihood that a given seed match complies with all requirements for a *bona fide* miRNA target site is low. The previously observed sequence-specific off-target effects might be in part caused by the high cytosolic concentration of siRNA after transfection and it is currently unclear if the expression of redirected miRNA induces similar off-target effects.

The upregulation of genes encoding target sites for endogenous miRNA and the downregulation of genes encoding seed matches in RNAi-TCR gene-modified T cells would indicate a saturation of the RNAi machinery or the induction of sequence-specific off-target effects, respectively, but the relevance of such perturbations has to be confirmed in functional assays. Therefore in this study, the specificity of the induced RNAi was controlled by functional reconstitution experiments. Mouse RNAi-TCR gene-modified T cells showed no functional disadvantage compared to conventional TCR gene-modified T cells in a tumor suppression model and in *in vitro* experiments (Fig. 19 and 20). In this study, only few initial *in vitro* experiments were conducted using human RNAi-TCR gene-modified T cells and conventional TCR gene-modified T cells (Fig. 25). Further investigations are needed to confirm that the human RNAi-TCR gene-modified T cells harbor no functional deficits due to the expression of the miRNA compared to conventional TCR gene-modified T cells.

4.4 Simultaneous expression of miRNA and transgenes

The expression of transcripts encoding miRNA and transgenes naturally results in low protein levels of the transgene, because the processing of the miRNA produces truncated mRNA. Either the 5' cap or the poly(A)-tail is lost if the miRNA is positioned in front or behind the transgene, respectively. Intronic miRNA has the potential to resolve this issue, as the splicing mechanism can religate the mRNA after the miRNA has been excised. This has been first demonstrated using plasmid-based vectors [263,264]. In retroviral vectors, however, efficiently spliced introns are in general not retained during the production of viral particles in the packing cell lines. Exceptions are introns that contain the packing signal (Ψ), because this configuration ensures that only unspliced messages are packaged into the virions. In case of the γ-retroviral vector MP71, a minimal splice acceptor has been used to construct such an intron in the 5' leader sequence encoding the packing signal [265]. This intron is only weakly spliced and therfore the positioning of the miRNA cassette into the intron only partially restored the expression of the transgene. It is therefore plausible, that the usage of a more efficient

intron would further improve transgene expression, which is desirable to replace as much as possible of remaining endogenous TCR. Indeed, the usage of optimized TCR genes in the RNAi-TCR replacement vector resulted in higher P14 TCR surface levels and in a somewhat lower incidence of TI-GVHD indicating that TCR gene optimization is able to partially alleviate the negative effect of the introduced miRNA on transgene expression (Fig. 18 and 22). In case of the MP71 vector, however, the improvement of the splicing signals of the intron is not a feasible strategy, as this would decrease the titer of the vector particles.

To construct an improved RNAi-TCR replacement vector with respect to transgene expression, one might consider further vector systems that are available for the genetic modification of human T cells. A lentiviral vector can be constructed similar to the MP71-based RNAi-TCR replacement vector by inserting the miRNA cassette into the 5' intron encoding the packing signal. In contrast to γ-retroviral vectors, the export of unspliced RNA in lentiviral vector systems is mediated through the interaction of the viral REV protein with the Rev-responsive element (RRE) encoded in the 5' intron [266]. Therefore, increasing the splicing efficiency might have only a limited effect on the vector titer due to the presence of REV in the packing cell line [267]. One study reported that even a miRNA-encoding intron without further regulatory elements was efficiently retained in a lentiviral vector, although this has not been confirmed by analyzing the integrated proviruses in transduced cells [268].

Since plasmid vectors are propagated in bacteria, the usage of strong introns is permitted. Stable genomic integration of transgene expression cassettes encoded by plasmid vectors in human T cells can be achieved using transposases like SleepingBeauty or piggyBac [269,270,271]. The SleepingBeauty transposase has been reconstructed from non-functional sequences encoded in fish DNA and was further modified by *in vitro* evolution [272,273]. In contrast, piggyBac is an active insect transposon that was shown to be functional in mammalian cells [274]. These enzymes bind to characteristic recognition sequences flanking the expression cassette on the plasmid, excise the enclosed DNA and integrated the full cassette into the genome. Both components of these vector systems, the donor plasmid and the transposase, are typically transfected simultaneously into T cells by electroporation. The transposase is only needed short time and can be expressed from a second plasmid or delivered as mRNA or protein. Initial experiments with transposon vectors constructed analogous to the viral RNAi-TCR replacement vector but with different splicing signals have confirmed the expatiations. The transgene expression is not longer negatively influenced if the miRNA is encoded in an efficiently spliced intron.

4.5 Knockout of the endogenous TCR by genome editing

Genome editing by programmable nucleases represents an attractive alternative to RNAi-based gene knockout strategies. Zinc-finger nucleases (ZFN), transcription activator-like effector nucleases (TALEN) or RNA-guided nucleases based on the prokaryotic CRISPER/Cas system can be used for the sequence-specific introduction of double-strand breaks (DSB) in genomic DNA [275,276,277,278,279].

The error prone repair of DSB by nonhomologous end joining often creates frameshift mutations, which result in the abort of functional protein expression of the target gene. TCR gene-modified T cells with edited endogenous TCR genes have already been generated using ZNF and TALEN by Provasi et al. and Berdien et al., respectively [219,220]. In principle, such TCRαβ-edited T cells are ideal, because the do not require the constant suppression of the endogenous TCR genes like in the RNAi approach and they are completely devoid of functional endogenous TCR protein. However, so far the complicated process to select T cells with the desired genotype without establishing clonal cultures prevents the implementation of these techniques into clinically feasible protocols.

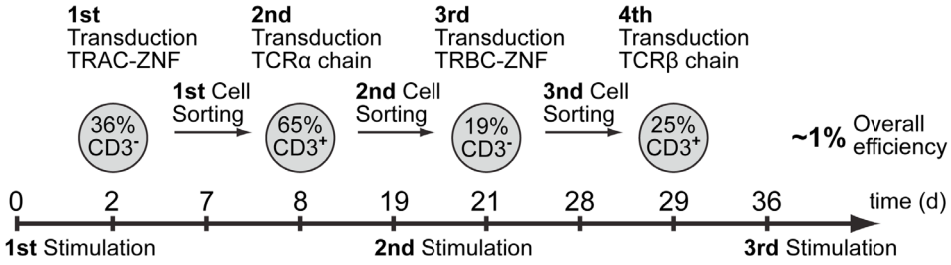

Figure 26: *Strategy to isolated T cells with ZNF-edited endogenous TCR genes and integrated therapeutic TCR genes by CD3 surface expression.*
The isolation of TCR gene-modified T cells with ZNF-edited endogenous TCR genes on the basis of CD3 surface expression requires a stepwise protocol. The knockout of one of both endogenous TCR genes generates a population of CD3-negative T cells, which can be sorted. Transduction of one therapeutic TCR chains into the CD3-negative T cells restores CD3 surface expression and enables sorting of CD3-positive T cells. Instead of sorting the CD3-positive T cells after the fourth transduction, the population is selectively expanded by CD3 stimulation. The total yield is calculated based on the efficiencies of the genetic manipulations of each step (mean values, *n*=4). Additional time and expansion steps will be required to produce the amount of cells needed for clinical application. All data from Provasi et al. (ref. 219).

Provasi et al. used a protocol for the selection of T cells based on the surface expression of the CD3/TCR complex and Berdien et al. used the same strategy afterwards (Fig. 26) [219,220]. In the first step, one of the endogenous TCR genes is edited and the population carrying inactivating mutations at he targeted locus becomes CD3-negative, because no TCRαβ dimers are expressed at the cell surface. This population is then sorted and CD3 surface expression is restored by the transduction of the respective therapeutic TCR chain, which forms TCRαβ dimers with the remaining endogenous TCR chains. Next, the CD3-positive T cells are sorted and the process is repeated for the second TCR chain. The CD3-positive T cells at the end of the process are not sorted but selectively expanded by TCR stimulation. Berdien et al. reported higher efficiencies for the editing of the TCR genes by TALEN (TCRα: 58%, TCRβ: 41%) compared to efficiencies of the ZNF reported by Provasi et al., but as long as an arguably impossible efficiency of 100% in each of the step is not achieved, the T cells have to be sorted multiple times. Although the use of RNA-guided nucleases for example would allow to edited both TCR loci at the same time, T cells harboring just one edited TCR chain locus and T cells with frameshift mutations at both loci cannot be differentiated on the basis of CD3 surface expression.

Hence, neither the development of more efficient nucleases nor the simultaneous editing of both TCR loci will allow simplifying the protocol. The major problem to be solved in the future is how to select the T cells with the desired genotype, which is both endogenous TCR loci mutated and both therapeutic TCR chains integrated, in a reasonable protocol. In contrast, the RNAi-TCR replacement vector delivers both therapeutic TCR chains and the miRNA for the suppression of both endogenous TCR chains at once and the expression of all components is under the control of the same promoter ensuring that they are all expressed simultaneously.

Furthermore, although frameshift mutations may destroy the functional expression of the target gene, mRNA is transcribed and, given that the repair of DSB results in random insertions and deletions, it is not excluded that some of the transcripts will be translated. Therefore, this approach bears a certain risk that the introduced frameshift mutations lead to new immunogenic epitopes causing the rejection of the edited T cells in an immunocompetent host. Since this issue has not been addressed in the literature, it is unclear if and to which extend this indeed could happen.

4.6 Alternative strategies of T cell-based cancer immunotherapy

Several distinct strategies were established that rely on T cell-based cancer immunotherapy and include the transfer of gene-modified cells but avoid the transfer of TCR genes into mature α/β T cells. The most successful of these strategies uses chimeric antigen receptors (CAR) to generate redirected T cells for the treatment of hematological malignancies. CAR are constructed using the variable regions of an antigen-specific antibody that are joined together by an flexible linker and fused to a transmembrane domain and an intracellular signaling domain. The first generation of CAR employed signaling moieties derived from the CD3ζ chain or the γ chain of the Fc receptor [280]. CAR-modified T cells are able to recognize cell surface proteins on the target cells but cannot interact with professional antigen-presenting cells of the immune system, which usually provide costimulatory signals in addition to the antigenic stimulus in form of peptide-MHC complexes. The lack of costimulation resulted in poor engraftment and proliferation of the CAR-modified T cells. Therefore, new generations of CAR were designed that included signaling moieties from costimulatory receptors like CD28 or CD137 (4-1BB) [281,282,283]. In case of a CAR specific for the B cell marker CD19, the combination of CD3ζ- and CD137-derived signaling moieties was shown to result in improved antigen-driven proliferation and tumor killing in a xenograft mouse model [284]. This CAR was subsequently successfully applied in clinical trials for the treatment of chronic and acute lymphoid leukemia [285,286,287]. The genetic modification of T cells with CAR circumvents the issue of mixed TCR dimers and CAR-modified T cells are able to recognize antigens in an MHC-independent manner. However, the disadvantage of this approach is that only surface-expressed proteins can be targeted, but the most suitable tumor antigens in terms of their restricted expression in normal tissue are intracellular proteins. The treatment of refractory leukemia represents a situation in which the therapy-induced loss of B cells that also express CD19 is an acceptable side effect.

Several different designs were proposed for the construction of single-chain TCR (scTCR) analogous to CAR. In general, the construction of scTCR is more difficult compared to CAR because of an inherent instability of the TCR V domains in the absence of the TCR C domains [288]. The three extracellular domains of the first scTCR were composed of a TCR Vα domain linked to a TCR Vβ domain that was connected to a Cβ domain, whereas the transmembrane region and the intracellular region of this construct were derived from the CD3ζ chain (Vα-Vβ-Cβ-CD3ζ) [289]. Human T cells transduced with such a three-domain scTCR could be activated in an antigen-specific manner, but the construct was poorly expressed at the cell surface [290]. Transduced mouse T cells expressing three-domain scTCR constructed with different transmembrane and signaling domains were shown to require higher amounts of antigen for activation and to secrete much less INF-γ as compared to TCR-transduced T cells [291]. Another study showed that the surface expression of three-domain scTCR on the surface of transduced human T cells could be increased by using the mouse TCR Cβ domain for the construction of the scTCR and by coexpressing a construct encoding the mouse TCR Cα domain [292]. It was assumed, that the scTCR associates with the Cα domain and forms a four-domain complex similar to the TCR heterodimer. However, the stabilization of the TCR V domains by the introduction of several mutations allowed the construct of two-domain scTCR (Vα-Vβ-CD28-CD137-CD3ζ) that were stably expressed at the cell surface without TCR C domains [293]. This study also demonstrated, that three-domain scTCR can ignore the linked TCR Vα domain and are able to form mixed TCR dimers with endogenous TCRα chains. Therefore, mixed TCR dimer formation is only prevented when the scTCR construct does not contain a TCR C region, but whether the two-domain design is generally applicable for human TCR remains to be shown. It was reported that some human TCR V regions are more amenable for such an approach than others [294]. Another important issue might be the avidity of scTCR-modified T cells because two-domain scTCR without TCR C regions do not associate with CD3 proteins. Consequently, they cannot form oligomers on the cell surface and are not able to serially engage with peptide-MHC complexes at the immunological synapse. Both events are used to explain that T cells show a higher functional avidity as one might expect considering the moderate affinities of TCR compared to antibodies. Hence, it was recommended to use affinity-enhanced TCR for the construction of two-domain scTCR [293].

The genetic modification of hematopoietic stem cells (HSC) by the introduction of TCR genes was proposed as a further strategy to provide the patient with antigen-specific T cells [295,296]. After being implanted, the TCR gene-modified HSC give rise to T cell progenitors that mature in the thymus. It was shown in mouse models, that the expression of the transferred TCR in the thymus prevents the rearrangement of the endogenous TCR genes [239,297,298]. The value of this strategy for the treatment of patients with advanced cancer is currently unclear. High numbers of *ex vivo* activated and expanded antigen-specific T cells are used in conventional adoptive T cell therapy to overcome the tolerance of the host to the tumor, whereas antigen-specific T cells derived from TCR gene-modified HSC mature slowly in the host environment and in the absence of signals of acute inflammation. In

addition, T cells expressing high-affinity TCR for self-derived antigens like TAA are deleted in the thymus.

4.7 The therapeutic potential of different T cell subtypes

The success of adoptive T cell therapy is intimately linked to the intrinsic properties of the transferred T cells. Naive CD8 T cells (T_N) differentiate upon antigen encounter into short-lived effector T cells (T_E) and long-lived memory T cells (T_M), which can be further subdivided into central memory T cells (T_{CM}) and effector memory T cells (T_{EM}). It has been demonstrated, that mice were more efficiently protected against viral and bacterial infections if they received prior to the challenge antigen-specific CD8 T_{CM} cells in comparison to CD8 T_{EM} cells [299]. So far, TCR gene-modified T cells for the clinical trials were generated from bulk lymphocytes, which consist of about 40% of T_N cells, less than 30% of T_{EM} cells and less than 10% of T_{CM} cells [300]. One promising strategy to improve the *in vivo* properties of the T cell graft is to start the culture with sorted T_{CM} cells. In a nonhuman primate model, only antigen-specific CD8 T cell clones derived from T_{CM} cells expanded and persisted long-term after transfer, although the T cell clones lost the phenotypic markers of T_{CM} cells during the 49 days of *in vitro* culture and acquired the phenotype of T_E cells [301]. These data argues for stable epigenetic determination of T_{CM} cells, which is retained during stimulation and expansion of the T cells *in vitro*. This aspect is of great importance, because the activation of the T cells is an indispensable step in viral transduction protocols.

Other strategies aiming to generate T cell populations with an improved phenotype for adoptive T cell therapy suggest to use the least differentiated T_N cell subtype and to block the differentiation of the T cells in the *in vitro* culture using cytokines or pharmacological substances. The rational behind is that the more the T cells progress into the direction of terminal differentiation, the more they loose their capacity for self-renewal and to give rise to other T cell subtypes. The idea of a gradual loss of potential during differentiation was supported by experiments in which the ability of transferred T cells to mediate tumor regression in mice decreased with progressing differentiation states [302]. In addition, a rare T cell subtype was identified presumably representing an intermediate state between T_N and T_M cells, which was thought to constantly replenish the pool of T_M cells. Stimulation of purified human CD8 T_N cells in the presence of substances triggering Wnt/β-Catenin signaling or IL-7 and IL-15 induced the differentiation of the cells into this intermediate subtype, which was suggested instead of T_{CM} cells for adoptive T cell therapy [303,304,305]. However, the relevance of this subtype for the generation of the T cell memory pool was questioned by experiments in which single antigen-specific T_N and T_{CM} cells were compared for their ability to confer immunological protection to mice [306]. The immune responses derived from single transferred T_N and T_{CM} cells were equal in size and diversity. Moreover, single T_{CM} cells derived from single transferred T_N cells after infection were transferred into secondary hosts and single T_{CM} cells generated through the infection of the secondary hosts were thereafter transferred into tertiary hosts that were also challenged by infection. No differences in the

proliferative capacity or in the developmental potential of the transferred T cell clones in the three hosts were observed, arguing against gradual accumulation of inherited restrictions in case of T_{CM} cells.

TCR gene therapy has not yet exploited the possibility to choose a T cell population of a defined subtype in clinical trials. An increasing body of evidence pinpoints to T_{CM} cells as the T cell subtype with the best properties for therapy but it is currently unclear if it is required to start with sorted T_{CM} cells or if culture conditions can be established that allow the generation of T_{CM} cells from bulk T cell cultures. In a clinical pilot study, antigen-specific CD8 T cell clones that were generated from T_N cells in the presence of IL-21 partially acquired T_{CM} markers and persisted long-term in the patient after transfer, whereas T cell clones generated with IL-2 disappeared after a few days [307]. If the cytokine-induced T_{CM} cells are as stable as natural T_{CM} cells, than both T_N and T_{CM} cells can be considered in the future for the generation of TCR gene-modified T cells with improved in *vivo* qualities.

5 Material and Methods

5.1 Material

5.1.1 Mice

C57BL/6 and B6.SJL mice (CD45.1) were purchased from Charles River (Sulzfeld, Germany). Transgenic mice, expressing either the H2-Db-restricted TCR I (Vα3, Vβ7) specific for the simian virus 40 large tumor antigen epitope I ($SV40_I$) or the H2-Db-restricted P14 TCR (Vα2, Vβ8) specific for the LMCV GP33-41 epitope were purchased from The Jackson Laboratory (Sulzfeld, Germany) [308,309]. Female mice were used at ages ranging from 10 to 12 weeks. Experiments were conducted in specific pathogen-free (SPF), environment-controlled animal facilities at the Max Delbrück Center for Molecular Medicine (Berlin, Germany) and at the Netherlands Cancer Institute (Amsterdam, Netherlands). The experiments were approved by the responsible national animal ethics committees and performed in accordance with national and institutional guidelines.

5.1.2 Cell lines

The mouse fibroblast cell line NIH/3T3 (ATCC: CRL-1658, American Type Culture Collection, Manassas, Virginia, USA) and human kidney HEK 293T cells (ATCC: CRL-11268) were cultured in Dulbecco's modified Eagles medium (DMEM GlutaMAX, Life Technologies Karlsruhe, Germany) supplemented with 10% heat-inactivated fetal calf serum (FCS, PAN-Biotech, Aidenbach, Germany) and 100 IU/ml Penicillin/Streptomycin (Life Technologies) [310]. The packing cell line Platinum-E (Plat-E, Cell Biolabs *via* BioCat, Heidelberg, Germany) is a derivative of the HEK 293T cell line expressing the MLV genes gag-pol and env [311]. Plat-E cells were cultured in the same medium as NIH/3T3 cells, but with addition of 10 µg/ml blasticidin and 1 µg/ml puromycin (both Sigma-Aldrich, Taufkirchen, Germany). The B16-GP33 cell line is a derivative of the B16.F10 mouse melanoma cell line expressing the LCMV-derived GP33 antigen [312]. B16-GP33 cells were cultured in the same medium as NIH/3T3 cells, but under G418 selection (1 mg/ml) (Life Technologies). The B3Z cell line is a mouse T cell hybridoma generated by the fusion of an ovalbumin-specific T cell clone with a derivative of the mouse BW5147 thymoma cell line that was transfected with an NFAT-controlled β-galactosidase gene [313]. The human T2 cell line is HLA-2-positive but TAP-deficient (ATCC: CRL-1992). The Jurkat cell line (DMSZ: ACC 282, Deutsche Sammlung von Mikroorganismen und Zellkulturen, Braunschweig, Germany) has been established from a patient with acute lymphoblastic leukemia [314]. B3Z cells, T2 cells and Jurkat cells were cultured in Roswell Park Memorial Institute 1640 medium (RPMI 1640 GlutaMAX, Life Technologies) supplemented with 10% heat-inactivated FCS (PAN-Biotech), 100 IU/ml Penicillin/Streptomycin (Life Technologies) and 1 mM sodium pyruvat (Life Technologies).

5.1.3 Peptides

Synthesized peptides were purchased from Biosynthan (Berlin, Germany) as HPLC-purified and lyophilized products (Tab. 1). The C-terminal cysteine of the native GP33 peptide was replaced with a methionine to prevent disulfide bond formation [315].

Table 1: Peptides used for T cell stimulation

Name	*Gene*	*Position*	*MHC*	*Peptide*
GP33	LCMV GP1	33-41	H2-Db	KAVYNFATC/M
MAGE A1	Human MAGE A1	278–286	HLA-A*0201	KVLEYVIKV

5.1.4 Antibodies and MHC multimers

Table 2: MHC multimers specific for mouse and human TCR

Name	*Peptide*	*MHC*	*Fluorophore*	*Binds to*	*Supplier*
Db-GP33	KAVYNFATC	H-2Db	APC	P14 TCR	MBL *via* Biomol (Eching, Germany)
Db-$SV40_I$	SAINNYAQKL	H-2Db	PE	TCR I	
A2-MAGE A1	KVLEYVIKV	HLA-A*02:01	APC	1367 TCR	

Table 3: Antibodies specific for mouse surface antigens

Specificity	*Clone*	*Antibody*	*Fluorophore*	*Supplier*
CD3ε	17A2	Rat IgG2b	APC	BioLegend (London, UK)
CD8α	53-6.7	Rat IgG2a	PE	BD Bioscience (Heidelberg, Germany)
mTRBC	H57-597	Hamster IgG	APC	BioLegend
TCR Vα2	B20.1	Rat IgG2a	APC	BioLegend
TCR Vβ8.1	KJ16-133.18	Rat IgG2a	FITC	BioLegend
CD16/CD32	2.4G2	Rat IgG2b	-	BD Bioscience

Table 4: Antibodies specific for human surface antigens

Specificity	*Clone*	*Antibody*	*Fluorophore*	*Supplier*
CD3ε	UCHT1	Mouse IgG1	APC	BD Bioscience
CD8α	HIT8a	Mouse IgG1	FITC	BioLegend
CD8α	RPA-T8	Mouse IgG1	APC	BD Bioscience
TCR Vα2	F1	Mouse IgG2a	FITC	Thermo Scientific (Rockford, Illinois, USA)
TCR Vα7.2	3C10	Mouse IgG1	FITC	BioLegend
TCR Vα12.1	6D6.6	Mouse IgG1	FITC	Thermo Scientific
TCR Vβ1	BL37.2	Rat IgG1	PE	Beckman Coulter (Krefeld, Germany)
TCR Vβ2	MPB2D5	Mouse IgG1	PE	Beckman Coulter
TCR Vβ3	CH92	Mouse IgM	FITC	Beckman Coulter
TCR Vβ3	JOVI-3	Mouse IgG2a	PE	Ancell *via* Biomol
TCR Vβ5.1	IMMU 157	Mouse IgG2a	PE	Beckman Coulter

TCR Vβ13.6	JU74.3	Mouse IgG1	PE	Beckman Coulter
TCR Vβ14	CAS1.1.3	Mouse IgG1	PE	Beckman Coulter
TCR Vβ22	IM2051	Mouse IgG1	PE	Beckman Coulter

5.1.5 Synthesized DNA oligonucleotides

Synthesized DNA oligonucleotides were purchased from Eurofins MWG (Ebersberg, Germany). Characters in bold encode restriction sites or single-stranded overhangs compatible with restriction sites. Antisense sequences are underlined and loop sequences are italicized.

Table 5: PCR primer used to generate reporter plasmids for the RNAi reporter assay

Name	*Sequence*	*Applied for*
mTRAC-XhoI-FWD	GC **CTCGAGA** CAT CCA GAA CCC AGA ACC T	Cloning of mouse TRAC into psiCHECK2
mTRAC-NotI-REV	T **GCGGCCGC** TTT CTG AAT CAC CTT TAA TGA TGT	
mTRACco-XhoI-FWD	GC **CTCGAGA** GTC AAG CCC GAC ATC CAG AAC	Cloning of codon-optimized mouse TRAC into psiCHECK2
mTRACco-NotI-REV	T **GCGGCCGC** AAT TCT CAT CAG CTG CTC CAC AG	
mTRBC-XhoI-FWD	GC **CTCGAGA** GGA TCT GAG AAA TGT GAC TCC AC	Cloning of mouse TRBC1/2 into psiCHECK2
mTRBC1-NotI-REV	T **GCGGCCGC** TCA TGA ATT CTT TCT TTT GAC CAT A	
mTRBC2-NotI-REV	T **GCGGCCGC** TCA GGA ATT TTT TTT CTT GAC CAT G	
mTRBC2co-XhoI-FWD	G **CCTCGAGA** CCT GAC CGT CCT GGA AGA	Cloning of codon-optimized mouse TRBC2 into psiCHECK2
mTRBC2co-NotI-REV	T **GCGGCCGC** GCT GTT CTT CTT CTT CAC CAT	
Renilla-Seq-FWD	AAG GAG AAG GGC GAG GTT AG	Sequencing of psiCHECK2
HsvTk-Seq-REV	CAA ACC CTA ACC ACC GCT TA	

Table 6: DNA oligonucleotides encoding shRNA

Name	*Sequence*	*shRNA characteristics*
POScontr-FWD	**GATC** CCC GCTGGACTCCTTCATCAAC *TTCAAGAGA* GTTGATGAAGGAGTCCAGC TTT TTG GAA A	shRNA directed at the renilla ORF. Antisense sequence: 19 nt
POScontr-REV	**AGCT** TTT CCA AAA A GCTGGACTCCTTCATCAAC *TCTCTTGAA* GTTGATGAAGGAGTCCAGC GGG	
NEGcontr-FWD	**GATC** CCC CAACAAGATGAAGAGCACC *TTCAAGAGA* GGTGCTCTTCATCTTGTTG TTT TTG GAA A	shRNA not targeting any mouse gene. Antisense sequence: 19 nt
NEGcontr-REV	**AGCT** TTT CCA AAA A CAACAAGATGAAGAGCACC *TCTCTTGAA* GGTGCTCTTCATCTTGTTG GGG	
mTRBC052-FWD	**GATC** CCC AAGCAGAGATTGCAAACAA *TTCAAGAGA* TTGTTTGCAATCTCTGCTT TTT TTG GAA A	shRNA directed at β052. Antisense sequence: 19 nt (mTRBC 52-70).
mTRBC052-REV	**AGCT** TTT CCA AAA A AAGCAGAGATTGCAAACAA *TCTCTTGAA* TTGTTTGCAATCTCTGCTT GGG	
mTRBC130-FWD	**GATC** CCC GCTGGTGGGTGAATGGCAA *TTCAAGAGA* TTGCCATTCACCCACCAGC TTT TTG GAA A	shRNA directed at β130. Antisense sequence: 19 nt (mTRBC 130-148).
mTRBC130-REV	**AGCT** TTT CCA AAA A GCTGGTGGGTGAATGGCAA *TCTCTTGAA* TTGCCATTCACCCACCAGC GGG	
mTRBC190-FWD	**GATC** CCC AGGAGAGCAATTATAGCTA *TTCAAGAGA* TAGCTATAATTGCTCTCCT TTT TTG GAA A	shRNA directed at β190. Antisense sequence: 19 nt (mTRBC 190-208).
mTRBC190-REV	**AGCT** TTT CCA AAA A AGGAGAGCAATTATAGCTA *TCTCTTGAA* TAGCTATAATTGCTCTCCT GGG	
mTRBC333-FWD	**GATC** CCC CCTGTCACACAGAACATCA *TTCAAGAGA* TGATGTTCTGTGTGACAGG TTT TTG GAA A	shRNA directed at β333. Antisense sequence: 19 nt (mTRBC 333-315).
mTRBC333-REV	**AGCT** TTT CCA AAA A CCTGTCACACAGAACATCA *TCTCTTGAA* TGATGTTCTGTGTGACAGG GGG	

mTRAC018-FWD	**GATC** CCC CCTGCTGTGTACCAGTTAA *TTCAAGAGA* TTAACTGGTACACAGCAGG TTT TTG GAA A	shRNA directed at α018. Antisense sequence: 19 nt (mTRAC 18-36).
mTRAC018-REV	**AGCT** TTT CCA AAA A CCTGCTGTGTACCAGTTAA *TCTCTTGAA* TTAACTGGTACACAGCAGG GGG	
mTRAC076-FWD	**GATC** CCC CCGACTTTGACTCCCAAAT *TTCAAGAGA* ATTTGGGAGTCAAAGTCGG TTT TTG GAA A	shRNA directed at α076. Antisense sequence: 19 nt (mTRAC 76-94).
mTRAC076-REV	**AGCT** TTT CCA AAA A CCGACTTTGACTCCCAAAT *TCTCTTGAA* ATTTGGGAGTCAAAGTCGG GGG	
mTRAC275-FWD	**GATC** CCC TGCCACGTTGACTGAGAAA *TTCAAGAGA* TTTCTCAGTCAACGTGGCA TTT TTG GAA A	shRNA directed at α275. Antisense sequence: 19 nt (mTRAC 275-293).
mTRAC275-REV	**AGCT** TTT CCA AAA A TGCCACGTTGACTGAGAAA *TCTCTTGAA* TTTCTCAGTCAACGTGGCA GGG	
mTRAC349-FWD	**GATC** CCC GAATCCTCCTGCTGAAAGT *TTCAAGAGA* ACTTTCAGCAGGAGGATTC TTT TTG GAA A	shRNA directed at α349. Antisense sequence: 19 nt (mTRAC 349-376).
mTRAC349-REV	**AGCT** TTT CCA AAA A GAATCCTCCTGCTGAAAGT *TCTCTTGAA* ACTTTCAGCAGGAGGATTC GGG	

Table 7: DNA oligonucleotides used to modify the MP71-GFP vector for the cloning of the miRNA

Name	*Sequence*	*Applied for*
5UTR-FWD	TTC CAC CGA GAT TTG GAG AC	PCR primer encoding restriction sites for the amplification a part of the 5' intron.
NotI-NsiI-MluI-REV	AT **GCGGCCGC** TAA **ATGCAT** TAA TT **ACGCGT** GCT AAT TTT CAG ACA AAT ACA GAA ACA	
NotI-5'Intron-NsI-FWD	TGA CAA AGT TAA GTA ATA GTC CCT CTC TCC AAA GCT CAC TTA CAG GC	Branchpoint and splice acceptor were introduced between NsiI and NotI to restore the 5' intron.
NotI-5'Intron-NsI-REV	**GGCC** GCC TGT AAG TGA GCT TTG GAG AGA GGG ACT ATT ACT TAA CTT TGT CA **TGCA**	
NotIX-MluI-NsiI-NotI-FWD	**GGCC** AAT AA **ACGCGT** TAA TT **ATGCAT** ATA GC	Introduction of MluI/NsiI into pMP71-GFP at an exonic position 5' of NotI.
NotIX-MluI-NsiI-NotI-REV	**GGCC** GCT AT **ATGCAT** AAT TA **ACGCGT** TTA TTG G	
EcoRI-MluI-NsiI-EcoRIX-FWD	**AATT** CT AA **ACGCGT** TAA TT **ATGCAT** ATA	Introduction of MluI/NsiI into pMP71-GFP at an exonic position 3' of EcoRI.
EcoRI-MluI-NsiI-EcoRIX-REV	**AATT** TAT **ATGCAT** AAT TA **ACGCGT** TTA G	

Table 8: AmiR backbone sequences without the miRNA hairpin

Name	*Sequence*	*Applied for*
AmiR-Backbone-FWD	**CGCG** AAC AAG AGA ACA AAG TGG AGT CTT TGT TGC CC **ACGCGT** AGC AT **ATGCAT** CAG AGC CTG CCT GGT GGC CCC TGA GAG ATT TGC **TGCA**	AmiR backbone cloned into pMP71-GFP using MluI/NsiI. New MluI/NsiI sites in the center allowed the subsequent cloning of miRNA hairpins.
AmiR-Backbone-REV	GCA AAT CTC TCA GGG GCC ACC AGG CAG GCT CTG **ATGCAT** ATG CT **ACGCGT** GGG CAA CAA AGA CTC CAC TTT GTT CTC TTG TT	

Table 9: AmiR hairpins directed at the mouse TCRα chain

Name	*Sequence*	*miRNA characteristics*
AmiRα018-B-FWD	**CGCG** TAG CTT CCC TGG CTC TTTAACTGGTACACAGCAGGTT GT *ACATGAG* ACT ACC TGC TGT GAA CCA GTT GAT GAG CTT GGG AAG CAT A **TGCA**	AmiR hairpin (format B) directed at α018. Antisense sequence: 22 nt (mTRAC 16-37).
AmiRα018-B-REV	TAT GCT TCC CAA GCT CAT CAA CTG GTT CAC AGC AGG TAG T *CTCATGT* AC AACCTGCTGTGTACCAGTTAAA GAG CCA GGG AAG CTA	
AmiRα018-C-FWD	**CGCG** TAG CTT CCC TGG CTC TTAACTGGTACACAGCAGGTTC GT *ACATGAG* ACC AAC CTG CTG TCT ACC GGT TAT GAG CTT GGG AAG CAT A **TGCA**	AmiR hairpin (format C) directed at α018.

AmiRα018-C-REV	TAT GCT TCC CAA GCT CAT AAC CGG TAG ACA GCA GGT TGG T *CTCATGT* AC GAACCTGCTGTGTACCAGTTAA GAG CCA GGG AAG CTA	Antisense sequence: 22 nt (mTRAC 15-36).
AmiRα089-C-FWD	**CGCG** TAG CTT CCC TGG CTC TTTCGGCACATTGATTTGGGAG GT *ACATGAG* ACG TCC CAA ATC ATT GTG CCG GAT GAG CTT GGG AAG CAT A **TGCA**	AmiR hairpin (format C) directed at α089. Antisense sequence: 22 nt (mTRAC 86-107).
AmiRα089-C-REV	TAT GCT TCC CAA GCT CAT CCG GCA CAA TGA TTT GGG ACG T *CTCATGT* AC CTCCCAAATCAATGTGCCGAAA GAG CCA GGG AAG CTA	
AmiRα121-C-FWD	**CGCG** TAG CTT CCC TGG CTC TTGTCAGTGATGAACGTTCCAG GT *ACATGAG* ACG TGG AAC GTT CTT CAC TGA TAT GAG CTT GGG AAG CAT A **TGCA**	AmiR hairpin (format C) directed at α121. Antisense sequence: 22 nt (mTRAC 118-139).
AmiRα121-C-REV	TAT GCT TCC CAA GCT CAT ATC AGT GAA GAA CGT TCC ACG T *CTCATGT* AC CTGGAACGTTCATCACTGACAA GAG CCA GGG AAG CTA	
AmiRα193-B-FWD	**CGCG** TAG CTT CCC TGG CTC GAAGCTTGTCTGGTTGCTCCAG GT *ACATGAG* ACG TGG AGC AAC CTG ACA AGT TTG GAG CTT GGG AAG CAT A **TGCA**	AmiR hairpin (format B) directed at α193. Antisense sequence: 22 nt (mTRAC 191-212).
AmiRα193-B-REV	TAT GCT TCC CAA GCT CCA AAC TTG TCA GGT TGC TCC ACG T *CTCATGT* AC CTGGAGCAACCAGACAAGCTTC GAG CCA GGG AAG CTA	
AmiRα193-C-FWD	**CGCG** TAG CTT CCC TGG CTC AAGCTTGTCTGGTTGCTCCAGG GT *ACATGAG* ACG CTG GAG CAA CGA GAC AAG TTA GAG CTT GGG AAG CAT A **TGCA**	AmiR hairpin (format C) directed at α193. Antisense sequence: 22 nt (mTRAC 190-211).
AmiRα193-C-REV	TAT GCT TCC CAA GCT CTA ACT TGT CTC GTT GCT CCA GCG T *CTCATGT* AC CCTGGAGCAACCAGACAAGCTT GAG CCA GGG AAG CTA	
AmiRα275-FWD	**CGCG** TAG CTT CCC TGG CTC TTTCTCAGTCAACGTGGCATC TGT *ACATGAG* ACT GAT GCC ACG TAG ACT GAG AAT GAG CTT GGG AAG CAT A **TGCA**	AmiR hairpin directed at α275. Antisense sequence: 21 nt (mTRAC 273-293).
AmiRα275-REV	TAT GCT TCC CAA GCT CAT TCT CAG TCT ACG TGG CAT CAG T *CTCATGT* ACA GATGCCACGTTGACTGAGAAA GAG CCA GGG AAG CTA	
AmiRα300-B-FWD	**CGCG** TAG CTT CCC TGG CTC TTTAGGTTCATATCTGTTTCAA GT *ACATGAG* ACA TGA AAC AGA TTT GAA CCT GAT GAG CTT GGG AAG CAT A **TGCA**	AmiR hairpin (format B) directed at α300. Antisense sequence: 22 nt (mTRAC 298-319).
AmiRα300-B-REV	TAT GCT TCC CAA GCT CAT CAG GTT CAA ATC TGT TTC ATG T *CTCATGT* AC TTGAAACAGATATGAACCTAAA GAG CCA GGG AAG CTA	
AmiRα300-C-FWD	**CGCG** TAG CTT CCC TGG CTC TTAGGTTCATATCTGTTTCAAA GT *ACATGAG* ACA TTG AAA CAG AAA TGA ACT TAT GAG CTT GGG AAG CAT A **TGCA**	AmiR hairpin (format C) directed at α300. Antisense sequence: 22 nt (mTRAC 297-318).
AmiRα300-C-REV	TAT GCT TCC CAA GCT CAT AAG TTC ATT TCT GTT TCA ATG T *CTCATGT* AC TTTGAAACAGATATGAACCTAA GAG CCA GGG AAG CTA	
AmiRα395-B-FWD	**CGCG** TAG CTT CCC TGG CTC TAAATCCGGCTACTTTCAGCAG GT *ACATGAG* ACG TGC TGA AAG TTG CCG GGT TTT GAG CTT GGG AAG CAT A **TGCA**	AmiR hairpin (format B) directed at α395. Antisense sequence: 22 nt (mTRAC 357-378).
AmiRα395-B-REV	TAT GCT TCC CAA GCT CAA AAC CCG GCA ACT TTC AGC ACG T *CTCATGT* AC CTGCTGAAAGTAGCCGGATTTA GAG CCA GGG AAG CTA	

Table 10: AmiR hairpins directed at the mouse TCRβ chain

Name	*Sequence*	*miRNA characteristics*
AmiRβ052-A-FWD	**CGCG** TAG CTT CCC TGG CTC TTGTTTGCAATCTCTGCTTT CTGT *ACATGAG* ACT GAA AGC AGA GTT TGC AAA CAT GAG CTT GGG AAG CAT A **TGCA**	AmiR hairpin (format A) directed at β052. Antisense sequence: 20 nt (mTRBC 51-70).
AmiRβ052-A-REV	TAT GCT TCC CAA GCT CAT GTT TGC AAA CTC TGC TTT CAG T *CTCATGT* ACA G AAAGCAGAGATTGCAA ACA AGA GCC AGG GAA GCT A	

AmiRβ052-B-FWD	**CGCG** TAG CTT CCC TGG CTC TTTGTTTGCAATCTCTGCTTTT GT *ACATGAG* ACT AAA GCA GAG AAT GCA AAC GAT GAG CTT GGG AAG CAT A **TGCA**	AmiR hairpin (format B) directed at β052. Antisense sequence: 22 nt (mTRBC 50-71).
AmiRβ052-B-REV	TAT GCT TCC CAA GCT CAT CGT TTG CAT TCT CTG CTT TAG T *CTCATGT* AC AAAAGCAGAGATTGCAAACAAA GAG CCA GGG AAG CTA	
AmiRβ130-B-FWD	**CGCG** TAG CTT CCC TGG CTC CTTGCCATTCACCCACCAGCTC GT *ACATGAG* ACC AGC TGG TGG GAG AAT GGC GAC GAG CTT GGG AAG CAT A **TGCA**	AmiR hairpin (format B) directed at β130. Antisense sequence: 22 nt (mTRBC 128-149).
AmiRβ130-B-REV	TAT GCT TCC CAA GCT CGT CGC CAT TCT CCC ACC AGC TGG T *CTCATGT* AC GAGCTGGTGGGTGAATGGCAAG GAG CCA GGG AAG CTA	
AmiRβ190-B-FWD	**CGCG** TAG CTT CCC TGG CTC GTAGCTATAATTGCTCTCCTTG GT *ACATGAG* ACG AAG GAG AGC ATT TAT AGC TGG GAG CTT GGG AAG CAT A **TGCA**	AmiR hairpin (format B) directed at β190. Antisense sequence: 22 nt (mTRBC 188-209).
AmiRβ190-B-REV	TAT GCT TCC CAA GCT CCC AGC TAT AAA TGC TCT CCT TCG T *CTCATGT* AC CAAGGAGAGCAATTATAGCTAC GAG CCA GGG AAG CTA	
AmiRβ333-B-FWD	**CGCG** TAG CTT CCC TGG CTC CTGATGTTCTGTGTGACAGGTT GT *ACATGAG* ACT ACC TGT CAC AGA GAA CAT TAC GAG CTT GGG AAG CAT A **TGCA**	AmiR hairpin (format B) directed at β333. Antisense sequence: 22 nt (mTRBC 331-352).
AmiRβ333-B-REV	TAT GCT TCC CAA GCT CGT AAT GTT CTC TGT GAC AGG TAG T *CTCATGT* AC AACCTGTCACACAGAACATCAG GAG CCA GGG AAG CTA	

Table 11: AmiR hairpins directed at the human TCRα chain

Name	*Sequence*	*miRNA characteristics*
AmiRα094-FWD	**CGCG** TAG CTT CCC TGG CTC TTACTTTGTGACACATTTGTTT GT *ACATGAG* ACT AAC AAA TGT GAC ACA AGG TAC GAG CTT GGG AAG CAT A **TGCA**	AmiR hairpin (format C) directed at α094. Antisense sequence: 22 nt (hTRAC 91-112).
AmiRα094-REV	TAT GCT TCC CAA GCT CGT ACC TTG TGT CAC ATT TGT TAG T *CTCATGT* AC AAACAAATGTGTCACAAAGTAA GAG CCA GGG AAG CTA	
AmiRα109-FWD	**CGCG** TAG CTT CCC TGG CTC TACACATCAGAATCCTTACTTT GT *ACATGAG* ACT AAG TAA GGA TAC TGG TGT GTC GAG CTT GGG AAG CAT A **TGCA**	AmiR hairpin (format C) directed at α109. Antisense sequence: 22 nt (hTRAC 106-127).
AmiRα109-REV	TAT GCT TCC CAA GCT CGA CAC ACC AGT ATC CTT ACT TAG T *CTCATGT* AC AAAGTAAGGATTCTGATGTGTA GAG CCA GGG AAG CTA	
AmiRα116-FWD	**CGCG** TAG CTT CCC TGG CTC TGTGATATACACATCAGAATCC GT *ACATGAG* ACA GAT TCT GAT GAG TAT ATC GCT GAG CTT GGG AAG CAT A **TGCA**	AmiR hairpin (format C) directed at α116. Antisense sequence: 22 nt (hTRAC 113-134).
AmiRα116-REV	TAT GCT TCC CAA GCT CAG CGA TAT ACT CAT CAG AAT CTG T *CTCATGT* AC GGATTCTGATGTGTATATCACA GAG CCA GGG AAG CTA	
AmiRα146-FWD	**CGCG** TAG CTT CCC TGG CTC CATAGACCTCATGTCTAGCACA GT *ACATGAG* ACA GTG CTA GAC AAG AGG TCT GTC GAG CTT GGG AAG CAT A **TGCA**	AmiR hairpin (format C) directed at α146. Antisense sequence: 22 nt (hTRAC 143-164).
AmiRα146-REV	TAT GCT TCC CAA GCT CGA CAG ACC TCT TGT CTA GCA CTG T *CTCATGT* AC TGTGCTAGACATGAGGTCTATG GAG CCA GGG AAG CTA	
AmiRα197-FWD	**CGCG** TAG CTT CCC TGG CTC TGCAAAGTCAGATTTGTTGCTC GT *ACATGAG* ACT AGC AAC AAA TAT GAT TTT GCT GAG CTT GGG AAG CAT A **TGCA**	AmiR hairpin (format C) directed at α197. Antisense sequence: 22 nt (hTRAC 194-215).
AmiRα197-REV	TAT GCT TCC CAA GCT CAG CAA AAT CAT ATT TGT TGC TAG T *CTCATGT* AC GAGCAACAAATCTGACTTTGCA GAG CCA GGG AAG CTA	
AmiRα233-FWD	**CGCG** TAG CTT CCC TGG CTC TTCTGGAATAATGCTGTTGTTG GT *ACATGAG* ACG AAC AAC AGC AGT ATT CCG GAT GAG CTT GGG AAG CAT A **TGCA**	AmiR hairpin (format C) directed at α233. Antisense sequence: 22 nt (hTRAC 230-251).
AmiRα233-REV	TAT GCT TCC CAA GCT CAT CCG GAA TAC TGC TGT TGT TCG T *CTCATGT* AC CAACAACAGCATTATTCCAGAA GAG CCA GGG AAG CTA	

AmiRα307-FWD	**CGCG** TAG CTT CCC TGG CTC TTCGTATCTGTTTCAAAGCTTT GT *ACATGAG* ACT AAG CTT TGA ATC AGA TAT GAC GAG CTT GGG AAG CAT A **TGCA**	AmiR hairpin (format C) directed at α307. Antisense sequence: 22 nt (hTRAC 304-325).
AmiRα307-REV	TAT GCT TCC CAA GCT CGT CAT ATC TGA TTC AAA GCT TAG T *CTCATGT* AC AAAGCTTTGAAACAGATACGAA GAG CCA GGG AAG CTA	
AmiRα317-FWD	**CGCG** TAG CTT CCC TGG CTC AAAGTTTAGGTTCGTATCTGTT GT *ACATGAG* ACT ACA GAT ACG ATC CTA AAT TTC GAG CTT GGG AAG CAT A **TGCA**	AmiR hairpin (format C) directed at α317. Antisense sequence: 22 nt (hTRAC 314-335).
AmiRα317-REV	TAT GCT TCC CAA GCT CGA AAT TTA GGA TCG TAT CTG TAG T *CTCATGT* AC AACAGATACGAACCTAAACTTT GAG CCA GGG AAG CTA	
AmiRα319-FWD	**CGCG** TAG CTT CCC TGG CTC TGAAAGTTTAGGTTCGTATCTG GT *ACATGAG* ACA AGA TAC GAA CAT AAA TTT TCT GAG CTT GGG AAG CAT A **TGCA**	AmiR hairpin (format C) directed at α319. Antisense sequence: 22 nt (hTRAC 316-337).
AmiRα319-REV	TAT GCT TCC CAA GCT CAG AAA ATT TAT GTT CGT ATC TTG T *CTCATGT* AC CAGATACGAACCTAAACTTTCA GAG CCA GGG AAG CTA	
AmiRα384-FWD	**CGCG** TAG CTT CCC TGG CTC TCATGAGCAGATTAAACCCGGC GT *ACATGAG* ACA CCG GGT TTA AGC TGC TCG TGC GAG CTT GGG AAG CAT A **TGCA**	AmiR hairpin (format C) directed at α384. Antisense sequence: 22 nt (hTRAC 381-402).
AmiRα384-REV	TAT GCT TCC CAA GCT CGC ACG AGC AGC TTA AAC CCG GTG T *CTCATGT* AC GCCGGGTTTAATCTGCTCATGA GAG CCA GGG AAG CTA	

Table 12: AmiR hairpins directed at the human TCRβ chain

Name	*Sequence*	*miRNA characteristics*
AmiRβ028-FWD	**CGCG** TAG CTT CCC TGG CTC GGCTCAAACACAGCGACCTCGG GT *ACATGAG* ACG CGA GGT CGC TCT GTT TGG GCG GAG CTT GGG AAG CAT A **TGCA**	AmiR hairpin (format C) directed at β028. Antisense sequence: 22 nt (hTRBC 25-46).
AmiRβ028-REV	TAT GCT TCC CAA GCT CCG CCC AAA CAG AGC GAC CTC GCG T *CTCATGT* AC CCGAGGTCGCTGTGTTTGAGCC GAG CCA GGG AAG CTA	
AmiRβ032-FWD	**CGCG** TAG CTT CCC TGG CTC TGATGGCTCAAACACAGCGACC GT *ACATGAG* ACC GTC GCT GTG TAT GAG CCG TCT GAG CTT GGG AAG CAT A **TGCA**	AmiR hairpin (format C) directed at β032. Antisense sequence: 22 nt (hTRBC 29-50).
AmiRβ032-REV	TAT GCT TCC CAA GCT CAG ACG GCT CAT ACA CAG CGA CGG T *CTCATGT* AC GGTCGCTGTGTTTGAGCCATCA GAG CCA GGG AAG CTA	
AmiRβ034-FWD	**CGCG** TAG CTT CCC TGG CTC TCTGATGGCTCAAACACAGCGA GT *ACATGAG* ACA CGC TGT GTT TCA GCC ATC GGT GAG CTT GGG AAG CAT A **TGCA**	AmiR hairpin (format C) directed at β034. Antisense sequence: 22 nt (hTRBC 31-52).
AmiRβ034-REV	TAT GCT TCC CAA GCT CAC CGA TGG CTG AAA CAC AGC GTG T *CTCATGT* AC TCGCTGTGTTTGAGCCATCAGA GAG CCA GGG AAG CTA	
AmiRβ035-FWD	**CGCG** TAG CTT CCC TGG CTC TTCTGATGGCTCAAACACAGCG GT *ACATGAG* ACG GCT GTG TTT GTG CCA TCG GAT GAG CTT GGG AAG CAT A **TGCA**	AmiR hairpin (format C) directed at β035. Antisense sequence: 22 nt (hTRBC 32-53).
AmiRβ035-REV	TAT GCT TCC CAA GCT CAT CCG ATG GCA CAA ACA CAG CCG T *CTCATGT* AC CGCTGTGTTTGAGCCATCAGAA GAG CCA GGG AAG CTA	
AmiRβ041-FWD	**CGCG** TAG CTT CCC TGG CTC CTCTGCTTCTGATGGCTCAAAC GT *ACATGAG* ACC TTT GAG CCA TGA GAA GCG GAC GAG CTT GGG AAG CAT A **TGCA**	AmiR hairpin (format C) directed at β041. Antisense sequence: 22 nt (hTRBC 38-59).
AmiRβ041-REV	TAT GCT TCC CAA GCT CGT CCG CTT CTC ATG GCT CAA AGG T *CTCATGT* AC GTTTGAGCCATCAGAAGCAGAG GAG CCA GGG AAG CTA	
AmiRβ202-FWD	**CGCG** TAG CTT CCC TGG CTC TATCTGGAGTCATTGAGGGCGG GT *ACATGAG* ACG CGC CCT CAA TCA CTC CAG GTT GAG CTT GGG AAG CAT A **TGCA**	AmiR hairpin (format C) directed at β202. Antisense sequence: 22 nt (hTRBC 199-220).
AmiRβ202-REV	TAT GCT TCC CAA GCT CAA CCT GGA GTG ATT GAG GGC GCG T *CTCATGT* AC CCGCCCTCAATGACTCCAGATA GAG CCA GGG AAG CTA	

AmiRβ203-FWD	**CGCG** TAG CTT CCC TGG CTC GTATCTGGAGTCATTGAGGGCG GT *ACATGAG* ACG GCC CTC AAT GTC TCC AGG TAG GAG CTT GGG AAG CAT A **TGCA**	AmiR hairpin (format C) directed at β203. Antisense sequence: 22 nt (hTRBC 200-221).
AmiRβ203-REV	TAT GCT TCC CAA GCT CCT ACC TGG AGA CAT TGA GGG CCG T *CTCATGT* AC CGCCCTCAATGACTCCAGATAC GAG CCA GGG AAG CTA	
AmiRβ204-FWD	**CGCG** TAG CTT CCC TGG CTC AGTATCTGGAGTCATTGAGGGC GT *ACATGAG* ACA CCC TCA ATG AGT CCA GAT GCA GAG CTT GGG AAG CAT A **TGCA**	AmiR hairpin (format C) directed at β204. Antisense sequence: 22 nt (hTRBC 201-222).
AmiRβ204-REV	TAT GCT TCC CAA GCT CTG CAT CTG GAC TCA TTG AGG GTG T *CTCATGT* AC GCCCTCAATGACTCCAGATACT GAG CCA GGG AAG CTA	
AmiRβ205-FWD	**CGCG** TAG CTT CCC TGG CTC CAGTATCTGGAGTCATTGAGGG GT *ACATGAG* ACG CCT CAA TGA CAC CAG ATA TTC GAG CTT GGG AAG CAT A **TGCA**	AmiR hairpin (format C) directed at β205. Antisense sequence: 22 nt (hTRBC 202-223).
AmiRβ205-REV	TAT GCT TCC CAA GCT CGA ATA TCT GGT GTC ATT GAG GCG T *CTCATGT* AC CCCTCAATGACTCCAGATACTG GAG CCA GGG AAG CTA	
AmiRβ272-FWD	**CGCG** TAG CTT CCC TGG CTC TTGACAGCGGAAGTGGTTGCGG GT *ACATGAG* ACG CGC AAC CAC TAC CGC TGT TAT GAG CTT GGG AAG CAT A **TGCA**	AmiR hairpin (format C) directed at β272. Antisense sequence: 22 nt (hTRBC 269-290).
AmiRβ272-REV	TAT GCT TCC CAA GCT CAT AAC AGC GGT AGT GGT TGC GCG T *CTCATGT* AC CCGCAACCACTTCCGCTGTCAA GAG CCA GGG AAG CTA	
AmiRβ313-FWD	**CGCG** TAG CTT CCC TGG CTC TGGGTCCACTCGTCATTCTCCG GT *ACATGAG* ACG GGA GAA TGA CCA GTG GAC TCT GAG CTT GGG AAG CAT A **TGCA**	AmiR hairpin (format C) directed at β313. Antisense sequence: 22 nt (hTRBC 310-331).
AmiRβ313-REV	TAT GCT TCC CAA GCT CAG AGT CCA CTG GTC ATT CTC CCG T *CTCATGT* AC CGGAGAATGACGAGTGGACCCA GAG CCA GGG AAG CTA	
AmiRβ433-FWD	**CGCG** TAG CTT CCC TGG CTC ATCTCATAGAGGATGGTGGCAG GT *ACATGAG* ACG TGC CAC CAT CGT CTA TGG GAA GAG CTT GGG AAG CAT A **TGCA**	AmiR hairpin (format C) directed at β433. Antisense sequence: 22 nt (hTRBC 430-451).
AmiRβ433-REV	TAT GCT TCC CAA GCT CTT CCC ATA GAC GAT GGT GGC ACG T *CTCATGT* AC CTGCCACCATCCTCTATGAGAT GAG CCA GGG AAG CTA	
AmiRβ508-FWD	**CGCG** TAG CTT CCC TGG CTC TCCTTTCTCTTGACCATGGCCA GT *ACATGAG* ACA GGC CAT GGT CTA GAG AAG GGT GAG CTT GGG AAG CAT A **TGCA**	AmiR hairpin (format C) directed at β508. Antisense sequence: 22 nt (hTRBC 505-526).
AmiRβ508-REV	TAT GCT TCC CAA GCT CAC CCT TCT CTA GAC CAT GGC CTG T *CTCATGT* AC TGGCCATGGTCAAGAGAAAGGA GAG CCA GGG AAG CTA	

Table 13: PCR primer for the cloning of the full-length human miR17, mouse miR155 and AmiR

Name	*Sequence*	*Applied for*
miR17-BssHII-FWD-1	TTGAA **GCGCGC** GAG GTG TTA ATT CTA ATT ATC T	Cloning of human miR17 (252 bp) from genomic DNA into the modified MP71-GFP vector. Generation of full-length miR17 by overlap PCR.
miR17-MluI-NsiI-REV-2	AACTT **ATGCAT** GAAT **ACGCGT** CTC AAC ATC AGC AGG CCC TGC AC	
miR155-BssHII-FWD-1	TTG AA **GCGCGC** CTT ATC CTC TGG CTG CTG GAG G	Cloning of mouse miR155 (181 bp) from genomic DNA into the modified MP71-GFP vector. Generation of full-length miR155 by overlap PCR.
miR155-MluI-NsiI-REV-2	AACTT **ATGCAT** GAAT **ACGCGT** GTG GCC ATT TGT TCC ATG TGA G	
AmiR-BssHII-FWD-1	TTGAA **GCGCGC** CAA GAG AAC AAA GTG	Generation of full-length AmiR by overlap PCR.
AmiR-MluI-NsiI-REV-2	AACTT **ATGCAT** GAAT **ACGCGT** AA ATC TC	

Table 14: Full-length AmiR sequence encoding the AmiRβ333-B hairpin (mouse miRβ)

Name	*Sequence*	*miRNA characteristics*
mouse miRβ-FWD	TTGAA **GCGCGC** CAA GAG AAC AAA GTG GAG TCT TTG TTG CCC ACA CCC AGC TTC CCT GGC TC CTGATGTTCTGTGTGACAGGTT GT *ACATGAG* ACT ACC TGT CAC	full-length AmiR (format B) directed at β333. Antisense sequence: 22 nt (mTRBC 331-352).
mouse miRβ-REV	AACTT **ATGCAT** GAAT **ACGCGT** AAA TCT CTC AGG GGC CAC CAG GCA GGC TCT GCT GCA GAT GCT TCC CAA GCT CGT AAT GTT CTC TGT GAC AGG TAG T *CTCATGT* AC AACCTGTCAC	

Table 15: miRNA hairpins for the generation of full-length miR17 directed at the mouse TCRβ chain

Name	*Sequence*	*miRNA characteristics*
miR17β052-A-REV-1	GAT G *CACATAT* CAC TGC AAGCAGAGATTGCAAACAA ACA TTA TTC TGA CTG GTC	miR17 hairpin (format A) directed at β052. Antisense sequence: 19 nt (mTRBC 52-70).
miR17β052-A-FWD-2	GCA GTG *ATATGTG* CAT CTG AAG CAC AGT TTG CAA ACC TCG CAT TAT GGT GAC AGC T	
miR17β052-B-REV-1	TAT G *CACATAT* CA AAAAGCAGAGATTGCAAACAAAC ACA TTA TTC TGA CTG GTC	miR17 hairpin (format B) directed at β052. Antisense sequence: 23 nt (mTRBC 50-72).
miR17β052-B-FWD-2	TTT TTG *ATATGTG* CAT AAA GCA GAC ATA GTA AAC AAG TAG CAT TAT GGT GAC AGC T	

Table 16: miRNA hairpins for the generation of full-length miR155 directed at the mouse TCRα chain

Name	*Sequence*	*miRNA characteristics*
miR155α018-C-REV-1	CAG *TCAGAGGC* CAA AAC AACCTGCTGTGTACCAGTTAA CAG CAT ACA GCC TTC AG	miR155 hairpin (format C) directed at α018. Antisense sequence: 21 nt (mTRAC 16-36).
miR155α018-C-FWD-2	TTG TTT TG *GCCTCTGA* CTG ACA ACC TGC TGT ACC AGT TAA CAG GAC ACA AGG CCT G	
miR155α018-C+-REV-1	CAG *TCAGAGGC* CAA A AGAACCTGCTGTGTACCAGTTAA CAG CAT ACA GCC TTC AG	miR155 hairpin (format C+) directed at α018. Antisense sequence: 23 nt (mTRAC 16-36).
miR155α018-C+-FWD-2	TTC TTT TG *GCCTCTGA* CTG AGA ACC TGC TGT ACC AGT TAA CAG GAC ACA AGG CCT G	
miR155α300-B-REV-1	CAG *TCAGAGGC* CAA AAC TGAAACAGATATGAACCTAAA CAG CAT ACA GCC TTC AG	miR155 hairpin (format B) directed at α300. Antisense sequence: 21 nt (mTRAC 299-319).
miR155α300-B-FWD-2	CAG TTT TG *GCCTCTGA* CTG ACT GAA ACA GAT GAA CCT AAA CAG GAC ACA AGG CCT G	
miR155α300-B+-REV-1	CAG *TCAGAGGC* CAA AA TTGAAACAGATATGAACCTAAA CAG CAT ACA GCC TTC AG	miR155 hairpin (format B+) directed at α300. Antisense sequence: 22 nt (mTRAC 298-319).
miR155α300-B+-FWD-2	CAA TTT TG *GCCTCTGA* CTGA TTG AAA CAG ATG AAC CTA AAC AGG ACA CAA GGC CTG	

Table 17: miRNA hairpins for the generation of full-length AmiR directed at the human TCRα chain

Name	*Sequence*	*miRNA characteristics*
AmiRα109-C-REV-1	CTT ACT TAG T *CTCATGT* AC AAAGTAAGGATTCTGATGTGTA GAG CCA GGG AAG CTG G	AmiR hairpin (format C) directed at α109. Antisense sequence: 22 nt (hTRAC 106-127).
AmiRα109-C-FWD-2	TTT GT *ACATGAG* ACT AAG TAA GGA TAC TGG TGT GTC GAG CTT GGG AAG CAT CTG	
AmiRα319-C-REV-1	CGT ATC TTG T *CTCATGT* AC CAGATACGAACCTAAACTTTCA GAG CCA GGG AAG CTG G	AmiR hairpin (format C) directed at α319. Antisense sequence: 22 nt (hTRAC 316-337).
AmiRα319-C-FWD-2	CTG GT *ACATGAG* ACA AGA TAC GAA CAT AAA TTT TCT GAG CTT GGG AAG CAT CTG	

Table 18: miRNA hairpins for the generation of full-length AmiR directed at the human TCRβ chain

Name	*Sequence*	*miRNA characteristics*
AmiRβ034-C-REV-1	CAG CGT GT *CTCATGT* AC TCGCTGTGTTTGAGCCATCAGA GAG CCA GGG AAG CTG G	AmiR hairpin (format C) directed at β034. Antisense sequence: 22 nt (hTRBC 31-52).
AmiRβ034-C-FWD-2	CGA GT *ACATGAG* ACA CGC TGT GTT TCA GCC ATC GGT GAG CTT GGG AAG CAT CTG	
AmiRβ433-C-REV-1	GGC ACG T *CTCATGT* AC CTGCCACCATCCTCTATGAGAT GAG CCA GGG AAG CTG G	AmiR hairpin (format C) directed at β433. Antisense sequence: 22 nt (hTRBC 430-451).
AmiRβ433-C-FWD-2	CAG GT *ACATGAG* ACG TGC CAC CAT CGT CTA TGG GAA GAG CTT GGG AAG CAT CTG	

Table 19: miRNA hairpins for the generation of full-length miR155 directed at the human TCRα chain

Name	*Sequence*	*miRNA characteristics*
miR155α109-C-REV-1	CAG *TCAGAGG* CCA AAA C AAGTAAGGATTCTGATGTGTA CAG CAT ACA GCC TTC AG	miR155 hairpin (format C) directed at α109. Antisense sequence: 21 nt (hTRAC 107-127).
miR155α109-C-FWD-2	TTG TTT TG *GCCTCTGA* CTG ACA AGT AAG GAC TGA TGT GTA CAG GAC ACA AGG CCT G	
miR155α319-C-REV-1	CAG *TCAGAGG* CCA AAA C AGATACGAACCTAAACTTTCA CAG CAT ACA GCC TTC AG	miR155 hairpin (format C) directed at α319. Antisense sequence: 21 nt (hTRAC 317-337).
miR155α319-C-FWD-2	CTG TTT TG *GCCTCTGA* CTG ACA GAT ACG AAT AAA CTT TCA CAG GAC ACA AGG CCT G	

Table 20: miRNA hairpins for the generation of full-length miR155 directed at the human TCRβ chain

Name	*Sequence*	*miRNA characteristics*
miR155β034-C-REV-1	CAG *TCAGAGG* CCA AAA C CGCTGTGTTTGAGCCATCAGA CAG CAT ACA GCC TTC AG	miR155 hairpin (format C) directed at β034. Antisense sequence: 21 nt (hTRBC 32-52).
miR155β034-C-FWD-2	CGG TTT TG *GCCTCTGA* CTG ACC GCT GTG TTA GCC ATC AGA CAG GAC ACA AGG CCT G	
miR155β433-C-REV-1	CAG *TCAGAGG* CCA AAA C TGCCACCATCCTCTATGAGAT CAG CAT ACA GCC TTC AG	miR155 hairpin (format C) directed at α433. Antisense sequence: 21 nt (hTRBC 431-451).
miR155β433-C-FWD-2	CAG TTT TG *GCCTCTGA* CTG ACT GCC ACC ATT CTA TGA GAT CAG GAC ACA AGG CCT G	

5.2 Methods

5.2.1 RNAi target site prediction

Reference sequences of mouse and human TCR C regions were received from the GeneBank sequence database (Tab. 21) [316]. The C region of the TCRα chain is encoded by a single gene segment designated TRAC. The sequences of the first three TRAC exons were used as input for four web-based RNAi target site prediction programs (Tab. 22). TCRβ chains are made of either of two C regions encoded by TRBC1 and TRBC2. The sequences of all four TRBC2 exons were used for the target site prediction and afterwards, target sites that were not present in the TRBC1 sequences were removed. Furthermore, target sites with a difference of 5' end sense and 5' end antisense energy of >-0.5 k/mol were removed from the results of the WIsiRNA program and target sites with a predicted efficiency score of less than 0.8 were removed from the results of the OligoWalk program. The lists of target sites for the mouse and human TCR C regions were further processed as described in the section

2.1.2 of the Results chapter (Fig. 6). Target sites were named after the first nucleotide of the 19-mer sequences.

Table 21: Gene sequences used for RNAi target site prediction

	Mus musculus		*Homo sapiens*	
Name	*Gene ID*	*GeneBank*	*Gene ID*	*GeneBank*
TRAC	100101484	M64239.1	28755	X02883.1
TRBC1	100125262	AH002088.2	28639	M12887.1
TRBC2	100125263	AH002089.1	28638	M12888.1

Table 22: RNAi target site prediction programs

Program	*Web address*	*Reference*
WIsiRNA	www.sirna.wi.mit.edu	Yuan et al.[317]
BlockIT	www.rnaidesigner.lifetechnologies.com	-
siDESIGN	www.dharmacon.gelifesciences.com	-
OligoWalk	www.rna.urmc.rochester.edu	Lu et al.[318]

5.2.2 Construction of plasmid vectors for the reporter assay

The plasmid siCHECK-2 (Fig. 27), which harbors firefly and renilla luciferase genes under the control of separate promoters, was purchased from Promega (Mannheim, Germany). Reporter plasmids were generated by cloning the sequences of the mouse TCR C regions into the 3' UTR of the renilla luciferase gene using the XhoI and NotI restriction sites. Native sequences (mTRAC, mTRBC1, mTRBC2) were amplified from cDNA by PCR (Phusion high-fidelity DNA polymerase, Thermo Scientific). Total RNA was isolated from splenocytes of C57BL/6 mice (RNeasy Mini Kit, Qiagen, Hildesheim, Germany) and converted into cDNA using reverse transcriptase (Superscript II, Life Technologies) and oligo(dT) primers (Promega). Codon-optimized sequences (mTRACco and mTRBC2co) were amplified by PCR from a plasmid (provided by P. Meyerhuber, MDC, Berlin). The plasmid encoded the genes of a human TCR with mouse constant regions specific for epidermal growth factor receptor 2 (HER2) [319], which were codon-optimized by GeneArt (Regensburg, Germany). PCR primers (Tab. 5) encoding NotI and XhoI restriction sites were designed using Primer3 software [320]. PCR products and the siCHECK-2 plasmid were digested with NotI and XhoI restriction enzymes (Fermentas, St. Leon-Rot, Germany). Afterwards, the digested plasmid was dephosphorylated with alkaline phosphatase (Roche, Mannheim, Germany). The DNA preparations were subjected to gel electrophoresis and linearized DNA of the expected size was isolated (Invisorb Spin DNA Extraction Kit, STRATEC Biomedical, Berlin, Germany). Five siCHECK-2 plasmids encoding different mouse TCR C regions (mTRAC, mTRACco, mTRBC1, mTRBC2 and mTRBC2co) were generated by ligation of the linearized vector with the respective PCR products (Rapid DNA Ligation Kit, Roche) and used for the transformation of chemically competent *E.coli* cells (MACH1, Life Technologies). Plasmid DNA was isolated from 2-ml cultures grown from single colonies (Invisorb Spin Plasmid Mini Two, Invitek) and

sequenced by MWG. Plasmids with the correct sequence were used for the production of larger quantities of plasmid DNA (Plasmid Midi Kit, Qiagen).

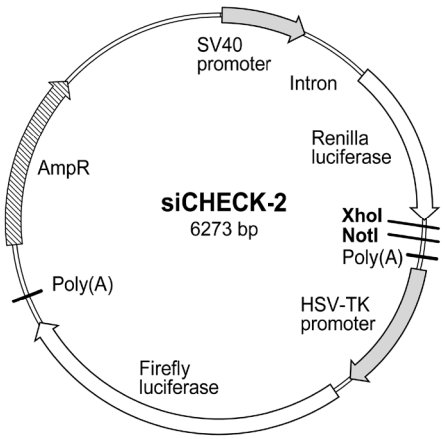

Figure 27: *Map of the siCHECK-2 vector.*
The siCHECK-2 plasmid was used in the dual-luciferase reporter assay. It encodes two luciferases. The renilla luciferase is used to assess the RNAi effect and the firefly luciferase is used for data normalization. To construct reporter plasmids, a sequence of interest is cloned in the 3' UTR of the renilla luciferase using XhoI and NotI restriction sites. Renilla luciferase expression is controlled by a simian virus 40 (SV40) enhancer and early promoter. Firefly luciferse expression is controlled by a herpes simplex virus-thymidine kinase (HSV-TK) promoter.

The effector plasmid SUPERIOR.puro (Fig. 28), which harbors a pol III H1 promoter for the expression of shRNA, was purchased from Oligoengine (Seattle, Washington, USA). DNA oligonucleotides encoding shRNA directed at the predicted target sites were constructed according to the manufacturer's instructions and synthesized by MWG (Tab. 6). The forward strands encoded the 19-mer target sequences in sense and antisense orientation connected by a loop of 9 nt. Five thymidine residues at the 3' end served as a stop signal for the transcription. The vector was digested using the restriction enzymes HindIII and BglII (Fermentas), dephosphorylated and purified by gel electrophoresis. The forward and reverse strands of the DNA oligonucleotides encoding the shRNA (Tab. 6) were phosphorylated using polynucleotide kinase (PNK, Roche). Then, the mixture was heated to 95° C for 5 min and both strands were annealed by cooling down slowly. Annealed oligonucleotides possessed single-stranded overhangs that were compatible with the HindIII and BglII restriction sites of the vector. The shRNA-encoding vectors were generated by ligation of the oligonucleotides with the linearized vector. Four shRNA plasmids directed at the mouse TCRα chain, four shRNA plasmids directed at the mouse TCRβ chain and two control shRNA plasmids were generated (Tab. 6). Plasmids were propagated in *E.coli* as described above and sequenced by MWG.

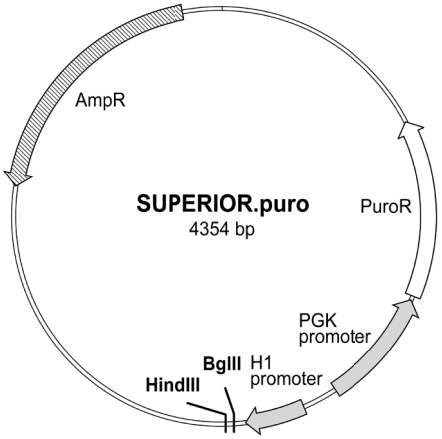

Figure 28: *Map of the SUPERIOR.puro vector.* The SUPERIOR.puro vector harbors an H1 promoter for the expression of short hairpin RNA (shRNA). This polymerase III promoter produces uncapped RNA transcripts without poly(A)-tails. DNA oligonucleotides encoding the shRNA were synthesized and introduced using the HindIII and BglII restriction sites.

5.2.3 Dual-luciferase reporter assay

A mixture of the reporter and effector plasmids were transfected into mouse NIH/3T3 fibroblasts and two days later, the amount of renilla and firefly luciferase was determined using the dual-luciferase reporter assay system (Promega) according to the manufacturer's instructions. One day before transfection, $5x10^4$ cells per well were seeded into tissue culture-treated 24-well plates. Cells were transfected in triplicates using the calcium phosphate method. Each well was transfected with a total amount of 3 µg DNA containing 0.4 µg of the reporter plasmid. First, the reporter and effector plasmid were mixed in a molar ratio of 1:2. Then, the promoterless plasmid SL1190 was used to adjust the total DNA amount. $CaCl_2$ solution (2.5 M) was added to a concentration of 250 mM and H_2O was used to adjust the mixture to a volume of 25 µL per well. The solution was mixed under agitation with an equal amount of transfection buffer (1% HEPES, 1.5 mM Na_2HPO_4, 270 mM NaCl, 10 mM KCl, pH 6.76). After 15 min of incubation, 50 µl per well was added dropwise onto the cells and 6 h later, the medium was exchanged. One transfection mix sufficient for three wells was prepared for each reporter and effector plasmid combination. Two days after the transfection, the medium was removed, the cells were washed with PBS, 100 µl passive lysis buffer (Promega) per well were added, the plates were placed on a rocking platform for 15 min and the lysates were collected in 1.5 ml tubes that were placed on ice. 20 µl of the lysates were transferred to 96-well black microplates with white wells (Berthold Technologies, Bad Wildbad, Germany). The light signals produced by the luciferase enzymes after adding substrates were measured using a Mithras LB 940 Multimode Microplate Reader (Berthold Technologies) equipped with automatic injectors. First, 100 µl LARII reagent (Promega) were added to the first well and after 2 s delay, the light signal was measured for 10 s. Then, 100 µl Stop&Glow reagent (Promega) were added to the same well and the light signal was measured again as described. The procedure was repeated for each well. The first light signal is proportional to the amount of firefly luciferase in the lysates and the second signal is proportional to the amount of renilla luciferase. The ratio of both signals was calculated and compared to the ratio of the negative control.

5.2.4 Introduction of miRNA into the MP71-GFP vector

The general cloning procedures were performed as described. The γ-retroviral vector MP71-GFP (Fig. 29) was modified in two steps: First, new restriction sites were introduced and second, these restriction sites were used to introduce miRNA sequences.

In the first step, MluI and NsiI restriction sites were introduced into plasmids of the viral vector MP71-GFP (Fig. 29). Synthesized DNA oligonucleotides (Tab. 7) were used to introduce the restriction sites in exonic positions either 5' or 3' of GFP. The oligonucleotides were designed with single-stranded overhangs that were compatible either to the NotI or EcoRI restriction sites flanking the GFP encoding sequence. The introduction of the MluI and NsiI restriction sites into the 5' intron of the MP71-GFP vector was achieved in a two-step process: First, a part of the intron was amplified by PCR from the MP71-GFP plasmid using the primer 5UTR-FWD and NotI-NsiI-MluI-REV (Tab. 7). The PCR product was cloned into the MP71-GFP vector using BglII and NotI restriction sites. This procedure placed the MluI and NsiI restriction sites in the middle of the intronic sequence, but the 3' sequences of the intron were lost during the procedure. In the subsequent step, the intron was restored by the introduction of synthesized DNA (Tab. 7) between the NsiI and NotI restriction sites.

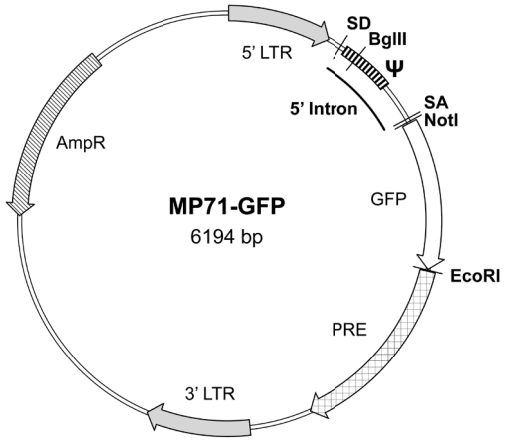

Figure 29: *Map of the MP71-GFP vector.* The MP71 vector harbors long terminal repeats (LTR) of the myeloproliferative sarcoma virus. The transgene is flanked by NotI and EcoRI restriction sites and followed by a posttranscriptional regulatory element (PRE) of the woodchuck hepatitis virus. The splice donor (SD) and splice acceptor (SA) sites of the intron, which contains the packaging signal (Ψ), are indicated.

In the second step, miRNA sequences were introduced into the modified MP71-GFP vectors harboring the MluI and NsiI restriction sites at either one of the three positions (Fig. 15A). Two strategies were used: either the AmiR backbone sequence was introduced first and the hairpins were introduced afterwards (Fig. 12A) or full-length miRNA was introduced in a single cloning step (Fig 12B). The AmiR backbone sequence was introduced using synthesizes oligonucleotides (Tab. 8) with compatible overhangs. The MluI and NsiI restriction sites of the vector were destroyed through the integration and a new pair of MluI and NsiI restriction sites was introduced by the oligonucleotides allowing the subsequent cloning of the miRNA hairpin (Fig. 12B). Ten miRNA vectors directed at the mouse TCRα chain (Tab. 9), five miRNA vectors directed at the mouse TCRβ chain (Tab. 10), ten miRNA vectors directed at the human TCRα chain (Tab. 11) and 13 miRNA vectors directed at the

human TCRβ chain (Tab. 12) were cloned using an MP71-GFP vector harboring the AmiR backbone sequence in the 5' intron.

5.2.5 Generation of full-length miRNA by overlap PCR

The sequences of full-length miRNA harboring new hairpin sequences and restriction sites at both ends (Fig. 12B) were generated by overlap PCR using plasmids encoding the full-length miRNA sequences as templates. The native sequences of human miR17 (252 bp) and mouse miR155 (181 bp) were amplified by PCR from genomic DNA that was isolated from T cells (Invisorb Spin Tissue Mini Kit, Invitek). Forward primers encoded a BssHII restriction site, which is compatible with the MluI restriction site, and reverse primers encoded MluI and NsiI restriction sites (Tab. 13). The AmiR sequence (185 bp) was generated by PCR using synthesized DNA oligonucleotides as template (Tab. 14). The forward and reverse oligonucleotides encoded either half of the miRNA sequence and possessed overlapping ends. The oligonucleotides were annealed and elongated by PCR. In a subsequent PCR, the full-length double-stranded DNA fragment was amplified using the primers AmiR-BssHII-FWD-1 and AmiR-MluI-NsiI-REV-2 (Tab. 13). The AmiR, miR155 and miR17 PCR products were digested with BssHII and NsiI (Fermentas) and introduced into the modified MP71-GFP vectors using the MluI and NsiI restriction sites.

To generate miRNA with a hairpin of choice, oligonucleotides were synthesized encoding the new hairpin and a part of the miRNA backbone sequence. In two separate PCR (Phusion high-fidelity DNA polymerase, Thermo Scientific), the oligonucleotides were used as primers together with primers binding to the ends of the miRNA (Fig. 30A). Plasmids encoding miRNA with a different hairpin served as template. The products of both PCR were subjected to gel electrophoresis and DNA of the expected size was isolated (Invisorb Spin DNA Extraction Kit, STRATEC Biomedical). The PCR products were annealed in a subsequent PCR reaction without additional primer or template DNA (Fig. 30B). The annealing PCR comprises five cycles of 94 °C for 20 s followed by slow cooling to 50 °C (0.5 °C/s) and 72 °C for 10 s each. Then, primers that bind to both ends of the miRNA (Tab. 13) were added to the PCR reaction and the full-length construct encoding the new hairpin was amplified (Fig. 30C). The PCR products were cloned into the modified MP71-GFP vectors harboring the MluI and NsiI restriction sites as described above. The full-length miRNA encoded MluI and NsiI restriction sites at the 3' end, so that the inserts after being cloned into the vector provided the restriction sites for the next miRNA integration (Fig. 12B). Two miRNA based on the miR17 sequence and directed at the mouse TCRβ chain (Tab. 15), four miRNA based on the miR155 sequence and directed at the mouse TCRα chain (Tab. 16), two miRNA based on the AmiR sequence and directed at the human TCRα chain (Tab. 17), two miRNA based on the AmiR sequence and directed at the human TCRβ chain (Tab. 18), two miRNA based on the miR155 sequence and directed at the human TCRα chain (Tab. 19) and two miRNA based on the miR155 sequence and directed at the human TCRβ chain (Tab. 20) were generated using this strategy.

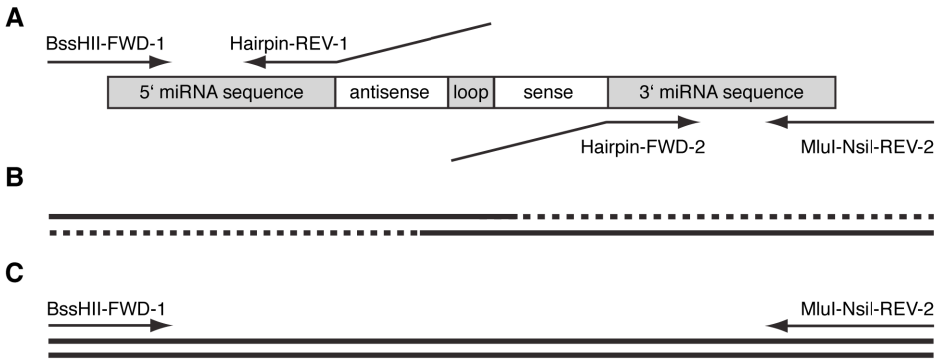

Figure 30: *Generation of full-length miRNA by overlap PCR.*
(**A**) In the first step, the 5' and 3' sequences of the miRNA were separately amplified by PCR using primers encoding the new miRNA hairpin. A plasmid harboring the miRNA sequence with a different hairpin served as template. Afterwards, the products of both PCR were purified. (**B**) Both PCR products were annealed and elongated in a PCR without primer. (**C**) After the annealing step, primers binding to both ends of the miRNA were added and the full-length miRNA sequence encoding the new hairpin was amplified by PCR.

5.2.6 Generation of RNAi-TCR replacement vectors

RNAi-TCR replacement vectors were generated by exchanging the GFP gene of the miRNA-expressing MP71-GFP vectors for a TCR cassette using the NotI and EcoRI restriction sites flanking GFP (Fig. 29). MP71 vectors encoding the native and optimized sequences of the P14 TCR were provided by M. Leisegang and S. Reuss, respectively (both MDC, Berlin) [207,250]. The fully codon-optimized P14 TCR genes harbored a threonine to cysteine mutation at the position 187 in the TCRα chain and a serine to cysteine mutation at the position 199 in the TCRβ chain. The native P14 TCR genes were rendered RNAi-resistant by the introduction of four silent mutations at the RNAi target sites (Fig. 31). The codon changes, which were identical to those in the codon-optimized TCR constant regions, were introduced by overlap PCR. The procedure was similar to the one described for the generation of full-length miRNA (Fig. 30).

TCRα constant region (4 mutations)

```
     Phe Glu Thr Asp Met Asn Leu Asn
nat: ttT GAA ACA GAT ATG AAC CTA AAc
 mu: ttC GAG ACA GAC ATG AAC CTG AAc
```

TCRβ constant region (4 mutations)

```
     Lys Pro Val Thr Gln Asn Ile Ser
nat: aAA CCT GTC ACA CAG AAC ATC AGt
 mu: aAG CCC GTG ACC CAG AAC ATC AGt
```

Figure 31: *The native P14 TCR genes were rendered RNAi-resistant by silent mutations.*
The native (nat) sequences of the P14 TCRα and β chains were modified by the introduction of synonymous codons to protect the TCR from the RNAi effect. The codons of the RNAi target sites were changed into the same codons that were used in the codon-optimized P14 TCR chains. Upper-case letters are used for the nucleotides of the target site sequence. Mutated nucleotides are underlined.

MP71 vectors encoding two versions of the human, MAGE A1-reactive 1367 TCR were provided by the AG Blankenstein (MDC, Berlin). One vector encoded codon-optimized TCR genes that differed at the RNAi target sites from the native TCR sequences and were used to construct the RNAi-TCR replacement vector. The other vector harbored codon-optimized TCR genes that were additionally

modified by the introduction of two additional cysteines and nine residues of the mouse TCR C region. These modifications improve the surface expression of the TCR in TCR gene-modified T cells and induce preferential pairing of the TCR chains [211,212,213,214].

5.2.7 Production of viral supernatants

Ecotropic retroviral particles were produced by transfecting Plat-E cells with the respective MP71 plasmids using the calcium phosphate method. One day before the transfection, $4x10^6$ cells per well in 3 ml medium (without blasticidin and puromycin) were seeded into tissue culture-treated 6-well plates. The next day, each well was transfected with 18 µg plasmid DNA using the following procedure: First, a 150 µl solution containing the DNA in H_2O and 250 mM $CaCl_2$ was prepared. Then, the solution was mixed under agitation with an equal amount of transfection buffer (1% HEPES, 1.5 mM Na_2HPO_4, 270 mM NaCl, 10 mM KCl, pH 6.76). After 15min of incubation, 300 µl per well was added dropwise onto the cells and 6 h later, the medium was exchanged. Supernatants containing the viral particles were harvested 48 h after transfection, filtrated (0.45-µm pore size) and frozen (-80 °C). Amphotropic retroviral particles were produced by transfecting HEK 293T cells with the respective MP71 plasmid and two plasmids encoding the MLV env (10A1) and gag/pol genes in a ratio of 1:1:1 (each 6 µg) following the same protocol as described above but with the exception that $1x10^6$ cells per well were seeded into 6-well plates one day before the transfection.

5.2.8 Titration of viral supernatants

Batches of viral supernatant were produced for each vector, frozen (-80 °C) in aliquots and the titer of the viral supernatants was determined by transducing activated splenocytes (C57BL/6) with diluted supernatants. The transduction efficiency was assessed four days after transduction by flow cytometry and the dilution required to obtain a transduction rate of 50% was determined (Fig. 32). The transduction rates achieved with supernatants generated with the miR-P14 vector were somewhat lower compared to supernatants generated with the P14 vector. Therefore, the supernatants of the P14 and miR-P14 vector had to be diluted to a concentration of 50% and 70%, respectively. Higher transduction rates were achieved with the supernatants of the miR-P14opt and P14opt vector encoding the genetically optimized TCR genes with and without the miRNA. In addition, there was only a small difference between both supernatants. A concentration of 20% and 25% was required for the supernatants generated with the P14opt and miR-P14opt vector, respectively, in order to achieve a transduction rate of 50%.

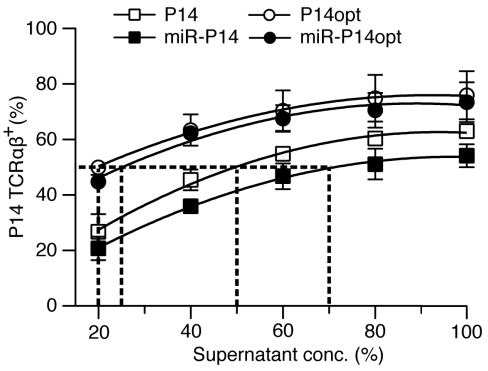

Figure 32: *Titration of viral supernatants.* Polyclonal T cells (C57BL/6) were transduced with diluted viral supernatant and transduction (Td) efficiencies were determined as percentage of CD8/P14 TCRαβ T cells four days after Td. Dotted lines indicate the concentration required to achieve Td efficiency of 50%. Plot shows the mean ±SD of three independent experiments (*n*=3).

5.2.9 Isolation, transduction and culture of mouse splenocytes

10-12 week old mice were sacrificed, spleens were removed and single-cell suspensions were generated by passing the spleens through a 40-µm cell strainer. The cells were spun down and resuspended in 4 ml ACK lysis buffer (150 mM NH_4Cl, 1 mM $KHCO_3$, 100 nM Na_2EDTA, pH 7.2-7.4). Lysis of red blood cells was stopped after 90 s by adding mouse T cell culture medium (mTCM, RPMI 1640 GlutaMAX (Life Technologies), 10% heat-inactivated FCS (PAN-Biotech), 1 mM sodium pyruvate, 1 mM HEPES, 100 IU/ml Penicillin/Streptomycin, 50 µM 2-mercaptoethanol (all Life Technolgies). Cells were washed in mTCM, adjusted to $2x10^6$/ml and activated for 24 h with 1 µg/ml anti-CD3 mAb, 0.1 µg/ml anti-CD28 mAb (both BD Biosciences) and 10 IU/ml Proleukin (Novartis, Nuremberg, Germany). Mouse splenocytes were subjected to two rounds of transduction. For the first transduction the culture medium was exchanged, the cell density was adjusted to $1x10^6$ cells/ml and $4x10^5$ beads/ml mouse T-Activator CD3/CD28 (Life Technologies), 10 IU/ml Proleukin and 4 µg/ml protamine sulfate (Sigma-Aldrich, Taufkirchen, Germany) were added. Then, $1x10^6$ activated splenocytes per well were transferred to the virus-coated plates, which were prepared as follows: 0.5 ml viral supernatant per well was transferred to RetroNectin-coated (12.5 µg/ml, Takara, Saint-Germain-en-Laye, France) 24-well non-tissue culture plates, centrifuged (3000 g, 4 °C) for 3 h and immediately discharged before the activated splenocytes were transferred to the plates. Next, the splenocytes were centrifuged (800 g, 32 °C) for 20 min and cultured over night. For the second transduction, 1 ml viral supernatant supplemented with 10 IU Proleukin (Novartis) and 4 µg protamine sulfate (Sigma-Aldrich) per well was added and the cells were centrifuged (800 g, 32 °C) for 1.5 h. After transduction, the cells were washed and adjusted to $1x10^6$/ml in mTCM supplemented with 10 ng/ml human recombinant IL-15 (Peprotech, Hamburg, Germany). This step was repeated every 3-4 d during prolonged culture of the transduced splenocytes.

5.2.10 Isolation, transduction and culture of human T cells

Peripheral blood was drawn from healthy donors after giving informed consent and diluted 1:1 in human T cell culture medium (hTCM, RPMI 1640 GlutaMAX (Life Technologies), 10% heat-inactivated FCS (PAN-Biotech), 1 mM sodium pyruvate, 10 mM HEPES, 100 IU/ml Penicillin/Streptomycin (all Life Technolgies)). Peripheral blood mononuclear cells (PBMC) were isolated by density gradient centrifugation (Biocoll, Biochrom). PBMC were washed in hTCM, adjusted to $1x10^6$ cells/ml and 100 IU/ml Proleukin (Novartis) were added. The cells were transferred to 24-well plates (1 ml/well), which were coated with CD3-specific mAb (5 µg/ml) and CD28-specific mAb (1 µg/ml) (both BD Bioscience). Human T cells were subjected to two rounds of transduction. The first transduction was performed after the T cells were activated for 48 h on the mAb-coated plates. 1 ml viral supernatant supplemented with 8 µg protamine sulfate and 100 IU Proleukin per well was added and the cells were centrifuged (800 g, 32 °C) for 1.5 h. The next day, the cells were transferred into the virus-coated plates, which were prepared as follows: 3 ml viral supernatant per well was transferred to RetroNectin-coated (12.5 µg/ml) 6-well non-tissue culture plates, centrifuged (3000 g, 4 °C) for 3 h and immediately discharged before the activated T cells were transferred to the plates. 3 ml hTCM supplemented with 4 µg protamine sulfate and 100 IU Proleukin per well was added and the cells were centrifuged (800 g, 32 °C) for 1.5 h. After the transduction, hTCM supplemented with 100 IU Proleukin was added to the cells as required on a daily basis for a week. Afterwards, the medium was completely exchanged for fresh hTCM supplemented with 10 IU Proleukin to rest the cells. Two days later, functional assays were performed.

5.2.11 Transduction of T cell lines

Mouse B3Z cells and human Jurkat cells were subjected to a single round of transduction. $1x10^5$ cells per well in 1 ml medium were transferred to RetroNectin-coated (12.5 µg/ml) 24-well non-tissue culture plates. 1 ml viral supernatant per well supplemented with 8 µg protamine sulfate was added and the cells were centrifuged (800 g, 32 °C) for 1.5 h.

5.2.12 Analysis of surface protein by flow cytometry

If not stated otherwise, flow cytometry data were acquired 4-6 d after transduction. Approximately $5x10^6$ cells were stained with saturating amounts of mAb or MHC multimer. Cells were stained in buffer (PBS, 2 mM EDTA, 2% FCS, 0.05% NaN_3) for 30 min at 4 °C in the dark, washed twice and resuspended in buffer containing SYTOX Blue (Life Technologies), which stains dead cells. Immunofluorescence was measured using a FACS Canto II cytometer (BD Biosciences) or a MACS Quant Analyzer (Miltenyi Biotec, Bergisch Gladbach, Germany). Data were analyzed using FlowJo software (Tree Star, Ashland OR, USA). Relative median fluorescence intensities (MFI) values were calculated by dividing the MFI of the samples by the MFI of the control sample as specified in the figure legends. TCR surface levels of GFP-expressing mouse T cells and B3Z cells were determined using APC-

labeled anti-mouse mAb directed against mTRBC or CD3ε (Tab. 3). P14 TCR chain expression was analyzed using FITC-labeled anti-mouse TCR Vβ8 mAb, PE-labeled anti-mouse CD8α mAb and APC-labeled anti-mouse TCR Vα2 mAb (Tab. 3). TCR-transgenic T cells were stained with PE-labeled Db-$SV40_I$ multimer and APC-labeled Db-GP33 multimer (Tab. 2). P14 TCR chain pairing was analyzed using PE-labeled anti-mouse CD8α mAb (Tab. 3) and APC-labeled Db-GP33 multimer (Tab. 2). Adoptively transferred T cells were analyzed by staining peripheral blood samples after ACK lysis of the red blood cells with unlabeled anti-mouse CD16/CD32 mAb, FITC-labeled anti-mouse CD8α mAb, PE-labeled anti-mouse CD45.1 mAb (Tab. 3) and Db-GP33 multimer (Tab. 2). TCR surface levels of GFP-expressing human T cells and Jurkat cells were determined using APC-labeled anti-human CD3 mAb (Tab. 4). 1367 TCR chain pairing was analyzed using FITC-labeled anti-human CD8α mAb (Tab. 4) and APC-labeled A2-MAGE A1 multimer (Tab. 2). The expression of endogenous TCRα chains on the surface of 1367 TCR-transduced T cells was analyzed using a mixture of FITC-labeled anti-human TCR Vα2, Vα7.2 and Vα12.1 mAb, PE-labeled anti-human TCR Vβ7 mAb and APC-labeled anti-human CD8 mAb (Tab 4). The expression of endogenous TCRβ chains on the surface of 1367 TCR-transduced T cells was analyzed using FITC-labeled anti-human TCR Vβ3 mAb, a mixture of PE-labeled anti-human TCR Vβ1, Vβ2, Vβ5.1, Vβ13.6, Vβ14 and Vβ22 mAb and APC-labeled anti-human CD8 mAb (Tab 4).

5.2.13 Melanoma lung metastases model

B16-GP33 cells were split and seeded at low density one day before being harvested. $1x10^6$ cells per mice (C57BL/6, 10-12 weeks old) were injected into the tail vein. Three days later, $2x10^6$ P14 TCR-expressing CD8 T cells (B6.SJL) per mice were injected similarly. Seven and 14 days after T cell transfer, blood samples were taken from the sub-mandibular vain and analyzed by flow cytometry. After two weeks, one mice of each group was sacrificed and tumor growth was inspected. All mice of the control group were sacrificed two weeks after the T cell transfer and the mice of the treatment groups were sacrificed after 21 days. The lungs were removed and the number of macroscopically visible metastases on the lung surface was determined.

5.2.14 TI-GVHD model

The experiments using the TI-GVHD mouse model were conducted in cooperation with G. Bendle and C. Linneman (group of Prof. T. N. Schumacher, The Netherlands Cancer Institute, Amsterdam) in Amsterdam and Berlin. Single-cell suspensions of mouse splenocytes (C57BL/6, 10-12 weeks) were prepared as described (5.2.9). The cell density was adjusted to $3x10^6$ cells/ml and concovalin A (2 µg/ml, Sigma-Aldrich) and IL-7 (1 ng/ml, Preprotech) was added. The cells were transferred to 24-well plates (1 ml/well) and incubated for 48 h before they were subjected to one round of transduction. Activated splenocytes were spun down, resuspended in viral supernatant ($6x10^6$ cells/ml) and transferred to RetroNectin-coated (12.5 µg/ml) 24-well non-tissue culture plates (0.5 ml/well). The cells were centrifuged (800 g, 23 °C) for 1.5 h and incubated over night. The next day, the transduction

rate was determined by flow cytometry and an unsorted population of cells containing $1x10^6$ P14 TCR-expressing CD8 T cells was transferred via the tail vain into the mice (C57BL/6, 10-12 weeks) that were treated one day before with total body irradiation (TBI, 5 Gy). Ten days after the T cell transfer, the mice received $7.2x10^5$ IU Proleukin intraperitoneally twice a day for thee days. During the experiment, the mice were monitored thoroughly several times a day (weight, appearance, behavior) and peripheral blood samples were analyzed to confirm the engraftment and expansion of the transferred T cells. Group assignments were blinded.

5.2.15 Histological analysis

Histological specimens from the TI-GVHD mouse model were analyzed in cooperation with S. Schulz (Institute of Pathology, Charité Campus Mitte, Berlin). Spleen and bone marrow (femur) of mice were collected and fixed with 4% buffered paraformaldehyde (Roti-Histofix, Carl Roth, Karlsruhe, Germany). Bones were decalcified using EDTA. Paraffin-embedded tissues were cut in sections (3 µm thickness), dried (70 °C, 30 min), deparaffinized in xylene and dehydrated through graded alcohols. Sections were stained using hematoxylin and eosin (H&E) and analyzed using a brightfield microscope (BX53, Olympus, Hamburg, Germany) equipped with a digital camera (DP25, Olympus).

5.2.16 Cytokine secretion assay

To analyze antigen-stimulated cytokine secretion of transduced mouse T cells, $5x10^4$ CD8/P14 TCR T cells were cocultured with $5x10^4$ syngeneic mouse splenocytes preloaded with GP33 peptide (Tab. 1) in round-bottom 96-well plates for 24 h. The INF-γ concentration in the supernatant was determined by enzyme linked immunosorbent assay (ELISA, BD Bioscience) using flat-bottom 96-well ELISA plates (MaxiSorp, Thermo Scientific). Human 1367 TCR-transduced T cells were analyzed following the same protocol but using T2 cells preloaded with MAGE A1 peptide (Tab. 1) for stimulation and an ELISA kit for human INF-γ (BD Bioscience).

6 Abbreviations

aa	amino acid
Ago	Argonaut
AIRE	autoimmune regulator
AmiR	artificial miRNA
APC	allophycocyanin
APC	antigen presenting cell
as	antisense sequence
ATP	adenosine triphosphate
ATT	adoptive T cell therapy
AU	arbitrary unit
BLAST	basic local alignment search tool
BM	bone marrow
bp	base pair
C domain	constant domain
C region	constant region
C segment	constant segment
C-terminus	carboxyl-terminus
CAR	chimeric antigen receptor
CD	cluster of differentiation
CDK4	cyclin-dependent kinase 4
cDNA	complementary DNA
CDR	complementarity determining region
CEA	carcinoembryonic antigen
CMV	cytomegalovirus
contr.	control
CR	complete reponse
CT antigen	cancer/testis antigen
D segment	diversity segment
DGCR8	DiGeorge critical region 8
DLI	donor lymphocyte infusion
DMEM	Dulbecco's modified Eagles medium
DNA	deoxyribonucleic acid
dsRNA	double-stranded RNA
E. coli	Escherichia coli
EBV	Epstein-Barr virus
EDTA	ethylenediaminetetraacetic acid
ELISA	enzyme-linked immunosorbant assay
endo.	endogenous
ER	endoplasmic reticulum
ERAAP	ER aminopeptidase associated with antigen processing
ex.	exonic
FCS	fetal calf serum
FITC	fluorescein isothiocyanate
GFP	green fluorescent protein
GP	glycoprotein
GVHD	graft-versus-host disease
GVL	graft-versus-leukemia

H&E	hematoxylin and eosin
HEPES	hydroxyethyl-piperazineethane-sulfonic acid
HLA	human leukocyte antigen
HSC	hematopoietic stem cells
hTCM	medium for human T cells
IFN	interferon
Ig	immunoglobulin
IL	interleukin
int.	intronic
ITAM	immunoreceptor tyrosine-based activation motif
J segment	joining segment
LCMV	lymphocyte choriomeningitis virus
LTR	long terminal repeat
mAb	monoclonal antibody
MAGE	melanoma antigen
MART-1	melanoma antigen recognized by T cells 1
MCA	methylcholanthrene
MFI	median fluorescence intensity
mHAg	minor histocompatibility antigen
MHC	major histocompatibility complex
miRNA	micro RNA
Mo-MLV	Moloney murine leukemia virus
MPSV	myeloproliferative sarcoma virus
mRNA	messenger RNA
mTCM	medium for mouse T cells
mTRA	mouse TCRβ chain
mTRAC	mouse TCRα chain constant region
mTRB	mouse TCRα chain
mTRBC	mouse TCRβ chain constant region
N-terminus	amino-terminus
NMA	nonmyeloablative
nt	nucleotide
ORF	open reading frame
PALS	periarterial lymphatic sheaths
PBL	peripheral blood lymphocytes
PBMC	peripheral blood mononuclear cells
PCR	polymerase chain reaction
PE	phycoerythrin
pol	polymerase
PR	partial response
PRE	posttranscriptional regulatory element
RCC	renal cell carcinoma
RefSeq	reference sequence database
RISC	RNA-induced silencing complex
RNA	ribonucleic acid
RNAi	RNA interference
RPMI	Roswell Park Memorial Institute
RRE	Rev-responsive element
SA	splice acceptor
scTCR	single-chain TCR

SD	standard deviation
SD	splice donor
SELEX	systematic evolution of ligands by exponential enrichment
shRNA	short hairpin RNA
siRNA	small interfering RNA
ss	sense sequence
TAA	tumor-associated antigen
TALEN	transcription activator-like effector nuclease
TAP	transporter associated with antigen processing
TBI	total body irradiation
T_{CM} cell	central memory T cell
TCR	T cell receptor
Td	transduction
T_E cell	effector T cell
T_{EM} cell	effector memory T cell
Tg	transgenic
TI-GVHD	TCR gene transfer-induced graft-versus-host disease
TIL	tumor-infiltrating lymphocytes
T_M cell	memory T cell
T_m domain	transmembrane domain
T_N cell	naive T cell
TSA	tumor-specific antigen
UTR	untranslated region
V domain	variable domain
V region	variable region
V segment	variable segment
ZFN	zinc-finger nuclease
β2M	β2-microglobulin

7 Literature

[1] Cantor, H. and Boyse, E. A. (1975): Functional subclasses of T-lymphocytes bearing different Ly antigens. I. The generation of functionally distinct T-cell subclasses is a differentiative process independent of antigen, J Exp Med 141 [6], pp. 1376-89. URL: http://www.ncbi.nlm.nih.gov/entrez/query.fcgi?cmd=Retrieve&db=PubMed&dopt=Citation&list_uids=1092798

[2] Kisielow, P.; Hirst, J. A.; Shiku, H.; Beverley, P. C.; Hoffman, M. K.; Boyse, E. A. and Oettgen, H. F. (1975): Ly antigens as markers for functionally distinct subpopulations of thymus-derived lymphocytes of the mouse, Nature 253 [5488], pp. 219-20. URL: http://www.ncbi.nlm.nih.gov/entrez/query.fcgi?cmd=Retrieve&db=PubMed&dopt=Citation&list_uids=234178

[3] Evans, R. L.; Breard, J. M.; Lazarus, H.; Schlossman, S. F. and Chess, L. (1977): Detection, isolation, and functional characterization of two human T-cell subclasses bearing unique differentiation antigens, J Exp Med 145 [1], pp. 221-33. URL: http://www.ncbi.nlm.nih.gov/entrez/query.fcgi?cmd=Retrieve&db=PubMed&dopt=Citation&list_uids=137269

[4] Kung, P.; Goldstein, G.; Reinherz, E. L. and Schlossman, S. F. (1979): Monoclonal antibodies defining distinctive human T cell surface antigens, Science 206 [4416], pp. 347-9. URL: http://www.ncbi.nlm.nih.gov/entrez/query.fcgi?cmd=Retrieve&db=PubMed&dopt=Citation&list_uids=314668

[5] Reinherz, E. L.; Kung, P. C.; Goldstein, G. and Schlossman, S. F. (1979): Separation of functional subsets of human T cells by a monoclonal antibody, Proc Natl Acad Sci U S A 76 [8], pp. 4061-5. URL: http://www.ncbi.nlm.nih.gov/entrez/query.fcgi?cmd=Retrieve&db=PubMed&dopt=Citation&list_uids=315070

[6] Reinherz, E. L.; Meuer, S.; Fitzgerald, K. A.; Hussey, R. E.; Levine, H. and Schlossman, S. F. (1982): Antigen recognition by human T lymphocytes is linked to surface expression of the T3 molecular complex, Cell 30 [3], pp. 735-43. URL: http://www.ncbi.nlm.nih.gov/entrez/query.fcgi?cmd=Retrieve&db=PubMed&dopt=Citation&list_uids=6982759

[7] Köhler, G. and Milstein, C. (1975): Continuous cultures of fused cells secreting antibody of predefined specificity, Nature 256 [5517], pp. 495-7. URL: http://www.ncbi.nlm.nih.gov/entrez/query.fcgi?cmd=Retrieve&db=PubMed&dopt=Citation&list_uids=1172191

[8] Allison, J. P.; McIntyre, B. W. and Bloch, D. (1982): Tumor-specific antigen of murine T-lymphoma defined with monoclonal antibody, J Immunol 129 [5], pp. 2293-300. URL: http://www.ncbi.nlm.nih.gov/entrez/query.fcgi?cmd=Retrieve&db=PubMed&dopt=Citation&list_uids=6181166

[9] Meuer, S. C.; Fitzgerald, K. A.; Hussey, R. E.; Hodgdon, J. C.; Schlossman, S. F. and Reinherz, E. L. (1983): Clonotypic structures involved in antigen-specific human T cell function. Relationship to the T3 molecular complex, J Exp Med 157 [2], pp. 705-19. URL: http://www.ncbi.nlm.nih.gov/entrez/query.fcgi?cmd=Retrieve&db=PubMed&dopt=Citation&list_uids=6185617

[10] Haskins, K.; Kubo, R.; White, J.; Pigeon, M.; Kappler, J. and Marrack, P. (1983): The major histocompatibility complex-restricted antigen receptor on T cells. I. Isolation with a monoclonal antibody, J Exp Med 157 [4], pp. 1149-69. URL: http://www.ncbi.nlm.nih.gov/entrez/query.fcgi?cmd=Retrieve&db=PubMed&dopt=Citation&list_uids=6601175

[11] Kappler, J.; Kubo, R.; Haskins, K.; White, J. and Marrack, P. (1983): The mouse T cell receptor: comparison of MHC-restricted receptors on two T cell hybridomas, Cell 34 [3], pp. 727-37. URL: http://www.ncbi.nlm.nih.gov/entrez/query.fcgi?cmd=Retrieve&db=PubMed&dopt=Citation&list_uids=6605198

[12] Reinherz, E. L.; Meuer, S. C.; Fitzgerald, K. A.; Hussey, R. E.; Hodgdon, J. C.; Acuto, O. and Schlossman, S. F. (1983): Comparison of T3-associated 49- and 43-kilodalton cell surface molecules on individual human T-cell clones: evidence for peptide variability in T-cell receptor structures, Proc Natl Acad Sci U S A 80 [13], pp. 4104-8. URL: http://www.ncbi.nlm.nih.gov/entrez/query.fcgi?cmd=Retrieve&db=PubMed&dopt=Citation&list_uids=6602985

[13] Hedrick, S. M.; Cohen, D. I.; Nielsen, E. A. and Davis, M. M. (1984): Isolation of cDNA clones encoding T cell-specific membrane-associated proteins, Nature 308 [5955], pp. 149-53. URL: http://www.ncbi.nlm.nih.gov/entrez/query.fcgi?cmd=Retrieve&db=PubMed&dopt=Citation&list_uids=6199676

[14] Hedrick, S. M.; Nielsen, E. A.; Kavaler, J.; Cohen, D. I. and Davis, M. M. (1984): Sequence relationships between putative T-cell receptor polypeptides and immunoglobulins, Nature 308 [5955], pp. 153-8. URL: http://www.ncbi.nlm.nih.gov/entrez/query.fcgi?cmd=Retrieve&db=PubMed&dopt=Citation&list_uids=6546606

[15] Yanagi, Y.; Yoshikai, Y.; Leggett, K.; Clark, S. P.; Aleksander, I. and Mak, T. W. (1984): A human T cell-specific cDNA clone encodes a protein having extensive homology to immunoglobulin chains, Nature 308 [5955], pp. 145-9. URL: http://www.ncbi.nlm.nih.gov/entrez/query.fcgi?cmd=Retrieve&db=PubMed&dopt=Citation&list_uids=6336315

[16] Chien, Y.; Becker, D. M.; Lindsten, T.; Okamura, M.; Cohen, D. I. and Davis, M. M. (1984): A third type of murine T-cell receptor gene, Nature 312 [5989], pp. 31-5. URL: http://www.ncbi.nlm.nih.gov/entrez/query.fcgi?cmd=Retrieve&db=PubMed&dopt=Citation&list_uids=6548551

[17] Saito, H.; Kranz, D. M.; Takagaki, Y.; Hayday, A. C.; Eisen, H. N. and Tonegawa, S. (1984): Complete primary structure of a heterodimeric T-cell receptor deduced from cDNA sequences, Nature 309 [5971], pp. 757-62. URL: http://www.ncbi.nlm.nih.gov/entrez/query.fcgi?cmd=Retrieve&db=PubMed&dopt=Citation&list_uids=6330561

[18] Yanagi, Y.; Chan, A.; Chin, B.; Minden, M. and Mak, T. W. (1985): Analysis of cDNA clones specific for human T cells and the alpha and beta chains of the T-cell receptor heterodimer from a human T-cell line, Proc Natl Acad Sci U S A 82 [10], pp. 3430-4. URL: http://www.ncbi.nlm.nih.gov/entrez/query.fcgi?cmd=Retrieve&db=PubMed&dopt=Citation&list_uids=3873654

[19] Hozumi, N. and Tonegawa, S. (1976): Evidence for somatic rearrangement of immunoglobulin genes coding for variable and constant regions, Proc Natl Acad Sci U S A 73 [10], pp. 3628-32. URL: http://www.ncbi.nlm.nih.gov/entrez/query.fcgi?cmd=Retrieve&db=PubMed&dopt=Citation&list_uids=824647

[20] Arstila, T. P.; Casrouge, A.; Baron, V.; Even, J.; Kanellopoulos, J. and Kourilsky, P. (1999): A direct estimate of the human alphabeta T cell receptor diversity, Science 286 [5441], pp. 958-61. URL: http://www.ncbi.nlm.nih.gov/entrez/query.fcgi?cmd=Retrieve&db=PubMed&dopt=Citation&list_uids=10542151

[21] Robins, H. S.; Campregher, P. V.; Srivastava, S. K.; Wacher, A.; Turtle, C. J.; Kahsai, O.; Riddell, S. R.; Warren, E. H. and Carlson, C. S. (2009): Comprehensive assessment of T-cell receptor beta-chain diversity in alphabeta T cells, Blood 114 [19], pp. 4099-107. URL: http://www.ncbi.nlm.nih.gov/entrez/query.fcgi?cmd=Retrieve&db=PubMed&dopt=Citation&list_uids=19706884

[22] Yoshikai, Y.; Clark, S. P.; Taylor, S.; Sohn, U.; Wilson, B. I.; Minden, M. D. and Mak, T. W. (1985): Organization and sequences of the variable, joining and constant region genes of the human T-cell receptor alpha-chain, Nature 316 [6031], pp. 837-40. URL: http://www.ncbi.nlm.nih.gov/entrez/query.fcgi?cmd=Retrieve&db=PubMed&dopt=Citation&list_uids=2993909

[23] Toyonaga, B.; Yoshikai, Y.; Vadasz, V.; Chin, B. and Mak, T. W. (1985): Organization and sequences of the diversity, joining, and constant region genes of the human T-cell receptor

beta chain, Proc Natl Acad Sci U S A 82 [24], pp. 8624-8. URL: http://www.ncbi.nlm.nih.gov/entrez/query.fcgi?cmd=Retrieve&db=PubMed&dopt=Citation&list_uids=3866244

[24] Marie-Paule Lefranc, Gerard Lefranc (2001): The T Cell Receptor FactsBook, Academic Press, ISBN: 978-0-12-441352-8.

[25] Schatz, D. G.; Oettinger, M. A. and Baltimore, D. (1989): The V(D)J recombination activating gene, RAG-1, Cell 59 [6], pp. 1035-48. URL: http://www.ncbi.nlm.nih.gov/entrez/query.fcgi?cmd=Retrieve&db=PubMed&dopt=Citation&list_uids=2598259

[26] Oettinger, M. A.; Schatz, D. G.; Gorka, C. and Baltimore, D. (1990): RAG-1 and RAG-2, adjacent genes that synergistically activate V(D)J recombination, Science 248 [4962], pp. 1517-23. URL: http://www.ncbi.nlm.nih.gov/entrez/query.fcgi?cmd=Retrieve&db=PubMed&dopt=Citation&list_uids=2360047

[27] van Gent, D. C.; Ramsden, D. A. and Gellert, M. (1996): The RAG1 and RAG2 proteins establish the 12/23 rule in V(D)J recombination, Cell 85 [1], pp. 107-13. URL: http://www.ncbi.nlm.nih.gov/entrez/query.fcgi?cmd=Retrieve&db=PubMed&dopt=Citation&list_uids=8620529

[28] Mombaerts, P.; Iacomini, J.; Johnson, R. S.; Herrup, K.; Tonegawa, S. and Papaioannou, V. E. (1992): RAG-1-deficient mice have no mature B and T lymphocytes, Cell 68 [5], pp. 869-77. URL: http://www.ncbi.nlm.nih.gov/entrez/query.fcgi?cmd=Retrieve&db=PubMed&dopt=Citation&list_uids=1547488

[29] Shinkai, Y.; Rathbun, G.; Lam, K. P.; Oltz, E. M.; Stewart, V.; Mendelsohn, M.; Charron, J.; Datta, M.; Young, F.; Stall, A. M. and et al. (1992): RAG-2-deficient mice lack mature lymphocytes owing to inability to initiate V(D)J rearrangement, Cell 68 [5], pp. 855-67. URL: http://www.ncbi.nlm.nih.gov/entrez/query.fcgi?cmd=Retrieve&db=PubMed&dopt=Citation&list_uids=1547487

[30] Uematsu, Y.; Ryser, S.; Dembic, Z.; Borgulya, P.; Krimpenfort, P.; Berns, A.; von Boehmer, H. and Steinmetz, M. (1988): In transgenic mice the introduced functional T cell receptor beta gene prevents expression of endogenous beta genes, Cell 52 [6], pp. 831-41. URL: http://www.ncbi.nlm.nih.gov/entrez/query.fcgi?cmd=Retrieve&db=PubMed&dopt=Citation&list_uids=3258191

[31] Saint-Ruf, C.; Ungewiss, K.; Groettrup, M.; Bruno, L.; Fehling, H. J. and von Boehmer, H. (1994): Analysis and expression of a cloned pre-T cell receptor gene, Science 266 [5188], pp. 1208-12. URL: http://www.ncbi.nlm.nih.gov/entrez/query.fcgi?cmd=Retrieve&db=PubMed&dopt=Citation&list_uids=7973703

[32] Ramiro, A. R.; Trigueros, C.; Marquez, C.; San Millan, J. L. and Toribio, M. L. (1996): Regulation of pre-T cell receptor (pT alpha-TCR beta) gene expression during human thymic development, J Exp Med 184 [2], pp. 519-30. URL: http://www.ncbi.nlm.nih.gov/entrez/query.fcgi?cmd=Retrieve&db=PubMed&dopt=Citation&list_uids=8760805

[33] Casanova, J. L.; Romero, P.; Widmann, C.; Kourilsky, P. and Maryanski, J. L. (1991): T cell receptor genes in a series of class I major histocompatibility complex-restricted cytotoxic T lymphocyte clones specific for a Plasmodium berghei nonapeptide: implications for T cell allelic exclusion and antigen-specific repertoire, J Exp Med 174 [6], pp. 1371-83. URL: http://www.ncbi.nlm.nih.gov/entrez/query.fcgi?cmd=Retrieve&db=PubMed&dopt=Citation&list_uids=1836010

[34] Malissen, M.; Trucy, J.; Jouvin-Marche, E.; Cazenave, P. A.; Scollay, R. and Malissen, B. (1992): Regulation of TCR alpha and beta gene allelic exclusion during T-cell development, Immunol Today 13 [8], pp. 315-22. URL: http://www.ncbi.nlm.nih.gov/entrez/query.fcgi?cmd=Retrieve&db=PubMed&dopt=Citation&list_uids=1324691

[35] Padovan, E.; Casorati, G.; Dellabona, P.; Meyer, S.; Brockhaus, M. and Lanzavecchia, A. (1993): Expression of two T cell receptor alpha chains: dual receptor T cells, Science 262 [5132], pp. 422-4. URL:

http://www.ncbi.nlm.nih.gov/entrez/query.fcgi?cmd=Retrieve&db=PubMed&dopt=Citation&list_uids=8211163

[36] Han, A.; Glanville, J.; Hansmann, L. and Davis, M. M. (2014): Linking T-cell receptor sequence to functional phenotype at the single-cell level, Nat Biotechnol. URL: http://www.ncbi.nlm.nih.gov/entrez/query.fcgi?cmd=Retrieve&db=PubMed&dopt=Citation&list_uids=24952902

[37] Padovan, E.; Giachino, C.; Cella, M.; Valitutti, S.; Acuto, O. and Lanzavecchia, A. (1995): Normal T lymphocytes can express two different T cell receptor beta chains: implications for the mechanism of allelic exclusion, J Exp Med 181 [4], pp. 1587-91. URL: http://www.ncbi.nlm.nih.gov/entrez/query.fcgi?cmd=Retrieve&db=PubMed&dopt=Citation&list_uids=7699339

[38] Gilfillan, S.; Dierich, A.; Lemeur, M.; Benoist, C. and Mathis, D. (1993): Mice lacking TdT: mature animals with an immature lymphocyte repertoire, Science 261 [5125], pp. 1175-8. URL: http://www.ncbi.nlm.nih.gov/entrez/query.fcgi?cmd=Retrieve&db=PubMed&dopt=Citation&list_uids=8356452

[39] Komori, T.; Okada, A.; Stewart, V. and Alt, F. W. (1993): Lack of N regions in antigen receptor variable region genes of TdT-deficient lymphocytes, Science 261 [5125], pp. 1171-5. URL: http://www.ncbi.nlm.nih.gov/entrez/query.fcgi?cmd=Retrieve&db=PubMed&dopt=Citation&list_uids=8356451

[40] Weiss, A. and Stobo, J. D. (1984): Requirement for the coexpression of T3 and the T cell antigen receptor on a malignant human T cell line, J Exp Med 160 [5], pp. 1284-99. URL: http://www.ncbi.nlm.nih.gov/entrez/query.fcgi?cmd=Retrieve&db=PubMed&dopt=Citation&list_uids=6208306

[41] Reth, M. (1989): Antigen receptor tail clue, Nature 338 [6214], pp. 383-4. URL: http://www.ncbi.nlm.nih.gov/entrez/query.fcgi?cmd=Retrieve&db=PubMed&dopt=Citation&list_uids=2927501

[42] Bentley, G. A.; Boulot, G.; Karjalainen, K. and Mariuzza, R. A. (1995): Crystal structure of the beta chain of a T cell antigen receptor, Science 267 [5206], pp. 1984-7. URL: http://www.ncbi.nlm.nih.gov/entrez/query.fcgi?cmd=Retrieve&db=PubMed&dopt=Citation&list_uids=7701320

[43] Fields, B. A.; Ober, B.; Malchiodi, E. L.; Lebedeva, M. I.; Braden, B. C.; Ysern, X.; Kim, J. K.; Shao, X.; Ward, E. S. and Mariuzza, R. A. (1995): Crystal structure of the V alpha domain of a T cell antigen receptor, Science 270 [5243], pp. 1821-4. URL: http://www.ncbi.nlm.nih.gov/entrez/query.fcgi?cmd=Retrieve&db=PubMed&dopt=Citation&list_uids=8525376

[44] Garcia, K. C.; Degano, M.; Stanfield, R. L.; Brunmark, A.; Jackson, M. R.; Peterson, P. A.; Teyton, L. and Wilson, I. A. (1996): An alphabeta T cell receptor structure at 2.5 A and its orientation in the TCR-MHC complex, Science 274 [5285], pp. 209-19. URL: http://www.ncbi.nlm.nih.gov/entrez/query.fcgi?cmd=Retrieve&db=PubMed&dopt=Citation&list_uids=8824178

[45] Garboczi, D. N.; Ghosh, P.; Utz, U.; Fan, Q. R.; Biddison, W. E. and Wiley, D. C. (1996): Structure of the complex between human T-cell receptor, viral peptide and HLA-A2, Nature 384 [6605], pp. 134-41. URL: http://www.ncbi.nlm.nih.gov/entrez/query.fcgi?cmd=Retrieve&db=PubMed&dopt=Citation&list_uids=8906788

[46] Call, M. E.; Pyrdol, J.; Wiedmann, M. and Wucherpfennig, K. W. (2002): The organizing principle in the formation of the T cell receptor-CD3 complex, Cell 111 [7], pp. 967-79. URL: http://www.ncbi.nlm.nih.gov/entrez/query.fcgi?cmd=Retrieve&db=PubMed&dopt=Citation&list_uids=12507424

[47] Schamel, W. W.; Arechaga, I.; Risueno, R. M.; van Santen, H. M.; Cabezas, P.; Risco, C.; Valpuesta, J. M. and Alarcon, B. (2005): Coexistence of multivalent and monovalent TCRs explains high sensitivity and wide range of response, J Exp Med 202 [4], pp. 493-503. URL: http://www.ncbi.nlm.nih.gov/entrez/query.fcgi?cmd=Retrieve&db=PubMed&dopt=Citation&list_uids=16087711

[48] Lillemeier, B. F.; Mortelmaier, M. A.; Forstner, M. B.; Huppa, J. B.; Groves, J. T. and Davis, M. M. (2010): TCR and Lat are expressed on separate protein islands on T cell membranes and

concatenate during activation, Nat Immunol 11 [1], pp. 90-6. URL: http://www.ncbi.nlm.nih.gov/entrez/query.fcgi?cmd=Retrieve&db=PubMed&dopt=Citation&list_uids=20010844

[49] Sherman, E.; Barr, V.; Manley, S.; Patterson, G.; Balagopalan, L.; Akpan, I.; Regan, C. K.; Merrill, R. K.; Sommers, C. L.; Lippincott-Schwartz, J. and Samelson, L. E. (2011): Functional nanoscale organization of signaling molecules downstream of the T cell antigen receptor, Immunity 35 [5], pp. 705-20. URL: http://www.ncbi.nlm.nih.gov/entrez/query.fcgi?cmd=Retrieve&db=PubMed&dopt=Citation&list_uids=22055681

[50] Campi, G.; Varma, R. and Dustin, M. L. (2005): Actin and agonist MHC-peptide complex-dependent T cell receptor microclusters as scaffolds for signaling, J Exp Med 202 [8], pp. 1031-6. URL: http://www.ncbi.nlm.nih.gov/entrez/query.fcgi?cmd=Retrieve&db=PubMed&dopt=Citation&list_uids=16216891

[51] Yokosuka, T.; Sakata-Sogawa, K.; Kobayashi, W.; Hiroshima, M.; Hashimoto-Tane, A.; Tokunaga, M.; Dustin, M. L. and Saito, T. (2005): Newly generated T cell receptor microclusters initiate and sustain T cell activation by recruitment of Zap70 and SLP-76, Nat Immunol 6 [12], pp. 1253-62. URL: http://www.ncbi.nlm.nih.gov/entrez/query.fcgi?cmd=Retrieve&db=PubMed&dopt=Citation&list_uids=16273097

[52] Kumar, R.; Ferez, M.; Swamy, M.; Arechaga, I.; Rejas, M. T.; Valpuesta, J. M.; Schamel, W. W.; Alarcon, B. and van Santen, H. M. (2011): Increased sensitivity of antigen-experienced T cells through the enrichment of oligomeric T cell receptor complexes, Immunity 35 [3], pp. 375-87. URL: http://www.ncbi.nlm.nih.gov/entrez/query.fcgi?cmd=Retrieve&db=PubMed&dopt=Citation&list_uids=21903423

[53] Zinkernagel, R. M. and Doherty, P. C. (1974): Restriction of in vitro T cell-mediated cytotoxicity in lymphocytic choriomeningitis within a syngeneic or semiallogeneic system, Nature 248 [5450], pp. 701-2. URL: http://www.ncbi.nlm.nih.gov/entrez/query.fcgi?cmd=Retrieve&db=PubMed&dopt=Citation&list_uids=4133807

[54] Bevan, M. J. (1977): In a radiation chimaera, host H-2 antigens determine immune responsiveness of donor cytotoxic cells, Nature 269 [5627], pp. 417-8. URL: http://www.ncbi.nlm.nih.gov/entrez/query.fcgi?cmd=Retrieve&db=PubMed&dopt=Citation&list_uids=302918

[55] Zinkernagel, R. M.; Callahan, G. N.; Klein, J. and Dennert, G. (1978): Cytotoxic T cells learn specificity for self H-2 during differentiation in the thymus, Nature 271 [5642], pp. 251-3. URL: http://www.ncbi.nlm.nih.gov/entrez/query.fcgi?cmd=Retrieve&db=PubMed&dopt=Citation&list_uids=304527

[56] Zijlstra, M.; Bix, M.; Simister, N. E.; Loring, J. M.; Raulet, D. H. and Jaenisch, R. (1990): Beta 2-microglobulin deficient mice lack CD4-8+ cytolytic T cells, Nature 344 [6268], pp. 742-6. URL: http://www.ncbi.nlm.nih.gov/entrez/query.fcgi?cmd=Retrieve&db=PubMed&dopt=Citation&list_uids=2139497

[57] Koller, B. H.; Marrack, P.; Kappler, J. W. and Smithies, O. (1990): Normal development of mice deficient in beta 2M, MHC class I proteins, and CD8+ T cells, Science 248 [4960], pp. 1227-30. URL: http://www.ncbi.nlm.nih.gov/entrez/query.fcgi?cmd=Retrieve&db=PubMed&dopt=Citation&list_uids=2112266

[58] Cosgrove, D.; Gray, D.; Dierich, A.; Kaufman, J.; Lemeur, M.; Benoist, C. and Mathis, D. (1991): Mice lacking MHC class II molecules, Cell 66 [5], pp. 1051-66. URL: http://www.ncbi.nlm.nih.gov/entrez/query.fcgi?cmd=Retrieve&db=PubMed&dopt=Citation&list_uids=1909605

[59] Grusby, M. J.; Johnson, R. S.; Papaioannou, V. E. and Glimcher, L. H. (1991): Depletion of CD4+ T cells in major histocompatibility complex class II-deficient mice, Science 253 [5026], pp. 1417-20. URL:

http://www.ncbi.nlm.nih.gov/entrez/query.fcgi?cmd=Retrieve&db=PubMed&dopt=Citation&list_uids=1910207

[60] Kisielow, P.; Teh, H. S.; Bluthmann, H. and von Boehmer, H. (1988): Positive selection of antigen-specific T cells in thymus by restricting MHC molecules, Nature 335 [6192], pp. 730-3. URL: http://www.ncbi.nlm.nih.gov/entrez/query.fcgi?cmd=Retrieve&db=PubMed&dopt=Citation&list_uids=3262831

[61] Hogquist, K. A.; Gavin, M. A. and Bevan, M. J. (1993): Positive selection of CD8+ T cells induced by major histocompatibility complex binding peptides in fetal thymic organ culture, J Exp Med 177 [5], pp. 1469-73. URL: http://www.ncbi.nlm.nih.gov/entrez/query.fcgi?cmd=Retrieve&db=PubMed&dopt=Citation&list_uids=8478616

[62] Ashton-Rickardt, P. G.; Van Kaer, L.; Schumacher, T. N.; Ploegh, H. L. and Tonegawa, S. (1993): Peptide contributes to the specificity of positive selection of CD8+ T cells in the thymus, Cell 73 [5], pp. 1041-9. URL: http://www.ncbi.nlm.nih.gov/entrez/query.fcgi?cmd=Retrieve&db=PubMed&dopt=Citation&list_uids=8500174

[63] Hogquist, K. A.; Jameson, S. C.; Heath, W. R.; Howard, J. L.; Bevan, M. J. and Carbone, F. R. (1994): T cell receptor antagonist peptides induce positive selection, Cell 76 [1], pp. 17-27. URL: http://www.ncbi.nlm.nih.gov/entrez/query.fcgi?cmd=Retrieve&db=PubMed&dopt=Citation&list_uids=8287475

[64] Takahama, Y.; Suzuki, H.; Katz, K. S.; Grusby, M. J. and Singer, A. (1994): Positive selection of CD4+ T cells by TCR ligation without aggregation even in the absence of MHC, Nature 371 [6492], pp. 67-70. URL: http://www.ncbi.nlm.nih.gov/entrez/query.fcgi?cmd=Retrieve&db=PubMed&dopt=Citation&list_uids=7915400

[65] Surh, C. D. and Sprent, J. (1994): T-cell apoptosis detected in situ during positive and negative selection in the thymus, Nature 372 [6501], pp. 100-3. URL: http://www.ncbi.nlm.nih.gov/entrez/query.fcgi?cmd=Retrieve&db=PubMed&dopt=Citation&list_uids=7969401

[66] Kappler, J. W.; Roehm, N. and Marrack, P. (1987): T cell tolerance by clonal elimination in the thymus, Cell 49 [2], pp. 273-80. URL: http://www.ncbi.nlm.nih.gov/entrez/query.fcgi?cmd=Retrieve&db=PubMed&dopt=Citation&list_uids=3494522

[67] Woodland, D. L.; Lund, F. E.; Happ, M. P.; Blackman, M. A.; Palmer, E. and Corley, R. B. (1991): Endogenous superantigen expression is controlled by mouse mammary tumor proviral loci, J Exp Med 174 [5], pp. 1255-8. URL: http://www.ncbi.nlm.nih.gov/entrez/query.fcgi?cmd=Retrieve&db=PubMed&dopt=Citation&list_uids=1658187

[68] Derbinski, J.; Schulte, A.; Kyewski, B. and Klein, L. (2001): Promiscuous gene expression in medullary thymic epithelial cells mirrors the peripheral self, Nat Immunol 2 [11], pp. 1032-9. URL: http://www.ncbi.nlm.nih.gov/entrez/query.fcgi?cmd=Retrieve&db=PubMed&dopt=Citation&list_uids=11600886

[69] Anderson, M. S.; Venanzi, E. S.; Klein, L.; Chen, Z.; Berzins, S. P.; Turley, S. J.; von Boehmer, H.; Bronson, R.; Dierich, A.; Benoist, C. and Mathis, D. (2002): Projection of an immunological self shadow within the thymus by the aire protein, Science 298 [5597], pp. 1395-401. URL: http://www.ncbi.nlm.nih.gov/entrez/query.fcgi?cmd=Retrieve&db=PubMed&dopt=Citation&list_uids=12376594

[70] Gallegos, A. M. and Bevan, M. J. (2004): Central tolerance to tissue-specific antigens mediated by direct and indirect antigen presentation, J Exp Med 200 [8], pp. 1039-49. URL: http://www.ncbi.nlm.nih.gov/entrez/query.fcgi?cmd=Retrieve&db=PubMed&dopt=Citation&list_uids=15492126

[71] McCaughtry, T. M.; Baldwin, T. A.; Wilken, M. S. and Hogquist, K. A. (2008): Clonal deletion of thymocytes can occur in the cortex with no involvement of the medulla, J Exp Med 205 [11],

pp. 2575-84. URL: http://www.ncbi.nlm.nih.gov/entrez/query.fcgi?cmd=Retrieve&db=PubMed&dopt=Citation&list_uids=18936237

[72] Ziegler, K. and Unanue, E. R. (1981): Identification of a macrophage antigen-processing event required for I-region-restricted antigen presentation to T lymphocytes, J Immunol 127 [5], pp. 1869-75. URL: http://www.ncbi.nlm.nih.gov/entrez/query.fcgi?cmd=Retrieve&db=PubMed&dopt=Citation&list_uids=6795263

[73] Ziegler, H. K. and Unanue, E. R. (1982): Decrease in macrophage antigen catabolism caused by ammonia and chloroquine is associated with inhibition of antigen presentation to T cells, Proc Natl Acad Sci U S A 79 [1], pp. 175-8. URL: http://www.ncbi.nlm.nih.gov/entrez/query.fcgi?cmd=Retrieve&db=PubMed&dopt=Citation&list_uids=6798568

[74] Shimonkevitz, R.; Kappler, J.; Marrack, P. and Grey, H. (1983): Antigen recognition by H-2-restricted T cells. I. Cell-free antigen processing, J Exp Med 158 [2], pp. 303-16. URL: http://www.ncbi.nlm.nih.gov/entrez/query.fcgi?cmd=Retrieve&db=PubMed&dopt=Citation&list_uids=6193218

[75] Allen, P. M.; Strydom, D. J. and Unanue, E. R. (1984): Processing of lysozyme by macrophages: identification of the determinant recognized by two T-cell hybridomas, Proc Natl Acad Sci U S A 81 [8], pp. 2489-93. URL: http://www.ncbi.nlm.nih.gov/entrez/query.fcgi?cmd=Retrieve&db=PubMed&dopt=Citation&list_uids=6201858

[76] Babbitt, B. P.; Allen, P. M.; Matsueda, G.; Haber, E. and Unanue, E. R. (1985): Binding of immunogenic peptides to Ia histocompatibility molecules, Nature 317 [6035], pp. 359-61. URL: http://www.ncbi.nlm.nih.gov/entrez/query.fcgi?cmd=Retrieve&db=PubMed&dopt=Citation&list_uids=3876513

[77] Buus, S.; Colon, S.; Smith, C.; Freed, J. H.; Miles, C. and Grey, H. M. (1986): Interaction between a "processed" ovalbumin peptide and Ia molecules, Proc Natl Acad Sci U S A 83 [11], pp. 3968-71. URL: http://www.ncbi.nlm.nih.gov/entrez/query.fcgi?cmd=Retrieve&db=PubMed&dopt=Citation&list_uids=3487084

[78] Buus, S. and Werdelin, O. (1986): A group-specific inhibitor of lysosomal cysteine proteinases selectively inhibits both proteolytic degradation and presentation of the antigen dinitrophenyl-poly-L-lysine by guinea pig accessory cells to T cells, J Immunol 136 [2], pp. 452-8. URL: http://www.ncbi.nlm.nih.gov/entrez/query.fcgi?cmd=Retrieve&db=PubMed&dopt=Citation&list_uids=3079785

[79] Takahashi, H.; Cease, K. B. and Berzofsky, J. A. (1989): Identification of proteases that process distinct epitopes on the same protein, J Immunol 142 [7], pp. 2221-9. URL: http://www.ncbi.nlm.nih.gov/entrez/query.fcgi?cmd=Retrieve&db=PubMed&dopt=Citation&list_uids=2466893

[80] Townsend, A. R.; Rothbard, J.; Gotch, F. M.; Bahadur, G.; Wraith, D. and McMichael, A. J. (1986): The epitopes of influenza nucleoprotein recognized by cytotoxic T lymphocytes can be defined with short synthetic peptides, Cell 44 [6], pp. 959-68. URL: http://www.ncbi.nlm.nih.gov/entrez/query.fcgi?cmd=Retrieve&db=PubMed&dopt=Citation&list_uids=2420472

[81] Bjorkman, P. J.; Saper, M. A.; Samraoui, B.; Bennett, W. S.; Strominger, J. L. and Wiley, D. C. (1987): Structure of the human class I histocompatibility antigen, HLA-A2, Nature 329 [6139], pp. 506-12. URL: http://www.ncbi.nlm.nih.gov/entrez/query.fcgi?cmd=Retrieve&db=PubMed&dopt=Citation&list_uids=3309677

[82] Bjorkman, P. J.; Saper, M. A.; Samraoui, B.; Bennett, W. S.; Strominger, J. L. and Wiley, D. C. (1987): The foreign antigen binding site and T cell recognition regions of class I histocompatibility antigens, Nature 329 [6139], pp. 512-8. URL:

http://www.ncbi.nlm.nih.gov/entrez/query.fcgi?cmd=Retrieve&db=PubMed&dopt=Citation&list_uids=2443855

[83] Brown, J. H.; Jardetzky, T. S.; Gorga, J. C.; Stern, L. J.; Urban, R. G.; Strominger, J. L. and Wiley, D. C. (1993): Three-dimensional structure of the human class II histocompatibility antigen HLA-DR1, Nature 364 [6432], pp. 33-9. URL: http://www.ncbi.nlm.nih.gov/entrez/query.fcgi?cmd=Retrieve&db=PubMed&dopt=Citation&list_uids=8316295

[84] Demotz, S.; Grey, H. M.; Appella, E. and Sette, A. (1989): Characterization of a naturally processed MHC class II-restricted T-cell determinant of hen egg lysozyme, Nature 342 [6250], pp. 682-4. URL: http://www.ncbi.nlm.nih.gov/entrez/query.fcgi?cmd=Retrieve&db=PubMed&dopt=Citation&list_uids=2480524

[85] Rötzschke, O.; Falk, K.; Wallny, H. J.; Faath, S. and Rammensee, H. G. (1990): Characterization of naturally occurring minor histocompatibility peptides including H-4 and H-Y, Science 249 [4966], pp. 283-7. URL: http://www.ncbi.nlm.nih.gov/entrez/query.fcgi?cmd=Retrieve&db=PubMed&dopt=Citation&list_uids=1695760

[86] Wallny, H. J. and Rammensee, H. G. (1990): Identification of classical minor histocompatibility antigen as cell-derived peptide, Nature 343 [6255], pp. 275-8. URL: http://www.ncbi.nlm.nih.gov/entrez/query.fcgi?cmd=Retrieve&db=PubMed&dopt=Citation&list_uids=1689009

[87] Falk, K.; Rötzschke, O. and Rammensee, H. G. (1990): Cellular peptide composition governed by major histocompatibility complex class I molecules, Nature 348 [6298], pp. 248-51. URL: http://www.ncbi.nlm.nih.gov/entrez/query.fcgi?cmd=Retrieve&db=PubMed&dopt=Citation&list_uids=2234092

[88] Rötzschke, O.; Falk, K.; Deres, K.; Schild, H.; Norda, M.; Metzger, J.; Jung, G. and Rammensee, H. G. (1990): Isolation and analysis of naturally processed viral peptides as recognized by cytotoxic T cells, Nature 348 [6298], pp. 252-4. URL: http://www.ncbi.nlm.nih.gov/entrez/query.fcgi?cmd=Retrieve&db=PubMed&dopt=Citation&list_uids=1700304

[89] Falk, K.; Rötzschke, O.; Stevanovic, S.; Jung, G. and Rammensee, H. G. (1991): Allele-specific motifs revealed by sequencing of self-peptides eluted from MHC molecules, Nature 351 [6324], pp. 290-6. URL: http://www.ncbi.nlm.nih.gov/entrez/query.fcgi?cmd=Retrieve&db=PubMed&dopt=Citation&list_uids=1709722

[90] Jardetzky, T. S.; Lane, W. S.; Robinson, R. A.; Madden, D. R. and Wiley, D. C. (1991): Identification of self peptides bound to purified HLA-B27, Nature 353 [6342], pp. 326-9. URL: http://www.ncbi.nlm.nih.gov/entrez/query.fcgi?cmd=Retrieve&db=PubMed&dopt=Citation&list_uids=1922338

[91] Hunt, D. F.; Henderson, R. A.; Shabanowitz, J.; Sakaguchi, K.; Michel, H.; Sevilir, N.; Cox, A. L.; Appella, E. and Engelhard, V. H. (1992): Characterization of peptides bound to the class I MHC molecule HLA-A2.1 by mass spectrometry, Science 255 [5049], pp. 1261-3. URL: http://www.ncbi.nlm.nih.gov/entrez/query.fcgi?cmd=Retrieve&db=PubMed&dopt=Citation&list_uids=1546328

[92] Chicz, R. M.; Urban, R. G.; Gorga, J. C.; Vignali, D. A.; Lane, W. S. and Strominger, J. L. (1993): Specificity and promiscuity among naturally processed peptides bound to HLA-DR alleles, J Exp Med 178 [1], pp. 27-47. URL: http://www.ncbi.nlm.nih.gov/entrez/query.fcgi?cmd=Retrieve&db=PubMed&dopt=Citation&list_uids=8315383

[93] Michalek, M. T.; Grant, E. P.; Gramm, C.; Goldberg, A. L. and Rock, K. L. (1993): A role for the ubiquitin-dependent proteolytic pathway in MHC class I-restricted antigen presentation, Nature 363 [6429], pp. 552-4. URL: http://www.ncbi.nlm.nih.gov/entrez/query.fcgi?cmd=Retrieve&db=PubMed&dopt=Citation&list_uids=8389422

[94] Rock, K. L.; Gramm, C.; Rothstein, L.; Clark, K.; Stein, R.; Dick, L.; Hwang, D. and Goldberg, A. L. (1994): Inhibitors of the proteasome block the degradation of most cell proteins and the

generation of peptides presented on MHC class I molecules, Cell 78 [5], pp. 761-71. URL: http://www.ncbi.nlm.nih.gov/entrez/query.fcgi?cmd=Retrieve&db=PubMed&dopt=Citation&list_uids=8087844

[95] Paz, P.; Brouwenstijn, N.; Perry, R. and Shastri, N. (1999): Discrete proteolytic intermediates in the MHC class I antigen processing pathway and MHC I-dependent peptide trimming in the ER, Immunity 11 [2], pp. 241-51. URL: http://www.ncbi.nlm.nih.gov/entrez/query.fcgi?cmd=Retrieve&db=PubMed&dopt=Citation&list_uids=10485659

[96] Cascio, P.; Hilton, C.; Kisselev, A. F.; Rock, K. L. and Goldberg, A. L. (2001): 26S proteasomes and immunoproteasomes produce mainly N-extended versions of an antigenic peptide, EMBO J 20 [10], pp. 2357-66. URL: http://www.ncbi.nlm.nih.gov/entrez/query.fcgi?cmd=Retrieve&db=PubMed&dopt=Citation&list_uids=11350924

[97] Serwold, T.; Gonzalez, F.; Kim, J.; Jacob, R. and Shastri, N. (2002): ERAAP customizes peptides for MHC class I molecules in the endoplasmic reticulum, Nature 419 [6906], pp. 480-3. URL: http://www.ncbi.nlm.nih.gov/entrez/query.fcgi?cmd=Retrieve&db=PubMed&dopt=Citation&list_uids=12368856

[98] Saric, T.; Chang, S. C.; Hattori, A.; York, I. A.; Markant, S.; Rock, K. L.; Tsujimoto, M. and Goldberg, A. L. (2002): An IFN-gamma-induced aminopeptidase in the ER, ERAP1, trims precursors to MHC class I-presented peptides, Nat Immunol 3 [12], pp. 1169-76. URL: http://www.ncbi.nlm.nih.gov/entrez/query.fcgi?cmd=Retrieve&db=PubMed&dopt=Citation&list_uids=12436109

[99] York, I. A.; Chang, S. C.; Saric, T.; Keys, J. A.; Favreau, J. M.; Goldberg, A. L. and Rock, K. L. (2002): The ER aminopeptidase ERAP1 enhances or limits antigen presentation by trimming epitopes to 8-9 residues, Nat Immunol 3 [12], pp. 1177-84. URL: http://www.ncbi.nlm.nih.gov/entrez/query.fcgi?cmd=Retrieve&db=PubMed&dopt=Citation&list_uids=12436110

[100] Neefjes, J. J.; Momburg, F. and Hammerling, G. J. (1993): Selective and ATP-dependent translocation of peptides by the MHC-encoded transporter, Science 261 [5122], pp. 769-71. URL: http://www.ncbi.nlm.nih.gov/entrez/query.fcgi?cmd=Retrieve&db=PubMed&dopt=Citation&list_uids=8342042

[101] Androlewicz, M. J.; Anderson, K. S. and Cresswell, P. (1993): Evidence that transporters associated with antigen processing translocate a major histocompatibility complex class I-binding peptide into the endoplasmic reticulum in an ATP-dependent manner, Proc Natl Acad Sci U S A 90 [19], pp. 9130-4. URL: http://www.ncbi.nlm.nih.gov/entrez/query.fcgi?cmd=Retrieve&db=PubMed&dopt=Citation&list_uids=8415666

[102] Ehrlich, P. (1909): Über den jetzigen Stand der Karzinomforschung, Ned. Tijdschr. Geneeskd 5, pp. 273–290.

[103] Little, C. C. and Tyzzer, E. E. (1916): Further experimental studies on the inheritance of susceptibility to a Transplantable tumor, Carcinoma (J. W. A.) of the Japanese waltzing Mouse, J Med Res 33 [3], pp. 393-453. URL: http://www.ncbi.nlm.nih.gov/entrez/query.fcgi?cmd=Retrieve&db=PubMed&dopt=Citation&list_uids=19972275

[104] Gorer, P. A.; Lyman, S. and Snaell, G. D. (1948): Studies on the genetic and antigenic basis of tumour transplantation: linkage between a histocompatibility gene and “fused” in mice, Proc. R. Soc. Lond. 135, pp. 499–505.

[105] Gross, Ludwik (1943): Intradermal immunization of C3H mice against a sarcoma that originated in an animal of the same line, Cancer Res [3], pp. 326-333.

[106] Foley, E. J. (1953): Antigenic properties of methylcholanthrene-induced tumors in mice of the strain of origin, Cancer Res 13 [12], pp. 835-7. URL: http://www.ncbi.nlm.nih.gov/entrez/query.fcgi?cmd=Retrieve&db=PubMed&dopt=Citation&list_uids=13116120

[107] Prehn, R. T. and Main, J. M. (1957): Immunity to methylcholanthrene-induced sarcomas, J Natl Cancer Inst 18 [6], pp. 769-78. URL:

http://www.ncbi.nlm.nih.gov/entrez/query.fcgi?cmd=Retrieve&db=PubMed&dopt=Citation&list_uids=13502695

[108] Klein, G.; Sjogren, H. O.; Klein, E. and Hellstrom, K. E. (1960): Demonstration of resistance against methylcholanthrene-induced sarcomas in the primary autochthonous host, Cancer Res 20, pp. 1561-72. URL: http://www.ncbi.nlm.nih.gov/entrez/query.fcgi?cmd=Retrieve&db=PubMed&dopt=Citation&list_uids=13756652

[109] Burnet, M. (1964): Immunological Factors in the Process of Carcinogenesis, Br Med Bull 20, pp. 154-8. URL: http://www.ncbi.nlm.nih.gov/entrez/query.fcgi?cmd=Retrieve&db=PubMed&dopt=Citation&list_uids=14168097

[110] Burnet, F. M. (1970): The concept of immunological surveillance, Prog Exp Tumor Res. [13], pp. 1-27.

[111] Dunn, G. P.; Bruce, A. T.; Ikeda, H.; Old, L. J. and Schreiber, R. D. (2002): Cancer immunoediting: from immunosurveillance to tumor escape, Nat Immunol 3 [11], pp. 991-8. URL: http://www.ncbi.nlm.nih.gov/entrez/query.fcgi?cmd=Retrieve&db=PubMed&dopt=Citation&list_uids=12407406

[112] van der Bruggen, P.; Traversari, C.; Chomez, P.; Lurquin, C.; De Plaen, E.; Van den Eynde, B.; Knuth, A. and Boon, T. (1991): A gene encoding an antigen recognized by cytolytic T lymphocytes on a human melanoma, Science 254 [5038], pp. 1643-7. URL: http://www.ncbi.nlm.nih.gov/entrez/query.fcgi?cmd=Retrieve&db=PubMed&dopt=Citation&list_uids=1840703

[113] Traversari, C.; van der Bruggen, P.; Luescher, I. F.; Lurquin, C.; Chomez, P.; Van Pel, A.; De Plaen, E.; Amar-Costesec, A. and Boon, T. (1992): A nonapeptide encoded by human gene MAGE-1 is recognized on HLA-A1 by cytolytic T lymphocytes directed against tumor antigen MZ2-E, J Exp Med 176 [5], pp. 1453-7. URL: http://www.ncbi.nlm.nih.gov/entrez/query.fcgi?cmd=Retrieve&db=PubMed&dopt=Citation&list_uids=1402688

[114] Brichard, V.; Van Pel, A.; Wolfel, T.; Wolfel, C.; De Plaen, E.; Lethe, B.; Coulie, P. and Boon, T. (1993): The tyrosinase gene codes for an antigen recognized by autologous cytolytic T lymphocytes on HLA-A2 melanomas, J Exp Med 178 [2], pp. 489-95. URL: http://www.ncbi.nlm.nih.gov/entrez/query.fcgi?cmd=Retrieve&db=PubMed&dopt=Citation&list_uids=8340755

[115] Coulie, P. G.; Brichard, V.; Van Pel, A.; Wolfel, T.; Schneider, J.; Traversari, C.; Mattei, S.; De Plaen, E.; Lurquin, C.; Szikora, J. P.; Renauld, J. C. and Boon, T. (1994): A new gene coding for a differentiation antigen recognized by autologous cytolytic T lymphocytes on HLA-A2 melanomas, J Exp Med 180 [1], pp. 35-42. URL: http://www.ncbi.nlm.nih.gov/entrez/query.fcgi?cmd=Retrieve&db=PubMed&dopt=Citation&list_uids=8006593

[116] Kawakami, Y.; Eliyahu, S.; Delgado, C. H.; Robbins, P. F.; Rivoltini, L.; Topalian, S. L.; Miki, T. and Rosenberg, S. A. (1994): Cloning of the gene coding for a shared human melanoma antigen recognized by autologous T cells infiltrating into tumor, Proc Natl Acad Sci U S A 91 [9], pp. 3515-9. URL: http://www.ncbi.nlm.nih.gov/entrez/query.fcgi?cmd=Retrieve&db=PubMed&dopt=Citation&list_uids=8170938

[117] Wolfel, T.; Hauer, M.; Schneider, J.; Serrano, M.; Wolfel, C.; Klehmann-Hieb, E.; De Plaen, E.; Hankeln, T.; Meyer zum Buschenfelde, K. H. and Beach, D. (1995): A p16INK4a-insensitive CDK4 mutant targeted by cytolytic T lymphocytes in a human melanoma, Science 269 [5228], pp. 1281-4. URL: http://www.ncbi.nlm.nih.gov/entrez/query.fcgi?cmd=Retrieve&db=PubMed&dopt=Citation&list_uids=7652577

[118] Vigneron, N.; Stroobant, V.; Van den Eynde, B. J. and van der Bruggen, P. (2013): Database of T cell-defined human tumor antigens: the 2013 update, Cancer Immun 13, p. 15. URL: http://www.ncbi.nlm.nih.gov/entrez/query.fcgi?cmd=Retrieve&db=PubMed&dopt=Citation&list_uids=23882160

[119] Willimsky, G. and Blankenstein, T. (2005): Sporadic immunogenic tumours avoid destruction by inducing T-cell tolerance, Nature 437 [7055], pp. 141-6. URL: http://www.ncbi.nlm.nih.gov/entrez/query.fcgi?cmd=Retrieve&db=PubMed&dopt=Citation&list_uids=16136144

[120] Goulmy, E.; Gratama, J. W.; Blokland, E.; Zwaan, F. E. and van Rood, J. J. (1983): A minor transplantation antigen detected by MHC-restricted cytotoxic T lymphocytes during graft-versus-host disease, Nature 302 [5904], pp. 159-61. URL: http://www.ncbi.nlm.nih.gov/entrez/query.fcgi?cmd=Retrieve&db=PubMed&dopt=Citation&list_uids=6186923

[121] den Haan, J. M.; Meadows, L. M.; Wang, W.; Pool, J.; Blokland, E.; Bishop, T. L.; Reinhardus, C.; Shabanowitz, J.; Offringa, R.; Hunt, D. F.; Engelhard, V. H. and Goulmy, E. (1998): The minor histocompatibility antigen HA-1: a diallelic gene with a single amino acid polymorphism, Science 279 [5353], pp. 1054-7. URL: http://www.ncbi.nlm.nih.gov/entrez/query.fcgi?cmd=Retrieve&db=PubMed&dopt=Citation&list_uids=9461441

[122] Barnes, D. W.; Corp, M. J.; Loutit, J. F. and Neal, F. E. (1956): Treatment of murine leukaemia with X rays and homologous bone marrow; preliminary communication, Br Med J 2 [4993], pp. 626-7. URL: http://www.ncbi.nlm.nih.gov/entrez/query.fcgi?cmd=Retrieve&db=PubMed&dopt=Citation&list_uids=13356034

[123] Barnes, D. W. and Loutit, J. F. (1957): Treatment of murine leukaemia with x-rays and homologous bone marrow. II, Br J Haematol 3 [3], pp. 241-52. URL: http://www.ncbi.nlm.nih.gov/entrez/query.fcgi?cmd=Retrieve&db=PubMed&dopt=Citation&list_uids=13460193

[124] Weiden, P. L.; Flournoy, N.; Thomas, E. D.; Prentice, R.; Fefer, A.; Buckner, C. D. and Storb, R. (1979): Antileukemic effect of graft-versus-host disease in human recipients of allogeneic-marrow grafts, N Engl J Med 300 [19], pp. 1068-73. URL: http://www.ncbi.nlm.nih.gov/entrez/query.fcgi?cmd=Retrieve&db=PubMed&dopt=Citation&list_uids=34792

[125] Weiden, P. L.; Sullivan, K. M.; Flournoy, N.; Storb, R. and Thomas, E. D. (1981): Antileukemic effect of chronic graft-versus-host disease: contribution to improved survival after allogeneic marrow transplantation, N Engl J Med 304 [25], pp. 1529-33. URL: http://www.ncbi.nlm.nih.gov/entrez/query.fcgi?cmd=Retrieve&db=PubMed&dopt=Citation&list_uids=7015133

[126] Apperley, J. F.; Jones, L.; Hale, G.; Waldmann, H.; Hows, J.; Rombos, Y.; Tsatalas, C.; Marcus, R. E.; Goolden, A. W.; Gordon-Smith, E. C. and et al. (1986): Bone marrow transplantation for patients with chronic myeloid leukaemia: T-cell depletion with Campath-1 reduces the incidence of graft-versus-host disease but may increase the risk of leukaemic relapse, Bone Marrow Transplant 1 [1], pp. 53-66. URL: http://www.ncbi.nlm.nih.gov/entrez/query.fcgi?cmd=Retrieve&db=PubMed&dopt=Citation&list_uids=3332120

[127] Maraninchi, D.; Gluckman, E.; Blaise, D.; Guyotat, D.; Rio, B.; Pico, J. L.; Leblond, V.; Michallet, M.; Dreyfus, F.; Ifrah, N. and et al. (1987): Impact of T-cell depletion on outcome of allogeneic bone-marrow transplantation for standard-risk leukaemias, Lancet 2 [8552], pp. 175-8. URL: http://www.ncbi.nlm.nih.gov/entrez/query.fcgi?cmd=Retrieve&db=PubMed&dopt=Citation&list_uids=2885638

[128] Goldman, J. M.; Gale, R. P.; Horowitz, M. M.; Biggs, J. C.; Champlin, R. E.; Gluckman, E.; Hoffmann, R. G.; Jacobsen, S. J.; Marmont, A. M.; McGlave, P. B. and et al. (1988): Bone marrow transplantation for chronic myelogenous leukemia in chronic phase. Increased risk for relapse associated with T-cell depletion, Ann Intern Med 108 [6], pp. 806-14. URL: http://www.ncbi.nlm.nih.gov/entrez/query.fcgi?cmd=Retrieve&db=PubMed&dopt=Citation&list_uids=3285744

[129] Horowitz, M. M.; Gale, R. P.; Sondel, P. M.; Goldman, J. M.; Kersey, J.; Kolb, H. J.; Rimm, A. A.; Ringden, O.; Rozman, C.; Speck, B. and et al. (1990): Graft-versus-leukemia reactions after bone marrow transplantation, Blood 75 [3], pp. 555-62. URL:

http://www.ncbi.nlm.nih.gov/entrez/query.fcgi?cmd=Retrieve&db=PubMed&dopt=Citation&list_uids=2297567

[130] Kolb, H. J.; Mittermuller, J.; Clemm, C.; Holler, E.; Ledderose, G.; Brehm, G.; Heim, M. and Wilmanns, W. (1990): Donor leukocyte transfusions for treatment of recurrent chronic myelogenous leukemia in marrow transplant patients, Blood 76 [12], pp. 2462-5. URL: http://www.ncbi.nlm.nih.gov/entrez/query.fcgi?cmd=Retrieve&db=PubMed&dopt=Citation&list_uids=2265242

[131] Cullis, J. O.; Jiang, Y. Z.; Schwarer, A. P.; Hughes, T. P.; Barrett, A. J. and Goldman, J. M. (1992): Donor leukocyte infusions for chronic myeloid leukemia in relapse after allogeneic bone marrow transplantation, Blood 79 [5], pp. 1379-81. URL: http://www.ncbi.nlm.nih.gov/entrez/query.fcgi?cmd=Retrieve&db=PubMed&dopt=Citation&list_uids=1536963

[132] Drobyski, W. R.; Roth, M. S.; Thibodeau, S. N. and Gottschall, J. L. (1992): Molecular remission occurring after donor leukocyte infusions for the treatment of relapsed chronic myelogenous leukemia after allogeneic bone marrow transplantation, Bone Marrow Transplant 10 [3], pp. 301-4. URL: http://www.ncbi.nlm.nih.gov/entrez/query.fcgi?cmd=Retrieve&db=PubMed&dopt=Citation&list_uids=1422483

[133] Bar, B. M.; Schattenberg, A.; Mensink, E. J.; Geurts Van Kessel, A.; Smetsers, T. F.; Knops, G. H.; Linders, E. H. and De Witte, T. (1993): Donor leukocyte infusions for chronic myeloid leukemia relapsed after allogeneic bone marrow transplantation, J Clin Oncol 11 [3], pp. 513-9. URL: http://www.ncbi.nlm.nih.gov/entrez/query.fcgi?cmd=Retrieve&db=PubMed&dopt=Citation&list_uids=8445426

[134] Helg, C.; Roux, E.; Beris, P.; Cabrol, C.; Wacker, P.; Darbellay, R.; Wyss, M.; Jeannet, M.; Chapuis, B. and Roosnek, E. (1993): Adoptive immunotherapy for recurrent CML after BMT, Bone Marrow Transplant 12 [2], pp. 125-9. URL: http://www.ncbi.nlm.nih.gov/entrez/query.fcgi?cmd=Retrieve&db=PubMed&dopt=Citation&list_uids=8401357

[135] Porter, D. L.; Roth, M. S.; McGarigle, C.; Ferrara, J. L. and Antin, J. H. (1994): Induction of graft-versus-host disease as immunotherapy for relapsed chronic myeloid leukemia, N Engl J Med 330 [2], pp. 100-6. URL: http://www.ncbi.nlm.nih.gov/entrez/query.fcgi?cmd=Retrieve&db=PubMed&dopt=Citation&list_uids=8259165

[136] Kolb, H. J.; Schattenberg, A.; Goldman, J. M.; Hertenstein, B.; Jacobsen, N.; Arcese, W.; Ljungman, P.; Ferrant, A.; Verdonck, L.; Niederwieser, D.; van Rhee, F.; Mittermueller, J.; de Witte, T.; Holler, E. and Ansari, H. (1995): Graft-versus-leukemia effect of donor lymphocyte transfusions in marrow grafted patients, Blood 86 [5], pp. 2041-50. URL: http://www.ncbi.nlm.nih.gov/entrez/query.fcgi?cmd=Retrieve&db=PubMed&dopt=Citation&list_uids=7655033

[137] Chalandon, Y.; Passweg, J. R.; Schmid, C.; Olavarria, E.; Dazzi, F.; Simula, M. P.; Ljungman, P.; Schattenberg, A.; de Witte, T.; Lenhoff, S.; Jacobs, P.; Volin, L.; Iacobelli, S.; Finke, J.; Niederwieser, D. and Guglielmi, C. (2010): Outcome of patients developing GVHD after DLI given to treat CML relapse: a study by the Chronic Leukemia Working Party of the EBMT, Bone Marrow Transplant 45 [3], pp. 558-64. URL: http://www.ncbi.nlm.nih.gov/entrez/query.fcgi?cmd=Retrieve&db=PubMed&dopt=Citation&list_uids=19633691

[138] Warren, E. H.; Greenberg, P. D. and Riddell, S. R. (1998): Cytotoxic T-lymphocyte-defined human minor histocompatibility antigens with a restricted tissue distribution, Blood 91 [6], pp. 2197-207. URL: http://www.ncbi.nlm.nih.gov/entrez/query.fcgi?cmd=Retrieve&db=PubMed&dopt=Citation&list_uids=9490709

[139] Mutis, T.; Verdijk, R.; Schrama, E.; Esendam, B.; Brand, A. and Goulmy, E. (1999): Feasibility of immunotherapy of relapsed leukemia with ex vivo-generated cytotoxic T lymphocytes specific for hematopoietic system-restricted minor histocompatibility antigens, Blood 93 [7], pp. 2336-41. URL:

http://www.ncbi.nlm.nih.gov/entrez/query.fcgi?cmd=Retrieve&db=PubMed&dopt=Citation&list_uids=10090944

[140] Reddehase, M. J.; Weiland, F.; Munch, K.; Jonjic, S.; Luske, A. and Koszinowski, U. H. (1985): Interstitial murine cytomegalovirus pneumonia after irradiation: characterization of cells that limit viral replication during established infection of the lungs, J Virol 55 [2], pp. 264-73. URL: http://www.ncbi.nlm.nih.gov/entrez/query.fcgi?cmd=Retrieve&db=PubMed&dopt=Citation&list_uids=2991554

[141] Borysiewicz, L. K.; Morris, S.; Page, J. D. and Sissons, J. G. (1983): Human cytomegalovirus-specific cytotoxic T lymphocytes: requirements for in vitro generation and specificity, Eur J Immunol 13 [10], pp. 804-9. URL: http://www.ncbi.nlm.nih.gov/entrez/query.fcgi?cmd=Retrieve&db=PubMed&dopt=Citation&list_uids=6196203

[142] Reusser, P.; Riddell, S. R.; Meyers, J. D. and Greenberg, P. D. (1991): Cytotoxic T-lymphocyte response to cytomegalovirus after human allogeneic bone marrow transplantation: pattern of recovery and correlation with cytomegalovirus infection and disease, Blood 78 [5], pp. 1373-80. URL: http://www.ncbi.nlm.nih.gov/entrez/query.fcgi?cmd=Retrieve&db=PubMed&dopt=Citation&list_uids=1652311

[143] Riddell, S. R.; Watanabe, K. S.; Goodrich, J. M.; Li, C. R.; Agha, M. E. and Greenberg, P. D. (1992): Restoration of viral immunity in immunodeficient humans by the adoptive transfer of T cell clones, Science 257 [5067], pp. 238-41. URL: http://www.ncbi.nlm.nih.gov/entrez/query.fcgi?cmd=Retrieve&db=PubMed&dopt=Citation&list_uids=1352912

[144] Rooney, C. M.; Smith, C. A.; Ng, C. Y.; Loftin, S.; Li, C.; Krance, R. A.; Brenner, M. K. and Heslop, H. E. (1995): Use of gene-modified virus-specific T lymphocytes to control Epstein-Barr-virus-related lymphoproliferation, Lancet 345 [8941], pp. 9-13. URL: http://www.ncbi.nlm.nih.gov/entrez/query.fcgi?cmd=Retrieve&db=PubMed&dopt=Citation&list_uids=7799740

[145] Haque, T.; Wilkie, G. M.; Taylor, C.; Amlot, P. L.; Murad, P.; Iley, A.; Dombagoda, D.; Britton, K. M.; Swerdlow, A. J. and Crawford, D. H. (2002): Treatment of Epstein-Barr-virus-positive post-transplantation lymphoproliferative disease with partly HLA-matched allogeneic cytotoxic T cells, Lancet 360 [9331], pp. 436-42. URL: http://www.ncbi.nlm.nih.gov/entrez/query.fcgi?cmd=Retrieve&db=PubMed&dopt=Citation&list_uids=12241714

[146] Comoli, P.; Labirio, M.; Basso, S.; Baldanti, F.; Grossi, P.; Furione, M.; Vigano, M.; Fiocchi, R.; Rossi, G.; Ginevri, F.; Gridelli, B.; Moretta, A.; Montagna, D.; Locatelli, F.; Gerna, G. and Maccario, R. (2002): Infusion of autologous Epstein-Barr virus (EBV)-specific cytotoxic T cells for prevention of EBV-related lymphoproliferative disorder in solid organ transplant recipients with evidence of active virus replication, Blood 99 [7], pp. 2592-8. URL: http://www.ncbi.nlm.nih.gov/entrez/query.fcgi?cmd=Retrieve&db=PubMed&dopt=Citation&list_uids=11895798

[147] Balch, C. M.; Gershenwald, J. E.; Soong, S. J.; Thompson, J. F.; Atkins, M. B.; Byrd, D. R.; Buzaid, A. C.; Cochran, A. J.; Coit, D. G.; Ding, S.; Eggermont, A. M.; Flaherty, K. T.; Gimotty, P. A.; Kirkwood, J. M.; McMasters, K. M.; Mihm, M. C., Jr.; Morton, D. L.; Ross, M. I.; Sober, A. J. and Sondak, V. K. (2009): Final version of 2009 AJCC melanoma staging and classification, J Clin Oncol 27 [36], pp. 6199-206. URL: http://www.ncbi.nlm.nih.gov/entrez/query.fcgi?cmd=Retrieve&db=PubMed&dopt=Citation&list_uids=19917835

[148] Morgan, D. A.; Ruscetti, F. W. and Gallo, R. (1976): Selective in vitro growth of T lymphocytes from normal human bone marrows, Science 193 [4257], pp. 1007-8. URL: http://www.ncbi.nlm.nih.gov/entrez/query.fcgi?cmd=Retrieve&db=PubMed&dopt=Citation&list_uids=181845

[149] Cheever, M. A.; Greenberg, P. D.; Fefer, A. and Gillis, S. (1982): Augmentation of the anti-tumor therapeutic efficacy of long-term cultured T lymphocytes by in vivo administration of purified interleukin 2, J Exp Med 155 [4], pp. 968-80. URL:

http://www.ncbi.nlm.nih.gov/entrez/query.fcgi?cmd=Retrieve&db=PubMed&dopt=Citation&list_uids=6977616

[150] Hefeneider, S. H.; Conlon, P. J.; Henney, C. S. and Gillis, S. (1983): In vivo interleukin 2 administration augments the generation of alloreactive cytolytic T lymphocytes and resident natural killer cells, J Immunol 130 [1], pp. 222-7. URL: http://www.ncbi.nlm.nih.gov/entrez/query.fcgi?cmd=Retrieve&db=PubMed&dopt=Citation&list_uids=6600178

[151] Donohue, J. H.; Rosenstein, M.; Chang, A. E.; Lotze, M. T.; Robb, R. J. and Rosenberg, S. A. (1984): The systemic administration of purified interleukin 2 enhances the ability of sensitized murine lymphocytes to cure a disseminated syngeneic lymphoma, J Immunol 132 [4], pp. 2123-8. URL: http://www.ncbi.nlm.nih.gov/entrez/query.fcgi?cmd=Retrieve&db=PubMed&dopt=Citation&list_uids=6607956

[152] Taniguchi, T.; Matsui, H.; Fujita, T.; Takaoka, C.; Kashima, N.; Yoshimoto, R. and Hamuro, J. (1983): Structure and expression of a cloned cDNA for human interleukin-2, Nature 302 [5906], pp. 305-10. URL: http://www.ncbi.nlm.nih.gov/entrez/query.fcgi?cmd=Retrieve&db=PubMed&dopt=Citation&list_uids=6403867

[153] Devos, R.; Plaetinck, G.; Cheroutre, H.; Simons, G.; Degrave, W.; Tavernier, J.; Remaut, E. and Fiers, W. (1983): Molecular cloning of human interleukin 2 cDNA and its expression in E. coli, Nucleic Acids Res 11 [13], pp. 4307-23. URL: http://www.ncbi.nlm.nih.gov/entrez/query.fcgi?cmd=Retrieve&db=PubMed&dopt=Citation&list_uids=6306584

[154] Rosenberg, S. A.; Grimm, E. A.; McGrogan, M.; Doyle, M.; Kawasaki, E.; Koths, K. and Mark, D. F. (1984): Biological activity of recombinant human interleukin-2 produced in Escherichia coli, Science 223 [4643], pp. 1412-4. URL: http://www.ncbi.nlm.nih.gov/entrez/query.fcgi?cmd=Retrieve&db=PubMed&dopt=Citation&list_uids=6367046

[155] Bindon, C.; Czerniecki, M.; Ruell, P.; Edwards, A.; McCarthy, W. H.; Harris, R. and Hersey, P. (1983): Clearance rates and systemic effects of intravenously administered interleukin 2 (IL-2) containing preparations in human subjects, Br J Cancer 47 [1], pp. 123-33. URL: http://www.ncbi.nlm.nih.gov/entrez/query.fcgi?cmd=Retrieve&db=PubMed&dopt=Citation&list_uids=6600395

[156] Lotze, M. T.; Frana, L. W.; Sharrow, S. O.; Robb, R. J. and Rosenberg, S. A. (1985): In vivo administration of purified human interleukin 2. I. Half-life and immunologic effects of the Jurkat cell line-derived interleukin 2, J Immunol 134 [1], pp. 157-66. URL: http://www.ncbi.nlm.nih.gov/entrez/query.fcgi?cmd=Retrieve&db=PubMed&dopt=Citation&list_uids=3871099

[157] Lotze, M. T.; Matory, Y. L.; Ettinghausen, S. E.; Rayner, A. A.; Sharrow, S. O.; Seipp, C. A.; Custer, M. C. and Rosenberg, S. A. (1985): In vivo administration of purified human interleukin 2. II. Half life, immunologic effects, and expansion of peripheral lymphoid cells in vivo with recombinant IL 2, J Immunol 135 [4], pp. 2865-75. URL: http://www.ncbi.nlm.nih.gov/entrez/query.fcgi?cmd=Retrieve&db=PubMed&dopt=Citation&list_uids=2993418

[158] Rosenberg, S. A.; Lotze, M. T.; Muul, L. M.; Leitman, S.; Chang, A. E.; Ettinghausen, S. E.; Matory, Y. L.; Skibber, J. M.; Shiloni, E.; Vetto, J. T. and et al. (1985): Observations on the systemic administration of autologous lymphokine-activated killer cells and recombinant interleukin-2 to patients with metastatic cancer, N Engl J Med 313 [23], pp. 1485-92. URL: http://www.ncbi.nlm.nih.gov/entrez/query.fcgi?cmd=Retrieve&db=PubMed&dopt=Citation&list_uids=3903508

[159] Rosenberg, S. A. (2014): IL-2: The First Effective Immunotherapy for Human Cancer, J Immunol 192 [12], pp. 5451-8. URL: http://www.ncbi.nlm.nih.gov/entrez/query.fcgi?cmd=Retrieve&db=PubMed&dopt=Citation&list_uids=24907378

[160] Law, T. M.; Motzer, R. J.; Mazumdar, M.; Sell, K. W.; Walther, P. J.; O'Connell, M.; Khan, A.; Vlamis, V.; Vogelzang, N. J. and Bajorin, D. F. (1995): Phase III randomized trial of interleukin-2

with or without lymphokine-activated killer cells in the treatment of patients with advanced renal cell carcinoma, Cancer 76 [5], pp. 824-32. URL: http://www.ncbi.nlm.nih.gov/entrez/query.fcgi?cmd=Retrieve&db=PubMed&dopt=Citation&list_uids=8625186

[161] Rosenberg, S. A.; Lotze, M. T.; Yang, J. C.; Topalian, S. L.; Chang, A. E.; Schwartzentruber, D. J.; Aebersold, P.; Leitman, S.; Linehan, W. M.; Seipp, C. A. and et al. (1993): Prospective randomized trial of high-dose interleukin-2 alone or in conjunction with lymphokine-activated killer cells for the treatment of patients with advanced cancer, J Natl Cancer Inst 85 [8], pp. 622-32. URL: http://www.ncbi.nlm.nih.gov/entrez/query.fcgi?cmd=Retrieve&db=PubMed&dopt=Citation&list_uids=8468720

[162] Atkins, M. B.; Lotze, M. T.; Dutcher, J. P.; Fisher, R. I.; Weiss, G.; Margolin, K.; Abrams, J.; Sznol, M.; Parkinson, D.; Hawkins, M.; Paradise, C.; Kunkel, L. and Rosenberg, S. A. (1999): High-dose recombinant interleukin 2 therapy for patients with metastatic melanoma: analysis of 270 patients treated between 1985 and 1993, J Clin Oncol 17 [7], pp. 2105-16. URL: http://www.ncbi.nlm.nih.gov/entrez/query.fcgi?cmd=Retrieve&db=PubMed&dopt=Citation&list_uids=10561265

[163] Fyfe, G.; Fisher, R. I.; Rosenberg, S. A.; Sznol, M.; Parkinson, D. R. and Louie, A. C. (1995): Results of treatment of 255 patients with metastatic renal cell carcinoma who received high-dose recombinant interleukin-2 therapy, J Clin Oncol 13 [3], pp. 688-96. URL: http://www.ncbi.nlm.nih.gov/entrez/query.fcgi?cmd=Retrieve&db=PubMed&dopt=Citation&list_uids=7884429

[164] Payne, R.; Glenn, L.; Hoen, H.; Richards, B.; Smith, J. W., 2nd; Lufkin, R.; Crocenzi, T. S.; Urba, W. J. and Curti, B. D. (2014): Durable responses and reversible toxicity of high-dose interleukin-2 treatment of melanoma and renal cancer in a Community Hospital Biotherapy Program, J Immunother Cancer 2, p. 13. URL: http://www.ncbi.nlm.nih.gov/entrez/query.fcgi?cmd=Retrieve&db=PubMed&dopt=Citation&list_uids=24855563

[165] Yron, I.; Wood, T. A., Jr.; Spiess, P. J. and Rosenberg, S. A. (1980): In vitro growth of murine T cells. V. The isolation and growth of lymphoid cells infiltrating syngeneic solid tumors, J Immunol 125 [1], pp. 238-45. URL: http://www.ncbi.nlm.nih.gov/entrez/query.fcgi?cmd=Retrieve&db=PubMed&dopt=Citation&list_uids=6966652

[166] Muul, L. M.; Spiess, P. J.; Director, E. P. and Rosenberg, S. A. (1987): Identification of specific cytolytic immune responses against autologous tumor in humans bearing malignant melanoma, J Immunol 138 [3], pp. 989-95. URL: http://www.ncbi.nlm.nih.gov/entrez/query.fcgi?cmd=Retrieve&db=PubMed&dopt=Citation&list_uids=3100623

[167] Rosenberg, S. A.; Spiess, P. and Lafreniere, R. (1986): A new approach to the adoptive immunotherapy of cancer with tumor-infiltrating lymphocytes, Science 233 [4770], pp. 1318-21. URL: http://www.ncbi.nlm.nih.gov/entrez/query.fcgi?cmd=Retrieve&db=PubMed&dopt=Citation&list_uids=3489291

[168] Rosenberg, S. A.; Packard, B. S.; Aebersold, P. M.; Solomon, D.; Topalian, S. L.; Toy, S. T.; Simon, P.; Lotze, M. T.; Yang, J. C.; Seipp, C. A. and et al. (1988): Use of tumor-infiltrating lymphocytes and interleukin-2 in the immunotherapy of patients with metastatic melanoma. A preliminary report, N Engl J Med 319 [25], pp. 1676-80. URL: http://www.ncbi.nlm.nih.gov/entrez/query.fcgi?cmd=Retrieve&db=PubMed&dopt=Citation&list_uids=3264384

[169] Rosenberg, S. A.; Yannelli, J. R.; Yang, J. C.; Topalian, S. L.; Schwartzentruber, D. J.; Weber, J. S.; Parkinson, D. R.; Seipp, C. A.; Einhorn, J. H. and White, D. E. (1994): Treatment of patients with metastatic melanoma with autologous tumor-infiltrating lymphocytes and interleukin 2, J Natl Cancer Inst 86 [15], pp. 1159-66. URL: http://www.ncbi.nlm.nih.gov/entrez/query.fcgi?cmd=Retrieve&db=PubMed&dopt=Citation&list_uids=8028037

[170] Dudley, M. E.; Wunderlich, J. R.; Robbins, P. F.; Yang, J. C.; Hwu, P.; Schwartzentruber, D. J.; Topalian, S. L.; Sherry, R.; Restifo, N. P.; Hubicki, A. M.; Robinson, M. R.; Raffeld, M.; Duray, P.; Seipp, C. A.; Rogers-Freezer, L.; Morton, K. E.; Mavroukakis, S. A.; White, D. E. and Rosenberg, S. A. (2002): Cancer regression and autoimmunity in patients after clonal repopulation with antitumor lymphocytes, Science 298 [5594], pp. 850-4. URL: http://www.ncbi.nlm.nih.gov/entrez/query.fcgi?cmd=Retrieve&db=PubMed&dopt=Citation&list_uids=12242449

[171] Rosenberg, S. A.; Yang, J. C.; Sherry, R. M.; Kammula, U. S.; Hughes, M. S.; Phan, G. Q.; Citrin, D. E.; Restifo, N. P.; Robbins, P. F.; Wunderlich, J. R.; Morton, K. E.; Laurencot, C. M.; Steinberg, S. M.; White, D. E. and Dudley, M. E. (2011): Durable complete responses in heavily pretreated patients with metastatic melanoma using T-cell transfer immunotherapy, Clin Cancer Res 17 [13], pp. 4550-7. URL: http://www.ncbi.nlm.nih.gov/entrez/query.fcgi?cmd=Retrieve&db=PubMed&dopt=Citation&list_uids=21498393

[172] Dembic, Z.; Haas, W.; Weiss, S.; McCubrey, J.; Kiefer, H.; von Boehmer, H. and Steinmetz, M. (1986): Transfer of specificity by murine alpha and beta T-cell receptor genes, Nature 320 [6059], pp. 232-8. URL: http://www.ncbi.nlm.nih.gov/entrez/query.fcgi?cmd=Retrieve&db=PubMed&dopt=Citation&list_uids=2421164

[173] Clay, T. M.; Custer, M. C.; Sachs, J.; Hwu, P.; Rosenberg, S. A. and Nishimura, M. I. (1999): Efficient transfer of a tumor antigen-reactive TCR to human peripheral blood lymphocytes confers anti-tumor reactivity, J Immunol 163 [1], pp. 507-13. URL: http://www.ncbi.nlm.nih.gov/entrez/query.fcgi?cmd=Retrieve&db=PubMed&dopt=Citation&list_uids=10384155

[174] Cooper, L. J.; Kalos, M.; Lewinsohn, D. A.; Riddell, S. R. and Greenberg, P. D. (2000): Transfer of specificity for human immunodeficiency virus type 1 into primary human T lymphocytes by introduction of T-cell receptor genes, J Virol 74 [17], pp. 8207-12. URL: http://www.ncbi.nlm.nih.gov/entrez/query.fcgi?cmd=Retrieve&db=PubMed&dopt=Citation&list_uids=10933734

[175] Sadovnikova, E.; Jopling, L. A.; Soo, K. S. and Stauss, H. J. (1998): Generation of human tumor-reactive cytotoxic T cells against peptides presented by non-self HLA class I molecules, Eur J Immunol 28 [1], pp. 193-200. URL: http://www.ncbi.nlm.nih.gov/entrez/query.fcgi?cmd=Retrieve&db=PubMed&dopt=Citation&list_uids=9485199

[176] Wilde, S.; Sommermeyer, D.; Frankenberger, B.; Schiemann, M.; Milosevic, S.; Spranger, S.; Pohla, H.; Uckert, W.; Busch, D. H. and Schendel, D. J. (2009): Dendritic cells pulsed with RNA encoding allogeneic MHC and antigen induce T cells with superior antitumor activity and higher TCR functional avidity, Blood 114 [10], pp. 2131-9. URL: http://www.ncbi.nlm.nih.gov/entrez/query.fcgi?cmd=Retrieve&db=PubMed&dopt=Citation&list_uids=19587379

[177] Li, L. P.; Lampert, J. C.; Chen, X.; Leitao, C.; Popovic, J.; Muller, W. and Blankenstein, T. (2010): Transgenic mice with a diverse human T cell antigen receptor repertoire, Nat Med 16 [9], pp. 1029-34. URL: http://www.ncbi.nlm.nih.gov/entrez/query.fcgi?cmd=Retrieve&db=PubMed&dopt=Citation&list_uids=20693993

[178] Holler, P. D.; Holman, P. O.; Shusta, E. V.; O'Herrin, S.; Wittrup, K. D. and Kranz, D. M. (2000): In vitro evolution of a T cell receptor with high affinity for peptide/MHC, Proc Natl Acad Sci U S A 97 [10], pp. 5387-92. URL: http://www.ncbi.nlm.nih.gov/entrez/query.fcgi?cmd=Retrieve&db=PubMed&dopt=Citation&list_uids=10779548

[179] Li, Y.; Moysey, R.; Molloy, P. E.; Vuidepot, A. L.; Mahon, T.; Baston, E.; Dunn, S.; Liddy, N.; Jacob, J.; Jakobsen, B. K. and Boulter, J. M. (2005): Directed evolution of human T-cell receptors with picomolar affinities by phage display, Nat Biotechnol 23 [3], pp. 349-54. URL: http://www.ncbi.nlm.nih.gov/entrez/query.fcgi?cmd=Retrieve&db=PubMed&dopt=Citation&list_uids=15723046

[180] Fujio, K.; Misaki, Y.; Setoguchi, K.; Morita, S.; Kawahata, K.; Kato, I.; Nosaka, T.; Yamamoto, K. and Kitamura, T. (2000): Functional reconstitution of class II MHC-restricted T cell immunity mediated by retroviral transfer of the alpha beta TCR complex, J Immunol 165 [1], pp. 528-32. URL: http://www.ncbi.nlm.nih.gov/entrez/query.fcgi?cmd=Retrieve&db=PubMed&dopt=Citation&list_uids=10861092

[181] Kessels, H. W.; Wolkers, M. C.; van den Boom, M. D.; van der Valk, M. A. and Schumacher, T. N. (2001): Immunotherapy through TCR gene transfer, Nat Immunol 2 [10], pp. 957-61. URL: http://www.ncbi.nlm.nih.gov/entrez/query.fcgi?cmd=Retrieve&db=PubMed&dopt=Citation&list_uids=11577349

[182] de Witte, M. A.; Coccoris, M.; Wolkers, M. C.; van den Boom, M. D.; Mesman, E. M.; Song, J. Y.; van der Valk, M.; Haanen, J. B. and Schumacher, T. N. (2006): Targeting self-antigens through allogeneic TCR gene transfer, Blood 108 [3], pp. 870-7. URL: http://www.ncbi.nlm.nih.gov/entrez/query.fcgi?cmd=Retrieve&db=PubMed&dopt=Citation&list_uids=16861342

[183] Morgan, R. A.; Dudley, M. E.; Wunderlich, J. R.; Hughes, M. S.; Yang, J. C.; Sherry, R. M.; Royal, R. E.; Topalian, S. L.; Kammula, U. S.; Restifo, N. P.; Zheng, Z.; Nahvi, A.; de Vries, C. R.; Rogers-Freezer, L. J.; Mavroukakis, S. A. and Rosenberg, S. A. (2006): Cancer regression in patients after transfer of genetically engineered lymphocytes, Science 314 [5796], pp. 126-9. URL: http://www.ncbi.nlm.nih.gov/entrez/query.fcgi?cmd=Retrieve&db=PubMed&dopt=Citation&list_uids=16946036

[184] Johnson, L. A.; Morgan, R. A.; Dudley, M. E.; Cassard, L.; Yang, J. C.; Hughes, M. S.; Kammula, U. S.; Royal, R. E.; Sherry, R. M.; Wunderlich, J. R.; Lee, C. C.; Restifo, N. P.; Schwarz, S. L.; Cogdill, A. P.; Bishop, R. J.; Kim, H.; Brewer, C. C.; Rudy, S. F.; VanWaes, C.; Davis, J. L.; Mathur, A.; Ripley, R. T.; Nathan, D. A.; Laurencot, C. M. and Rosenberg, S. A. (2009): Gene therapy with human and mouse T-cell receptors mediates cancer regression and targets normal tissues expressing cognate antigen, Blood 114 [3], pp. 535-46. URL: http://www.ncbi.nlm.nih.gov/entrez/query.fcgi?cmd=Retrieve&db=PubMed&dopt=Citation&list_uids=19451549

[185] Parkhurst, M. R.; Yang, J. C.; Langan, R. C.; Dudley, M. E.; Nathan, D. A.; Feldman, S. A.; Davis, J. L.; Morgan, R. A.; Merino, M. J.; Sherry, R. M.; Hughes, M. S.; Kammula, U. S.; Phan, G. Q.; Lim, R. M.; Wank, S. A.; Restifo, N. P.; Robbins, P. F.; Laurencot, C. M. and Rosenberg, S. A. (2011): T cells targeting carcinoembryonic antigen can mediate regression of metastatic colorectal cancer but induce severe transient colitis, Mol Ther 19 [3], pp. 620-6. URL: http://www.ncbi.nlm.nih.gov/entrez/query.fcgi?cmd=Retrieve&db=PubMed&dopt=Citation&list_uids=21157437

[186] Palmer, D. C.; Chan, C. C.; Gattinoni, L.; Wrzesinski, C.; Paulos, C. M.; Hinrichs, C. S.; Powell, D. J., Jr.; Klebanoff, C. A.; Finkelstein, S. E.; Fariss, R. N.; Yu, Z.; Nussenblatt, R. B.; Rosenberg, S. A. and Restifo, N. P. (2008): Effective tumor treatment targeting a melanoma/melanocyte-associated antigen triggers severe ocular autoimmunity, Proc Natl Acad Sci U S A 105 [23], pp. 8061-6. URL: http://www.ncbi.nlm.nih.gov/entrez/query.fcgi?cmd=Retrieve&db=PubMed&dopt=Citation&list_uids=18523011

[187] Bos, R.; van Duikeren, S.; Morreau, H.; Franken, K.; Schumacher, T. N.; Haanen, J. B.; van der Burg, S. H.; Melief, C. J. and Offringa, R. (2008): Balancing between antitumor efficacy and autoimmune pathology in T-cell-mediated targeting of carcinoembryonic antigen, Cancer Res 68 [20], pp. 8446-55. URL: http://www.ncbi.nlm.nih.gov/entrez/query.fcgi?cmd=Retrieve&db=PubMed&dopt=Citation&list_uids=18922918

[188] Linette, G. P.; Stadtmauer, E. A.; Maus, M. V.; Rapoport, A. P.; Levine, B. L.; Emery, L.; Litzky, L.; Bagg, A.; Carreno, B. M.; Cimino, P. J.; Binder-Scholl, G. K.; Smethurst, D. P.; Gerry, A. B.; Pumphrey, N. J.; Bennett, A. D.; Brewer, J. E.; Dukes, J.; Harper, J.; Tayton-Martin, H. K.; Jakobsen, B. K.; Hassan, N. J.; Kalos, M. and June, C. H. (2013): Cardiovascular toxicity and titin cross-reactivity of affinity-enhanced T cells in myeloma and melanoma, Blood 122 [6], pp. 863-71. URL: http://www.ncbi.nlm.nih.gov/entrez/query.fcgi?cmd=Retrieve&db=PubMed&dopt=Citation&list_uids=23770775

[189] Connerotte, T.; Van Pel, A.; Godelaine, D.; Tartour, E.; Schuler-Thurner, B.; Lucas, S.; Thielemans, K.; Schuler, G. and Coulie, P. G. (2008): Functions of Anti-MAGE T-cells induced in melanoma patients under different vaccination modalities, Cancer Res 68 [10], pp. 3931-40. URL: http://www.ncbi.nlm.nih.gov/entrez/query.fcgi?cmd=Retrieve&db=PubMed&dopt=Citation&list_uids=18483279

[190] Cameron, B. J.; Gerry, A. B.; Dukes, J.; Harper, J. V.; Kannan, V.; Bianchi, F. C.; Grand, F.; Brewer, J. E.; Gupta, M.; Plesa, G.; Bossi, G.; Vuidepot, A.; Powlesland, A. S.; Legg, A.; Adams, K. J.; Bennett, A. D.; Pumphrey, N. J.; Williams, D. D.; Binder-Scholl, G.; Kulikovskaya, I.; Levine, B. L.; Riley, J. L.; Varela-Rohena, A.; Stadtmauer, E. A.; Rapoport, A. P.; Linette, G. P.; June, C. H.; Hassan, N. J.; Kalos, M. and Jakobsen, B. K. (2013): Identification of a Titin-derived HLA-A1-presented peptide as a cross-reactive target for engineered MAGE A3-directed T cells, Sci Transl Med 5 [197], p. 197ra103. URL: http://www.ncbi.nlm.nih.gov/entrez/query.fcgi?cmd=Retrieve&db=PubMed&dopt=Citation&list_uids=23926201

[191] Morgan, R. A.; Chinnasamy, N.; Abate-Daga, D.; Gros, A.; Robbins, P. F.; Zheng, Z.; Dudley, M. E.; Feldman, S. A.; Yang, J. C.; Sherry, R. M.; Phan, G. Q.; Hughes, M. S.; Kammula, U. S.; Miller, A. D.; Hessman, C. J.; Stewart, A. A.; Restifo, N. P.; Quezado, M. M.; Alimchandani, M.; Rosenberg, A. Z.; Nath, A.; Wang, T.; Bielekova, B.; Wuest, S. C.; Akula, N.; McMahon, F. J.; Wilde, S.; Mosetter, B.; Schendel, D. J.; Laurencot, C. M. and Rosenberg, S. A. (2013): Cancer regression and neurological toxicity following anti-MAGE-A3 TCR gene therapy, J Immunother 36 [2], pp. 133-51. URL: http://www.ncbi.nlm.nih.gov/entrez/query.fcgi?cmd=Retrieve&db=PubMed&dopt=Citation&list_uids=23377668

[192] Chinnasamy, N.; Wargo, J. A.; Yu, Z.; Rao, M.; Frankel, T. L.; Riley, J. P.; Hong, J. J.; Parkhurst, M. R.; Feldman, S. A.; Schrump, D. S.; Restifo, N. P.; Robbins, P. F.; Rosenberg, S. A. and Morgan, R. A. (2011): A TCR targeting the HLA-A*0201-restricted epitope of MAGE-A3 recognizes multiple epitopes of the MAGE-A antigen superfamily in several types of cancer, J Immunol 186 [2], pp. 685-96. URL: http://www.ncbi.nlm.nih.gov/entrez/query.fcgi?cmd=Retrieve&db=PubMed&dopt=Citation&list_uids=21149604

[193] Geiss, G. K.; Bumgarner, R. E.; Birditt, B.; Dahl, T.; Dowidar, N.; Dunaway, D. L.; Fell, H. P.; Ferree, S.; George, R. D.; Grogan, T.; James, J. J.; Maysuria, M.; Mitton, J. D.; Oliveri, P.; Osborn, J. L.; Peng, T.; Ratcliffe, A. L.; Webster, P. J.; Davidson, E. H.; Hood, L. and Dimitrov, K. (2008): Direct multiplexed measurement of gene expression with color-coded probe pairs, Nat Biotechnol 26 [3], pp. 317-25. URL: http://www.ncbi.nlm.nih.gov/entrez/query.fcgi?cmd=Retrieve&db=PubMed&dopt=Citation&list_uids=18278033

[194] Robbins, P. F.; Morgan, R. A.; Feldman, S. A.; Yang, J. C.; Sherry, R. M.; Dudley, M. E.; Wunderlich, J. R.; Nahvi, A. V.; Helman, L. J.; Mackall, C. L.; Kammula, U. S.; Hughes, M. S.; Restifo, N. P.; Raffeld, M.; Lee, C. C.; Levy, C. L.; Li, Y. F.; El-Gamil, M.; Schwarz, S. L.; Laurencot, C. and Rosenberg, S. A. (2011): Tumor regression in patients with metastatic synovial cell sarcoma and melanoma using genetically engineered lymphocytes reactive with NY-ESO-1, J Clin Oncol 29 [7], pp. 917-24. URL: http://www.ncbi.nlm.nih.gov/entrez/query.fcgi?cmd=Retrieve&db=PubMed&dopt=Citation&list_uids=21282551

[195] Chen, J. L.; Dunbar, P. R.; Gileadi, U.; Jager, E.; Gnjatic, S.; Nagata, Y.; Stockert, E.; Panicali, D. L.; Chen, Y. T.; Knuth, A.; Old, L. J. and Cerundolo, V. (2000): Identification of NY-ESO-1 peptide analogues capable of improved stimulation of tumor-reactive CTL, J Immunol 165 [2], pp. 948-55. URL: http://www.ncbi.nlm.nih.gov/entrez/query.fcgi?cmd=Retrieve&db=PubMed&dopt=Citation&list_uids=10878370

[196] Robbins, P. F.; Li, Y. F.; El-Gamil, M.; Zhao, Y.; Wargo, J. A.; Zheng, Z.; Xu, H.; Morgan, R. A.; Feldman, S. A.; Johnson, L. A.; Bennett, A. D.; Dunn, S. M.; Mahon, T. M.; Jakobsen, B. K. and Rosenberg, S. A. (2008): Single and dual amino acid substitutions in TCR CDRs can enhance antigen-specific T cell functions, J Immunol 180 [9], pp. 6116-31. URL:

http://www.ncbi.nlm.nih.gov/entrez/query.fcgi?cmd=Retrieve&db=PubMed&dopt=Citation&list_uids=18424733

[197] Schumacher, T. N. (2002): T-cell-receptor gene therapy, Nat Rev Immunol 2 [7], pp. 512-9. URL: http://www.ncbi.nlm.nih.gov/entrez/query.fcgi?cmd=Retrieve&db=PubMed&dopt=Citation&list_uids=12094225

[198] Bendle, G. M.; Linnemann, C.; Hooijkaas, A. I.; Bies, L.; de Witte, M. A.; Jorritsma, A.; Kaiser, A. D.; Pouw, N.; Debets, R.; Kieback, E.; Uckert, W.; Song, J. Y.; Haanen, J. B. and Schumacher, T. N. (2010): Lethal graft-versus-host disease in mouse models of T cell receptor gene therapy, Nat Med 16 [5], pp. 565-70, 1p following 570. URL: http://www.ncbi.nlm.nih.gov/entrez/query.fcgi?cmd=Retrieve&db=PubMed&dopt=Citation&list_uids=20400962

[199] van Loenen, M. M.; de Boer, R.; Amir, A. L.; Hagedoorn, R. S.; Volbeda, G. L.; Willemze, R.; van Rood, J. J.; Falkenburg, J. H. and Heemskerk, M. H. (2010): Mixed T cell receptor dimers harbor potentially harmful neoreactivity, Proc Natl Acad Sci U S A 107 [24], pp. 10972-7. URL: http://www.ncbi.nlm.nih.gov/entrez/query.fcgi?cmd=Retrieve&db=PubMed&dopt=Citation&list_uids=20534461

[200] Ahmadi, M.; King, J. W.; Xue, S. A.; Voisine, C.; Holler, A.; Wright, G. P.; Waxman, J.; Morris, E. and Stauss, H. J. (2011): CD3 limits the efficacy of TCR gene therapy in vivo, Blood 118 [13], pp. 3528-37. URL: http://www.ncbi.nlm.nih.gov/entrez/query.fcgi?cmd=Retrieve&db=PubMed&dopt=Citation&list_uids=21750319

[201] Sommermeyer, D.; Neudorfer, J.; Weinhold, M.; Leisegang, M.; Engels, B.; Noessner, E.; Heemskerk, M. H.; Charo, J.; Schendel, D. J.; Blankenstein, T.; Bernhard, H. and Uckert, W. (2006): Designer T cells by T cell receptor replacement, Eur J Immunol 36 [11], pp. 3052-9. URL: http://www.ncbi.nlm.nih.gov/entrez/query.fcgi?cmd=Retrieve&db=PubMed&dopt=Citation&list_uids=17051621

[202] Heemskerk, M. H.; Hagedoorn, R. S.; van der Hoorn, M. A.; van der Veken, L. T.; Hoogeboom, M.; Kester, M. G.; Willemze, R. and Falkenburg, J. H. (2007): Efficiency of T-cell receptor expression in dual-specific T cells is controlled by the intrinsic qualities of the TCR chains within the TCR-CD3 complex, Blood 109 [1], pp. 235-43. URL: http://www.ncbi.nlm.nih.gov/entrez/query.fcgi?cmd=Retrieve&db=PubMed&dopt=Citation&list_uids=16968899

[203] Engels, B.; Cam, H.; Schuler, T.; Indraccolo, S.; Gladow, M.; Baum, C.; Blankenstein, T. and Uckert, W. (2003): Retroviral vectors for high-level transgene expression in T lymphocytes, Hum Gene Ther 14 [12], pp. 1155-68. URL: http://www.ncbi.nlm.nih.gov/entrez/query.fcgi?cmd=Retrieve&db=PubMed&dopt=Citation&list_uids=12908967

[204] Schambach, A.; Wodrich, H.; Hildinger, M.; Bohne, J.; Krausslich, H. G. and Baum, C. (2000): Context dependence of different modules for posttranscriptional enhancement of gene expression from retroviral vectors, Mol Ther 2 [5], pp. 435-45. URL: http://www.ncbi.nlm.nih.gov/entrez/query.fcgi?cmd=Retrieve&db=PubMed&dopt=Citation&list_uids=11082317

[205] Engels, B.; Noessner, E.; Frankenberger, B.; Blankenstein, T.; Schendel, D. J. and Uckert, W. (2005): Redirecting human T lymphocytes toward renal cell carcinoma specificity by retroviral transfer of T cell receptor genes, Hum Gene Ther 16 [7], pp. 799-810. URL: http://www.ncbi.nlm.nih.gov/entrez/query.fcgi?cmd=Retrieve&db=PubMed&dopt=Citation&list_uids=16000062

[206] Scholten, K. B.; Kramer, D.; Kueter, E. W.; Graf, M.; Schoedl, T.; Meijer, C. J.; Schreurs, M. W. and Hooijberg, E. (2006): Codon modification of T cell receptors allows enhanced functional expression in transgenic human T cells, Clin Immunol 119 [2], pp. 135-45. URL: http://www.ncbi.nlm.nih.gov/entrez/query.fcgi?cmd=Retrieve&db=PubMed&dopt=Citation&list_uids=16458072

[207] Leisegang, M.; Engels, B.; Meyerhuber, P.; Kieback, E.; Sommermeyer, D.; Xue, S. A.; Reuss, S.; Stauss, H. and Uckert, W. (2008): Enhanced functionality of T cell receptor-redirected T cells is

defined by the transgene cassette, J Mol Med (Berl) 86 [5], pp. 573-83. URL: http://www.ncbi.nlm.nih.gov/entrez/query.fcgi?cmd=Retrieve&db=PubMed&dopt=Citation&list_uids=18335188

[208] Kuball, J.; Schmitz, F. W.; Voss, R. H.; Ferreira, E. A.; Engel, R.; Guillaume, P.; Strand, S.; Romero, P.; Huber, C.; Sherman, L. A. and Theobald, M. (2005): Cooperation of human tumor-reactive CD4+ and CD8+ T cells after redirection of their specificity by a high-affinity p53A2.1-specific TCR, Immunity 22 [1], pp. 117-29. URL: http://www.ncbi.nlm.nih.gov/entrez/query.fcgi?cmd=Retrieve&db=PubMed&dopt=Citation&list_uids=15664164

[209] Cohen, C. J.; Zhao, Y.; Zheng, Z.; Rosenberg, S. A. and Morgan, R. A. (2006): Enhanced antitumor activity of murine-human hybrid T-cell receptor (TCR) in human lymphocytes is associated with improved pairing and TCR/CD3 stability, Cancer Res 66 [17], pp. 8878-86. URL: http://www.ncbi.nlm.nih.gov/entrez/query.fcgi?cmd=Retrieve&db=PubMed&dopt=Citation&list_uids=16951205

[210] Voss, R. H.; Kuball, J.; Engel, R.; Guillaume, P.; Romero, P.; Huber, C. and Theobald, M. (2006): Redirection of T cells by delivering a transgenic mouse-derived MDM2 tumor antigen-specific TCR and its humanized derivative is governed by the CD8 coreceptor and affects natural human TCR expression, Immunol Res 34 [1], pp. 67-87. URL: http://www.ncbi.nlm.nih.gov/entrez/query.fcgi?cmd=Retrieve&db=PubMed&dopt=Citation&list_uids=16720899

[211] Sommermeyer, D. and Uckert, W. (2010): Minimal amino acid exchange in human TCR constant regions fosters improved function of TCR gene-modified T cells, J Immunol 184 [11], pp. 6223-31. URL: http://www.ncbi.nlm.nih.gov/entrez/query.fcgi?cmd=Retrieve&db=PubMed&dopt=Citation&list_uids=20483785

[212] Bialer, G.; Horovitz-Fried, M.; Ya'acobi, S.; Morgan, R. A. and Cohen, C. J. (2010): Selected murine residues endow human TCR with enhanced tumor recognition, J Immunol 184 [11], pp. 6232-41. URL: http://www.ncbi.nlm.nih.gov/entrez/query.fcgi?cmd=Retrieve&db=PubMed&dopt=Citation&list_uids=20427762

[213] Cohen, C. J.; Li, Y. F.; El-Gamil, M.; Robbins, P. F.; Rosenberg, S. A. and Morgan, R. A. (2007): Enhanced antitumor activity of T cells engineered to express T-cell receptors with a second disulfide bond, Cancer Res 67 [8], pp. 3898-903. URL: http://www.ncbi.nlm.nih.gov/entrez/query.fcgi?cmd=Retrieve&db=PubMed&dopt=Citation&list_uids=17440104

[214] Kuball, J.; Dossett, M. L.; Wolfl, M.; Ho, W. Y.; Voss, R. H.; Fowler, C. and Greenberg, P. D. (2007): Facilitating matched pairing and expression of TCR chains introduced into human T cells, Blood 109 [6], pp. 2331-8. URL: http://www.ncbi.nlm.nih.gov/entrez/query.fcgi?cmd=Retrieve&db=PubMed&dopt=Citation&list_uids=17082316

[215] Thomas, S.; Xue, S. A.; Cesco-Gaspere, M.; San Jose, E.; Hart, D. P.; Wong, V.; Debets, R.; Alarcon, B.; Morris, E. and Stauss, H. J. (2007): Targeting the Wilms tumor antigen 1 by TCR gene transfer: TCR variants improve tetramer binding but not the function of gene modified human T cells, J Immunol 179 [9], pp. 5803-10. URL: http://www.ncbi.nlm.nih.gov/entrez/query.fcgi?cmd=Retrieve&db=PubMed&dopt=Citation&list_uids=17947653

[216] Voss, R. H.; Willemsen, R. A.; Kuball, J.; Grabowski, M.; Engel, R.; Intan, R. S.; Guillaume, P.; Romero, P.; Huber, C. and Theobald, M. (2008): Molecular design of the Calphabeta interface favors specific pairing of introduced TCRalphabeta in human T cells, J Immunol 180 [1], pp. 391-401. URL: http://www.ncbi.nlm.nih.gov/entrez/query.fcgi?cmd=Retrieve&db=PubMed&dopt=Citation&list_uids=18097040

[217] Kuball, J.; Hauptrock, B.; Malina, V.; Antunes, E.; Voss, R. H.; Wolfl, M.; Strong, R.; Theobald, M. and Greenberg, P. D. (2009): Increasing functional avidity of TCR-redirected T cells by removing defined N-glycosylation sites in the TCR constant domain, J Exp Med 206 [2], pp. 463-75. URL:

http://www.ncbi.nlm.nih.gov/entrez/query.fcgi?cmd=Retrieve&db=PubMed&dopt=Citation&list_uids=19171765

[218] Haga-Friedman, A.; Horovitz-Fried, M. and Cohen, C. J. (2012): Incorporation of transmembrane hydrophobic mutations in the TCR enhance its surface expression and T cell functional avidity, J Immunol 188 [11], pp. 5538-46. URL: http://www.ncbi.nlm.nih.gov/entrez/query.fcgi?cmd=Retrieve&db=PubMed&dopt=Citation&list_uids=22544927

[219] Provasi, E.; Genovese, P.; Lombardo, A.; Magnani, Z.; Liu, P. Q.; Reik, A.; Chu, V.; Paschon, D. E.; Zhang, L.; Kuball, J.; Camisa, B.; Bondanza, A.; Casorati, G.; Ponzoni, M.; Ciceri, F.; Bordignon, C.; Greenberg, P. D.; Holmes, M. C.; Gregory, P. D.; Naldini, L. and Bonini, C. (2012): Editing T cell specificity towards leukemia by zinc finger nucleases and lentiviral gene transfer, Nat Med 18 [5], pp. 807-15. URL: http://www.ncbi.nlm.nih.gov/entrez/query.fcgi?cmd=Retrieve&db=PubMed&dopt=Citation&list_uids=22466705

[220] Berdien, B.; Mock, U.; Atanackovic, D. and Fehse, B. (2014): TALEN-mediated editing of endogenous T-cell receptors facilitates efficient reprogramming of T lymphocytes by lentiviral gene transfer, Gene Ther 21 [6], pp. 539-48. URL: http://www.ncbi.nlm.nih.gov/entrez/query.fcgi?cmd=Retrieve&db=PubMed&dopt=Citation&list_uids=24670996

[221] Okamoto, S.; Mineno, J.; Ikeda, H.; Fujiwara, H.; Yasukawa, M.; Shiku, H. and Kato, I. (2009): Improved expression and reactivity of transduced tumor-specific TCRs in human lymphocytes by specific silencing of endogenous TCR, Cancer Res 69 [23], pp. 9003-11. URL: http://www.ncbi.nlm.nih.gov/entrez/query.fcgi?cmd=Retrieve&db=PubMed&dopt=Citation&list_uids=19903853

[222] Okamoto, S.; Amaishi, Y.; Goto, Y.; Ikeda, H.; Fujiwara, H.; Kuzushima, K.; Yasukawa, M.; Shiku, H. and Mineno, J. (2012): A Promising Vector for TCR Gene Therapy: Differential Effect of siRNA, 2A Peptide, and Disulfide Bond on the Introduced TCR Expression, Mol Ther Nucleic Acids 1, p. e63. URL: http://www.ncbi.nlm.nih.gov/entrez/query.fcgi?cmd=Retrieve&db=PubMed&dopt=Citation&list_uids=23250361

[223] Liu, J.; Carmell, M. A.; Rivas, F. V.; Marsden, C. G.; Thomson, J. M.; Song, J. J.; Hammond, S. M.; Joshua-Tor, L. and Hannon, G. J. (2004): Argonaute2 is the catalytic engine of mammalian RNAi, Science 305 [5689], pp. 1437-41. URL: http://www.ncbi.nlm.nih.gov/entrez/query.fcgi?cmd=Retrieve&db=PubMed&dopt=Citation&list_uids=15284456

[224] Meister, G.; Landthaler, M.; Patkaniowska, A.; Dorsett, Y.; Teng, G. and Tuschl, T. (2004): Human Argonaute2 mediates RNA cleavage targeted by miRNAs and siRNAs, Mol Cell 15 [2], pp. 185-97. URL: http://www.ncbi.nlm.nih.gov/entrez/query.fcgi?cmd=Retrieve&db=PubMed&dopt=Citation&list_uids=15260970

[225] Pillai, R. S.; Bhattacharyya, S. N.; Artus, C. G.; Zoller, T.; Cougot, N.; Basyuk, E.; Bertrand, E. and Filipowicz, W. (2005): Inhibition of translational initiation by Let-7 MicroRNA in human cells, Science 309 [5740], pp. 1573-6. URL: http://www.ncbi.nlm.nih.gov/entrez/query.fcgi?cmd=Retrieve&db=PubMed&dopt=Citation&list_uids=16081698

[226] Humphreys, D. T.; Westman, B. J.; Martin, D. I. and Preiss, T. (2005): MicroRNAs control translation initiation by inhibiting eukaryotic initiation factor 4E/cap and poly(A) tail function, Proc Natl Acad Sci U S A 102 [47], pp. 16961-6. URL: http://www.ncbi.nlm.nih.gov/entrez/query.fcgi?cmd=Retrieve&db=PubMed&dopt=Citation&list_uids=16287976

[227] Wu, L.; Fan, J. and Belasco, J. G. (2006): MicroRNAs direct rapid deadenylation of mRNA, Proc Natl Acad Sci U S A 103 [11], pp. 4034-9. URL: http://www.ncbi.nlm.nih.gov/entrez/query.fcgi?cmd=Retrieve&db=PubMed&dopt=Citation&list_uids=16495412

[228] Elbashir, S. M.; Harborth, J.; Lendeckel, W.; Yalcin, A.; Weber, K. and Tuschl, T. (2001): Duplexes of 21-nucleotide RNAs mediate RNA interference in cultured mammalian cells,

Nature 411 [6836], pp. 494-8. URL: http://www.ncbi.nlm.nih.gov/entrez/query.fcgi?cmd=Retrieve&db=PubMed&dopt=Citation&list_uids=11373684

[229] Brummelkamp, T. R.; Bernards, R. and Agami, R. (2002): A system for stable expression of short interfering RNAs in mammalian cells, Science 296 [5567], pp. 550-3. URL: http://www.ncbi.nlm.nih.gov/entrez/query.fcgi?cmd=Retrieve&db=PubMed&dopt=Citation&list_uids=11910072

[230] Zeng, Y.; Wagner, E. J. and Cullen, B. R. (2002): Both natural and designed micro RNAs can inhibit the expression of cognate mRNAs when expressed in human cells, Mol Cell 9 [6], pp. 1327-33. URL: http://www.ncbi.nlm.nih.gov/entrez/query.fcgi?cmd=Retrieve&db=PubMed&dopt=Citation&list_uids=12086629

[231] Lee, Y.; Ahn, C.; Han, J.; Choi, H.; Kim, J.; Yim, J.; Lee, J.; Provost, P.; Radmark, O.; Kim, S. and Kim, V. N. (2003): The nuclear RNase III Drosha initiates microRNA processing, Nature 425 [6956], pp. 415-9. URL: http://www.ncbi.nlm.nih.gov/entrez/query.fcgi?cmd=Retrieve&db=PubMed&dopt=Citation&list_uids=14508493

[232] Gregory, R. I.; Yan, K. P.; Amuthan, G.; Chendrimada, T.; Doratotaj, B.; Cooch, N. and Shiekhattar, R. (2004): The Microprocessor complex mediates the genesis of microRNAs, Nature 432 [7014], pp. 235-40. URL: http://www.ncbi.nlm.nih.gov/entrez/query.fcgi?cmd=Retrieve&db=PubMed&dopt=Citation&list_uids=15531877

[233] Yi, R.; Qin, Y.; Macara, I. G. and Cullen, B. R. (2003): Exportin-5 mediates the nuclear export of pre-microRNAs and short hairpin RNAs, Genes Dev 17 [24], pp. 3011-6. URL: http://www.ncbi.nlm.nih.gov/entrez/query.fcgi?cmd=Retrieve&db=PubMed&dopt=Citation&list_uids=14681208

[234] Provost, P.; Dishart, D.; Doucet, J.; Frendewey, D.; Samuelsson, B. and Radmark, O. (2002): Ribonuclease activity and RNA binding of recombinant human Dicer, EMBO J 21 [21], pp. 5864-74. URL: http://www.ncbi.nlm.nih.gov/entrez/query.fcgi?cmd=Retrieve&db=PubMed&dopt=Citation&list_uids=12411504

[235] Schwarz, D. S.; Hutvagner, G.; Du, T.; Xu, Z.; Aronin, N. and Zamore, P. D. (2003): Asymmetry in the assembly of the RNAi enzyme complex, Cell 115 [2], pp. 199-208. URL: http://www.ncbi.nlm.nih.gov/entrez/query.fcgi?cmd=Retrieve&db=PubMed&dopt=Citation&list_uids=14567917

[236] Khvorova, A.; Reynolds, A. and Jayasena, S. D. (2003): Functional siRNAs and miRNAs exhibit strand bias, Cell 115 [2], pp. 209-16. URL: http://www.ncbi.nlm.nih.gov/entrez/query.fcgi?cmd=Retrieve&db=PubMed&dopt=Citation&list_uids=14567918

[237] Saetrom, P.; Snove, O.; Nedland, M.; Grunfeld, T. B.; Lin, Y.; Bass, M. B. and Canon, J. R. (2006): Conserved microRNA characteristics in mammals, Oligonucleotides 16 [2], pp. 115-44. URL: http://www.ncbi.nlm.nih.gov/entrez/query.fcgi?cmd=Retrieve&db=PubMed&dopt=Citation&list_uids=16764537

[238] Griffiths-Jones, S.; Saini, H. K.; van Dongen, S. and Enright, A. J. (2008): miRBase: tools for microRNA genomics, Nucleic Acids Res 36 [Database issue], pp. D154-8. URL: http://www.ncbi.nlm.nih.gov/entrez/query.fcgi?cmd=Retrieve&db=PubMed&dopt=Citation&list_uids=17991681

[239] Stärck, L.; Popp, K.; Pircher, H. and Uckert, W. (2014): Immunotherapy with TCR-redirected T cells: comparison of TCR-transduced and TCR-engineered hematopoietic stem cell-derived T cells, J Immunol 192 [1], pp. 206-13. URL: http://www.ncbi.nlm.nih.gov/entrez/query.fcgi?cmd=Retrieve&db=PubMed&dopt=Citation&list_uids=24293634

[240] Rosenberg, S. A. (2010): Of mice, not men: no evidence for graft-versus-host disease in humans receiving T-cell receptor-transduced autologous T cells, Mol Ther 18 [10], pp. 1744-5. URL:

http://www.ncbi.nlm.nih.gov/entrez/query.fcgi?cmd=Retrieve&db=PubMed&dopt=Citation&list_uids=20885433

[241] Davis, J. L.; Theoret, M. R.; Zheng, Z.; Lamers, C. H.; Rosenberg, S. A. and Morgan, R. A. (2010): Development of human anti-murine T-cell receptor antibodies in both responding and nonresponding patients enrolled in TCR gene therapy trials, Clin Cancer Res 16 [23], pp. 5852-61. URL: http://www.ncbi.nlm.nih.gov/entrez/query.fcgi?cmd=Retrieve&db=PubMed&dopt=Citation&list_uids=21138872

[242] Ellington, A. D. and Szostak, J. W. (1990): In vitro selection of RNA molecules that bind specific ligands, Nature 346 [6287], pp. 818-22. URL: http://www.ncbi.nlm.nih.gov/entrez/query.fcgi?cmd=Retrieve&db=PubMed&dopt=Citation&list_uids=1697402

[243] Tuerk, C. and Gold, L. (1990): Systematic evolution of ligands by exponential enrichment: RNA ligands to bacteriophage T4 DNA polymerase, Science 249 [4968], pp. 505-10. URL: http://www.ncbi.nlm.nih.gov/entrez/query.fcgi?cmd=Retrieve&db=PubMed&dopt=Citation&list_uids=2200121

[244] Wang, C.; Zhang, M.; Yang, G.; Zhang, D.; Ding, H.; Wang, H.; Fan, M.; Shen, B. and Shao, N. (2003): Single-stranded DNA aptamers that bind differentiated but not parental cells: subtractive systematic evolution of ligands by exponential enrichment, J Biotechnol 102 [1], pp. 15-22. URL: http://www.ncbi.nlm.nih.gov/entrez/query.fcgi?cmd=Retrieve&db=PubMed&dopt=Citation&list_uids=12668310

[245] Shangguan, D.; Li, Y.; Tang, Z.; Cao, Z. C.; Chen, H. W.; Mallikaratchy, P.; Sefah, K.; Yang, C. J. and Tan, W. (2006): Aptamers evolved from live cells as effective molecular probes for cancer study, Proc Natl Acad Sci U S A 103 [32], pp. 11838-43. URL: http://www.ncbi.nlm.nih.gov/entrez/query.fcgi?cmd=Retrieve&db=PubMed&dopt=Citation&list_uids=16873550

[246] Sefah, K.; Shangguan, D.; Xiong, X.; O'Donoghue, M. B. and Tan, W. (2010): Development of DNA aptamers using Cell-SELEX, Nat Protoc 5 [6], pp. 1169-85. URL: http://www.ncbi.nlm.nih.gov/entrez/query.fcgi?cmd=Retrieve&db=PubMed&dopt=Citation&list_uids=20539292

[247] Scholten, K. B.; Ruizendaal, J. J.; Graf, M.; Schoedl, T.; Kramer, D.; Meijer, C. J.; Man, S. and Hooijberg, E. (2010): Promiscuous behavior of HPV16E6 specific T cell receptor beta chains hampers functional expression in TCR transgenic T cells, which can be restored in part by genetic modification, Cell Oncol 32 [1-2], pp. 43-56. URL: http://www.ncbi.nlm.nih.gov/entrez/query.fcgi?cmd=Retrieve&db=PubMed&dopt=Citation&list_uids=20208133

[248] McManus, M. T.; Petersen, C. P.; Haines, B. B.; Chen, J. and Sharp, P. A. (2002): Gene silencing using micro-RNA designed hairpins, RNA 8 [6], pp. 842-50. URL: http://www.ncbi.nlm.nih.gov/entrez/query.fcgi?cmd=Retrieve&db=PubMed&dopt=Citation&list_uids=12088155

[249] Boden, D.; Pusch, O.; Silbermann, R.; Lee, F.; Tucker, L. and Ramratnam, B. (2004): Enhanced gene silencing of HIV-1 specific siRNA using microRNA designed hairpins, Nucleic Acids Res 32 [3], pp. 1154-8. URL: http://www.ncbi.nlm.nih.gov/entrez/query.fcgi?cmd=Retrieve&db=PubMed&dopt=Citation&list_uids=14966264

[250] Reuss, S.; Sebestyen, Z.; Heinz, N.; Loew, R.; Baum, C.; Debets, R. and Uckert, W. (2014): TCR-engineered T cells: a model of inducible TCR expression to dissect the interrelationship between two TCRs, Eur J Immunol 44 [1], pp. 265-74. URL: http://www.ncbi.nlm.nih.gov/entrez/query.fcgi?cmd=Retrieve&db=PubMed&dopt=Citation&list_uids=24114521

[251] Grimm, D.; Streetz, K. L.; Jopling, C. L.; Storm, T. A.; Pandey, K.; Davis, C. R.; Marion, P.; Salazar, F. and Kay, M. A. (2006): Fatality in mice due to oversaturation of cellular microRNA/short hairpin RNA pathways, Nature 441 [7092], pp. 537-41. URL: http://www.ncbi.nlm.nih.gov/entrez/query.fcgi?cmd=Retrieve&db=PubMed&dopt=Citation&list_uids=16724069

[252] An, D. S.; Qin, F. X.; Auyeung, V. C.; Mao, S. H.; Kung, S. K.; Baltimore, D. and Chen, I. S. (2006): Optimization and functional effects of stable short hairpin RNA expression in primary human lymphocytes via lentiviral vectors, Mol Ther 14 [4], pp. 494-504. URL: http://www.ncbi.nlm.nih.gov/entrez/query.fcgi?cmd=Retrieve&db=PubMed&dopt=Citation&list_uids=16844419

[253] Lo, H. L.; Chang, T.; Yam, P.; Marcovecchio, P. M.; Li, S.; Zaia, J. A. and Yee, J. K. (2007): Inhibition of HIV-1 replication with designed miRNAs expressed from RNA polymerase II promoters, Gene Ther 14 [21], pp. 1503-12. URL: http://www.ncbi.nlm.nih.gov/entrez/query.fcgi?cmd=Retrieve&db=PubMed&dopt=Citation&list_uids=17805304

[254] Giering, J. C.; Grimm, D.; Storm, T. A. and Kay, M. A. (2008): Expression of shRNA from a tissue-specific pol II promoter is an effective and safe RNAi therapeutic, Mol Ther 16 [9], pp. 1630-6. URL: http://www.ncbi.nlm.nih.gov/entrez/query.fcgi?cmd=Retrieve&db=PubMed&dopt=Citation&list_uids=18665161

[255] McBride, J. L.; Boudreau, R. L.; Harper, S. Q.; Staber, P. D.; Monteys, A. M.; Martins, I.; Gilmore, B. L.; Burstein, H.; Peluso, R. W.; Polisky, B.; Carter, B. J. and Davidson, B. L. (2008): Artificial miRNAs mitigate shRNA-mediated toxicity in the brain: implications for the therapeutic development of RNAi, Proc Natl Acad Sci U S A 105 [15], pp. 5868-73. URL: http://www.ncbi.nlm.nih.gov/entrez/query.fcgi?cmd=Retrieve&db=PubMed&dopt=Citation&list_uids=18398004

[256] Boudreau, R. L.; Martins, I. and Davidson, B. L. (2009): Artificial microRNAs as siRNA shuttles: improved safety as compared to shRNAs in vitro and in vivo, Mol Ther 17 [1], pp. 169-75. URL: http://www.ncbi.nlm.nih.gov/entrez/query.fcgi?cmd=Retrieve&db=PubMed&dopt=Citation&list_uids=19002161

[257] Castanotto, D.; Sakurai, K.; Lingeman, R.; Li, H.; Shively, L.; Aagaard, L.; Soifer, H.; Gatignol, A.; Riggs, A. and Rossi, J. J. (2007): Combinatorial delivery of small interfering RNAs reduces RNAi efficacy by selective incorporation into RISC, Nucleic Acids Res 35 [15], pp. 5154-64. URL: http://www.ncbi.nlm.nih.gov/entrez/query.fcgi?cmd=Retrieve&db=PubMed&dopt=Citation&list_uids=17660190

[258] Lai, E. C. (2002): Micro RNAs are complementary to 3' UTR sequence motifs that mediate negative post-transcriptional regulation, Nat Genet 30 [4], pp. 363-4. URL: http://www.ncbi.nlm.nih.gov/entrez/query.fcgi?cmd=Retrieve&db=PubMed&dopt=Citation&list_uids=11896390

[259] Jackson, A. L.; Bartz, S. R.; Schelter, J.; Kobayashi, S. V.; Burchard, J.; Mao, M.; Li, B.; Cavet, G. and Linsley, P. S. (2003): Expression profiling reveals off-target gene regulation by RNAi, Nat Biotechnol 21 [6], pp. 635-7. URL: http://www.ncbi.nlm.nih.gov/entrez/query.fcgi?cmd=Retrieve&db=PubMed&dopt=Citation&list_uids=12754523

[260] Birmingham, A.; Anderson, E. M.; Reynolds, A.; Ilsley-Tyree, D.; Leake, D.; Fedorov, Y.; Baskerville, S.; Maksimova, E.; Robinson, K.; Karpilow, J.; Marshall, W. S. and Khvorova, A. (2006): 3' UTR seed matches, but not overall identity, are associated with RNAi off-targets, Nat Methods 3 [3], pp. 199-204. URL: http://www.ncbi.nlm.nih.gov/entrez/query.fcgi?cmd=Retrieve&db=PubMed&dopt=Citation&list_uids=16489337

[261] Jackson, A. L.; Burchard, J.; Schelter, J.; Chau, B. N.; Cleary, M.; Lim, L. and Linsley, P. S. (2006): Widespread siRNA "off-target" transcript silencing mediated by seed region sequence complementarity, RNA 12 [7], pp. 1179-87. URL: http://www.ncbi.nlm.nih.gov/entrez/query.fcgi?cmd=Retrieve&db=PubMed&dopt=Citation&list_uids=16682560

[262] Grimson, A.; Farh, K. K.; Johnston, W. K.; Garrett-Engele, P.; Lim, L. P. and Bartel, D. P. (2007): MicroRNA targeting specificity in mammals: determinants beyond seed pairing, Mol Cell 27 [1], pp. 91-105. URL: http://www.ncbi.nlm.nih.gov/entrez/query.fcgi?cmd=Retrieve&db=PubMed&dopt=Citation&list_uids=17612493

[263] Chung, K. H.; Hart, C. C.; Al-Bassam, S.; Avery, A.; Taylor, J.; Patel, P. D.; Vojtek, A. B. and Turner, D. L. (2006): Polycistronic RNA polymerase II expression vectors for RNA interference based on BIC/miR-155, Nucleic Acids Res 34 [7], p. e53. URL: http://www.ncbi.nlm.nih.gov/entrez/query.fcgi?cmd=Retrieve&db=PubMed&dopt=Citation&list_uids=16614444

[264] Du, G.; Yonekubo, J.; Zeng, Y.; Osisami, M. and Frohman, M. A. (2006): Design of expression vectors for RNA interference based on miRNAs and RNA splicing, FEBS J 273 [23], pp. 5421-7. URL: http://www.ncbi.nlm.nih.gov/entrez/query.fcgi?cmd=Retrieve&db=PubMed&dopt=Citation&list_uids=17076699

[265] Hildinger, M.; Abel, K. L.; Ostertag, W. and Baum, C. (1999): Design of 5' untranslated sequences in retroviral vectors developed for medical use, J Virol 73 [5], pp. 4083-9. URL: http://www.ncbi.nlm.nih.gov/entrez/query.fcgi?cmd=Retrieve&db=PubMed&dopt=Citation&list_uids=10196304

[266] Malim, M. H.; Hauber, J.; Le, S. Y.; Maizel, J. V. and Cullen, B. R. (1989): The HIV-1 rev trans-activator acts through a structured target sequence to activate nuclear export of unspliced viral mRNA, Nature 338 [6212], pp. 254-7. URL: http://www.ncbi.nlm.nih.gov/entrez/query.fcgi?cmd=Retrieve&db=PubMed&dopt=Citation&list_uids=2784194

[267] Dull, T.; Zufferey, R.; Kelly, M.; Mandel, R. J.; Nguyen, M.; Trono, D. and Naldini, L. (1998): A third-generation lentivirus vector with a conditional packaging system, J Virol 72 [11], pp. 8463-71. URL: http://www.ncbi.nlm.nih.gov/entrez/query.fcgi?cmd=Retrieve&db=PubMed&dopt=Citation&list_uids=9765382

[268] Amendola, M.; Passerini, L.; Pucci, F.; Gentner, B.; Bacchetta, R. and Naldini, L. (2009): Regulated and multiple miRNA and siRNA delivery into primary cells by a lentiviral platform, Mol Ther 17 [6], pp. 1039-52. URL: http://www.ncbi.nlm.nih.gov/entrez/query.fcgi?cmd=Retrieve&db=PubMed&dopt=Citation&list_uids=19293777

[269] Singh, H.; Manuri, P. R.; Olivares, S.; Dara, N.; Dawson, M. J.; Huls, H.; Hackett, P. B.; Kohn, D. B.; Shpall, E. J.; Champlin, R. E. and Cooper, L. J. (2008): Redirecting specificity of T-cell populations for CD19 using the Sleeping Beauty system, Cancer Res 68 [8], pp. 2961-71. URL: http://www.ncbi.nlm.nih.gov/entrez/query.fcgi?cmd=Retrieve&db=PubMed&dopt=Citation&list_uids=18413766

[270] Nakazawa, Y.; Huye, L. E.; Dotti, G.; Foster, A. E.; Vera, J. F.; Manuri, P. R.; June, C. H.; Rooney, C. M. and Wilson, M. H. (2009): Optimization of the PiggyBac transposon system for the sustained genetic modification of human T lymphocytes, J Immunother 32 [8], pp. 826-36. URL: http://www.ncbi.nlm.nih.gov/entrez/query.fcgi?cmd=Retrieve&db=PubMed&dopt=Citation&list_uids=19752751

[271] Peng, P. D.; Cohen, C. J.; Yang, S.; Hsu, C.; Jones, S.; Zhao, Y.; Zheng, Z.; Rosenberg, S. A. and Morgan, R. A. (2009): Efficient nonviral Sleeping Beauty transposon-based TCR gene transfer to peripheral blood lymphocytes confers antigen-specific antitumor reactivity, Gene Ther 16 [8], pp. 1042-9. URL: http://www.ncbi.nlm.nih.gov/entrez/query.fcgi?cmd=Retrieve&db=PubMed&dopt=Citation&list_uids=19494842

[272] Ivics, Z.; Hackett, P. B.; Plasterk, R. H. and Izsvak, Z. (1997): Molecular reconstruction of Sleeping Beauty, a Tc1-like transposon from fish, and its transposition in human cells, Cell 91 [4], pp. 501-10. URL: http://www.ncbi.nlm.nih.gov/entrez/query.fcgi?cmd=Retrieve&db=PubMed&dopt=Citation&list_uids=9390559

[273] Mates, L.; Chuah, M. K.; Belay, E.; Jerchow, B.; Manoj, N.; Acosta-Sanchez, A.; Grzela, D. P.; Schmitt, A.; Becker, K.; Matrai, J.; Ma, L.; Samara-Kuko, E.; Gysemans, C.; Pryputniewicz, D.; Miskey, C.; Fletcher, B.; VandenDriessche, T.; Ivics, Z. and Izsvak, Z. (2009): Molecular evolution of a novel hyperactive Sleeping Beauty transposase enables robust stable gene transfer in vertebrates, Nat Genet 41 [6], pp. 753-61. URL:

http://www.ncbi.nlm.nih.gov/entrez/query.fcgi?cmd=Retrieve&db=PubMed&dopt=Citation&list_uids=19412179

[274] Ding, S.; Wu, X.; Li, G.; Han, M.; Zhuang, Y. and Xu, T. (2005): Efficient transposition of the piggyBac (PB) transposon in mammalian cells and mice, Cell 122 [3], pp. 473-83. URL: http://www.ncbi.nlm.nih.gov/entrez/query.fcgi?cmd=Retrieve&db=PubMed&dopt=Citation&list_uids=16096065

[275] Kim, Y. G.; Cha, J. and Chandrasegaran, S. (1996): Hybrid restriction enzymes: zinc finger fusions to Fok I cleavage domain, Proc Natl Acad Sci U S A 93 [3], pp. 1156-60. URL: http://www.ncbi.nlm.nih.gov/entrez/query.fcgi?cmd=Retrieve&db=PubMed&dopt=Citation&list_uids=8577732

[276] Christian, M.; Cermak, T.; Doyle, E. L.; Schmidt, C.; Zhang, F.; Hummel, A.; Bogdanove, A. J. and Voytas, D. F. (2010): Targeting DNA double-strand breaks with TAL effector nucleases, Genetics 186 [2], pp. 757-61. URL: http://www.ncbi.nlm.nih.gov/entrez/query.fcgi?cmd=Retrieve&db=PubMed&dopt=Citation&list_uids=20660643

[277] Li, T.; Huang, S.; Jiang, W. Z.; Wright, D.; Spalding, M. H.; Weeks, D. P. and Yang, B. (2011): TAL nucleases (TALNs): hybrid proteins composed of TAL effectors and FokI DNA-cleavage domain, Nucleic Acids Res 39 [1], pp. 359-72. URL: http://www.ncbi.nlm.nih.gov/entrez/query.fcgi?cmd=Retrieve&db=PubMed&dopt=Citation&list_uids=20699274

[278] Cong, L.; Ran, F. A.; Cox, D.; Lin, S.; Barretto, R.; Habib, N.; Hsu, P. D.; Wu, X.; Jiang, W.; Marraffini, L. A. and Zhang, F. (2013): Multiplex genome engineering using CRISPR/Cas systems, Science 339 [6121], pp. 819-23. URL: http://www.ncbi.nlm.nih.gov/entrez/query.fcgi?cmd=Retrieve&db=PubMed&dopt=Citation&list_uids=23287718

[279] Mali, P.; Yang, L.; Esvelt, K. M.; Aach, J.; Guell, M.; DiCarlo, J. E.; Norville, J. E. and Church, G. M. (2013): RNA-guided human genome engineering via Cas9, Science 339 [6121], pp. 823-6. URL: http://www.ncbi.nlm.nih.gov/entrez/query.fcgi?cmd=Retrieve&db=PubMed&dopt=Citation&list_uids=23287722

[280] Eshhar, Z.; Waks, T.; Gross, G. and Schindler, D. G. (1993): Specific activation and targeting of cytotoxic lymphocytes through chimeric single chains consisting of antibody-binding domains and the gamma or zeta subunits of the immunoglobulin and T-cell receptors, Proc Natl Acad Sci U S A 90 [2], pp. 720-4. URL: http://www.ncbi.nlm.nih.gov/entrez/query.fcgi?cmd=Retrieve&db=PubMed&dopt=Citation&list_uids=8421711

[281] Finney, H. M.; Lawson, A. D.; Bebbington, C. R. and Weir, A. N. (1998): Chimeric receptors providing both primary and costimulatory signaling in T cells from a single gene product, J Immunol 161 [6], pp. 2791-7. URL: http://www.ncbi.nlm.nih.gov/entrez/query.fcgi?cmd=Retrieve&db=PubMed&dopt=Citation&list_uids=9743337

[282] Finney, H. M.; Akbar, A. N. and Lawson, A. D. (2004): Activation of resting human primary T cells with chimeric receptors: costimulation from CD28, inducible costimulator, CD134, and CD137 in series with signals from the TCR zeta chain, J Immunol 172 [1], pp. 104-13. URL: http://www.ncbi.nlm.nih.gov/entrez/query.fcgi?cmd=Retrieve&db=PubMed&dopt=Citation&list_uids=14688315

[283] Imai, C.; Mihara, K.; Andreansky, M.; Nicholson, I. C.; Pui, C. H.; Geiger, T. L. and Campana, D. (2004): Chimeric receptors with 4-1BB signaling capacity provoke potent cytotoxicity against acute lymphoblastic leukemia, Leukemia 18 [4], pp. 676-84. URL: http://www.ncbi.nlm.nih.gov/entrez/query.fcgi?cmd=Retrieve&db=PubMed&dopt=Citation&list_uids=14961035

[284] Milone, M. C.; Fish, J. D.; Carpenito, C.; Carroll, R. G.; Binder, G. K.; Teachey, D.; Samanta, M.; Lakhal, M.; Gloss, B.; Danet-Desnoyers, G.; Campana, D.; Riley, J. L.; Grupp, S. A. and June, C. H. (2009): Chimeric receptors containing CD137 signal transduction domains mediate enhanced survival of T cells and increased antileukemic efficacy in vivo, Mol Ther 17 [8], pp. 1453-64. URL:

http://www.ncbi.nlm.nih.gov/entrez/query.fcgi?cmd=Retrieve&db=PubMed&dopt=Citation&list_uids=19384291

[285] Porter, D. L.; Levine, B. L.; Kalos, M.; Bagg, A. and June, C. H. (2011): Chimeric antigen receptor-modified T cells in chronic lymphoid leukemia, N Engl J Med 365 [8], pp. 725-33. URL: http://www.ncbi.nlm.nih.gov/entrez/query.fcgi?cmd=Retrieve&db=PubMed&dopt=Citation&list_uids=21830940

[286] Kalos, M.; Levine, B. L.; Porter, D. L.; Katz, S.; Grupp, S. A.; Bagg, A. and June, C. H. (2011): T cells with chimeric antigen receptors have potent antitumor effects and can establish memory in patients with advanced leukemia, Sci Transl Med 3 [95], p. 95ra73. URL: http://www.ncbi.nlm.nih.gov/entrez/query.fcgi?cmd=Retrieve&db=PubMed&dopt=Citation&list_uids=21832238

[287] Grupp, S. A.; Kalos, M.; Barrett, D.; Aplenc, R.; Porter, D. L.; Rheingold, S. R.; Teachey, D. T.; Chew, A.; Hauck, B.; Wright, J. F.; Milone, M. C.; Levine, B. L. and June, C. H. (2013): Chimeric antigen receptor-modified T cells for acute lymphoid leukemia, N Engl J Med 368 [16], pp. 1509-18. URL: http://www.ncbi.nlm.nih.gov/entrez/query.fcgi?cmd=Retrieve&db=PubMed&dopt=Citation&list_uids=23527958

[288] Richman, S. A.; Aggen, D. H.; Dossett, M. L.; Donermeyer, D. L.; Allen, P. M.; Greenberg, P. D. and Kranz, D. M. (2009): Structural features of T cell receptor variable regions that enhance domain stability and enable expression as single-chain ValphaVbeta fragments, Mol Immunol 46 [5], pp. 902-16. URL: http://www.ncbi.nlm.nih.gov/entrez/query.fcgi?cmd=Retrieve&db=PubMed&dopt=Citation&list_uids=18962897

[289] Chung, S.; Wucherpfennig, K. W.; Friedman, S. M.; Hafler, D. A. and Strominger, J. L. (1994): Functional three-domain single-chain T-cell receptors, Proc Natl Acad Sci U S A 91 [26], pp. 12654-8. URL: http://www.ncbi.nlm.nih.gov/entrez/query.fcgi?cmd=Retrieve&db=PubMed&dopt=Citation&list_uids=7809095

[290] Willemsen, R. A.; Weijtens, M. E.; Ronteltap, C.; Eshhar, Z.; Gratama, J. W.; Chames, P. and Bolhuis, R. L. (2000): Grafting primary human T lymphocytes with cancer-specific chimeric single chain and two chain TCR, Gene Ther 7 [16], pp. 1369-77. URL: http://www.ncbi.nlm.nih.gov/entrez/query.fcgi?cmd=Retrieve&db=PubMed&dopt=Citation&list_uids=10981663

[291] Zhang, T.; He, X.; Tsang, T. C. and Harris, D. T. (2004): Transgenic TCR expression: comparison of single chain with full-length receptor constructs for T-cell function, Cancer Gene Ther 11 [7], pp. 487-96. URL: http://www.ncbi.nlm.nih.gov/entrez/query.fcgi?cmd=Retrieve&db=PubMed&dopt=Citation&list_uids=15153936

[292] Voss, R. H.; Thomas, S.; Pfirschke, C.; Hauptrock, B.; Klobuch, S.; Kuball, J.; Grabowski, M.; Engel, R.; Guillaume, P.; Romero, P.; Huber, C.; Beckhove, P. and Theobald, M. (2010): Coexpression of the T-cell receptor constant alpha domain triggers tumor reactivity of single-chain TCR-transduced human T cells, Blood 115 [25], pp. 5154-63. URL: http://www.ncbi.nlm.nih.gov/entrez/query.fcgi?cmd=Retrieve&db=PubMed&dopt=Citation&list_uids=20378753

[293] Aggen, D. H.; Chervin, A. S.; Schmitt, T. M.; Engels, B.; Stone, J. D.; Richman, S. A.; Piepenbrink, K. H.; Baker, B. M.; Greenberg, P. D.; Schreiber, H. and Kranz, D. M. (2012): Single-chain ValphaVbeta T-cell receptors function without mispairing with endogenous TCR chains, Gene Ther 19 [4], pp. 365-74. URL: http://www.ncbi.nlm.nih.gov/entrez/query.fcgi?cmd=Retrieve&db=PubMed&dopt=Citation&list_uids=21753797

[294] Aggen, D. H.; Chervin, A. S.; Insaidoo, F. K.; Piepenbrink, K. H.; Baker, B. M. and Kranz, D. M. (2011): Identification and engineering of human variable regions that allow expression of stable single-chain T cell receptors, Protein Eng Des Sel 24 [4], pp. 361-72. URL: http://www.ncbi.nlm.nih.gov/entrez/query.fcgi?cmd=Retrieve&db=PubMed&dopt=Citation&list_uids=21159619

[295] Clay, T. M.; Custer, M. C.; Spiess, P. J. and Nishimura, M. I. (1999): Potential use of T cell receptor genes to modify hematopoietic stem cells for the gene therapy of cancer, Pathol Oncol Res 5 [1], pp. 3-15. URL: http://www.ncbi.nlm.nih.gov/entrez/query.fcgi?cmd=Retrieve&db=PubMed&dopt=Citation&list_uids=10079371

[296] Yang, L. and Baltimore, D. (2005): Long-term in vivo provision of antigen-specific T cell immunity by programming hematopoietic stem cells, Proc Natl Acad Sci U S A 102 [12], pp. 4518-23. URL: http://www.ncbi.nlm.nih.gov/entrez/query.fcgi?cmd=Retrieve&db=PubMed&dopt=Citation&list_uids=15758071

[297] Giannoni, F.; Hardee, C. L.; Wherley, J.; Gschweng, E.; Senadheera, S.; Kaufman, M. L.; Chan, R.; Bahner, I.; Gersuk, V.; Wang, X.; Gjertson, D.; Baltimore, D.; Witte, O. N.; Economou, J. S.; Ribas, A. and Kohn, D. B. (2013): Allelic exclusion and peripheral reconstitution by TCR transgenic T cells arising from transduced human hematopoietic stem/progenitor cells, Mol Ther 21 [5], pp. 1044-54. URL: http://www.ncbi.nlm.nih.gov/entrez/query.fcgi?cmd=Retrieve&db=PubMed&dopt=Citation&list_uids=23380815

[298] Vatakis, D. N.; Arumugam, B.; Kim, S. G.; Bristol, G.; Yang, O. and Zack, J. A. (2013): Introduction of exogenous T-cell receptors into human hematopoietic progenitors results in exclusion of endogenous T-cell receptor expression, Mol Ther 21 [5], pp. 1055-63. URL: http://www.ncbi.nlm.nih.gov/entrez/query.fcgi?cmd=Retrieve&db=PubMed&dopt=Citation&list_uids=23481324

[299] Wherry, E. J.; Teichgraber, V.; Becker, T. C.; Masopust, D.; Kaech, S. M.; Antia, R.; von Andrian, U. H. and Ahmed, R. (2003): Lineage relationship and protective immunity of memory CD8 T cell subsets, Nat Immunol 4 [3], pp. 225-34. URL: http://www.ncbi.nlm.nih.gov/entrez/query.fcgi?cmd=Retrieve&db=PubMed&dopt=Citation&list_uids=12563257

[300] Hinrichs, C. S.; Borman, Z. A.; Gattinoni, L.; Yu, Z.; Burns, W. R.; Huang, J.; Klebanoff, C. A.; Johnson, L. A.; Kerkar, S. P.; Yang, S.; Muranski, P.; Palmer, D. C.; Scott, C. D.; Morgan, R. A.; Robbins, P. F.; Rosenberg, S. A. and Restifo, N. P. (2011): Human effector CD8+ T cells derived from naive rather than memory subsets possess superior traits for adoptive immunotherapy, Blood 117 [3], pp. 808-14. URL: http://www.ncbi.nlm.nih.gov/entrez/query.fcgi?cmd=Retrieve&db=PubMed&dopt=Citation&list_uids=20971955

[301] Berger, C.; Jensen, M. C.; Lansdorp, P. M.; Gough, M.; Elliott, C. and Riddell, S. R. (2008): Adoptive transfer of effector CD8+ T cells derived from central memory cells establishes persistent T cell memory in primates, J Clin Invest 118 [1], pp. 294-305. URL: http://www.ncbi.nlm.nih.gov/entrez/query.fcgi?cmd=Retrieve&db=PubMed&dopt=Citation&list_uids=18060041

[302] Gattinoni, L.; Klebanoff, C. A.; Palmer, D. C.; Wrzesinski, C.; Kerstann, K.; Yu, Z.; Finkelstein, S. E.; Theoret, M. R.; Rosenberg, S. A. and Restifo, N. P. (2005): Acquisition of full effector function in vitro paradoxically impairs the in vivo antitumor efficacy of adoptively transferred CD8+ T cells, J Clin Invest 115 [6], pp. 1616-26. URL: http://www.ncbi.nlm.nih.gov/entrez/query.fcgi?cmd=Retrieve&db=PubMed&dopt=Citation&list_uids=15931392

[303] Gattinoni, L.; Zhong, X. S.; Palmer, D. C.; Ji, Y.; Hinrichs, C. S.; Yu, Z.; Wrzesinski, C.; Boni, A.; Cassard, L.; Garvin, L. M.; Paulos, C. M.; Muranski, P. and Restifo, N. P. (2009): Wnt signaling arrests effector T cell differentiation and generates CD8+ memory stem cells, Nat Med 15 [7], pp. 808-13. URL: http://www.ncbi.nlm.nih.gov/entrez/query.fcgi?cmd=Retrieve&db=PubMed&dopt=Citation&list_uids=19525962

[304] Gattinoni, L.; Lugli, E.; Ji, Y.; Pos, Z.; Paulos, C. M.; Quigley, M. F.; Almeida, J. R.; Gostick, E.; Yu, Z.; Carpenito, C.; Wang, E.; Douek, D. C.; Price, D. A.; June, C. H.; Marincola, F. M.; Roederer, M. and Restifo, N. P. (2011): A human memory T cell subset with stem cell-like properties, Nat Med 17 [10], pp. 1290-7. URL: http://www.ncbi.nlm.nih.gov/entrez/query.fcgi?cmd=Retrieve&db=PubMed&dopt=Citation&list_uids=21926977

[305] Cieri, N.; Camisa, B.; Cocchiarella, F.; Forcato, M.; Oliveira, G.; Provasi, E.; Bondanza, A.; Bordignon, C.; Peccatori, J.; Ciceri, F.; Lupo-Stanghellini, M. T.; Mavilio, F.; Mondino, A.; Bicciato, S.; Recchia, A. and Bonini, C. (2013): IL-7 and IL-15 instruct the generation of human memory stem T cells from naive precursors, Blood 121 [4], pp. 573-84. URL: http://www.ncbi.nlm.nih.gov/entrez/query.fcgi?cmd=Retrieve&db=PubMed&dopt=Citation&list_uids=23160470

[306] Graef, P.; Buchholz, V. R.; Stemberger, C.; Flossdorf, M.; Henkel, L.; Schiemann, M.; Drexler, I.; Hofer, T.; Riddell, S. R. and Busch, D. H. (2014): Serial transfer of single-cell-derived immunocompetence reveals stemness of CD8(+) central memory T cells, Immunity 41 [1], pp. 116-26. URL: http://www.ncbi.nlm.nih.gov/entrez/query.fcgi?cmd=Retrieve&db=PubMed&dopt=Citation&list_uids=25035956

[307] Chapuis, A. G.; Ragnarsson, G. B.; Nguyen, H. N.; Chaney, C. N.; Pufnock, J. S.; Schmitt, T. M.; Duerkopp, N.; Roberts, I. M.; Pogosov, G. L.; Ho, W. Y.; Ochsenreither, S.; Wolfl, M.; Bar, M.; Radich, J. P.; Yee, C. and Greenberg, P. D. (2013): Transferred WT1-reactive CD8+ T cells can mediate antileukemic activity and persist in post-transplant patients, Sci Transl Med 5 [174], p. 174ra27. URL: http://www.ncbi.nlm.nih.gov/entrez/query.fcgi?cmd=Retrieve&db=PubMed&dopt=Citation&list_uids=23447018

[308] Staveley-O'Carroll, K.; Schell, T. D.; Jimenez, M.; Mylin, L. M.; Tevethia, M. J.; Schoenberger, S. P. and Tevethia, S. S. (2003): In vivo ligation of CD40 enhances priming against the endogenous tumor antigen and promotes CD8+ T cell effector function in SV40 T antigen transgenic mice, J Immunol 171 [2], pp. 697-707. URL: http://www.ncbi.nlm.nih.gov/entrez/query.fcgi?cmd=Retrieve&db=PubMed&dopt=Citation&list_uids=12847236

[309] Pircher, H.; Michalopoulos, E. E.; Iwamoto, A.; Ohashi, P. S.; Baenziger, J.; Hengartner, H.; Zinkernagel, R. M. and Mak, T. W. (1987): Molecular analysis of the antigen receptor of virus-specific cytotoxic T cells and identification of a new V alpha family, Eur J Immunol 17 [12], pp. 1843-6. URL: http://www.ncbi.nlm.nih.gov/entrez/query.fcgi?cmd=Retrieve&db=PubMed&dopt=Citation&list_uids=2961577

[310] Jainchill, J. L.; Aaronson, S. A. and Todaro, G. J. (1969): Murine sarcoma and leukemia viruses: assay using clonal lines of contact-inhibited mouse cells, J Virol 4 [5], pp. 549-53. URL: http://www.ncbi.nlm.nih.gov/entrez/query.fcgi?cmd=Retrieve&db=PubMed&dopt=Citation&list_uids=4311790

[311] Morita, S.; Kojima, T. and Kitamura, T. (2000): Plat-E: an efficient and stable system for transient packaging of retroviruses, Gene Ther 7 [12], pp. 1063-6. URL: http://www.ncbi.nlm.nih.gov/entrez/query.fcgi?cmd=Retrieve&db=PubMed&dopt=Citation&list_uids=10871756

[312] Prevost-Blondel, A.; Zimmermann, C.; Stemmer, C.; Kulmburg, P.; Rosenthal, F. M. and Pircher, H. (1998): Tumor-infiltrating lymphocytes exhibiting high ex vivo cytolytic activity fail to prevent murine melanoma tumor growth in vivo, J Immunol 161 [5], pp. 2187-94. URL: http://www.ncbi.nlm.nih.gov/entrez/query.fcgi?cmd=Retrieve&db=PubMed&dopt=Citation&list_uids=9725210

[313] Karttunen, J.; Sanderson, S. and Shastri, N. (1992): Detection of rare antigen-presenting cells by the lacZ T-cell activation assay suggests an expression cloning strategy for T-cell antigens, Proc Natl Acad Sci U S A 89 [13], pp. 6020-4. URL: http://www.ncbi.nlm.nih.gov/entrez/query.fcgi?cmd=Retrieve&db=PubMed&dopt=Citation&list_uids=1378619

[314] Schneider, U.; Schwenk, H. U. and Bornkamm, G. (1977): Characterization of EBV-genome negative "null" and "T" cell lines derived from children with acute lymphoblastic leukemia and leukemic transformed non-Hodgkin lymphoma, Int J Cancer 19 [5], pp. 621-6. URL: http://www.ncbi.nlm.nih.gov/entrez/query.fcgi?cmd=Retrieve&db=PubMed&dopt=Citation&list_uids=68013

[315] Chen, W.; Yewdell, J. W.; Levine, R. L. and Bennink, J. R. (1999): Modification of cysteine residues in vitro and in vivo affects the immunogenicity and antigenicity of major

histocompatibility complex class I-restricted viral determinants, J Exp Med 189 [11], pp. 1757-64. URL: http://www.ncbi.nlm.nih.gov/entrez/query.fcgi?cmd=Retrieve&db=PubMed&dopt=Citation&list_uids=10359579

[316] Benson, D. A.; Cavanaugh, M.; Clark, K.; Karsch-Mizrachi, I.; Lipman, D. J.; Ostell, J. and Sayers, E. W. (2013): GenBank, Nucleic Acids Res 41 [Database issue], pp. D36-42. URL: http://www.ncbi.nlm.nih.gov/entrez/query.fcgi?cmd=Retrieve&db=PubMed&dopt=Citation&list_uids=23193287

[317] Yuan, B.; Latek, R.; Hossbach, M.; Tuschl, T. and Lewitter, F. (2004): siRNA Selection Server: an automated siRNA oligonucleotide prediction server, Nucleic Acids Res 32 [Web Server issue], pp. W130-4. URL: http://www.ncbi.nlm.nih.gov/entrez/query.fcgi?cmd=Retrieve&db=PubMed&dopt=Citation&list_uids=15215365

[318] Lu, Z. J. and Mathews, D. H. (2008): OligoWalk: an online siRNA design tool utilizing hybridization thermodynamics, Nucleic Acids Res 36 [Web Server issue], pp. W104-8. URL: http://www.ncbi.nlm.nih.gov/entrez/query.fcgi?cmd=Retrieve&db=PubMed&dopt=Citation&list_uids=18490376

[319] Meyerhuber, P.; Conrad, H.; Starck, L.; Leisegang, M.; Busch, D. H.; Uckert, W. and Bernhard, H. (2010): Targeting the epidermal growth factor receptor (HER) family by T cell receptor gene-modified T lymphocytes, J Mol Med (Berl) 88 [11], pp. 1113-21. URL: http://www.ncbi.nlm.nih.gov/entrez/query.fcgi?cmd=Retrieve&db=PubMed&dopt=Citation&list_uids=20700725

[320] Untergasser, A.; Nijveen, H.; Rao, X.; Bisseling, T.; Geurts, R. and Leunissen, J. A. (2007): Primer3Plus, an enhanced web interface to Primer3, Nucleic Acids Res 35 [Web Server issue], pp. W71-4. URL: http://www.ncbi.nlm.nih.gov/entrez/query.fcgi?cmd=Retrieve&db=PubMed&dopt=Citation&list_uids=17485472

8 Acknowledgements

Most of all, I would like to express my gratitude to my supervisor Wolfgang Uckert for giving me the opportunity to work in his laboratory on this interesting project. Furthermore, I would like to thank my colleagues of the AG Uckert for critical discussions, helpful suggestions and practical support. Also I am thankful to Ton Schumacher, Gavin Bendle, Carsten Linnemann, Laura Bies and Stephan Schulz for our successful cooperation. Carolin Genehr, Mareen Kamarys and Matthias Richter provided excellent technical assistance and I am grateful for their help.

9 Publications

Ammar I, Gogol-Döring A, Miskey C, **Bunse M**, Chen W, Uckert W, Izsák Z and Ivics Z (2014). Genome-Wide Profiling of Transposon and Retrovirus Integration Sites in Primary Human CD4+ T Cells. *Submitted*.

Bunse M, Bendle GM, Linnemann C, Bies L, Schulz S, Schumacher TN, and Uckert W (2014). RNAi-mediated TCR knockdown prevents autoimmunity in mice caused by mixed TCR dimers following TCR gene transfer. *Mol Ther* **22**: 1983-91.

Nauerth M, Weissbrich B, Knall R, Franz T, Dossinger G, Bet J, Paszkiewicz PJ, Pfeifer L, **Bunse M**, Uckert W, Holtappels R, Gillert-Marien D, Neuenhahn M, Krackhardt A, Reddehase MJ, Riddell SR, and Busch DH (2013). TCR-ligand koff rate correlates with the protective capacity of antigen-specific CD8+ T cells for adoptive transfer. *Sci Transl Med* **5**: 192ra187.

Dössinger G, **Bunse M**, Bet J, Albrecht J, Paszkiewicz PJ, Weissbrich B, Schiedewitz I, Henkel L, Schiemann M, Neuenhahn M, Uckert W, and Busch DH (2013). MHC multimer-guided and cell culture-independent isolation of functional T cell receptors from single cells facilitates TCR identification for immunotherapy. *PLoS One* **8**: e61384.

Cayeux S, Bukarica B, Buschow C, Charo J, **Bunse M**, Dörken B, and Blankenstein T (2007). In vivo splenic CD11c cells downregulate CD4 T-cell response thereby decreasing systemic immunity to gene-modified tumour cell vaccine. *Gene Ther* **14**: 1481-1491.

Oral presentations

Bunse M (2014, March 21). RNAi-mediated TCR knockdown prevents autoimmunity in mice caused by mixed TCR dimers following TCR gene transfer. *Presented at the XX Annual Meeting of the Germany Society of Gene Therapy (DG-GT).* Ulm, Germany.

Bunse M (2013, March 14). RNAi-assisted TCR protein replacement reduces severe autoimmune reactions caused by mixed TCR dimers. *Presented at the 7th International Cellular Therapy Symposium.* Erlangen, Germany.

Bunse M (2012, September 07). RNAi-assisted TCR protein replacement reduces severe autoimmune reactions caused by mixed TCR dimers. *Presented at the 3rd European Congress of Immunology.* Glasgow, Scotland.

Bunse M (2012, May 03). RNAi-assisted TCR protein replacement in T cells. *Presented at the 2nd Berlin Symposium on Adoptive T Cell Therapy.* Berlin, Germany.

Datum Unterschrift

10 Selbstständigkeitserklärung

Hiermit versichere ich, dass ich die vorliegende Dissertation selbstständig und nur unter Verwendung der angegebenen Hilfen und Hilfsmittel angefertigt habe. Ich habe mich anderwärts nicht um einen Doktorgrad beworben und besitze einen entsprechenden Doktorgrad nicht. Außerdem bestätige ich, dass mir die dem angestrebten Verfahren zugrunde liegende Promotionsordnung der Humboldt-Universität zu Berlin vom 01. September 2005 bekannt ist.

_____ _____

Datum Unterschrift